Sm-Nd and Rb-Sr ISOTOPIC SYSTEMATICS OF TEKTITES AND OTHER IMPACTITES, APPALACHIAN MAFIC ROCKS, AND MARINE CARBONATES AND PHOSPHATES

Thesis by

Henry Francis Shaw III

In Partial Fulfillment of the Requirements

for the Degree of

Doctor of Philosophy

California Institute of Technology

Pasadena, California

1984

(Submitted September 27, 1983)

Haec sic pernosces parva perductus opella;
namque alid ex alio clarescet nec tibi caeca
nox iter eripiet quin ultima naturai
pervideas: ita res accendent lumina rebus.

Leucretius, T. C.
De Rerum Natura
I: 1114-1117

ACKNOWLEDGMENTS

I would like to thank Professor G. J. Wasserburg for his guidance, interest, and alternating criticism and support of this work. He has always attempted to instill in me a sense of what constitutes an elegant experiment. I hope some small fraction of that wisdom has been successfully transferred. Dr. Dimitri A. Papanastassiou has unselfishly shared his time and extensive knowledge of mass-spectrometric and chemical procedures with me. Other members of the Lunatic Asylum, particularly Dr. James Chen, have by their enthusiasm and willingness to share their own special expertise, made the laboratory a stimulating place to work. Evelyn Brown's good humor, concern and desire to help contributed greatly to the smooth operation of the Asylum during my tenure there.

Special thanks are owed to Professor A. L. Albee firstly for encouraging me to come to Caltech and secondly for suggesting while I was casting about for a thesis topic that I should consider a problem involving isotopic measurements. His support and interest are gratefully acknowledged.

I have benefited from discussions and classes with many other faculty members during my stay at Caltech. I would particularly like to thank Professors T. J. Ahrens, S. Epstein, H. A. Lowenstam and E. M. Stolper for their continued interest in my work.

My interactions with the other students at Caltech were one of the most valuable parts of my education. Discussions with B. Gregory, S. B. Jacobsen, J. H. Jones and D. J. Piepgras were particularly helpful in formulating my own ideas. I would also like to thank Judith Wright-Clark (Univ. of Oregon) for teaching me what a conodont is.

Many people have contributed samples for the studies comprising this

thesis. In addition to those people acknowledged in Appendices I and II, I would like to thank Drs. Z. S. Altschuler (USGS, Reston), R. Ginsburg (Univ. of Miami), W. Holzer (Univ. of Oregon), Y. Kolodny (Jerusalem Univ.), and G. McLellan (Intl. Fertilizer Dev. Corp.) for the carbonate and phosphate samples discussed in Chapter III.

This work has been supported by NSF grants PHY79-23638A2, EAR79-19786, OCE81-08595, and NASA grant NGL-05-002-188.

ABSTRACT

This thesis is made up of three separate studies, each using the Sm-Nd and Rb-Sr isotopic systems to solve a problem of geologic interest.

In the first study it is shown that Sm-Nd and Rb-Sr analyses of tektites and other impactites can be used to place constraints on the age and provenance of the target materials which were impact melted to form these objects. Tektites have large negative values of $\varepsilon_{Nd}(0)$ which are uniform within each tektite group, while the $\varepsilon_{Sr}(0)$ values are large positive and show considerable variation within each group. The chemical, trace element, and isotopic compositions of tektites are consistent with their production by melting of sediments derived from old continental crust. Each tektite group is characterized by a uniform Nd model age, T^{Nd}_{CHUR}, interpreted as the time of formation of the crustal segment which weathered to form the parent sediment for the tektites: (1) ~ 1.15AE for Australasian tektites; (2) ~ 1.9AE for Ivory Coast tektites; (3) ~ 0.9AE for moldavites; (4) ~ 0.65AE for North American tektites; and (5) ~ 0.9AE for high-Si irghizites. Sr model ages, T^{Sr}_{UR}, are variable within each group, reflecting Rb-Sr fractionation during weathering and sedimentation. In the favorable limit of very high Rb/Sr ratios T^{Sr}_{UR} approaches the time of sedimentation of the parent material which melted to form the tektites. Australasian tektites are derived from ~ 0.25AE sediments, moldavites from ~ 0.0AE sediments, and Ivory Coast tektites from ~ 0.95AE sediments. The parent sediments of the other tektite groups have poorly constrained ages. The isotopic data on the moldavites and Ivory Coast tektites are consistent with their derivation from the Ries and Bosumtwi Craters, respectively. Irghizites are isotopically distinct from the Australasian tektites and are

probably not related. Sanidine spherules from an iridium-rich Cretaceous-Tertiary boundary clay were heavily overprinted with seawater-derived Sr and Nd during diagenesis. The inferred initial isotopic composition of the sanidine itself is $\varepsilon_{Nd}(T) = +2$ and $\varepsilon_{Sr}(T) = +5$. These results show that the spherules were not derived from old continental crust or meteoritic potassium feldspar. These objects may represent an impact melt of a mixture of basaltic oceanic crust and overlying sediments and are consistent with an oceanic impact at the Cretaceous-Tertiary boundary. The isotopic data are also consistent with an origin by authigenic growth of the spherules from young detrital material.

The second study in this thesis uses the Sm-Nd and Rb-Sr isotopic systematics of mafic rocks from the Appalachians to place constraints on their origin. Isotopic analyses of modern oceanic basalts and ophiolites have shown that both modern and ancient oceanic crust have a characteristic Nd and Sr isotopic signature indicative of derivation from a depleted mantle reservoir. It also appears that the Nd isotopic system is not appreciably disturbed by metamorphism. These isotopic characteristics have been extended to the Pt. Sal, Kings-Kaweah, and Josephine Ophiolites of California. These characteristics are used in an attempt to identify pieces of proto-Atlantic oceanic crust among the mafic and ultramafic rocks of the Appalachians. Sm-Nd mineral isochrons for the Baltimore Mafic Complex, Md (BMC) yield an age of 490±20 My which is interpreted as the igneous crystallization age. BMC whole rock samples do not define isochrons and have initial isotopic compositions of $-6.4 < \varepsilon_{Nd}(T) < -2.2$, $+51 < \varepsilon_{Sr}(T) < +115$. $\varepsilon_{Nd}(T)$ and $\varepsilon_{Sr}(T)$ are anti-correlated. This is not the signature of depleted mantle and oceanic crust, but is similar to old continental crust. It is proposed that the BMC is a mafic continental

intrusion, possibly subduction related, which was contaminated with old continental crust during emplacement. Whole rock samples from the Thetford Mines Complex, Qe (TMC) do not define isochrons and have $-1.5 < \varepsilon_{Nd}(T) < +4.2$, $+2.6 < \varepsilon_{Sr}(T) < +114$. These data do not in any way reflect the signature of normal oceanic crust. These results are in contrast with geologic relationships which show the TMC to have the characteristics of an ophiolite complex. The TMC is chemically and isotopically similar to a class of other ophiolites which have affinities to modern boninites. The TMC may therefore represent an ophiolite formed under an arc complex. The Chunky Gal Amphibolite, N.C., Lake Chatuge complex, N.C., and Hazen's Notch Amphibolite, Vt., were found to have a depleted mantle signature with $+5 < \varepsilon_{Nd}(T) < +8$ and may be fragments of oceanic crust. The Webster-Addie body, N.C., has $\varepsilon_{Nd}(T) \sim -1$, $\varepsilon_{Sr}(T) \sim +30$ and is not isotopically similar to oceanic crust or the other North Carolina mafic bodies analyzed. From these isotopic results it is clear that Appalachian mafic rocks have diverse origins, some are continental intrusives (BMC), others are probably fragments of oceanic crust (Vermont and N. Carolina amphibolites). Future models for the development of the Appalachians must allow for these various origins. The possibility that some ophiolites are not normal oceanic crust but have an origin in a partially continental setting or as anomalous oceanic crust will require further attention.

The final study is an exploration of the possibility of establishing the Nd isotopic variations in seawater over geologic time by analysing a marine sedimentary phase which records and preserves the $\varepsilon_{Nd}(T)$ value of the seawater in which it formed. Apatite and $CaCO_3$ (calcite and aragonite) are examined as possible such phases. Modern biogenic and inorganic calcite and aragonite were found to have low REE concentrations: Nd = 0.2 to 65 ppb. The $\varepsilon_{Nd}(0)$ values of Atlantic (-8.3 to -9.6) and

Pacific (-0.1 to -1.3) carbonates are distinctly different and reflect the isotopic composition of Nd in the seawater in which they formed. The high concentrations of REE measured in limestones and carbonate fossils cannot be primary but must be due to the presence of other phases in the carbonate of the introduction of REE during diagenesis. Modern biogenic apatite also has a low REE content (<150 ppb Nd), but appears to quickly scavenge REE from seawater. Levels up to 1000 ppm Nd can be reached by this process. Inorganically precipitated apatite from phosphorites also has high concentrations of seawater-derived REE. A seawater-like REE pattern with a characteristic negative Ce-anomaly is often preserved by sedimentary apatite and apatite samples of the same age from different localities bordering a common sea record a common value of $\varepsilon_{Nd}(T)$. These characteristics suggest that apatite can be used to trace the evolution of $\varepsilon_{Nd}(T)$ in ancient seawater. The values of $\varepsilon_{Nd}(T)$ in seawater as inferred from analyses of conodonts and phosphorite apatite range between -1.7 and -8.9 over the last 700My. These values lie in the range of modern seawater values and show no evidence for drastic changes in the sources for Nd in seawater during this time. High values of seawater $\varepsilon_{Nd}(T)$ in the Triassic and latest Precambrian may correlate with the breakup of large continental landmasses. The initial $\varepsilon_{Nd}(T) = -15.0$ of the 2AE old Rum Jungle phosphorite requires the presence of ~ 1.5AE old continental crust at 2AE ago. This demonstrates how the ε_{Nd} value of ancient seawater can be used to constrain the age of the exposed crust as a function of time.

TABLE OF CONTENTS

CHAPTER I

I.1. Introduction

The last decade has seen a flowering of the use of isotopic systematics in addressing problems of terrestrial geology, lunar geology, and early solar system history. In large part, the growth of this field has been spurred by the development of new laboratory techniques and the accessibility of instrumentation which permit the precise measurement of isotopic ratios for elements from hydrogen to uranium and beyond. Of particular interest are the isotopic systems involving radioactive decay. These systems are of interest because geology in its broadest sense is history; it is the science aimed at understanding the processes which have operated during the evolution of the solid bodies of our solar system. Because evolution implies change over some period of time, the ability to measure elapsed time is of fundamental importance to our science. Once the short timescale of man's recorded history is exceeded, the only chronometers that gauge absolute rather than relative time are those provided by radioactive nuclei. It is this ability to record chronometric information that sets the radioactive isotopic systems apart from other tracers of geologic processes, however imperfectly we may be able to extract the information contained there. In some applications the role of time in the interpretation of the isotopic data may be secondary. Nevertheless, the variations in the isotopic composition of a radioactive parent-daughter system will always reflect the timing of events in the evolution of the geologic system being studied.

This thesis presents the results of applying the Sm-Nd and Rb-Sr isotopic systems to three different problems of geologic interest. A brief discussion of these systems follows in section I.2. Each of the

problems uses the information provided by the isotopic systems in a somewhat different way and to a somewhat different end. Chapter II contains an examination of the Sm-Nd and Rb-Sr isotopic systematics of tektites and of sanidine spherules from an iridium-rich Cretaceous-Tertiary boundary clay. Both of these types of objects are thought to be produced by impact events. It will be shown that for tektites, the isotopic systematics can be interpreted in a model in which continental crust is weathered to form a sediment which is later impact-melted to form tektites. The model provides both the average age of the weathered crustal terrain as well as the time of sedimentation of the parent material for the tektites. These ages can then be used to help identify possible sites for the impact which produced the tektites. The interpretation of the sanidine spherule data is less clearcut but the data are consistent with impact melting of a mixture of continentally derived sediments and basaltic oceanic crust to produce the spherules. Alternatively, the spherules may be a product of late Cretaceous volcanism. Chapter III discusses the isotopic constraints provided by Sm-Nd and Rb-Sr systematics on the origin of mafic complexes and associated rocks of the Appalachian Mountains. In recent models of the evolution of the Appalachians, these mafic rocks have been interpreted as ophiolites or dismembered ophiolites. By comparing Nd and Sr isotopic data on these rocks with published and new data on established ophiolites and modern oceanic crust it will be shown that although some Appalachian mafic rocks have an oceanic isotopic signature other mafic complexes show no oceanic affinity, casting some doubt on the popular tectonic models for the Appalachians. Chapter IV is an exploration of the possibility of establishing a record of Nd isotopic variations in seawater over geologic

time. Such a record would contain information on the age of the exposed continents as a function of time and would thus constrain a growth curve for continental crust. The choice of a phase to analyze which records and preserves the record of seawater Nd is by no means resolved; this chapter presents results of analyses of modern and ancient marine carbonates and phosphates aimed at determining their suitability for this purpose.

I.2. Sm-Nd and Rb-Sr isotopic systematics

I.2.1. Systematics and Notation

The naturally occurring radioactive isotopes ^{87}Rb and ^{147}Sm decay with halflives $\tau^{Rb}_{1/2}$ = 49 AE and $\tau^{Sm}_{1/2}$ = 106 AE to the respective daughter isotopes ^{87}Sr and ^{143}Nd. Closed systems with differing parent-to-daughter ratios will evolve over time and develop measurable differences in the daughter element isotopic abundances. For Nd, these differences are conveniently represented using epsilon notation [DePaolo and Wasserburg, 1976a,b, 1977] in which $\varepsilon_{Nd}(T)$ is the deviation in parts in 10^4 of the sample isotopic composition from that of a nominal chondritic reservoir (CHUR) at time T:

$$\varepsilon_{Nd}(T) = \left[\left\{\left(\frac{^{143}Nd}{^{144}Nd}\right)_{SAMPLE}(T)/I_{CHUR}(T)\right\} - 1\right] \times 10^4 \qquad (1.1)$$

where

$$I_{CHUR}(T) = I_{CHUR}(0) - (^{147}Sm/^{144}Nd)_{CHUR} \cdot [\exp(\lambda^{Sm} \cdot T) - 1]. \qquad (1.2)$$

Table 1.1 lists the values used for the various model system parameters.

One can also reference the Sm/Nd ratios to this reservoir by defining the enrichment factor

$$f^{Sm/Nd} \equiv \{(({}^{147}Sm/ {}^{144}Nd)_{SAMPLE} / ({}^{147}Sm/ {}^{144}Nd)_{CHUR})-1\} \qquad (1.3)$$

Positive values of $f^{Sm/Nd}$ thus indicate light rare earth element (LREE) depletion relative to chondrites; negative values indicate LREE enrichment. One can similarly define ε_{Sr} with respect to a reservoir corresponding to the undifferentiated mantle (UR) with nominal values as given in Table 1.1 and with

$$\varepsilon_{Sr}(T) = [(\frac{{}^{87}Sr}{{}^{86}Sr})_{SAMPLE}(T)/I_{UR}(T))-1]\times 10^4 \quad ; \qquad (1.4)$$

$$I_{UR}(T) = I_{UR}(0) - ({}^{87}Rb/{}^{86}Sr)_{UR} \cdot [\exp(\lambda^{Rb}T) - 1]; \qquad (1.5)$$

$$f^{Rb/Sr} \equiv \{(({}^{87}Rb/{}^{86}Sr)_{SAMPLE} / ({}^{87}Rb/{}^{86}Sr)_{UR})-1\} \qquad (1.6)$$

[DePaolo and Wasserburg, 1976b; O'Nions *et al.*, 1977; Jacobsen and Wasserburg, 1981]. There is good reason to believe that the earth has approximately chondritic rare earth ratios. Although the $^{143}Nd/^{144}Nd$ ratios of chondrites vary somewhat along a ~ 4.5 AE Sm-Nd isochron, the Nd model system parameters are reasonably well established. The Sr model system, on the other hand, is based on a correlation between Nd and Sr

Table 1.1. Model System Parameters.

$\lambda^{Sm} = 6.54 \times 10^{-12} yr^{-1}$
$(^{147}Sm/^{144}Nd)_{CHUR} = 0.1967$
$I_{CHUR}(0) = 0.511847$
$Q^{Nd} = 25.13\ AE^{-1}$
$\lambda^{Rb} = 1.42 \times 10^{-11} yr^{-1}$
$(^{87}Rb/^{86}Sr)_{UR} = 0.0827$
$I_{UR}(0) = 0.7045$
$Q^{Sr} = 16.67\ AE^{-1}$

Refs. DePaolo and Wasserburg, 1976b; O'Nions et al., 1977; Jacobsen and Wasserburg, 1981; Wasserburg et al., 1981.

isotopic compositions in mantle-derived rocks and on the inference that the bulk silicate earth has a chondritic Sm/Nd ratio. The Sr parameters are therefore less well established. Nevertheless, the current estimate of $(^{87}Sr/^{86}Sr)_{UR} = 0.7045$ appears to be a reasonably close estimate of the bulk earth value.

I.2.2. Observed Isotopic Variations and Mantle Reservoirs

Isotopic analyses of young rocks thought to have been derived directly from the mantle in oceanic regions have shown that the present-day mantle is isotopically heterogeneous. The largest volume of rock is represented by mid-ocean ridge basalts (MORB) which have low values of $\varepsilon_{Sr}(0)$ and high values of $\varepsilon_{Nd}(0)$, implying that these rocks are derived from a large ion lithophile (LIL) and LREE depleted part of the mantle which has existed for a significant fraction of the earth's history. Other oceanic volcanics such as found on oceanic islands show a wide range of isotopic composition. In particular, it appears that there are at least two isotopically distinct, ancient mantle reservoirs capable of yielding basaltic magmas and which give rise to the general inverse correlation between $\varepsilon_{Nd}(0)$ and $\varepsilon_{Sr}(0)$ known as the mantle array: 1) a reservoir depleted of the LREE and LIL elements on an average of ~ 1.8 AE ago and characterized by negative values of $\varepsilon_{Sr}(0)$ (~ -20 to -30) and positive values of $\varepsilon_{Nd}(0)$ (~ +8 to +13) that is the source for present-day basaltic oceanic crust, and 2) a reservoir variously referred to as primitive or undepleted mantle with $\varepsilon_{Nd} \sim \varepsilon_{Sr} \sim 0$ [DePaolo and Wasserburg, 1976a,b, 1979b; DePaolo, 1983] or enriched mantle with $\varepsilon_{Sr} > 0$, $\varepsilon_{Nd} < 0$ [White and Hofmann, 1982; McCulloch et al., 1983]. Mixtures of magma derived from these two sources together with other less

clearly identified mantle sources appear to be responsible for the isotopic variation seen today in mantle derived rocks. The concept of endmember reservoirs is somewhat of an idealization; in actuality it is likely that there is a continuum of sources in the mantle which span the spectrum from depleted to enriched which were produced by fractionation of a primitive mantle at a variety of times and which today give rise to the spectrum of isotopic compositions observed in modern mantle-derived rocks [cf. Jacobsen and Wasserburg, 1979].

Old, LREE and LIL-enriched continental crust forms a complement to the depleted mantle reservoir and has characteristically negative values of $\varepsilon_{Nd}(0)$ and large positive values of $\varepsilon_{Sr}(0)$. Mixing of depleted mantle with crustal rocks has also been proposed as a mechanism for producing the parts of the mantle array populated by some continental flood basalts which have been regarded by DePaolo [1978, 1983] and DePaolo and Wasserburg [1979b] as being derived from a primitive mantle reservoir. The former point of view has recently been emphasized by Carlson et al. [1981, 1983].

I.2.3. Model Ages

The $^{143}Nd/^{144}Nd$ and $^{87}Sr/^{86}Sr$ ratios measured today in a sample derived T years ago from a reservoir with initial isotopic ratios $I_{Nd}(T)$ and $I_{Sr}(T)$ are given by:

$$(^{143}Nd/^{144}Nd)_M = I_{Nd}(T) + \left(\frac{^{147}Sm}{^{144}Nd}\right)_M \cdot [\exp(\lambda^{Sm} \cdot T) - 1] \qquad (1.7)$$

$$(^{87}Sr/^{86}Sr)_M = I_{Sr}(T) + \left(\frac{^{87}Rb}{^{86}Sr}\right)_M \cdot [\exp(\lambda^{Rb} \cdot T) - 1] \qquad (1.8)$$

where M denotes the measured value.

The model age is the time at which a sample last had the isotopic composition of a model reservoir. For Nd this reservoir is taken as the undifferentiated mantle (CHUR), and for Sr, the reference mantle reservoir (UR) is used as the model system. The model ages T^{Nd}_{CHUR} and T^{Sr}_{UR} are found by setting $I_{Nd}(T) = I_{CHUR}(T)$ and $I_{Sr}(T) = I_{UR}(T)$ and solving for T, where $I_{CHUR}(T)$ and $I_{UR}(T)$ are given by equations (1.2) and (1.5). The resulting model ages are then given by [McCulloch and Wasserburg, 1978]:

$$T^{Nd}_{CHUR} = \frac{1}{\lambda^{Sm}} \cdot \ln \left[1 + \frac{I_{CHUR}(0) - (^{143}Nd/^{144}Nd)_M}{(^{147}Sm/^{144}Nd)_{CHUR} - (^{147}Sm/^{144}Nd)_M}\right] \tag{1.9}$$

$$T^{Sr}_{UR} = \frac{1}{\lambda^{Rb}} \cdot \ln \left[1 + \frac{I_{UR}(0) - (^{87}Sr/^{86}Sr)_M}{(^{87}Rb/^{86}Sr)_{UR} - (^{87}Rb/^{86}Sr)_M}\right] \tag{1.10}$$

For $\lambda T << 1$, these equations have a particularly simple form when expressed in ε-notation:

$$T^{Nd}_{CHUR} = \frac{\varepsilon_{Nd}(0)}{Q^{Nd} \cdot f^{Sm/Nd}} \tag{1.11}$$

$$T^{Sr}_{UR} = \frac{\varepsilon_{Sr}(0)}{Q^{Sr} \cdot f^{Rb/Sr}} \tag{1.12}$$

The parameters Q^{Nd} and Q^{Sr} are constants which account for the evolution of the model system, and their values are given in Table 1.1.

If the assumptions built into the model age calculation are fulfilled (that the sample was derived from a reservoir with the isotopic characteristics of the model reservoirs and that the isotopic systems

have remained undisturbed since that time), then the model ages T_{UR}^{Sr} and T_{CHUR}^{Nd} should be concordant and will give the age of formation of the sample (i.e., the time at which the sample separated from the model reservoirs with major chemical fractionation of parent and daughter species).

CHAPTER II

Sm-Nd and Rb-Sr SYSTEMATICS of IMPACT PRODUCTS

II.1 Introduction

That major impact events have occurred on the surface of the earth is inarguable. One need only look at the cratered surface of the moon to infer that the earth must have been subject to a similar bombardment history. Indeed, over 100 terrestrial craterform structures, dating back to 2 AE, have been identified, all either associated with known meteorites or having shock metamorphic effects suggesting a hypervelocity impact origin [Grieve, 1982]. All of these structures are located on the continents, largely owing to the difficulty of detecting such structures given the low resolution of most bathymetric maps, but also due to the geologically young age of the ocean floor.

One way of studying the processes which occur during a large impact is to examine the material excavated from the impact site. This chapter presents a study of the Sm-Nd and Rb-Sr systematics of materials thought to represent the ejecta of large terrestrial impacts. It will be shown that the isotopic data can be used to infer some of the characteristics of both the impact site and the processes leading to the formation of the impact ejecta.

II.2 Tektites

II.2.1 Theories of origin

Tektites are naturally formed, siliceous, glassy objects, often with aerodynamic shapes suggesting that they were sculpted by high velocity passage through the earth's atmosphere. The first man known to have shown interest in tektites was a Cro-Magnon man living about 30,000

years ago in what is now Austria [O'Keefe, 1976]. Primitive man collected and traded tektite glass for use as talismans as well as for a tool-making material which could be chipped to a very sharp edge. The first scientific reference to tektites is due to Darwin [1844], who thought them a form of volcanic glass. Since that time, the origin of tektites has been the source of controversy. Much of the early debate centered on the whether tektites are naturally formed or were man-made objects. This debate was fueled by the unfortunate fact that the tektite field of central Europe lies in an area noted for considerable early experimentation in glassmaking. It was finally shown in the early part of this century that the chemical compo-s ition of tektites is unlike that of any early man-made glasses and that the melting point of tektite glass exceeds the temperatures attainable by early glassmaking furnaces [Suess, 1900; Johnsen, 1906]. It was thus established that tektites must be formed naturally. This presents a considerable problem, for in the thousands of years of man's awareness of tektites, an outcrop of tektite glass has never been found. To account for this, a variety of creative theories have been advanced to explain their origin. An incomplete list includes: formation by lightning strikes on soil or lightning strikes in a volcanic ash cloud; formation by fusion of meteorites during passage through the earth's atmosphere; fusion of meteors by passage too close to the sun; impact melting of terrestrial rocks; impact melting of lunar rocks; terrestrial volcanism; lunar volcanism; and collision of the earth with anti-matter. A full discussion of these and other theories is given in O'Keefe [1976]. Most of these suggestions have been examined and discarded, and today, most workers agree that the bulk of the physical and chemical data on tektites strongly supports

Figure 2.1. World map showing the locations of known tektite fields and suggested source craters. Locations of deep sea cores containing microtektites associated with the North American, Ivory Coast, and Australasian tektites are indicated by the symbols. (After Glass, 1979)

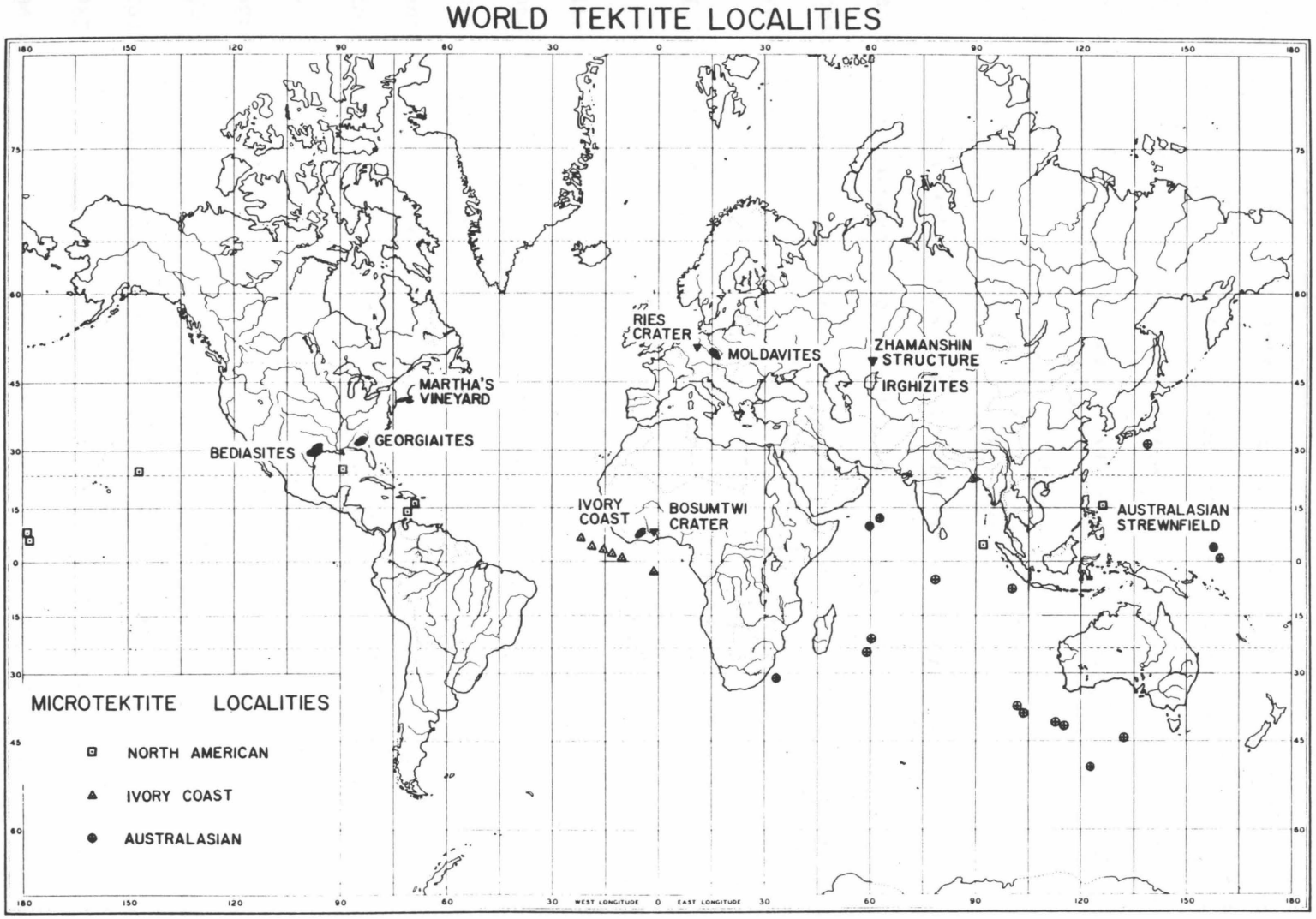
WORLD TEKTITE LOCALITIES
RIES CRATER
MOLDAVITES
ZHAMANSHIN STRUCTURE
IRGHIZITES
MARTHA'S VINEYARD
GEORGIAITES
BEDIASITES
IVORY COAST
BOSUMTWI CRATER
AUSTRALASIAN STREWNFIELD
MICROTEKTITE LOCALITIES
NORTH AMERICAN
IVORY COAST
AUSTRALASIAN
WEST LONGITUDE
EAST LONGITUDE

their formation by impact melting of terrestrial rocks or sediments by the fall of a large meteorite or comet nucleus [Taylor, 1973, 1975]. Prior to the return of the lunar samples, it was thought possible by many people that tektites might represent either lunar impact melts or the product of lunar volcanism. The results of analyses on returned lunar samples, however, do not support a lunar origin for tektites. Nevertheless, the lunar volcanic source retains some adherents [O'Keefe, 1976, 1981].

This chapter presents the results of a series of Nd and Sr isotopic measurements made on tektites in order to gain new insight into their origin. A model is then developed to explain the observed isotopic systematics.

II.2.2 Samples

Tektites are known to occur in four areas on earth (Fig. 2.1). Within each area, tektites have the same K-Ar or fission track age, presumably dating the time at which the tektites were last molten. These four groups consist of (1) the North American tektites (Georgiaites, Bediasites, and the Martha's Vineyard tektite), with ages of ~ 35 my [Zähringer, 1962; Störzer and Wagner, 1971]; (2) the central European moldavites which formed ~ 14 my ago [Gentner et al., 1963; Störzer and Wagner,1971]; (3) the Ivory Coast tektites of 1.3 my age [Zähringer, 1962; Fleischer et al., 1965]; and (4) the Australasian tektites (Australites, Indochinites, Philippinites, etc.) of ~ 0.7 my age [Zähringer, 1962; Fleischer and Price, 1964; Gentner et al., 1969]. In addition, the North American, Ivory Coast, and Australasian occurrences are associated with microtektites found in deep sea sediments of the same age as the land tektites [Glass, 1967, 1968; Glass et al., 1973]. It has been

estimated [Glass et al., 1979] that the total mass of tektite glass associated with the North American strewnfield, the largest of the four, is on the order of 10^{10} metric tons. As shown in Fig. 2.1, this material is globally distributed. For two of the tektite fields, impact structures have been identified which are spatially associated with the tektites and which have the appropriate age to be the site of a tektite-producing impact. The Ries Crater of Germany is associated with the moldavites and the Bosumtwi Crater of the Ivory Coast is associated with the Ivory Coast strewnfield. Impact sites for the North American and Australasian strewnfields have not been identified. Recently, glasses associated with the Zamanshin impact structure have been described from the region north of the Aral Sea, USSR [Florinskij, 1975, 1977; Taylor and McLennan, 1979; Bouska et al., 1981]. The tektite-like objects have been called irghizites and associated impact glasses, zhamanshinite. Determinations of the age of these objects range from 0.81 to 1.1 my [Sörzer and Wagner, 1977; Florenskij et al., 1979].

Samples from each of the four tektite fields and several irghizites have been analysed. In addition, a possible sedimentary parent material for the moldavites from the area around the Ries Crater was analysed. Work by Graup et al. [1981] has shown that this material, the Tertiary Upper Freshwater Molasse (OSM sands) has the appropriate chemical and Sr isotopic composition to be a precursor the the moldavites. Details of the samples and procedures used are given in Appendix I.

Table 2.1 Parameters for Nd,Sr isotopic evolution of tektites.

	$\varepsilon_{Nd}(0)$*	$f^{Sm/Nd}$†	T^{Nd}_{CHUR}(AE)	$\varepsilon_{Sr}(0)$+	$f^{Rb/Sr}$#	T^{Sr}_{UR}(AE)
Australasian Tektites						
Thailand A	-11.5±0.5	-0.4078	1.12±0.05	204.4±0.7	33.15	0.371±0.004
Thailand B	-11.8±0.5	-0.4075	1.15±0.05	203.0±0.6	29.90	0.407±0.004
Cambodia A	-11.8±0.4	-0.4047	1.15±0.05	199.8±0.4	32.82	0.365±0.004
Cambodia B	-11.2±0.7	-0.3942	1.14±0.2	212.5±0.4	34.62	0.368±0.004
Cambodia C	-12.2±0.4	-0.4129	1.17±0.07	207.6±0.4	35.72	0.348±0.003
HiCa Australite	-11.5±0.5 -11.4±0.4	-0.4050	1.13±0.2	134.6±0.6	15.05	0.536±0.005
HiMg Australite USNM 2536	-10.9±0.5	-0.4095	1.06±0.05	166.8±0.7	20.17	0.496±0.005
Microtektites° BG-1	—	—	—	174.6±9.9	17.48	0.59±0.05
BG-2	—	—	—	201.6±9.9	6.59	1.83±0.09
Moldavites						
USNM 2051	-9.8±0.5	-0.4461	0.88±0.04	242.4±0.6	25.68	0.566±0.006
USNM 2233	—	—	—	247.8±0.4	33.96	0.438±0.004
USNM 2226	—	—	—	261.4±0.5	35.56	0.441±0.005
USNM 2052	-9.8±0.5	-0.4077	0.96±0.04	268.6±0.7	41.09	0.392±0.006
OSM Sands						
OSM 050	-10.4±0.5	-0.4437	0.93±0.2	276.3±0.5	53.51	0.310±0.004
OSM D2	-9.9±0.5	-0.4851	0.81±0.2	247.9±0.8	25.53	0.583±0.007
Ivory Coast Tektites						
USNM 6011A	-20.2±0.6	-0.4207	1.91±0.05	267.4±0.4	6.58	2.44±0.62
USNM 6011B	—	—	—	270.7±0.6	6.85	2.37±0.67
USNM 6011C	-19.5±0.4	-0.4221	1.84±0.05	301.1±0.4	8.52	2.12±0.57

Table 2.1 (continued)

	$\varepsilon_{Nd}(0)$*	$f^{Sm/Nd}$†	T^{Nd}_{CHUR}(AE)	$\varepsilon_{Sr}(0)$+	$f^{Rb/Sr}$#	T^{Sr}_{UR}(AE)
North American Tektites						
Bediasites						
USNM 1880 B-229	-6.5±0.6	-0.3870	0.67±0.06	129.3±0.7	13.66	0.568±0.006
USNM 1880 B-306	-6.7±0.5	-0.3983	0.67±0.04	122.1±0.6	14.10	0.519±0.006
USNM 1880 B-312	-6.1±0.5	-0.3929	0.62±0.05	117.8±1.0	—	—
Georgiaites						
USNM 2339	-6.6±0.4	-0.3999	0.66±0.04	124.1±1.0	—	—
USNM 6178	—	—	—	114.3±0.4	13.32	0.515±0.005
Martha's Vineyard						
USNM 2082	-6.7±0.5	-0.4013	0.67±0.04	123.3±0.4	13.79	0.536±0.006
Irghizites						
USNM 5939 GpIV #12 low Si	+1.8±0.6	-0.2887	-0.25±0.09	7.25±1.6	0.32	1.34±0.30
USNM 5938 GpIII 3-1 high Si	-8.5±0.6	-0.4063	0.84±0.05	139.4±0.8	13.70	0.61±0.006
USNM 5938 GpIII 3-6 high Si	-9.3±0.5	-0.4069	0.91±0.05	138.7±0.7	13.70	0.61±0.006

*Referenced to $(^{143}Nd/^{144}Nd)_{CHUR} = 0.511847$.

†Referenced to $(^{147}Sm/^{144}Nd)_{CHUR} = 0.1967$.

+Referenced to $(^{87}Sr/^{86}Sr)_{UR} = 0.7045$.

#Referenced to $(^{87}Rb/^{86}Sr)_{UR} = 0.0827$.

°Data from Papanastassiou and Wasserburg, [1982]

Figure 2.2a. Histogram of $\varepsilon_{Nd}(0)$ comparing the Nd isotopic composition of tektites to other terrestrial materials. Tektites have the Nd isotopic composition of old continental crust. Each tektite group is characterized by a uniform value of $\varepsilon_{Nd}(0)$.

b. Histogram of $\varepsilon_{Sr}(0)$ showing range of Sr isotopic composition observed within a given tektite group. Tektites have the Sr isotopic composition of old continental crust. Sr data for old continental crust are not plotted but generally lie in the region $\varepsilon_{Sr}(0) > +50$. Patterns within histogram correspond to those used in Fig. 2.2a.

(Data on old continental crust, oceanic island arcs (ARCS), mid-ocean ridge basalts (MORB), and continental flood basalts (CFB) from DePaulo and Wasserburg, 1976a,b, 1977; Richard et al., 1976; O'Nions et al., 1977; McCulloch and Wasserburg, 1978

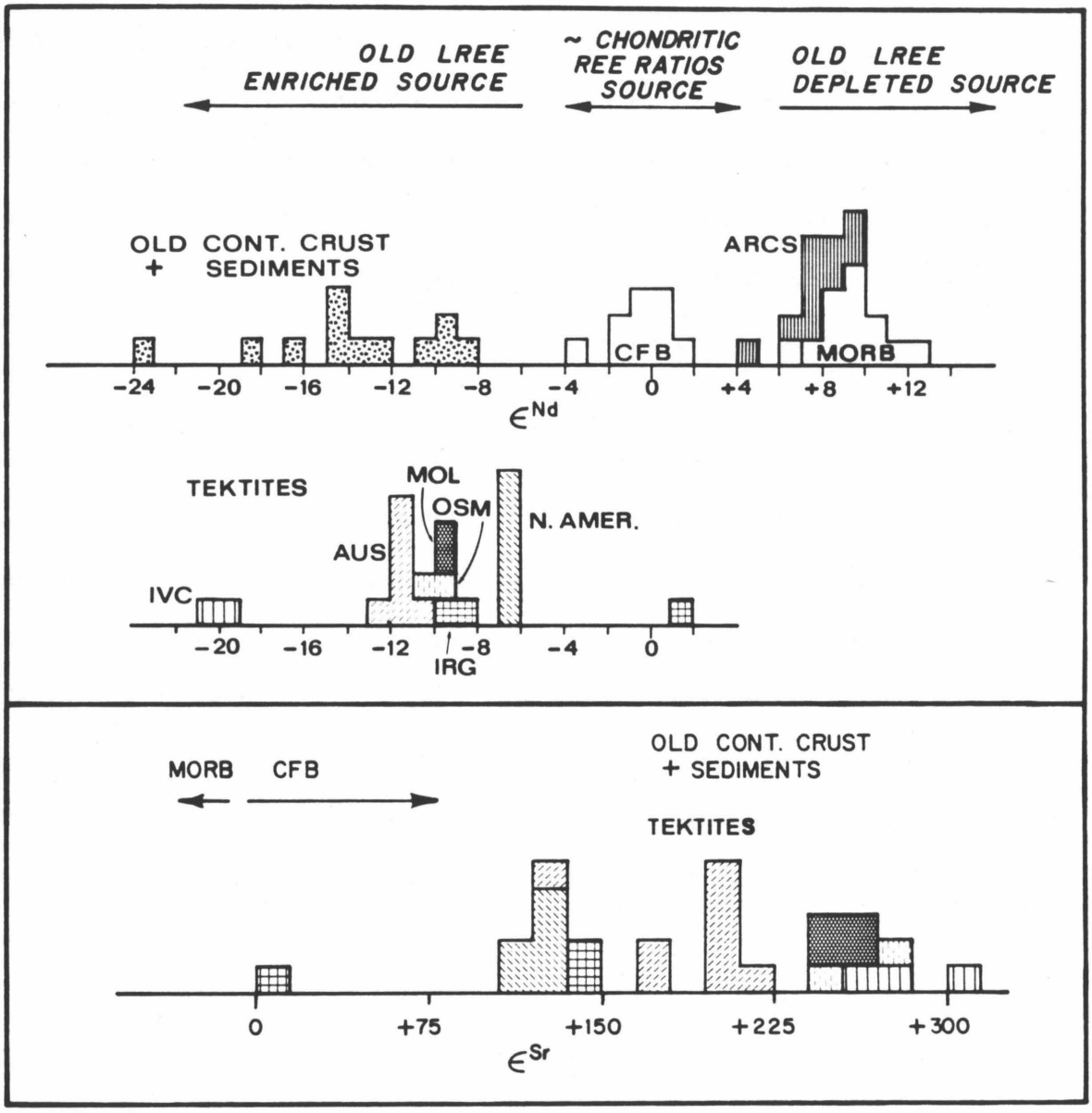
OLD LREE ENRICHED SOURCE
~ CHONDRITIC REE RATIOS SOURCE
OLD LREE DEPLETED SOURCE
OLD CONT. CRUST + SEDIMENTS
ARCS
CFB
MORB
-24
-20
-16
-12
-8
-4
0
+4
+8
+12
ϵ^{Nd}
TEKTITES
MOL
OSM
N. AMER.
AUS
IVC
-20
-16
-12
-8
-4
0
IRG
MORB
CFB
OLD CONT. CRUST + SEDIMENTS
TEKTITES
0
+75
+150
+225
+300
ϵ^{Sr}

II.2.3 Nd and Sr isotopic compositions

Unlike the chemical composition of an impact product, which may be strongly modified or fractionated by the impact process, the isotopic composition of an impactite will be identical to that of the target material. Any isotopic fractionation caused by the impact will be corrected for along with instrumental fractionation during routine processing of the raw isotopic data. The isotopic composition of the impact product can thus be used to fingerprint the target from which it formed.

The results of Nd and Sr analyses of tektites and related materials are presented in Table 2.1. As shown in Fig. 2.2, the large negative $\varepsilon_{Nd}(0)$ and positive $\varepsilon_{Sr}(0)$ characteristic of tektites are clear signatures of old continental crust [McCulloch and Wasserburg, 1978]. These data exclude the possible derivation of tektites from material recently derived from the mantle which has $\varepsilon_{Nd}(0)$ and $\varepsilon_{Sr}(0)$ near zero [DePaolo and Wasserburg, 1976a,b]. The data also rule out a basaltic oceanic crustal source which would have $\varepsilon_{Nd}(0)$ of +8 to +12 and $\varepsilon_{Sr}(0)$ of 0 to -30 [DePaolo and Wasserburg, 1976a,b; Richard et al., 1976; O'Nions et al., 1977]. High Si irghizites also have the characteristic isotopic composition of old continental crust.

A plot of $\varepsilon_{Nd}(0)$ vs. $\varepsilon_{Sr}(0)$ (Fig. 2.3) shows that the overlap in Sr isotopic composition between the various tektite groups is spread out in the second dimension provided by the Nd isotopic data. Each tektite group is characterized by a distinctive range of isotopic variations in $\varepsilon_{Sr}(0)$ at constant $\varepsilon_{Nd}(0)$. This is most clearly displayed by the Australasian tektites. The uniformity of the Nd isotopic composition and continuous range of Sr isotopic composition of the Australasian tektites

Figure 2.3. Plot of $\varepsilon_{Nd}(0)$ vs. $\varepsilon_{Sr}(0)$ for tektites. Each group has a distinctive range in isotopic composition. Variation in isotopic composition is mainly due to variation in $\varepsilon_{Sr}(0)$ at constant $\varepsilon_{Nd}(0)$. All the tektites lie in the region of this diagram populated by old, LREE, and LIL enriched upper continental crust.

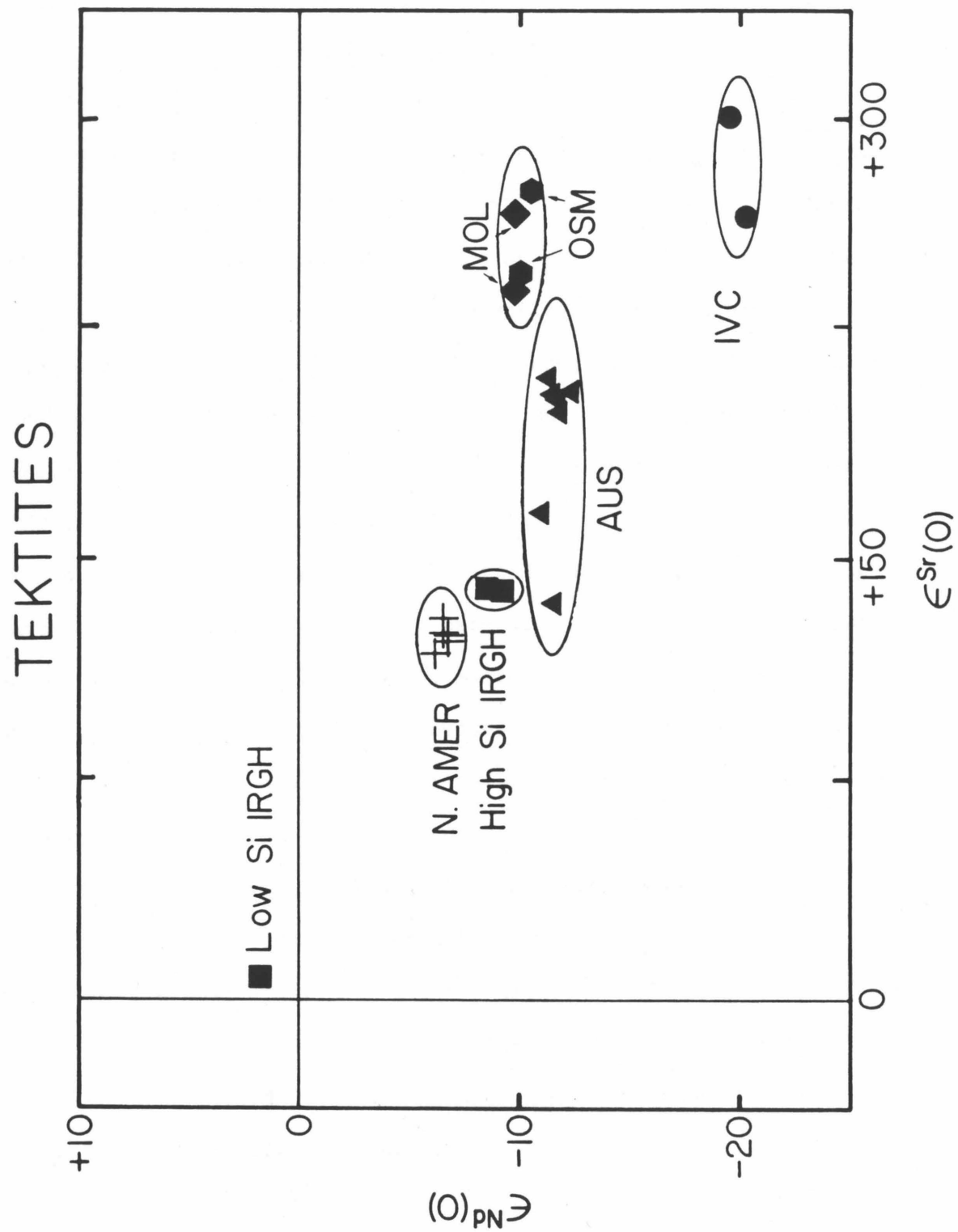
TEKTITES
Low Si IRGH
N. AMER
High Si IRGH
AUS
MOL
OSM
IVC
+10
0
-10
-20
+300
+150
0
$\epsilon_{Nd}(0)_{PN}$
$\epsilon^{Sr}(0)$

are hard to reconcile with the suggestion that the Indochinites and Australites are due to different impact events [Störzer and Wagner, 1980]. Instead, the Nd and Sr data support the interpretation that the entire strewnfield is due to a single event.

The OSM sand samples from the Ries Crater have $\varepsilon_{Nd}(0) \sim -10$ and $\varepsilon_{Sr}(0) = +250$ to $+280$ and closely match the range in isotopic composition of the moldavites. As suggested by Graup et al. [1981], this type of material is the likely parent for the moldavites. This result eliminates the long-standing problem of identifying a parent material for the moldavites in the Ries, a problem which has stood in the way of establishing a genetic relationship between the two. It is important to note that the OSM sands were a surficial deposit at the time of the impact. The thickness of the deposit at the time of impact is unknown but is thought to have been less than a few tens of meters, while the effects of cratering extend to a depth of 2 km [Bolten and Müller, 1969; David, 1969]. Laboratory experiments on impact processes have demonstrated that directional, high velocity jets of surficial target material are often produced upon impact [Kieffer, 1977]. The production of such jets could explain the highly localized distribution of the moldavites [Bouska, 1964].

The isotopic composition of Nd in the irghizites is different from that of the Australasian tektites. Although this does not completely rule out the Zhamanshin structure as a possible source for the Australasian strewnfield as suggested by Glass [1978], it does demonstrate that the high Si irghizites have a different parent material that the Australasian tektites despite their similarity in chemical composition [Taylor and McLennan, 1979; Bouska et al., 1981], thus reducing the likelihood of

there being a connection between these two groups. The higher Ni content of the irghizites as compared with the Australasian tektites [Taylor and McLennan, 1979] raises the possibility that the difference in isotopic composition between these groups may be due to a greater component of meteoritic component in the irghizites. Addition of projectile material with chondritic elemental abundances and isotopic composition ($\varepsilon_{Nd}(0)=0$, $\varepsilon_{Sr}(0) > +500$; Wetherill, 1975) to the parent material of the Australasian tektites would displace $\varepsilon_{Nd}(0)$ towards zero but would greatly increase $\varepsilon_{Sr}(0)$, contrary to what is observed (Fig. 2.3). One concludes that this mechanism cannot produce the irghizites and Australasian tektites from a common parent. The difference in isotopic composition between the high Si and low Si irghizites establishes that these two types have distinct parent materials and did not acquire their differences in chemistry through selective volatilization, partial melting, or other geologically recent processes acting on a common, homogeneous parent material. As described above, meteoritic contamination cannot explain the difference between the high and low Si irghizites.

The Martha's Vineyard tektite, USNM 2082, is the only tektite ever found at that locality and questions have been raised as to the authenticity of the find. The Nd and Sr isotopic composition of the Martha's Vineyard sample (Fig. 2.3, Table 2.1), is indistinguishable from the other North American tektites and it clearly had the same parent material as the Bediasites and Georgiaites, confirming its relationship to these groups. The possibility of human transport of the Martha's Vineyard tektite to the site of the find is unresolved, however.

II.2.4 Model ages and multistage isotopic evolution

In addition to being useful tracers, isotopic systems can be used to provide information on the timing of events in the history of an object. Table 2.1 lists values of T^{Nd}_{CHUR} and T^{Sr}_{UR} calculated for tektites. Examination of Table 2.1 shows that although the T^{Nd}_{CHUR} ages within each group are constant, the T^{Sr}_{UR} ages are quite variable and are generally less than T^{Nd}_{CHUR} for the same sample, indicating that the model assumptions given in section I.2.3 are not fulfilled.

A plot of T^{Sr}_{UR} vs $^{87}Rb/^{86}Sr$ using all the available isotopic analyses of Australasian tektites [Schnetzler and Pinson, 1964; Compston and Chapman, 1969; Papanastassiou and Wasserburg, 1981] defines a hyperbolic array with T^{Sr}_{UR} ranging from ~ 0.3 to 1.3 AE (1.8 AE if the microtektite point is included) with the model ages decreasing with increasing Rb/Sr ratio. This pattern is a result of the fact that on a Sr evolution diagram, these samples lie about a correlation line (Fig. 2.4b). A true isochronal relationship would correspond to a hyperbolic curve. These two ways of looking at the isotopic systematics are equivalent; however, a useful form of the alternate representation is developed below. In the discussion which follows, the Sr isotopic system is used as the example; an analogous development can be carried out for the Nd system.

It is desired to obtain an expression which will allow determination of the last time at which major chemical fractionation of the parent-daughter isotopes occurred for the following history. At some time a suite of samples with differing Rb/Sr ratios is derived from a homogeneous reservoir. Each of these samples then evolves isotopically until some

later time (or times) when major Rb/Sr fractionation again occurs. It is the last fractionation event of this type which is to be dated and the ability to date this event depends on large Rb/Sr fractionation occurring at that time. The basis for what follows is that for samples with very high Rb/Sr ratios, ages may be obtained even though the initial isotopic ratio is poorly known. In the limit of infinite Rb/Sr ratio, the initial isotopic ratio plays no part in determining the sample age so long as the initial ratio remains finite. The problem is to determine a method for extrapolating the Rb/Sr ratio of a suite of samples to infinity, making the age determination less ambiguous for a suite of samples which are correlated on an evolution diagram but which do not lie on an isochron.

For $\lambda T \ll 1$, the isotopic composition of Sr today in a sample which separated from a reservoir (not necessarily the model reservoir) at time T_1 and had an Rb/Sr ratio of R_1, and has been undisturbed since that time, is given by:

$$I^{Sr}(0) \cong I^{Sr}(T_1) + R_1 \cdot \lambda^{Rb} \cdot T_1 \qquad (2.1)$$

or in epsilon notation:

$$\varepsilon_{Sr}(0) \cong \varepsilon_{Sr}(T_1) + Q^{Sr} \cdot f_1^{Rb/Sr} \cdot T_1 \qquad (2.2)$$

Now if that sample had undergone a disturbance at time T_2 possibly changing the isotopic composition by amount ΔI^{Sr} and possibly changing the Rb/Sr ratio to a new value R_2, the isotopic composition would today be given by [Papanastassiou and Wasserburg, 1969]:

$$I^{Sr}(0) \cong I^{Sr}(T_1) + \Delta I^{Sr} + R_1 \cdot \lambda^{Rb} \cdot (T_1 - T_2) + R_2 \cdot \lambda^{Rb} \cdot T_2 \qquad (2.3)$$

In general, for n-1 disturbances at times $T_2 \cdots T_n$:

$$I^{Sr}(0) \cong I^{Sr}(T_1) + \sum_{j=1}^{n-1} [(T_j - T_{j+1}) \cdot R_j \cdot \lambda^{Rb} + \Delta I_{j+1}] + R_n \lambda^{Rb} T_n \qquad (2.4)$$

Dividing by $R_n \lambda^{Rb}$ and converting to epsilon notation one obtains:

$$\frac{\varepsilon_{Sr}(0)}{Q^{Sr} f_n^{Rb/Sr}} \cong \frac{1}{f_n^{Rb/Sr}} \cdot \left\{ \frac{\varepsilon_{Sr}(T_1)}{Q^{Sr}} + \sum_{j=1}^{n+1} \left(f_j^{Rb/Sr}(T_j - T_{j+1}) + \frac{\Delta\varepsilon_{Sr}^{j+1}}{Q^{Sr}} \right) \right\} + T_n \qquad (2.5)$$

where $\varepsilon_{Sr}(T_1)$ is the initial isotopic composition, $\Delta\varepsilon^j$ is the change in isotopic composition at time T_j, and $\frac{\varepsilon_{Sr}(0)}{Q^{Sr} f_n^{Rb/Sr}} \equiv T_{UR}^{Sr}$. Thus, in a plot of the quantity T_{UR}^{Sr} versus $1/f_n$ a suite of samples which have undergone multistage isotope evolution will lie in the wedge shaped region defined by the lines having slopes given by the bracketed terms above, and with common y-intercept T_n. This intercept value gives the time at which the suite last underwent parent-daughter fractionation. Note that this formalism provides a connection between the calculated model age T_{UR}^{Sr} and the actual times of disturbance $T_1 \cdots T_n$. The y-intercept value, however, gives a model-independent estimate of the age of last disturbance and corresponds to the age determined by the slope of an isochron. This analysis will now be applied to the model age patterns observed in tektites.

II.2.5 Tektite model ages

II.2.5.1 The model

The isotopic results presented here as well as studies of REE

patterns [Taylor, 1966, 1973; Frey, 1977, and others] major, minor, and trace element compositions [Taylor, 1966; Chapman and Scheiber, 1969; Taylor and McLennan, 1979], and oxygen isotopic work [Taylor and Epstein, 1962, 1966, 1969] are all consistent with the formation of tektites from terrestrial upper crustal rocks by impact melting. The data most closely match the characteristics of sedimentary rocks, sediments and soils, or meta-sediments. A three-stage model is postulated to explain the Sr and Nd systematics of tektites. In the first stage assume the derivation of a crustal segment with enrichment factors $f_1^{Rb/Sr}$ and $f_1^{Sm/Nd}$ from a uniform mantle reservoir at time T_1. At some later time T_2 this segment may undergo weathering and sedimentation producing a sedimentary rock with enrichment factors $f_2^{Rb/Sr}$ and $f_2^{Sm/Nd}$, which is then impact melted to form tektites at T_3 ($\cong$ 0) at which time selective volatilization may produce enrichment factors $f_3^{Rb/Sr}$, $f_3^{Sm/Nd}$. The Sm-Nd and Rb-Sr isotopic systems will behave quite differently in response to these processes. The major fractionation of Sm from Nd appears to occur during partial melting of mantle sources to produce crustal rocks. There are some data which indicate that the Sm-Nd system is relatively undisturbed by weathering and sedimentation [McCulloch and Wasserburg, 1978]. Further, the REE are both refractory and geochemically coherent; Sm and Nd will not be readily fractionated by differential volatilization upon impact melting. For Nd, then, $f_1^{Sm/Nd} \cong f_2^{Sm/Nd} \cong f_3^{Sm/Nd}$ and the equation reduces to that of single stage growth: $T_{CHUR}^{Nd} = T_1 = \varepsilon^{Nd}(0)/(Q^{Nd} \cdot f_1^{Sm/Nd})$. The T_{CHUR}^{Nd} model ages thus correspond to the concentration weighted mean model ages of the sources of the parent material of tektites (i.e., the original time of formation of the crustal segments from the mantle). In contrast, it is well established that sedimentary processes severely dis-

turb the Rb-Sr system, generally by increasing the Rb/Sr ratio in the sediment through preferential uptake of Rb relative to Sr in clays [Dasch, 1969; McCulloch and Wasserburg, 1978], or by decreasing the Rb/Sr ratio through addition of Sr-rich phases. The Rb/Sr system may also be disturbed by selective Rb volatilization upon melting. Depending on which process dominates, the Sr model age T_{UR}^{Sr} may be greater (Rb loss or Sr gain) or less (Rb gain) than T_{CHUR}^{Nd} for a given sample. It should be noted that the term "sedimentation" is used in a loosely defined sense; real sediments may have been reworked many times. What is dated is the last major parent-daughter fractionation event during which high Rb/Sr ratios were produced. This may occur during weathering, transport, or diagenesis of a sediment.

II.2.5.2 Australasian Tektites

Figure 2.4a is a plot of T_{UR}^{Sr} vs $1/f^{Rb/Sr}$ for Australasian tektites using the present data and data from the literature [Schnetzler and Pinson, 1964; Compston and Chapman, 1969; Papanastassiou and Wasserburg, 1981]. The T_{UR}^{Sr} ages for the samples in Table 2.1 range from ~ 0.36 to ~ 0.50 AE. The literature data extend this range down to 0.33 AE and up to 1.3 AE. The data define a wedge-shaped, linear array with a clustering in T_{UR}^{Sr} as $1/f^{Rb/Sr}$ tends toward zero. The array has a y-intercept of ~ 0.25 AE which is interpreted as the age of sedimentation for the parent material for these tektites. This age agrees well with the age of 0.1 to 0.3 AE calculated by Compston and Chapman [1969] from the correlation line on the Sr evolution diagram (Fig. 2.4b). The data point for one of the Indian Ocean microtektites falls within this array indicating that this microtektite shares a common precursor with the

Figure 2.4a. Plot of T_{UR}^{Sr} vs $1/f^{Rb/Sr}$ for Australasian tektites. The y-intercept value of ~ 0.25 AE gives the time of last Rb-Sr fractionation and corresponds to the time of sedimentation of a sedimentary parent material. Squares = macrotektites, crosses = microtektites.

b. Rb-Sr evolution diagram for Australasian tektites showing correlation line. Symbols as in Fig. 2.4a.

(Data sources: Schnetzler and Pinson, 1964; Compston and Chapman, 1969; Papanastassiou and Wasserburg, 1981; this work.)

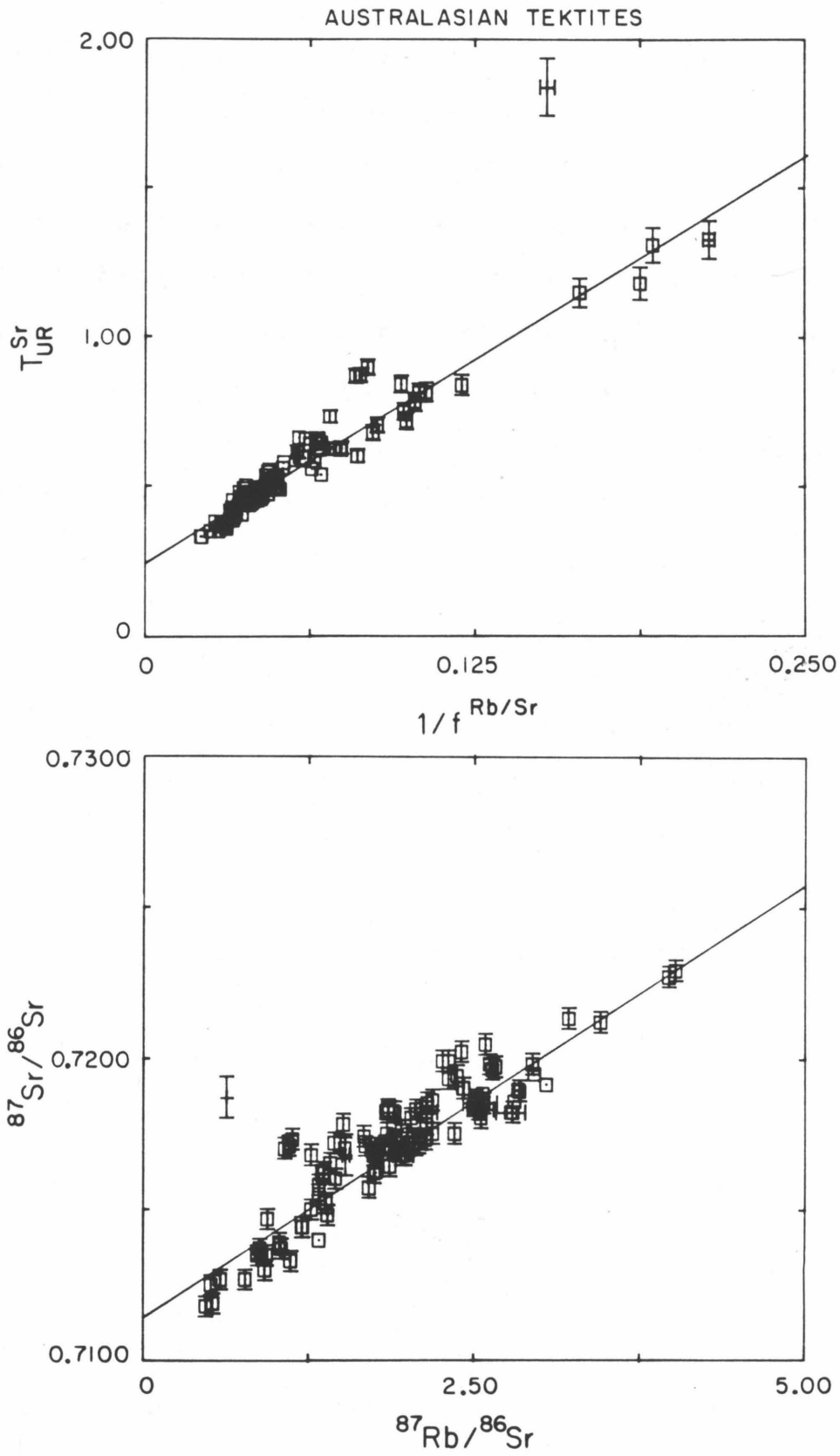
AUSTRALASIAN TEKTITES
2.00
1.00
0
T^{Sr}_{UR}
0
0.125
0.250
$1/f^{Rb/Sr}$
0.7300
0.7200
0.7100
$^{87}Sr/^{86}Sr$
0
2.50
5.00
$^{87}Rb/^{86}Sr$

macrotektites. The second microtektite is discrepant, having a higher model age than expected for its Rb/Sr ratio. Oddly, its isotopic characteristics are much more similar to those of the Ivory Coast tektites than the Australasian tektites. The general trend displayed in Fig. 2.4a strongly suggests a two-stage model with major Rb-Sr fractionation at 0.25 AE corresponding to the age of formation of the sediments which were the parent material. There is no evidence for significant Rb volatilization during tektite formation as selective volatilization would have produced an intercept of ~ 0 AE in Fig. 2.4a, corresponding to the time of melting. An exception may be the discrepant microtektite as Rb loss will increase the model age of a sample.

In contrast to the T_{UR}^{Sr} ages, the T_{CHUR}^{Nd} ages are quite uniform with total range in ages of 1.06 to 1.17 AE (Table 2.1). The uniformity of the Nd model ages suggests that the source terrains for the parent sediment were of approximately the same age, or that transport and sedimentation were effective at mixing material from sources of different ages. The value of ~ 1.15 AE for the T_{CHUR}^{Nd} ages implies that the parent sediments were dominantly derived from a Precambrian crustal segment.

The majority of these tektites have $T_{UR}^{Sr} < T_{CHUR}^{Nd}$ which is compatible with a model of increased Rb/Sr ratios in sediments by Rb uptake in clays. Four analyses from the literature, all high Ca Philippinites [Compston and Chapman, 1969; Chapman and Scheiber, 1969] have Sr model ages which exceed the Nd model age. These samples also have unusually high CaO and Sr contents. For the samples with $T_{UR}^{Sr} > T_{CHUR}^{Nd}$ the Rb/Sr ratio must have decreased during sedimentation by addition

of Sr, increasing the calculated model age. The strong correlation of Sr with CaO in the Australasian tektites [Compston and Chapman, 1969] suggests that the carrier of the Sr in the parental sediment was also a Ca-rich phase. Calcite is a common Ca- and Sr-rich and Rb-poor phase in terrestrial sediments and the observed correlations can be explained by variations in the calcite content of the parent material as discussed by Compston and Chapman [1969]. The initial Sr ratio for the high T_{UR}^{Sr} samples calculated for an age of 0.25 AE is ~ 0.710, thus the addition of a small amount of Permian marine carbonate with a relatively evolved $^{87}Sr/^{86}Sr$ ratio of ~ 0.708 [Peterman et al., 1970; Burke et al. 1982] as compared with $(^{87}Sr/^{86}Sr)_{UR}$ = 0.7045 to a detrital sediment with higher $^{87}Sr/^{86}Sr$ is not unreasonable on isotopic grounds and could account for the high model ages.

These data demonstrate that the source crater for the Australasian strewnfield lies in a target of late Paleozoic to early Mezozoic, continental sediment derived from a relatively young Precambrian cratonic source. If the source of the sediments actually contains a substantial amount of Archean crust, then the source area must also include a terrain of much younger rocks so that on average the age of the terrain is 1.15 AE. The data do not exclude the possibility that the impact structure is located underwater on a continental shelf or deep ocean basin mantled by continentally derived sediments of the above characteristics. Suggested source craters for the Australasian tektites include the Zhamanshin Crater [Glass, 1978] which was discussed and rejected above; the Elgygytgyn Crater of NE Siberia [Dietz, 1977]; and an unnamed NE Cambodian crater-like structure [Hartung and Rivolo, 1979]. The Elgygytgyn Crater is in a

terrain of plutonic and volcanic rocks of Mesozoic age [Nekrasov and Riudonis, 1973, cited in Dietz, 1977]. Unless these rocks have a large component of remelted Precambrian basement with negative $\varepsilon_{Nd}(0)$ then it would not be possible to produce tektites with the negative $\varepsilon_{Nd}(0)$ and Precambrian T^{Nd}_{CHUR} age observed for the Australasian objects. Elgygytgyn Crater is therefore an unlikely source for the Australasian tektites. Little is known about the geology in the area of the Cambodian structure. In the absence of more detailed information on the age and lithology of this site, little can be said of its merits.

II.2.5.3 North American Tektites

The North American tektites are characterized by a uniform T^{Nd}_{CHUR} age with a total range of from 0.62 to 0.67 AE (Table 2.1). This means that the material which melted to form the North American tektites came from a crustal segment which formed in very late Precambrian time. This relatively young age eliminates most of the Precambrian shield areas of North America as possible source terrains for the parent material of these tektites as well as sediments derived from these areas. The North American shale (NAS) composite [Haskin et al., 1966; McCulloch and Wasserburg, 1978] has $\varepsilon_{Nd}(0) = -14.4$ and $T^{Nd}_{CHUR} = 1.5$ AE, and is and is thought to be representative of the average mid-continental region. From a comparison with the tektite results it is clear that the Paleozoic sediments making up the NAS composite are derived from older Precambrian crustal material and cannot be typical of the parent material for the North American tektites. Late Precambrian crust of ~ 0.6 to 0.8 AE age in North America is largely restricted to the eastern and southeastern

Figure 2.5. Plot of T_{UR}^{Sr} vs $1/f^{Rb/Sr}$ for North American tektites and moldavites. The intercept for the moldavite array is well defined at ~ 0.015 AE and suggests that moldavites were formed from a geologically young parent sediment. North American tektites do not yield any new information.

(Data sources Schnetzler and Pinson, 1964; this work.)

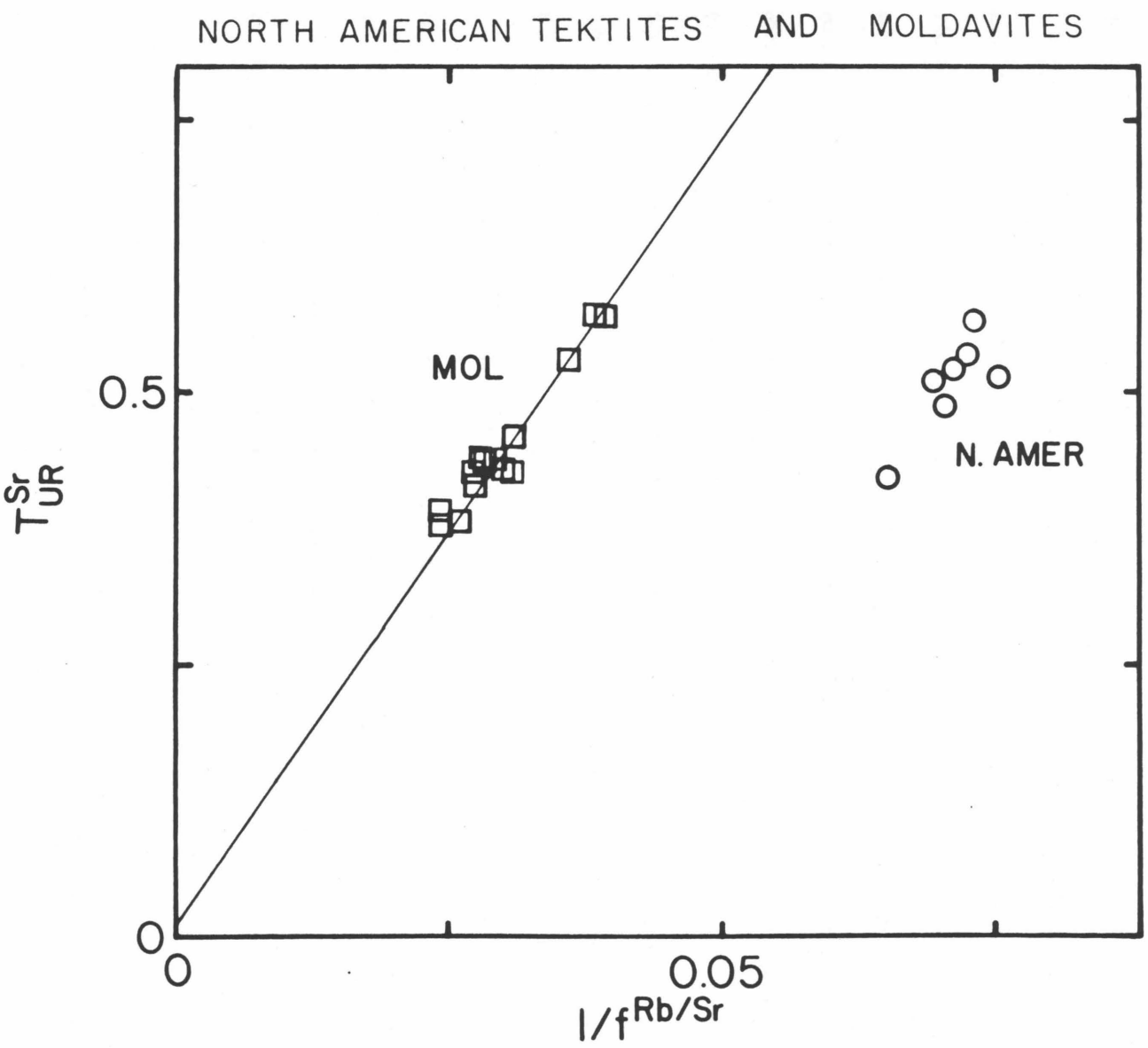
NORTH AMERICAN TEKTITES AND MOLDAVITES
MOL
N. AMER
0.5
0
0
0.05
T^{Sr}_{UR}
$1/f^{Rb/Sr}$

margin of the Appalachian orogenic belt and may underlie much of the Atlantic and Gulf coastal plains and continental shelves. The parent sediment for the North American tektites may have been derived from this terrain, however, no impact structure of the appropriate size and age has been identified there. The T^{Nd}_{CHUR} age may reflect a mixture of material from older and younger source terrains so that an average model age of $\sim$ 0.65 AE is obtained. Even in this case, the older shield areas of North America are still excluded as possible sources for a parent material because of the lack of young crustal material within these areas to mix with detritus from the ancient crust. Likewise, the Popigai astrobleme of Siberia could not be the source for the North American tektites as suggested by Dietz [1977]. This impact occurred on the Archean Anabar shield which gives K-Ar ages in the range of 2.7 to 1.9 AE [Rabkin, 1968] and is too old to satisfy the T^{Nd}_{CHUR} ages of the American tektites.

The T^{Sr}_{UR} model ages for the North American tektites in Table 2.1 range from 0.52 to 0.56 AE (down to 0.42 AE if literature data is included); in all cases slightly younger than the corresponding T^{Nd}_{CHUR} ages. Unfortunately, there is little spread in the Rb/Sr ratios for these samples and, more importantly, the samples do not have the extreme Rb enrichments that were observed in some of the Australasian tektites (Fig. 2.5). Because of these characteristics, little significant time information can be extracted from the Sr isotopic systematics. The Sr model ages are consistent with derivation of the tektites from a sediment, but do not demand a sedimentary parent. If the parent was a sediment, as suggested by other studies, there was relatively little parent-daughter fractionation at the time of sedimentation as reflected in the small differences between the T^{Nd}_{CHUR}

and T_{UR}^{Sr} ages and the $f^{Rb/Sr}$ values which are typical of old upper crustal igneous rocks.

In summary, the Nd isotopic data suggest that the source terrain of the parent material for the North American tektites was of ~ 0.65 AE age and cannot be any of the major ancient shield areas of North America or consequently from the areas covered by Paleozoic sediments derived from these Precambrian terranes. The Sr isotopic data suggest slight parent-daughter fractionation at some time after crustal formation in very late Precambrian time.

II.2.5.4 Ivory Coast Tektites

The T_{CHUR}^{Nd} model ages for the Ivory Coast tektites are ~ 1.9 AE (Table 2.1), which are in good agreement with whole rock Rb/Sr ages of the rocks around the Bosumtwi Crater and much of western Africa which range from 1.9 to 2.1 AE [Vachette, 1964; Schnetzler et al., 1966; Kolbe et al., 1967]. The Sr model ages for these samples range from 2.1 to 2.4 AE. In a plot of T_{UR}^{Sr} vs $1/f^{Rb/Sr}$, these data and literature analyses of the Ivory Coast tektites [Lippolt and Wasserburg, 1966; Schnetzler et al., 1966; Kolbe et al., 1967] appear to define a linear array (Fig. 2.6). Although these samples are not characterized by high Rb/Sr ratios, they are reasonably well correlated and yield a y-intercept of ~ 0.95 AE. These analyses have a range in T_{UR}^{Sr} from 1.9 to 2.8 AE, in all cases greater than the T_{CHUR}^{Nd} ages. In an evolution diagram the samples plot about a correlation line corresponding to 0.95 AE age. Selective volatilization of Rb during the melting of the tektite parent material, leading to increased values of the Rb/Sr ratio and T_{UR}^{Sr} could be the cause of the younger disturbance. In this case, however, one would expect an intercept value of ~ 0.0 AE

Figure 2.6. Plot of T_{UR}^{Sr} vs $1/f^{Rb/Sr}$ for Ivory Coast tektites. The intercept is reasonably well defined despite the lack of high Rb/Sr samples. The time of last parent-daughter fractionation is given by y-intercept value of ~ 0.95 AE.

(Data sources: Lippolt and Wasserburg, 1966; Schnetzler et al., 1966; this work.)

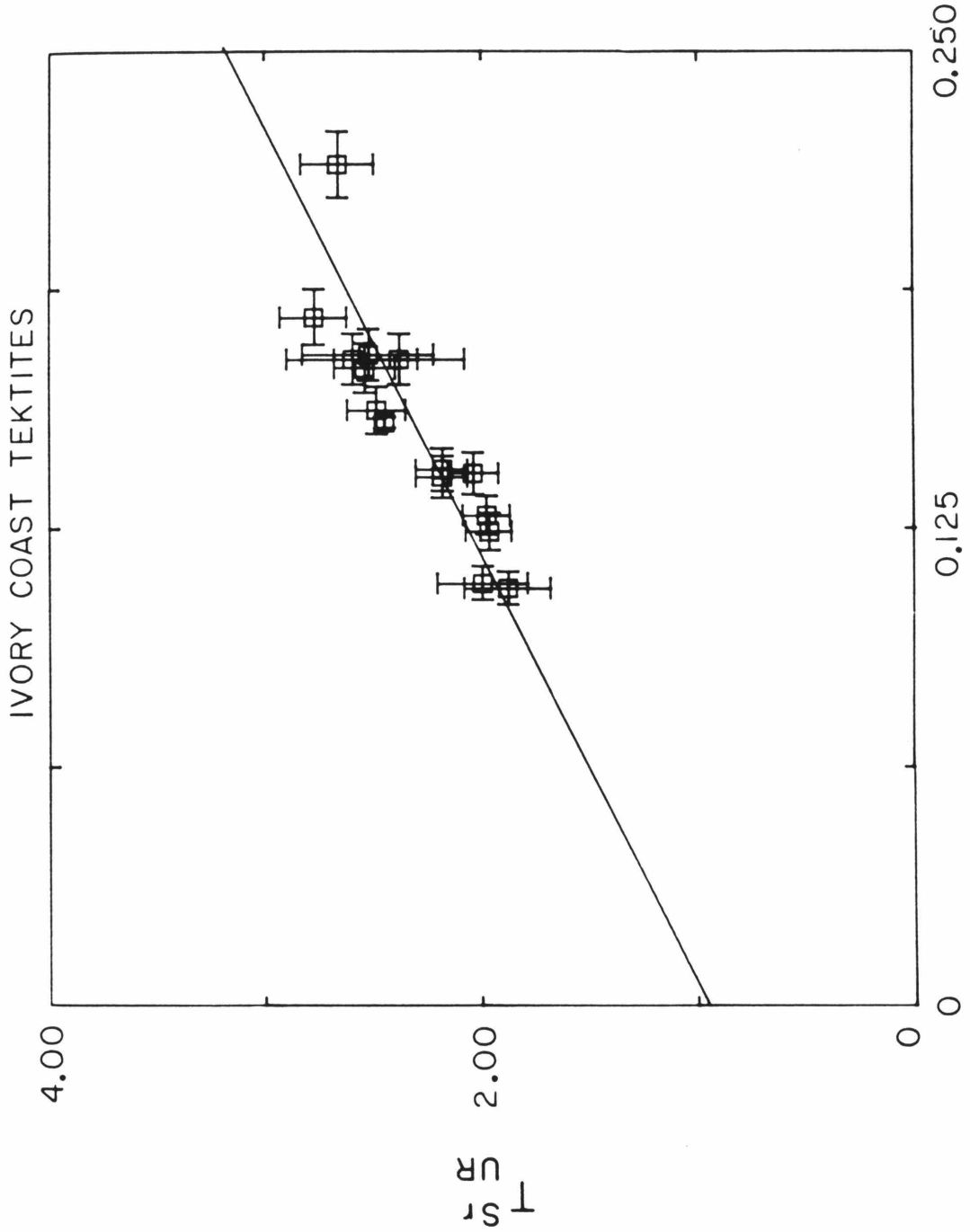
IVORY COAST TEKTITES
4.00
2.00
0
0
0.125
0.250
1 / f Rb/Sr
T Sr UR

in Fig. 2.6. Thus selective volatilization is not likely to have been an important process for these tektites. Alternatively, the parent material for the Ivory Coast tektites may be a sediment or a metamorphic rock in which the Rb/Sr ratio decreased relative to the crustal source material during sedimentation or metamorphism at ~ 0.95 AE. Taken together, the Nd and Sr data are consistent with formation by melting of material originally derived from the rather ancient basement around the Bosumtwi Crater. The actual target material has not been identified.

II.2.5.5 Moldavites

The T^{Nd}_{CHUR} ages for the moldavite samples are ~ 0.9 AE (Table 2.1), which agrees well with the age of the oldest known basement in the area of the Ries Crater. This basement was remobilized and partially melted at ~ 0.3 AE to form the terrain into which the Ries Crater was emplaced. The Sm-Nd isotopic systematics appear to be seeing through both this orogenic event and the tektite forming event back to the original time of formation of the crustal segment which was ultimately melted to form the tektites at 14 my. The lower Sr model ages of 0.39 to 0.57 AE (Table 2.1) indicate that the Rb-Sr system has been disturbed subsequent to the time of crustal formation. A plot of T^{Sr}_{UR} vs $1/f^{Rb/Sr}$ (Fig. 2.5) using literature analyses of moldavites [Schnetzler and Pinson, 1964; Schnetzler et al., 1969] yields a linear array with y-intercept of ~ 0.02 AE and with a variation in T^{Sr}_{UR} of from 0.37 AE to 0.58 AE. Similarly, in an evolution diagram the data plot along a sub-horizontal array of this age. Again the samples have a limited range of Rb/Sr ratios, but the intercept in the model age vs $1/f^{Rb/Sr}$ plot is reasonably well defined due to the high

Rb/Sr ratios. The young Sr age implies parent-daughter fractionation in the Sr isotopic system shortly before the tektite forming event leading to high Rb/Sr ratios in the parent. These results imply an origin for the moldavites by melting of a young sediment derived locally from the rocks around the Ries Crater. This interpretation of the Rb-Sr systematics is fully compatible with derivation of the moldavites from the Tertiary OSM sands.

II.2.5.6 Irghizites

The two high Si irghizite samples, USNM 5938 3-1 and USNM 5938 3-6, have T^{Nd}_{CHUR} model ages of ~ 0.88 AE and T^{Sr}_{UR} model ages of ~ 0.61 AE, (Table 2.1) the Nd data giving the original age of formation of the parent material and the Sr data suggesting that this material was disturbed at some later time. Florenskij et al. [1979] state that the Zhamanshin structure is in an area of Cretaceous and Tertiary sediments and Quaternary loess deposits underlain by Paleozoic metamorphic rocks. The data are consistent with derivation of the high Si irghizites from any of these materials if the crustal source(s) originally formed, on average, at ~ 0.9 AE ago. The low Si irghizite has a future T^{Nd}_{CHUR} model age of -0.25 AE due to its positive $\varepsilon_{Nd}(0)$ but negative $f^{Sm/Nd}$ values. In this case the model fails. Future Nd model ages are not uncommon among modern alkalic basalts of oceanic islands or continental rift settings. These basalts are also characterized by positive $\varepsilon_{Nd}(0)$ and are LREE enriched [O'Nions et al., 1977; Hawkesworth and Vollmer, 1979; Menzies and Murthy, 1980]. It is clear that these basalts are not derived from a mantle reservoir with the isotopic characteristics of CHUR, but instead

have had a time integrated LREE depletion. The observed REE patterns in the erupted basalts were imposed only shortly before eruption yielding the future model ages. The low Si irghizite may have been derived from similar basaltic material. Identification of the actual parent materials will depend on further field and laboratory studies of the area around the Zhamanshin structure.

II.2.6 Conclusions

Tektites are characterized by negative $\varepsilon_{Nd}(0)$ and positive $\varepsilon_{Sr}(0)$, which are clear signatures of old terrestrial continental crust. Each tektite group has a distinctive $\varepsilon_{Nd}(0)$ value and a range of $\varepsilon_{Sr}(0)$. Chemically and isotopically tektites are similar to terrestrial sediments derived from old continental crustal material. These results do not exclude the production of tektites by impact into an ocean basin or continental shelf if the impact site was mantled by sediments of continental derivation. The fact that the moldavites were probably formed by melting of the surficial OSM sands suggests more broadly that the tektite forming process does not always sample very deeply at the impact site. As a result, it may be possible to have an impact in an oceanic area which could produce tektites from only surficial sediments and not involve deeper mafic oceanic crust.

The recent discovery of live ^{10}Be, a short lived radionuclide ($T_{1/2}$ ~1.5 my) produced by spallation reactions in the upper atmosphere, in Australasian and Ivory Coast tektites [Pal *et al.*, 1982; Tera *et al.*, 1983] also implies that tektites are formed from surficial deposits. Calculations of impact dynamics indicate that it is the uppermost layers of the target which are involved in the early high speed ejecta [O'Keefe and

and Ahrens, 1982]. This ejecta consists of vaporized target, impact melt droplets (tektites), and finely divided target and projectile material. It is launched from the impact site at high velocity, along with the surrounding atmosphere, during the initial interaction of the impactor with the target. These calculations account for the fact that tektites are derived from surficial material and also dispose of the problem of propelling the tektites through the atmosphere to form a large strewnfield by using the the atmosphere itself to propel the molten target droplets.

Studies of sediments suggest that their Nd model ages reflect the age of their source terrain with major Sm-Nd fractionation occurring during partial melting of the mantle to form new crust. Surficial processes such as weathering do not appear to be effective in fractionating the rare earths. Thus the uniform Nd model age of each tektite field is interpreted as the age of formation of the crustal segment which weathered to form the parent sediment for the tektites. In contrast, it is well known that surficial processes severely disturb the Rb-Sr isotopic system generally by increasing the Rb/Sr ratio during weathering and sedimentation. This results in relatively young T_{UR}^{Sr} ages which reflect more recent events in the history of the tektite parent materials.

Inferences from the isotopic systematics as to the ages of the source terrains and sedimentary precursors for the various tektite groups are summarized in Table 2.2. In all cases the T_{CHUR}^{Nd} ages imply a Precambrian age for the crustal source terrains: ~ 0.6 AE for North American tektites, ~ 0.9 AE for both the irghizites and moldavites, ~ 1.15 AE for Australasian tektites, and ~ 1.9 AE for the Ivory Coast tektites. The T_{UR}^{Sr} ages suggest very young Rb-Sr fractionation in the moldavite

Table 2.2 Summary of age and provenance of tektite parent materials.

	Source Terrain age (AE)	Sedimentation age (AE)	Target
Australasian tektites	1.15	0.25	middle-late Paleozoic sediments derived from pЄ craton
North American tektites	0.65	<0.65	material derived from latest pЄ crust
Moldavites	0.90	0.01	very young sediments derived from late pЄ crust (Ries Crater)
Ivory Coast tektites	1.90	0.95	PЄ materials derived from old pЄ craton (Bosumtwi Crater)
High Si irghizites	0.88	?	sediments (?) derived from late pЄ crust (Zhamanshin Crater)
Low Si irghizites	?	--	basaltic material (Zhamanshin Crater)

parent material, and imply that the moldavites were derived from a very young sediment. The Tertiary OSM sands from around the Ries Crater have the appropriate age and isotopic composition to be the likely parent material for the moldavites. The Australasian tektites are characterized by major parent-daughter fractionation in their Sr isotopic system at ~ 0.25 AE, which is interpreted as the time of formation of a sediment which was melted to form these objects. The Nd isotopic composition of the high Si irghizites rules out any possibility of a common parent with the Australasian tektites. Parent-daughter fractionation in the Sr system of the Ivory Coast tektites last occurred at ~ 0.95 AE probably during an ancient sedimentation or metamorphic event producing the parent material which melted to form these objects. The data are consistent with derivation of the Ivory Coast tektites from Precambrian sediments in the Bosumtwi Crater. This is in consonance with conclusions about the origins of these objects by previous workers [Schnetzler and Pinson, 1964; Lippolt and Wasserburg, 1966; Schnetzler et al., 1966; Kolbe et al., 1967].

In summary, these data are consistent with tektite formation by melting of terrestrial sediments during a meteorite or comet impact onto a continent or continental shelf or ocean basin mantled by sediments of the appropriate age and provenance as described above. The thickness of the sedimentary cover may in some cases be rather modest (less than a few hundred meters).

Although it may be possible to create an ad hoc model involving a lunar origin for tektites, there is little in the way of positive evidence for such an origin in the considerable data which have been

gathered on these objects. In particular, it would be difficult to reconcile the data presented here with a lunar origin, especially in view of the agreement of the ages and isotopic characteristics of the Ries and Bosumtwi Craters with the moldavites and Ivory Coast tektites. Together with the discovery of live ^{10}Be unaccompanied by live ^{26}Al in tektites [Raisbeck et al., 1983] these results should be the final blow to the lunar theories. Instead, future research on tektites might profitably explore the processes that occur to form the molten and vaporized impact ejecta in more detail. Microtektites may hold some clues as to these processes. Microtektites are known to have a much wider range of chemical composition than the macrotektites of a given strewnfield [Glass, 1970; Glass and Zwart, 1979]. This greater variability may be due to either heterogeneities in the target or to fractionation processes occurring during impact. The results of Nd isotopic analyses may help in deciding between these options.

II.3 Sanidine Spherules from the Cretaceous-Tertiary Boundary

II.3.1 An impact at the Cretaceous-Tertiary boundary?

Recently, attention has been drawn to the terrestrial record of impacts by the discovery of anomalously high concentrations of iridium and other noble metals in the sediments marking the end of the Cretaceous period [Alvarez et al., 1980]. Iridium and the other siderophile noble metals are strongly depleted in terrestrial crustal rocks relative to their solar system abundances, occurring at levels of <<0.1ppb in most crustal rocks [Hertogen et al., 1980; Crocket, 1981]. Iridium concentrations in most chondritic and iron meteorites are much higher, on the order of 500ppm [Baedecker, 1971]. The Ir anomaly at the Cretaceous/Tertiary (K/T) boundary has consequently been interpreted as being due to the

infall of a large extraterrestrial body at that time. Following the initial discovery of the Ir anomaly in K/T boundary sediments in Italy, Denmark, and New Zealand [Alvarez et al., 1980], other workers have found the anomaly to be a worldwide phenomenon, occurring in both marine and non-marine sequences [Smit and Hertogen, 1980; Kyte et al., 1980; Ganapathy et al., 1981; Nazarov et al., 1982; Orth et al., 1982]. Figure 2.7 summarizes the localities at which Ir anomalies have been reported. On the basis of the observed noble metal concentrations amd the concentrations in meteoritic material, Alvarez et al. [1980] calculated minimum masses for the impacting body of between 2 and 6 x 10^{15} kg, corresponding to diameters of 5-16 km. Such objects impacting at velocities of ~20 km/s have a kinetic energy of ~10^{30} ergs or ~10^{8} megatons of TNT. This may be compared with the global nuclear arsenal of ~10^{4} megatons [Levi, 1983]. Although the detection of evidence for such a large impact is interesting in itself, an extraordinary amount of interest has been generated in the possibility of an impact at the K/T boundary due to the fact that the boundary marks a previously recognized major extinction event in the fossil record. Given the coincidence in timing and the undoubtedly severe ecological consequences of an impact of such magnitude, it was immediately proposed that the impact and its subsequent effects caused the extinction event [Alvarez et al., 1980]. This proposal has set off a heated debate both as to the nature of the extinction event (whether gradual, which would argue against a catastrophic cause, or abrupt) [Clemens, 1982; Thierstein, 1982; Schopf, 1982], and as to the interpretation of the Ir anomaly as being indicative of an impact [Rampino, 1982]. Little is known about the geochemistry of the noble metals during weathering,

Figure 2.7. Reported occurrences of anomalous Ir abundances. Values give an estimate of the integrated amount of Ir above the local background value in units of 10^{-9}g/cm^2. After Alvarez *et al.*, 1982a.

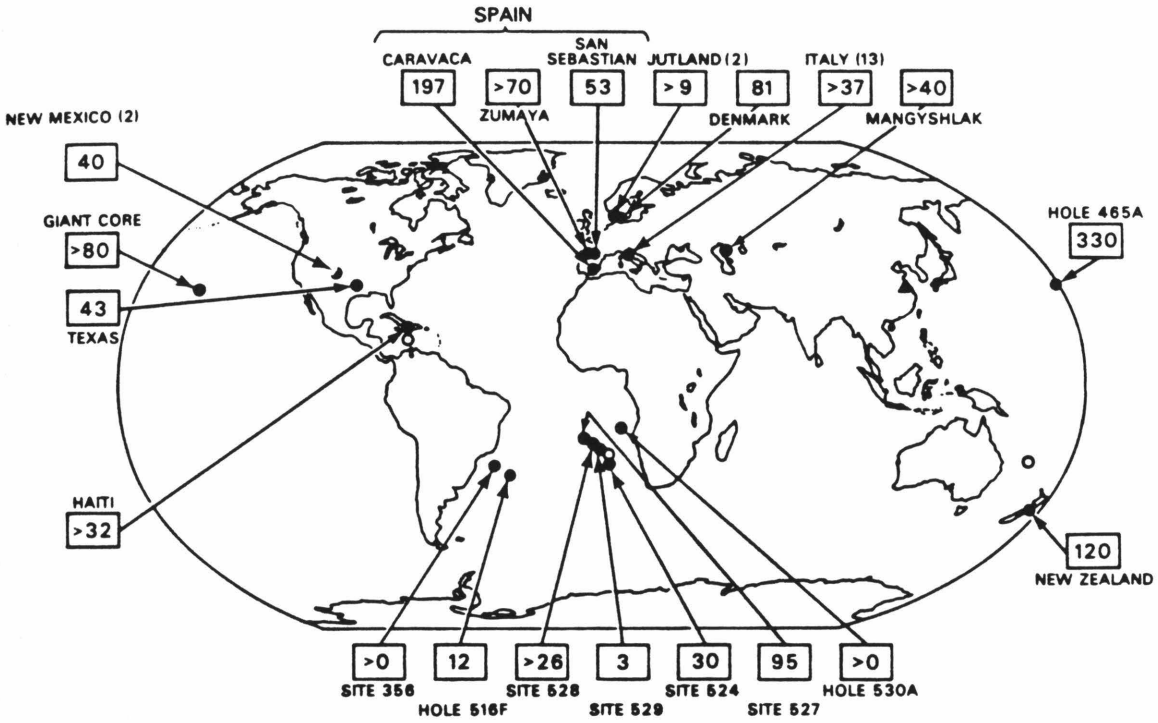

REPORTED K/T IRIDIUM ANOMALIES

transport, and diagenesis and it remains possible that the K/T Ir anomalies may be due to some wholly terrestrial cause such as a shift to reducing conditions in the oceans or an increase in global volcanism, both of which would also affect the biota. Additional sampling and analysis should reveal whether similar Ir anomalies are a common feature of the sedimentary record, in which case it is likely that they have an origin in ordinary sedimentary processes. Nevertheless, it is clear that impacts can and do product geochemical signatures similar to that at the K/T boundary. Kyte et al. [1981] have reported high Au and Ir abundances together with meteoritic debris in Pliocene sediments off the coast of Antarctica. They interpret these results as being due to the nearby fall of a small meteorite. Other studies have reported an Ir anomaly associated with sediments containing North American microtektites [Alvarez et al., 1982b; Ganapathy, 1982; Glass et al., 1982]. There remains some question as to whether the microtektites are found in the same layer as the Ir anomaly, however. It is interesting to note that the North American tektite event appears to coincide, or nearly coincide, with a significant though minor extinction event at the Eocene/Oligocene boundary.

A major stumbling block to the impact hypothesis is the lack of any identified crater of the appropriate size (~100 km diameter, Schmidt and Holsapple, 1982) and age to be the impact site. This has led to the suggestion that the impact occurred in an ocean basin, in which case the crater may never be found as ~25% of the ocean floor existing at the end of the Cretaceous has already been destroyed by subduction. Given that there is a strong contrast in Nd and Sr isotopic composition

between continental and oceanic crust, it was decided to examine material from the K/T boundary to see if there is isotopic evidence for either continental or oceanic impact as well as to see if there exists any isotopic signature of extraterrestrial material.

II.3.2 Samples and proceedures

In a study of the fossil assemblages across the K/T boundary, Smit and Klaver [1981] found large numbers (50-300 cm^{-3} of sediment) of small (50-1000μm) spherules in the Ir-rich layer in the Barranco del Gredero section, Caravaca, Spain. X-ray diffraction, electron probe and neutron activation analyses of the spherules showed that the they are dominantly sanidine with K/Na ~ 100, are rich in As, Se, Sb, Zn, and contain dark inclusions rich in Fe, Ni, and Co [Smit and Klaver, 1981]. Unlike the glassy tektites, the spherules are very finely crystalline and contain up to 20% void space which may have been occupied by another phase at one time. Since their initial discovery in the K/T boundary clay at Caravaca, similar spherules have been found in the boundary sediments in Tunisia, Texas, Montana, and the Pacific Ocean [Smit, pers. comm., 1982]. Smit and Klaver [1981] have argued that the sanidine spherules have the texture of quickly cooled liquid droplets. Epstein [1982] reported a very heavy oxygen isotopic composition of the spherules ($\delta^{18}O_{SMOW}$ = +27.5)and offered it as evidence of high temperature isotopic exchange with atmospheric oxygen ($\delta^{18}O^{ATM.}_{SMOW}$ ~ +24, Epstein and Mayeda, 1953). It is more likely, however, that low temperature exchange with sea water or pore fluids during devitrification or authigenic growth is reason for the heavy oxygen of the sanidine. It is the author's opinion that the spherules are the result of devitrification of microtektites

formed by the impact. It is clear from their chemistry, being nearly pure $KAlSi_3O_8$, that the devitrification process was not isochemical, as it is unlikely that a precursor glass of pure sanidine composition can be produced by impact onto any reasonable target material. The spherules remain enigmatic and need not represent an impact product. They may well be formed by authigenic growth from volcanic glass or other material. The apparently unique occurrence of the spherules in K/T boundary sediments, however, tends to argue for a rather special origin for these objects. As with the Ir anomaly itself, additional work may show that the occurrence is not unique and would invalidate this argument.

In order to remove secondary calcite as well as in an attempt to strip away the effects of diagenesis, several leaching experiments were performed on the spherules. Approximately 100 mg of sanidine spherules were hand-picked from carbonate nanofossils, lithic fragments, and organic matter in a concentrate of spherules from Caravaca. The spherules were then crushed, leached in cold 0.5M HCl, and rinsed with H_2O. This residue (residue 1) was spiked and analyzed. A sequential leaching experiment was carried out on a second, 262 mg separate of spherules. This separate was subjected to 4 acid leaches of increasing strength: cold 0.1M, 0.5M, 1.5M, and hot 1.5M HCl. Aliquots of all 4 leaches and the residue (residue 2) were spiked and analyzed. A 7.5 mg aliquot of residue 2 was subjected to a final leach in hot 3M HCl and the resulting residue (residue 3) analyzed. The Sr isotopic composition and concentration have also been measured in a hand-picked separate of carbonate fossils from the boundary clay. The results of these measurements are given in Table 2.3.

Table 2.3 Sanidine spherule data.

	ppm Sr	^{87}Rb nmoles	^{88}Sr nmoles	$^{87}Rb/^{86}Sr$	$\varepsilon_{Sr}(0)$*	ppm Nd	^{147}Sm pmoles	^{144}Nd pmoles	$^{147}Sm/^{144}Nd$	$\varepsilon_{Nd}(0)^{\dagger}$
Residue 1	60.1	--	--	3.10	+66.0 ±1.4	0.55	--	--	--	--
0.1 M leach	--	0.515 (1.08%)	886.3 (73.64%)	0.005	+44.8 ±0.7	--	--	43.9 (7.76%)	--	-6.93 ±.50
0.5 M leach	--	0.254 (0.53%)	148.5 (12.34%)	0.014)))	+43.7 ±0.7	--	--	253.0 (44.74%)	--	--
1.5 M leach	--	0.262 (0.55%)	68.4 (5.68%)	0.033)		--	--	149.0 (26.35%)	--	-5.56 ±.49
hot 1.5 M leach	--	1.400 (2.93%)	43.8 (3.64%)	0.267	+45.3 ±0.6	--	--	55.6 (9.83%)	--	-4.14 ±.46
Residue 2	24.9	45.3 (94.97%)	56.6 (4.70%)	6.70	+98.4 ±0.7	0.16	12.3	64.0 (11.32%)	.192	+1.93 ±.50
Residue 3	18.0	--	--	8.86	+106.4 ±2.5	0.11	--	--	--	--
Carbonate fossils	997.6	--	--	0.012	+45.3 ±0.6	--	--	--	--	--

*Referenced to $(^{87}Sr/^{86}Sr)_{UR} = 0.7045$.

†Referenced to $(^{143}Nd/^{144}Nd)_{CHUR} = 0.511847$.

Numbers in parentheses refer to the percentage of the element released in a sequential leaching experiment.

II.3.3 Results and discussion

In Fig. 2.6 the isotopic composition of Sr for the sequential leaches and residue 2 is plotted against the cumulative percent Sr released in the sequential leaching experiment. The bulk (~ 75%) of the Sr was removed in the first leach and ~ 96% removed in the combined leaches. The isotopic composition of the Sr in the leaches is $\varepsilon_{Sr}(0) \sim +45$ which is indistinguishable from that in the carbonate fossils (Table 2.3) and within the range of Cretaceous seawater Sr [Peterman et. al, 1970; Burke et al., 1982]. The residue has a significantly different isotopic composition of $\varepsilon_{Sr}(0) = +98.4$. The data for the carbonate fossils, residue 1 and residue 2, lie on a straight line mixing line in a plot of $\varepsilon_{Sr}(0)$ vs. 1/Sr (Fig. 2.9), showing that the bulk spherules have a Sr isotopic composition which is a mixture of Cretaceous seawater Sr represented by the fossils and a sanidine Sr endmember at higher $\varepsilon_{Sr}(0)$. Residue 3, the most strongly leached residue with $\varepsilon_{Sr}(0) = +106.4$ and ~ 18 ppm Sr does not lie on this mixing line, having lower $\varepsilon_{Sr}(0)$ than predicted from the mixing line. This represents the onset of Sr leaching from the sanidine itself. It is thus inferred that $\varepsilon_{Sr}(0)$ of the sanidine endmember is +106 as measured in residue 3. Residue 2 closely approached this value in the sequential leaching experiment. This value is higher than that reported by DePaolo et al. [1982] for an acid leached residue of spherules with 111 ppm Sr. It is clear that both their sample and that which was reported on by Shaw and Wasserburg [1982] were insufficiently leached and do not represent the sanidine endmember. It is the initial isotopic composition, however, which is of interest because that is what will reflect the isotopic composition of the source of the spherules.

Figure 2.8a. Plot showing measured $^{87}Sr/^{86}Sr$ vs. cumulative % Sr released in sequential leaching of sanidine spherules. Seawater data from Peterman et al., 1970; Burke et al., 1982.

b. Plot of cumulative % Rb vs cumulative % Sr released during sequential leaching of sanidine spherules. Sr is easily leached from the bulk spherules but Rb is strongly fixed in the sanidine lattice.

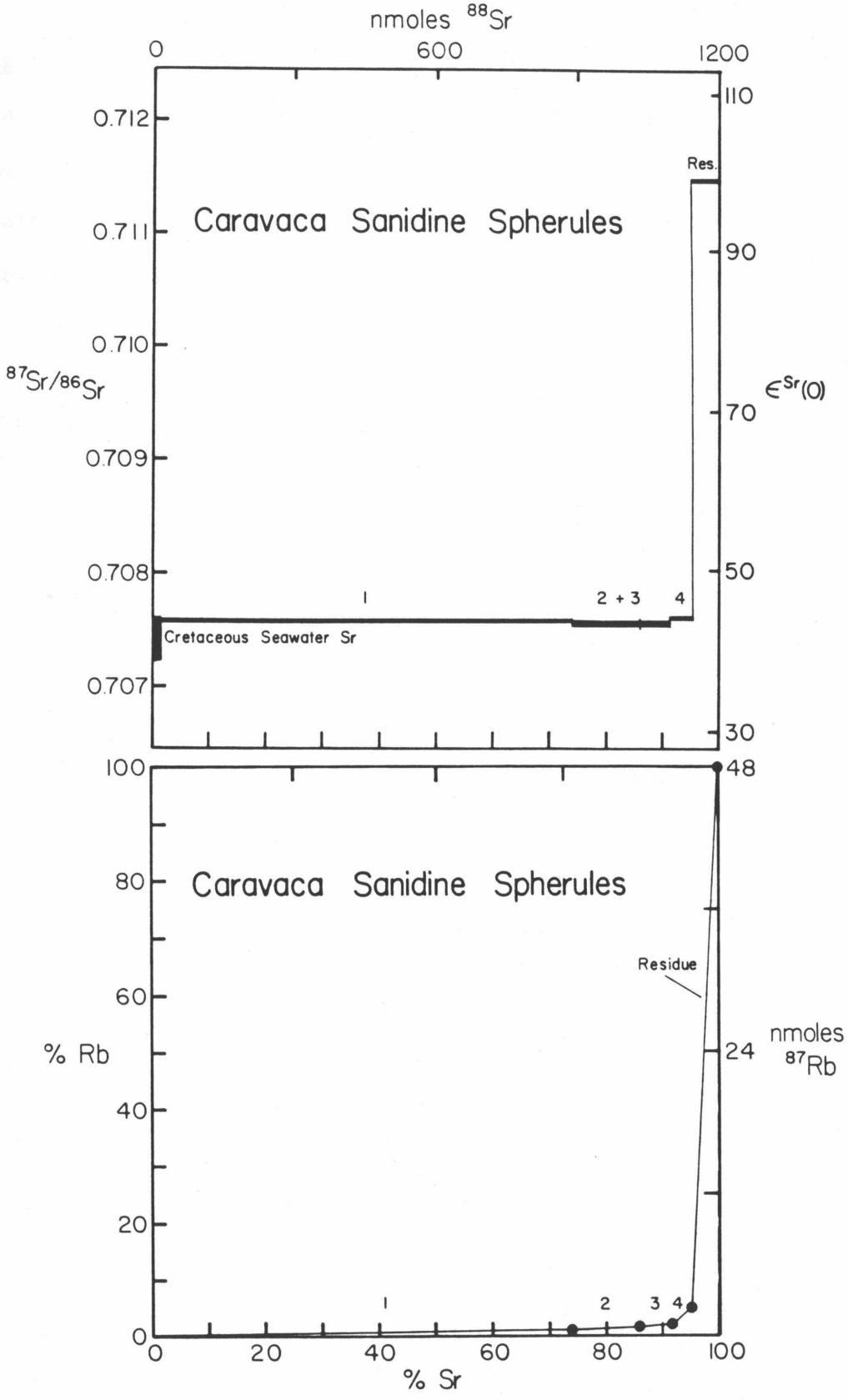
nmoles ^{88}Sr
0
600
1200
0.712
0.711
0.710
0.709
0.708
0.707
$^{87}Sr/^{86}Sr$
110
90
70
50
30
$\epsilon^{Sr}(0)$
Res.
Caravaca Sanidine Spherules
1
2 + 3
4
Cretaceous Seawater Sr
100
80
60
40
20
0
% Rb
48
24
nmoles ^{87}Rb
Caravaca Sanidine Spherules
Residue
1
2
3
4
0
20
40
60
80
100
% Sr

Figure 2.9. Plot of $^{87}Sr/^{86}Sr$ vs 1/Sr for Cretaceous-Tertiary boundary clay materials. Sanidine spherules lie on a mixing line between marine Sr and a sanidine Sr endmember. The inferred sanidine endmember isotopic composition is given by a horizontal extrapolation from the residue 3 value back to the mixing line.

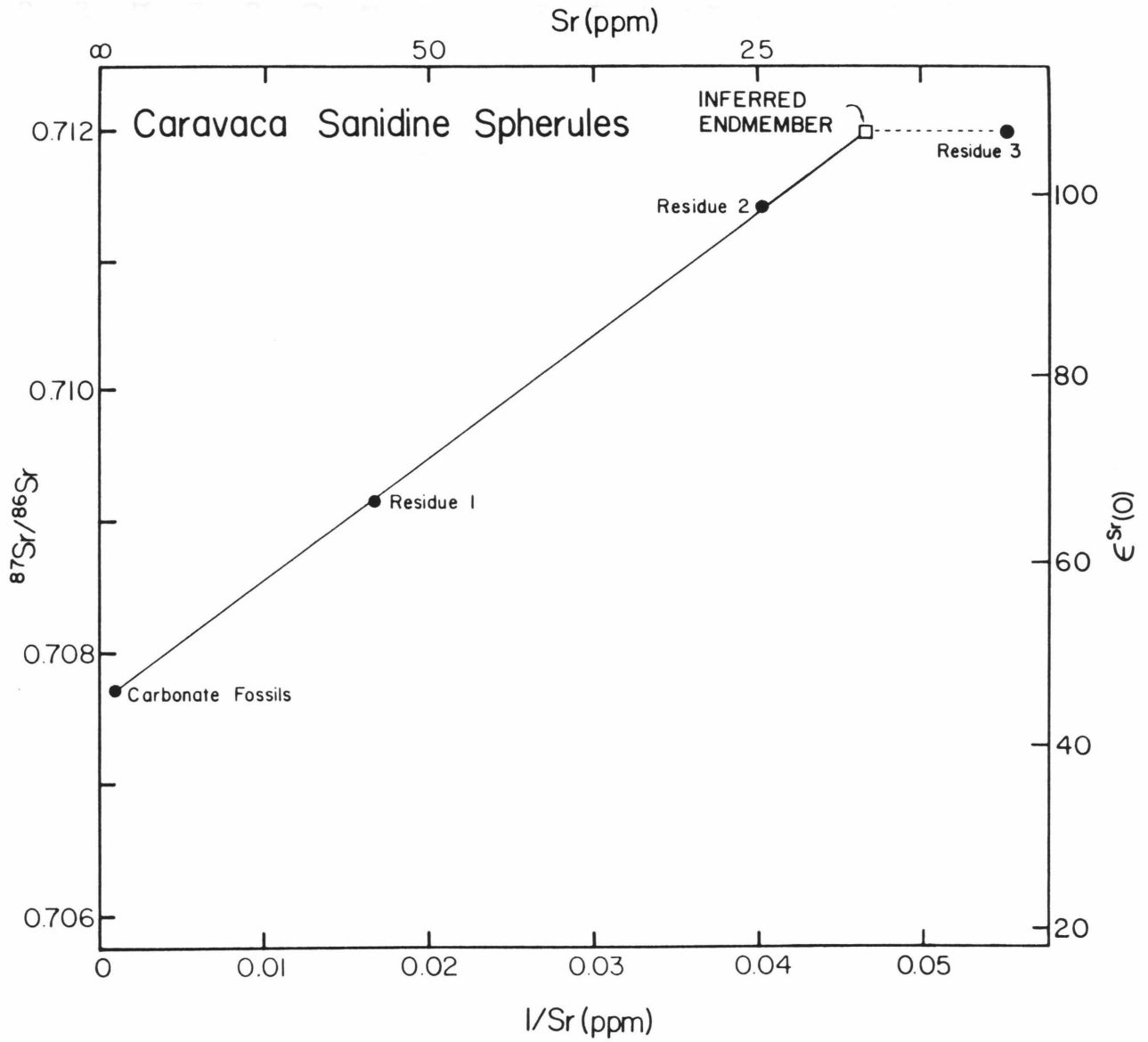
Sr (ppm)
∞
50
25
Caravaca Sanidine Spherules
INFERRED
ENDMEMBER
Residue 3
Residue 2
Residue 1
Carbonate Fossils
0.712
0.710
0.708
0.706
$^{87}Sr/^{86}Sr$
100
80
60
40
20
$\epsilon^{Sr}(0)$
0
0.01
0.02
0.03
0.04
0.05
1/Sr (ppm)

In order to determine the initial $\varepsilon_{Sr}(0)$ one must look at the behavior of Rb relative to Sr in the leaching experiment. Table 2.3 and Fig. 2.8b show that although ~ 96% of the Sr was removed in the 4 leaches, only 5% of the Rb was extracted. The bulk of the Rb remained in the residue and is associated with the high $\varepsilon_{Sr}(0)$ material. Rb in the bulk spherules is strongly fixed in the sanidine unlike Sr which must reside in easily acid leachable phases. If the Sr mixing relationship is used to determine the Sr concentration in the sanidine endmember (~ 22 ppm Sr) and assuming that all of the Rb in the bulk spherules is in the sanidine, then one can calculate a lower limit of $\varepsilon_{Sr}(T) = +1.1$ at 65 my. Similarly, using the same Sr concentration but assuming a Rb concentration equal to that in the most strongly leached residue one calculates an upper limit of $\varepsilon_{Sr}(T) = +11.0$. The parent material for the spherules must therefore have had $\varepsilon_{Sr}(T)$ between +1 and +11 ($^{87}Sr/^{86}Sr$ = 0.7045 to 0.7052).

Figure 2.10 shows $\varepsilon_{Nd}(0)$ vs. the cumulative percent Nd released by the leaching. Only 12% of the Nd remained in residue 2 which has a very low Nd concentration of 0.16 ppm and approximately chondritic Sm/Nd (Table 2.3). As a consequence of the chondritic Sm/Nd ratio, there is no age correction necessary for the ε_{Nd} data. The isotopic composition of residue 2 at $\varepsilon_{Nd}(0) = +1.9$ is significantly different from any of the leaches and is a lower limit on the endmember composition. On the basis of the Sr results it is argued that this value is close to the true isotopic composition in the sanidine endmember. The value of $\varepsilon_{Nd}(0) = -6.9$ for the isotopic composition of the most easily leached Nd is identical to the value found in a late Cretaceous phosphorite from Morocco [this work, Chapter IV] and suggests that, like the leachable Sr, this Nd is derived

Figure 2.10. Plot of $\varepsilon_{Nd}(0)$ vs. cumulative Nd released in sequential leaching of sanidine spherules.

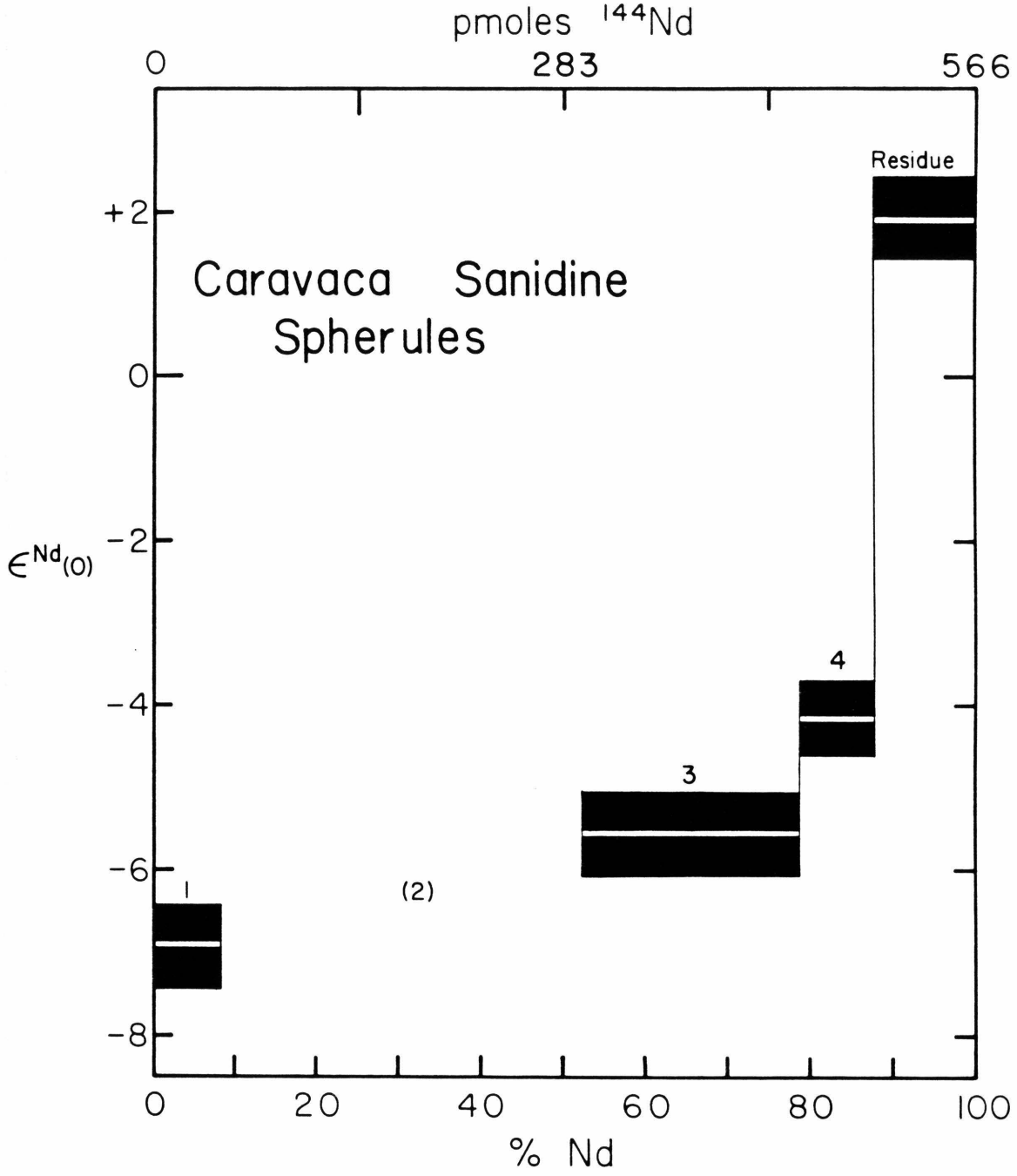
pmoles ^{144}Nd
0
283
566
Residue
+2
Caravaca Sanidine
Spherules
0
$\epsilon^{Nd}(0)$
-2
4
-4
3
-6
1
(2)
-8
0
20
40
60
80
100
% Nd

from seawater. DePaolo et al. [1982] reported a value of $\varepsilon_{Nd} = -6.0$ for acid leached spherules with 1.2 ppm Nd. As noted above, their sample and the sample which was initially reported on by Shaw and Wasserburg [1982] were insufficiently leached.

The value of $\varepsilon_{Nd} \sim +2$ and relatively unevolved initial $\varepsilon_{Sr}(T)$ of $\sim +5$ inferred to be characteristic of the sanidine clearly indicate that unlike tektites, the sanidine spherules could not have been derived from typical LREE enriched, high Rb/Sr old continental crust. Neither could they have been derived from meteoritic potassium feldspar [Smit and Klaver, 1981] as $\varepsilon_{Sr}(T)$ is too low. Strong chemical fractionation during spherule formation is required to explain their present high Rb/Sr ratio and other chemical characteristics (high K/Na, essentially pure sanidine, etc.). This means that simple impact melting resulting in a total melt of the target material could not have produced the spherules as they exist today. An impact process which could provide the necessary chemical fractionation is recondensation of volatilized target material. However, authigenic growth of these objects from either impact or volcanic material at low temperatures could also explain both the extremely low Na and Sr contents as well as the oxygen results of Epstein [1982]. In either case, the Sr and Nd results are consistent with an oceanic impact in which oceanic crust was a major component of the parent material for the spherules. Oceanic crust alone does not satisfy the isotopic constraints which require a mixture of oceanic crust with $\varepsilon_{Nd} \sim +8.0$, $\varepsilon_{Sr} \sim -25.0$ and a component with higher $\varepsilon_{Sr}(T)$ and lower $\varepsilon_{Nd}(T)$ such as continentally derived marine sediments. The isotopic results are also consistent with derivation of the sanidine spherules from crustal material which was relatively young

at 65 my. Thus a volcanic origin for the spherules is not ruled out by these data. Impact induced volcanism would not be an unexpected feature of an impact the size inferred for the K/T event; rapid, adiabatic rebound of the mantle beneath the impact site would cause extensive partial melting of the mantle and attendant volcanism. If volcanism continued for a significant period of time, the resulting volcanic edifice might obscure the craterform structure of the impact site, making recognition difficult.

CHAPTER III

Isotopic Constraints on the Origin of Appalachian Mafic Rocks

III.1 Introduction

The Appalachians have been called the "most elegant mountain chain on earth" [Rodgers, 1970]. Doubtless there are many who would dispute this assessment. Nevertheless, studies of this chain have played a significant role in the evolution of geological thinking about the nature of orogenic belts. It was in the Appalachians that the details of a major fold belt were first worked out [Rogers and Rogers, 1843], and the term geosyncline coined [Dana, 1843]. It was thus natural for Wilson [1966] to apply the then newly revived and revitalized concepts of plate tectonics to explain the evolution of the Appalachians. A key feature in the development of these ideas is the existence of a belt or series of parallel belts of mafic and ultramafic bodies which runs the length of the Appalachians from Newfoundland to Alabama. These bodies are largely restricted to the latest Precambrian to Ordovician eugeosynclinal rocks lying to the east of the chain of anticlinoria cored by Grenville age (1.0 - 1.3 AE) Precambrian basement. The majority of the bodies making up the belt are relatively small (<1 km), apparently rootless pods of peridotite which have been serpentinized to varying degrees. Also found within this belt are larger complexes of mafic and ultramafic rocks which range from relatively complete allochthonous sheets such as the Bay of Islands Ophiolite in Newfoundland, through bodies in which metamorphism and deformation have partially obscured an ophiolite stratigraphy, to bodies which have little if any recognizable stratigraphy, but because of their location in the belt

and mafic to ultramafic composition, have recently been described as dismembered or fragmented ophiolites.

Historically, the mafic and ultramafic rocks of the Appalachians have been interpreted as intrusive bodies, emplaced into an ensialic eugeosynclinal pile [Pratt and Lewis, 1905; Hess, 1939, 1955; Chidester and Cady, 1972], and which reached their present rootless stratigraphic position by diapiric rise of serpentinized peridotite. More recently, in light of the plate tectonic interpretation of ophiolites as fragments of obducted oceanic crust, the mafic and ultramafic rocks of the Appalachians have been interpreted as large and small fragments of proto-Atlantic oceanic crust and mantle which were incorporated into the Appalachian Orogen during the closure phase of a Wilson cycle [Church and Stevens, 1971; Williams, 1971; Dewey and Bird, 1971; Upadhyay et al., 1971; St. Julien, 1972; Laurent, 1975, 1977; Crowley, 1976; Morgan, 1977; Williams and Talkington, 1977; Malpas, 1977]. The objective of this study is to use the Sm-Nd and Rb-Sr isotopic systems to place constraints on the origin of several Appalachian mafic bodies in which either extensive metamorphism, or tectonism, or both has made their origin uncertain. Using criteria to be discussed below, it will be shown that the Baltimore Mafic Complex, Md and the Thetford Mines Complex, Qe, two large Appalachian mafic/ultramafic complexes, do not have the isotopic signature of oceanic crust. Several smaller mafic/ultramafic bodies from Vermont and N. Carolina, on the other hand, do have isotopic compositions which are consistent with an oceanic origin. Figure 3.1 shows the location within the Appalachians of the bodies studied.

Figure 3.1. Map of the Appalachians showing the locations of the mafic/ultramafic complexes studied. BMC=Baltimore Mafic Complex; BOI= Bay of Islands Ophiolite; TMC=Thetford Mines Complex; LC=Lake Chatuge Complex; CG=Chunky Gal/Buck Creek; W-A=Webster-Addie; Belv. Mtn.= Belvidere Mountain.

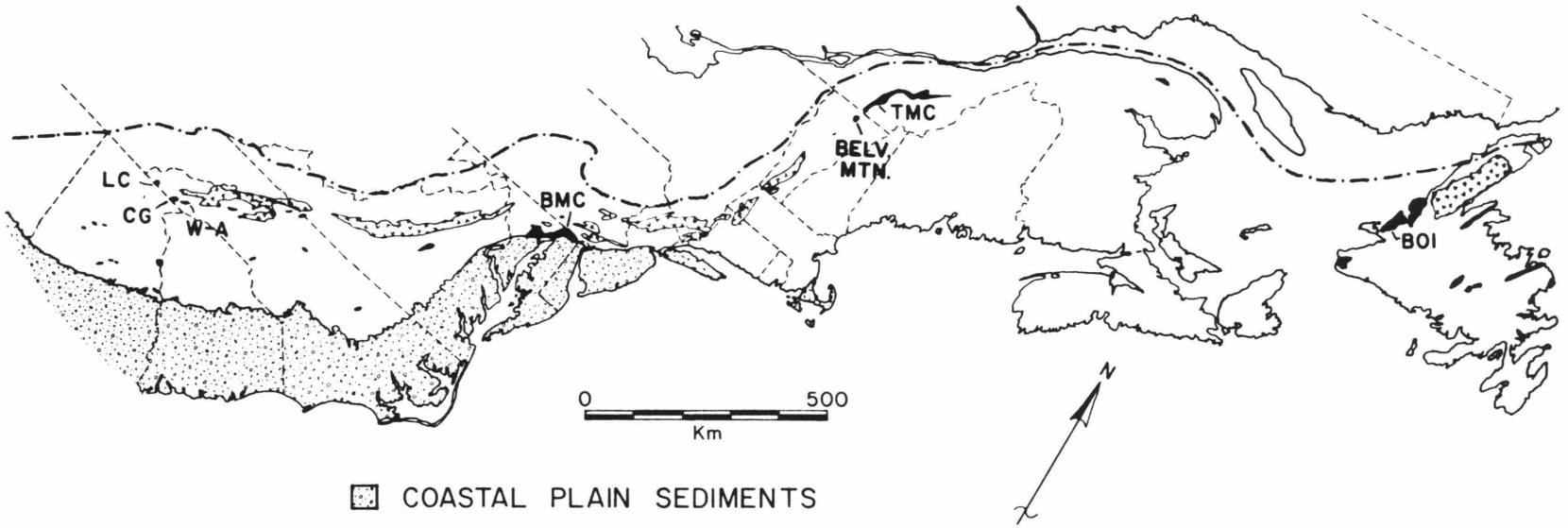
LC
CG
W-A
BMC
TMC
BELV
MTN.
BOI
0
500
Km
N
COASTAL PLAIN SEDIMENTS
MAFIC / ULTRAMAFIC COMPLEXES
pC BASEMENT
WESTERN LIMIT APPALACHIAN
DEFORMATION

III.2 Ophiolites

III.2.1 Geologic relationships

As originally introduced by Steinmann [1927], the term ophiolite carried no tectonic or genetic connotation, but simply referred to the common association of peridotite, serpentinite, gabbro, diabase, spilite, and deep-water marine sediments in the Mediterranean Alpine belts. This concept of a kindred relationship between diverse rock types was largely ignored by American geologists until the advent of plate tectonics. It was then realized that the ophiolite association consisted of the basic elements making up oceanic crust and that plate tectonics provided a means of incorporating segments of oceanic crust into orogenic belts [Coleman, 1971; Dewey and Bird, 1971; Moores and Vine, 1971; Church, 1972]. The idea that ophiolites represented fragments of oceanic crust and mantle overthrust or obducted onto continental margins at convergent plate boundaries has gained rapid acceptance. Although strictly speaking, an ophiolite must contain all the elements of the "Steinmann Trinity", (serpentinized ultramafic rocks, diabase-spillitic pillow basalts, and deep-water sediments), it has become common to talk of partial or dismembered ophiolites when one or more of the elements of the stratigraphy is missing. This is somewhat distressing as it has led to a tendency to identify every mafic or ultramafic rock in an orogenic belt as part of an ophiolite sequence. Furthermore, the word ophiolite has taken on the originally unintended genetic connotation of an oceanic origin. As will be shown in this chapter, these developments are not entirely warranted. It has also become clear that the original plate tectonic paradigm of ophiolites as obducted oceanic crust formed at a mid-ocean ridge cannot explain all ophiolites. It is likely that ophiolites can also form in other tectonic settings such as island arcs or marginal (back-arc) basins.

III.2.2 Isotopic systematics of ophiolites

Well characterized ophiolites such as the Bay of Islands Ophiolite, Newfoundland, and the Samail Ophiolite, Oman, have been found to have the characteristic isotopic signature of a depleted mantle source (see I.2.2) Figure 3.2 is a histogram of $\varepsilon_{Nd}(T)$ values for ophiolite samples. It can be clearly seen that in general, these values lie in the range of modern day MORB and island arc rocks.

In order to extend the isotopic observations on geologically well-characterized ophiolites, samples from three California ophiolites of Mesozoic age have been analysed: the Josephine Ophiolite [157 My, Harper, 1980; Harper and Saleeby, 1980], the Point Sal Ophiolite [160 My, Hopson and Frano, 1977] and the Kings-Kaweah Ophiolite [200 My, Saleeby, 1982]. In addition to the Sm-Nd and Rb-Sr analyses performed by the author, a joint study of the U-Th-Pb systematics of the same samples was initiated by James Chen [Chen and Shaw, 1982]. The results of this study are incorporated here. The Josephine Ophiolite and Kings-Kaweah Ophiolite have metamorphic histories comparable to that inferred for many of the Appalachian mafic complexes; both were metamorphosed to greenschist or amphibolite facies during regional metamorphic events after their emplacement onto the continental margin. The data for the California ophiolites are given in Tables 3.1 and 3.2 and Figs. 3.2-3.4. These rocks clearly have the Nd isotopic signature of the depleted mantle source characteristic of modern oceanic crust or oceanic island arcs, especially when allowance is made for the evolution of the source. For a depleted mantle with $f^{Sm/Nd} \sim +0.2$ one would expect this reservoir to evolve by $\sim +0.5$ ε_{Nd} units every 100 My. The present-day range of +8 to +13 ε_{Nd} for the MORB derived from

Figure 3.2. Histogram of $\varepsilon_{Nd}(T)$ values comparing mid-ocean ridge basalts, (MORB), oceanic island arcs and ocean island basalts [Carlson et al., 1978; Cohen et al., 1980; DePaolo, 1978; DePaolo and Wasserburg, 1976b, 1977; Dosso and Murthy, 1980; Hawkesworth et al., 1977; 1979a,b; Jahn et al., 1980; McCulloch and Perfit, 1981; Menzies and Murthy, 1980; O'Nions et al., 1977; 1978; Richard et al., 1976; Zindler et al., 1979] and ophiolites (key to ophiolites: Tr - Troodos, V - Vourinos, BC - Bett's Cove, BOI - Bay of Islands, S - Samail, PS - Pt. Sal, Jo - Josephine, KR - Kings-Kaweah, U - Kempersai, Urals, To - Toba, Japan) [Chen and Shaw, 1982; Coish et al., 1982; Edwards and Wasserburg, 1983; Hannah and Futa, 1982; Jacobsen and Wasserburg, 1979; McCulloch et al., 1981; Richard and Allegre, 1980].

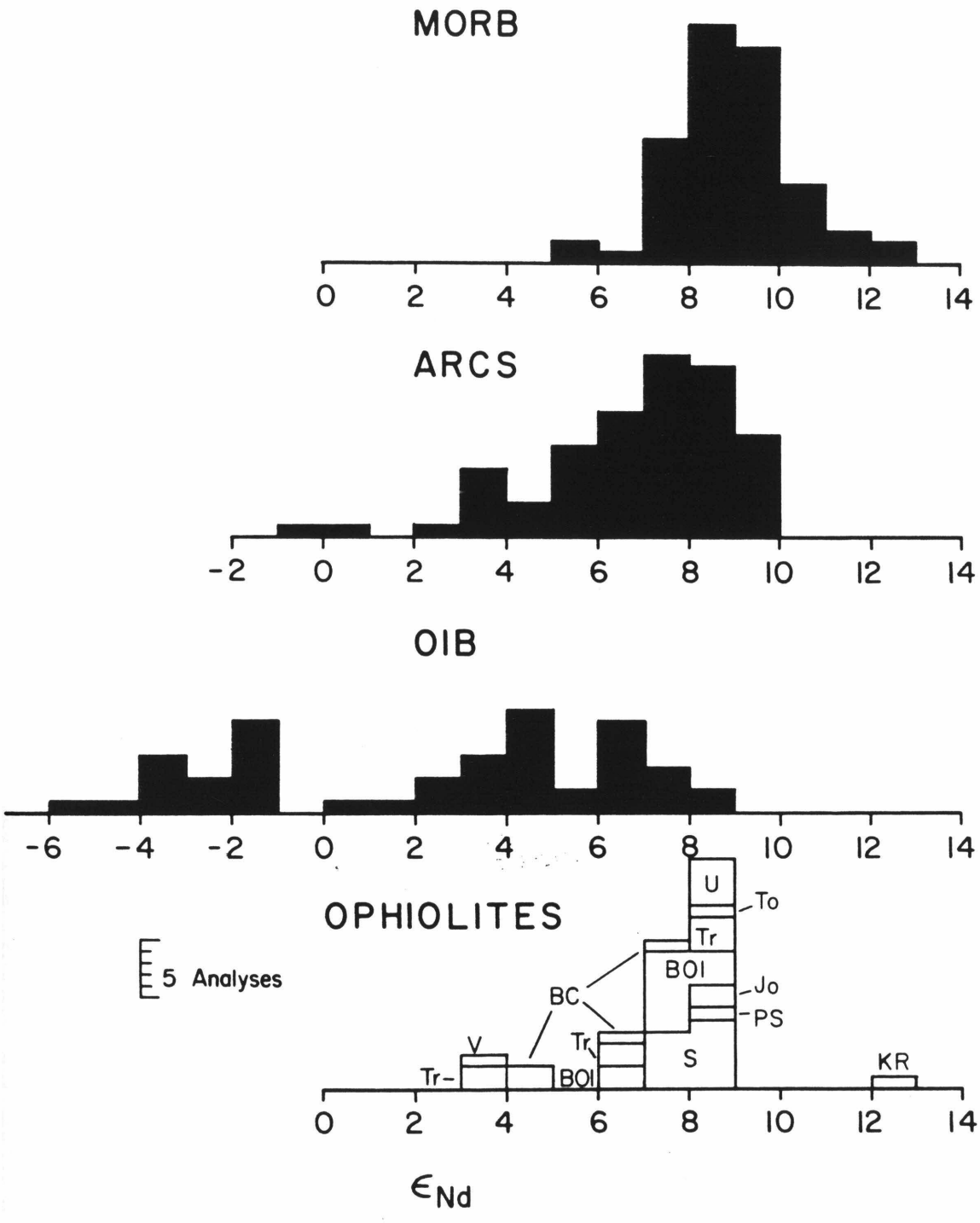
MORB
0 2 4 6 8 10 12 14
ARCS
-2 0 2 4 6 8 10 12 14
OIB
-6 -4 -2 0 2 4 6 8 10 12 14
OPHIOLITES
5 Analyses
U
To
Tr
BOI
Jo
PS
BC
V
Tr
Tr-
BOI
S
KR
0 2 4 6 8 10 12 14
ϵ_{Nd}

depleted oceanic mantle would thus correspond to a range of +5.5 to +10.5 at ~ 500 My ago. The effect of the evolution of the source is shown in Fig. 3.3. The value of $\varepsilon_{Nd}(T) = +12.4$ for the Kings-Kaweah sample deserves some comment. This value is among the highest reported for samples from a depleted mantle reservoir and implies that the Kings-Kaweah Ophiolite was derived from mantle which was either more highly depleted than average or was depleted at a much earlier-than-average time. Ophiolite localities showing such high ε_{Nd} values will require more attention in the future.

The Pb isotopic compositions of the California ophiolites are given in Table 3.2. As can be seen in Fig. 3.4, these and other ophiolites have the characteristic Pb isotopic composition of oceanic crust. The Kings-Kaweah sample again stands out as having among the least radiogenic Pb found in present day MORB. Unlike the Nd isotopic systematics which do not clearly differentiate between MORB and island arc rocks, the $^{207}Pb/^{204}Pb$ ratio for a given $^{206}Pb/^{204}Pb$ ratio of many arc rocks is distinctly higher than that defined by the main trend of oceanic basalts (Fig. 3.4). This has often been suggested to be due to the involvement of subducted oceanic sediments in the genesis island arc lavas. It may thus be possible in some cases to discriminate between ridge and arc generated ophiolites according to their Pb isotopic composition. Of the California ophiolites studied, the Point Sal Ophiolite appears on this basis to have island arc affinities, while the Kings-Kaweah sample is clearly derived from a strongly depleted reservior typical of MORB. The Josephine Ophiolite lies between these two extremes.

The Sr isotopic compositions of ophiolites range from depleted mantle values typical of fresh MORB to relatively radiogenic values. This dispersion is due to the relative ease with which the Sr isotopic system is

Table 3.1. Rb-Sr and Sm-Nd isotopic results: California ophiolites.

Sample	$\frac{143Nd}{144Nd}$*	ppm Nd	$\frac{147Sm}{144Nd}$+	$f^{Sm/Nd}$	$e_{Nd}(T)^a$	$\frac{87Sr}{86Sr}$*	ppm Sr	$\frac{87Rb}{86Sr}$+	$f^{Rb/Sr}$	$e_{Sr}(T)^a$
California Ophiolites[b]										
P-59	0.51229	1.25	0.223	0.134	+8.2	0.70333	298.7	0.0061	-0.926	-14.2
Pt. Sal Gabbro	±4				±0.9	±4				±0.6
JP-042	0.51238	0.74	0.275	0.396	+8.8	0.70349	88.4	0.0686	-0.171	-13.9
Josephine Gabbro	±2				±0.4	±3				±0.4
Y-13b	0.51238	1.14	0.257	0.305	+8.4	0.70342	214.7	0.0470#	-0.431	-14.2
Josephine Gabbro	±2				±0.4	±3				±0.4
Ca-10	0.51254	1.57	0.243	0.237	+12.4	0.70232	131.6	0.0061	-0.926	-27.9
Kings R. Gabbro	±3				±0.5	±3				±0.4

*Errors are 2s of the mean; 143Nd/144Nd normalized to 146Nd/142Nd = 0.636151; 87Sr/86Sr normalized to 86Sr/88Sr = 0.1194.

+Uncertainty = 0.2%

+Uncertainty = 1.0%. Rb measured on aliquot only--except as noted.

#Uncertainty = 0.4%. Rb measured on separated sample.

[b]Initial e values calculated using the ages: Pt. Sal = 160 My; Josephine Ophiolite = 157 My; Kings R. Ophiolite = 200 My.

Table 3.2 Pb isotopic results: California Ophiolites.

Sample	Conc (ppm) Pb	U	Th	Isotopic ratio $\frac{206_{Pb}}{204_{Pb}}$	$\frac{207_{Pb}}{204_{Pb}}$	$\frac{208_{Pb}}{204_{Pb}}$	$\frac{238_{U}}{204_{Pb}}$	$\frac{232_{Th}}{204_{Pb}}$
Kings-Kaweah Ophiolite								
Ca-10 #1	0.088	0.0039	------	17.438	15.385	36.935	2.7	-----
Ca-10 #2	0.058	0.0049	0.0116	17.545	15.406	37.102	5.2	2.4
Josephine Ophiolite								
JP-042	0.095	0.0029	0.0064	18.248	15.519	37.867	1.95	2.26
Y-13b	0.109	0.0029	------	18.242	15.519	37.864	1.68	----
Point Sal Ophiolite								
JS-PS-8-plag.	-----	------	------	18.407	15.575	38.132	----	----
P-59 #1	0.155	0.0031	------	18.612	15.557	38.034	1.26	----
P-59 #2	-----	------	------	18.609	15.566	38.100	----	----
JS-PS-9	0.0355	0.00038	------	18.379	15.562	38.119	0.60	----

All ratios have uncertainties of ~ 0.1% and are uncorrected for U, Th decay.
Data from Chen and Shaw, [1982], Chen, unpbl. data.

Figure 3.3. Plot of ε_{Nd} vs. ε_{Sr} showing the fields occupied by MORB, island arcs, and oceanic islands. Ophiolite data are superimposed on these fields. The solid symbols are the initial isotopic compositions. The open symbols indicate where the depleted mantle from which the ophiolites were derived would plot today assuming reasonable values for the depleted mantle of $f^{Sm/Nd} = +0.22$, $f^{Rb/Sr} = -0.9$. Representative analyses of the Bay of Islands Ophiolite [Jacobsen and Wasserburg, 1979] and Samail Ophiolite [McCulloch et al., 1981] are plotted to avoid cluttering the diagram. Nd-Sr relationships clearly show an oceanic affinity for ophiolites but are unable to clearly distinguish between MORB and island arc materials.

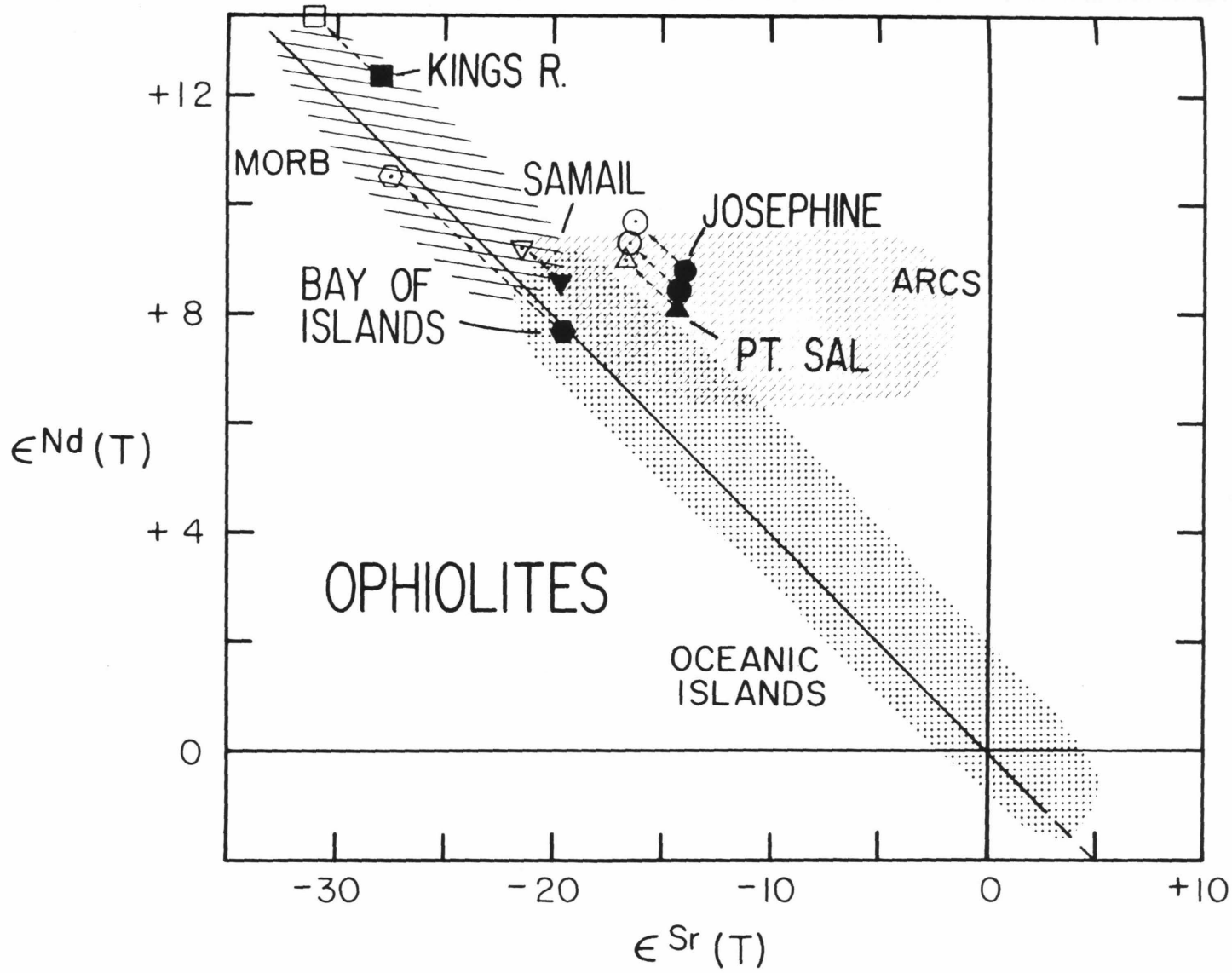
KINGS R.
MORB
SAMAIL
JOSEPHINE
ARCS
BAY OF ISLANDS
PT. SAL
OPHIOLITES
OCEANIC ISLANDS
+12
+8
+4
0
-30
-20
-10
0
+10
$\epsilon^{Nd}(T)$
$\epsilon^{Sr}(T)$

Figure 3.4. $^{208}Pb/^{204}Pb$ - $^{206}Pb/^{204}Pb$ and $^{207}Pb/^{204}Pb$ - $^{206}Pb/^{204}Pb$ plots of modern oceanic basalts, island arc magmas, oceanic sediments and ophiolites. The initial Pb isotopic compositions of ophiolites plot within the fields for MORB and arcs. The Point Sal Ophiolite is more similar to arcs than typical MORB. Note the primitive Pb isotopic composition of the Kings-Kaweah samples.

Oceanic data from Tatsumoto, [1978]; Cohen et al., [1980]; Dupre et al., [1980]; Sun et al., [1980]. Ophiolite data from Chen and Pallister, [1980]; Chen et al., [1981]; Göpel et al., [1982]; Chen and Shaw, [1982]; Chen, unpbl. data.

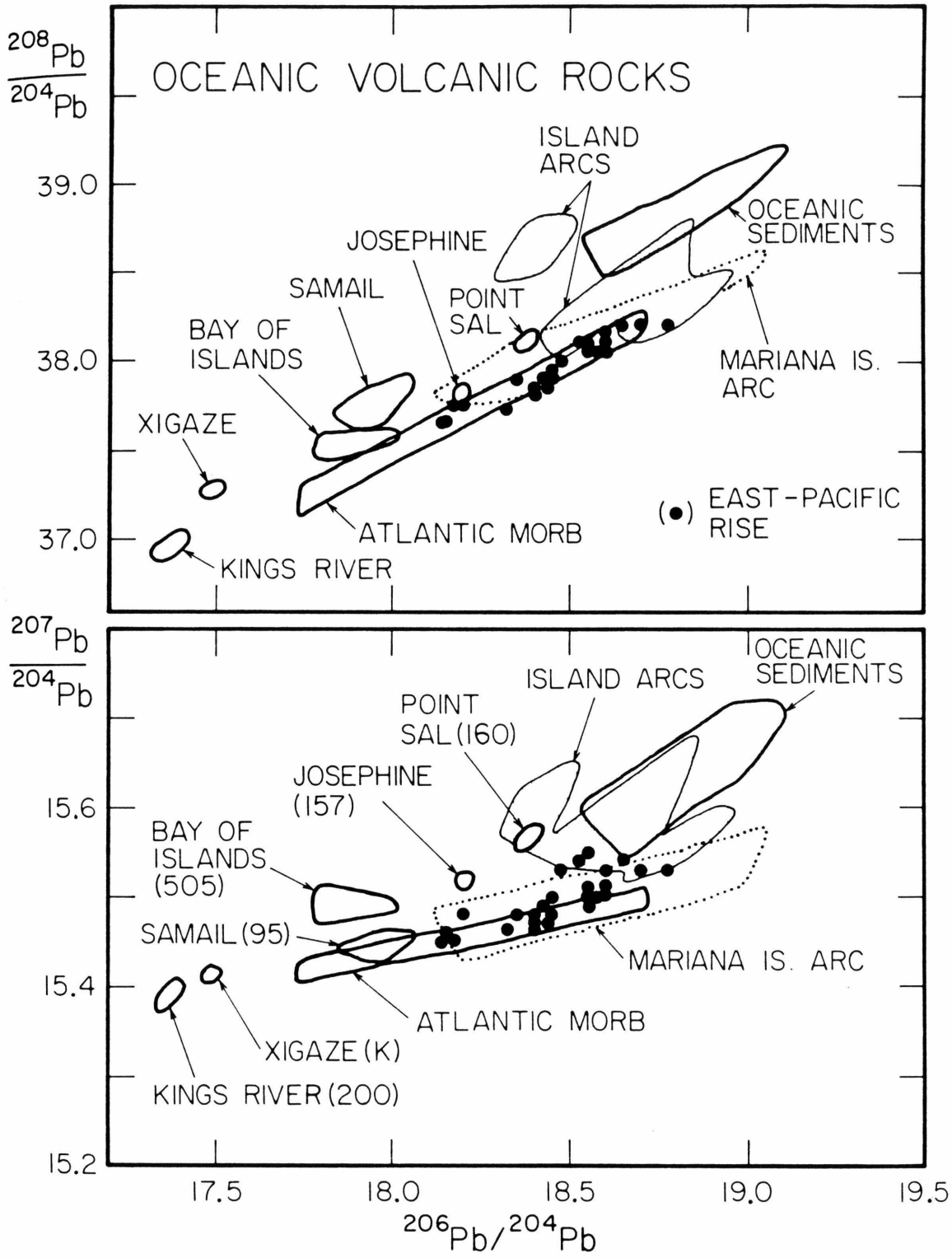
OCEANIC VOLCANIC ROCKS
208Pb/204Pb
39.0
38.0
37.0
ISLAND ARCS
OCEANIC SEDIMENTS
JOSEPHINE
SAMAIL
POINT SAL
BAY OF ISLANDS
MARIANA IS. ARC
XIGAZE
ATLANTIC MORB
(●) EAST-PACIFIC RISE
KINGS RIVER
207Pb/204Pb
15.6
15.4
15.2
ISLAND ARCS
OCEANIC SEDIMENTS
POINT SAL(160)
JOSEPHINE (157)
BAY OF ISLANDS (505)
SAMAIL(95)
MARIANA IS. ARC
ATLANTIC MORB
XIGAZE(K)
KINGS RIVER(200)
17.5
18.0
18.5
19.0
19.5
206Pb/204Pb

disturbed by exchange during both regional metamorphism and metamorphism on the seafloor [Jacobsen and Wasserburg, 1979; McCulloch et al., 1981]. This fact has limited the utility of the Sr isotopic system for constraining the origin of mafic rocks in complex orogenic terrains. In contrast, the Nd isotopic system appears to be relatively immune to such disturbances, suggesting that the distinctive Nd isotopic signature of oceanic crust is preserved during hydrothermal alteration on the sea floor and during obduction and regional metamorphism. Although the susceptibility of Nd and the REE in general to disturbance in response to different types of metamorphism is not well known, the available data suggests that the REE are quite robust. This feature could be of great importance in the Appalachians where metamorphism has obliterated the original mineralogy and modified the major element chemistry of most of the mafic and ultramafic rocks.

III.3 Baltimore Mafic Complex

III.3.1 Geologic setting

The Baltimore Mafic Complex (BMC) is made up of a discontinuous association of mafic and ultramafic bodies extending at least 150 km from southeastern Pennsylvania across Maryland into northern Virginia. As such, it represents the largest known Appalachian mafic complex south of Quebec. The Complex has a long history of studies dating back to the classic papers of Williams [1884, 1886, 1890] on the petrography of metamorphosed gabbros. A report by Hopson [1964] culminated the pre-plate tectonic studies of the geology of the Maryland Piedmont (see also Hertz, 1951; Southwick, 1970). In his interpretation, the ultramafic and gabbroic rocks of the BMC were to have intruded the sedimentary precursor of the

Wissahickon Formation late in the depositional history of a eugeosynclinal basin and prior to tectonism and regional metamorphism, the Wissahickon Formation being the latest deposited sediment in a deepening Cambro-Ordovician trough underlain by the Precambrian Baltimore Gneiss. The transition to deeper water in this interpretation is marked by the stratigraphic change from the older shallow water formations, the Setters Quartzite and Cockeysville Marble to the deep-water pelitic and psamitic sediments of the Wissahickon [Hopson, 1964].

More recent studies have shown that the Wissahickon in fact has little in the way of internal stratigraphy which can be traced. The current interpretation is that the Wissahickon is a terrain of broken blocks floating in an incoherent matrix of similar material [Crowley, 1976; Morgan, 1977]. What appeared to be a continuous stratigraphic succession is now believed to be due to overthrusting of deeper water sediments onto a shelf sequence. The BMC has been emplaced into this terrain. Crowley [1976] has argued that the Complex is allochthonous and this interpretation fits well with the chaotic nature of the enclosing rocks. His arguments rest on the following observations:

1. Mafic and ultramafic rocks are found only within the Wissahickon Fm.; no dikes, sills or evidence of intrusion are seen in the underlying rocks.
2. Internal layering of the complex is truncated at contacts with the Wissahickon Fm.
3. There is no evidence for a high temperature metamorphic aureole around the Complex.

On this basis, together with the fact that the BMC lies within the belt of mafic/ultramafic rocks extending the length of the Appalachians, the

Complex has been reinterpreted as a fragment of proto-Atlantic oceanic crust, i.e., an ophiolite. [Crowley, 1976; Morgan, 1977; Drake and Morgan, 1981].

In terms of ophiolite stratigraphy, the BMC consists only of a cumulate dunite-chromitite base overlain by cumulate pyroxenites which grade into cumulate and non-cumulate two-pyroxene gabbros, norites, and quartz gabbros. The BMC does not include tectonized harzburgite, a dike complex, pillow basalts or overlying marine sediments. Strictly speaking it is not an ophiolite as it does not contain all the elements of the ophiolite stratigraphy. The inferred order of crystallization of the gabbro and ultramafic cumulates is: olivine (+ chromite), olivine + orthopyroxene, olivine + orthopyroxene + clinopyroxene, two pyroxenes, two pyroxenes + plagioclase, two pyroxenes + plagioclase + hornblende (+ quartz). The entire complex has been metamorphosed to variable extent. On an outcrop scale one can follow the transition from a nearly pristine gabbro to a metagabbro in which pyroxene has been completely replaced by amphibole and calcic plagioclase by zoisite and sodic plagioclase.

Samples of a variety of lithologies and degrees of metamorphism have been analysed. Brief sample descriptions and a discussion of procedures is given in Appendix II.

III.3.2 Age of the Complex

Results for the Baltimore Mafic Complex are presented in Table 3.3 and Figs. 3.5-3.7. Figures 3.5a-c show Sm-Nd data on minerals separated from three samples of the BMC. The age and initial values are reported with 2σ errors calculated using the regression routine of Williamson [1968].

Table 3.3. Rb-Sr and Sm-Nd isotopic results: Appalachian matic complexes.

Sample	$\frac{^{143}Nd}{^{144}Nd}$*	ppm Nd	$\frac{^{147}Sm}{^{144}Nd}$‡	$f^{Sm/Nd}$	$\varepsilon_{Nd}(T)^a$	$\frac{^{87}Sr}{^{86}Sr}$*	ppm Sr	$\frac{^{87}Rb}{^{86}Sr}$+	$f^{Rb/Sr}$	$\varepsilon_{Sr}(T)^a$
Baltimore Mafic Complex										
Md-32 Norite	0.51132 ±2	16.1	0.131	-0.334	-6.2 ±0.5	0.71209 ±4	302.9	0.0104#	-0.874	+114.9 ±0.6
	0.51131 ±3	16.3	0.130	-0.337	-6.4 ±0.5	0.71214 ±4	302.9	--	--	--
Md-32 Plagioclase	0.51120 ±2	6.7	0.093	-0.526	--	0.71254 ±4	494.4	.0042#	0.949	
Md-32 Orthopyroxene	0.51140 ±2	4.0	0.152	-0.228	--	0.71272 ±4	8.55	.1161#	0.404	--
Md-32 Apatite	0.51135 ±2	796.9	0.135	-0.314	--	0.71214 ±3	205.6	.0100#	0.879	--
Md-3 Feldspathic websterite	0.51183 ±2	0.68	0.227	0.516	-2.2 ±0.4	0.70756 ±2	93.6	.0089	-0.893	+50.8 ±0.3
Md-3 Plagioclase	0.51130 ±2	0.12	0.068	-0.656	--	--	--	--	--	--
Md-3 Orthopyroxene	0.51188 ±2	0.21	0.253	0.285	--	--	--	--	--	--
Md-3 Clinopyroxene	0.51186 ±3	1.86	0.253	0.285	--	--	--	--	--	--

Table 3.3 (Continued).

Sample	$\frac{^{143}Nd}{^{144}Nd}$*	ppm Nd	$\frac{^{147}Sm}{^{144}Nd}$‡	$f^{Sm/Nd}$	$\varepsilon_{Nd}(T)^a$	$\frac{^{87}Sr}{^{86}Sr}$*	ppm Sr	$\frac{^{87}Rb}{^{86}Sr}$+	$f^{Rb/Sr}$	$\varepsilon_{Sr}(T)^a$
Md-44 Gabbro	0.51152 ±2	1.16	0.190	-0.035	-6.0 ±0.4	0.71052 ±8	131.0	0.0125	-0.849	+92.5 ±1.1
Md-44 Pyroxene	0.51160 ±2	1.55	0.220	0.119	--	--	--	--	--	--
Md-44 Plagioclase	0.51114 ±2	0.38	0.076	-0.612	--	--	--	--	--	--
Md-40 Metagabbro	0.51152 ±3	5.36	0.168	-0.143	-4.5 ±0.6	0.70970 ±3	85.1	0.0133	-0.839	+80.7 ±0.4
Md-30 Gabbro	0.51147 ±1	2.48	0.168	-0.144 ±0.3	-5.5 ±0.3	0.70950 ±3	180.0	0.0146	-0.823	+77.7 ±0.4
Md-15 Orthopyroxenite	0.51171 ±2	0.51	0.250	0.273	-6.1 ±0.4	0.71047 ±3	25.8	0.0193	-0.767	+91.0 ±0.4
Md-39 Hornblende Gabbro	0.51156 ±3	4.84	0.159	-0.194	-3.1 ±0.7	0.70916 ±4	142.5	0.0230#	-0.721	+72.1 ±0.6
Thetford Mines Samples										
Qe-18 Lower Pillow Basalt	0.51194 ±2	0.86	0.178	-0.097	+3.0 ±0.4	0.70763 ±3	53.5	0.1009	-0.220	+42.5 ±0.4
Qe-13A #3 Lower Pillow Basalt	0.51181 ±3	1.94	0.178	-0.097	+0.4 ±0.6	0.70761 ±4	72.3	0.0101	-0.878	+51.5 ±0.6

Table 3.3 (Continued).

Sample	$\frac{^{143}Nd}{^{144}Nd}$*	ppm Nd	$\frac{^{147}Sm}{^{144}Nd}$‡	$f^{Sm/Nd}$	$\varepsilon_{Nd}(T)^a$	$\frac{^{87}Sr}{^{86}Sr}$*	ppm Sr	$\frac{^{87}Rb}{^{86}Sr}$+	$f^{Rb/Sr}$	$\varepsilon_{Sr}(T)^a$
Qe-40 Upper Pillow Basalt	0.51197 ±2	1.05	0.201	0.022	+2.2 ±0.4					
Qe-8B Metadiabase	0.51209 ±2	1.43	0.205	0.044	+4.7 ±0.5	0.71287 ±4	98.6	0.3957	3.784	+87.2 ±0.6
Qe-12A Metagabbro	0.51205 ±1	0.96	0.211	0.072	+3.2 ±0.3	0.71202 ±3	94.5	0.0106	-0.872	+114.0 ±0.4
Qe-30A Metagabbro	0.51172 ±2	0.11	.1813	-0.078	-1.5 ±0.4	0.70412 ±4	88.4	0.0039	-0.953	+2.6 ±0.6
Qe-24 Clinopyroxenite	0.51242 ±2	0.11	0.326	0.655	+2.9 ±0.4	0.70936 ±5	6.58	0.2457	1.971	+52.6 ±0.7
Vermont Sample										
VJL-360C Hazens Notch Amphibolite	0.51232 ±3	6.9	0.217	0.101	+8.0 ±0.5	0.70412 ±3	63.1	0.1509#	0.824	-12.3 ±0.4
North Carolina Samples										
CG 12-1 Chunky Gal Amphibolite	0.51241 ±2	3.42	0.248	0.259	+7.7 ±0.4	0.70543 ±6	95.2	0.0143#	-0.827	+20.1 ±0.8

Table 3.3 (Continued).

Sample	$\frac{^{143}Nd}{^{144}Nd}$*	ppm Nd	$\frac{^{147}Sm}{^{144}Nd}$‡	$f^{Sm/Nd}$	$\varepsilon_{Nd}(T)^a$	$\frac{^{87}Sr}{^{86}Sr}$*	ppm Sr	$\frac{^{87}Rb}{^{86}Sr}$+	$f^{Rb/Sr}$	$\varepsilon_{Sr}(T)^a$
CG 2-18 Chunky Gal Amphibolite	0.51210 ±3	12.7	0.182	-0.073	+6.0 ±0.5	0.70680 ±5	340.4	0.0290	-0.649	+38.1 ±0.7
C-1 Lake Chatuge Amphibolite	0.51220 ±2	2.09	0.226	0.137	+5.1 ±0.5	0.70320 ±4	162.0	0.0258#	-0.688	-12.7 ±0.6
XTC-127 Webster-Addie websterite	0.51190 ±2	0.57	0.231	0.176	-1.1 ±0.4	0.70691 ±4	8.13	0.1323#	0.599	+29.2 ±0.6
XTC-127 leached residue	0.51207 ±1	0.31	0.278	0.414	-0.9 ±0.3	0.70654 ±4	7.30	--	--	--
Baltimore Gneiss, Wissahickon Schist Samples										
Md-7 Biotite Gneiss	0.51119 ±2	24.6	0.117	-0.407	-7.8† ±0.4	0.72947 ±3	199.0	1.363#	15.48	+227.4† ±0.4
Md-11 Augen Gneiss	0.51117 ±2	69.8	0.115	-0.415	-8.2† ±0.4	0.75406 ±6	128.8	3.225#	37.99	+393.2† ±0.9
RL 80-7 Wissahickon schist	0.51120 ±2	22.4	0.102	-0.484	-6.6† ±0.3	0.71773 ±3	123.6	0.6253#	6.561	+134.2† ±0.4

Table 3.3 (Continued).

---

*Errors are 2s of the mean; 143Nd/144Nd normalized to 146Nd/142Nd = 0.636151; 87Sr/86Sr normalized to 86Sr/88Sr = 0.1194.

+Uncertainty = 0.2%

+Uncertainty = 1.0%. Rb measured on aliquot only--except as noted.

#Uncertainty = 0.4%. Rb measured on separated sample.

†Initial e values calculated for 490 My.

aErrors on initial e values reflect only the analytical uncertainty and do not include errors due to age estimates.

Figure 3.5a. Sm-Nd evolution diagram showing internal isochron relationship for Baltimore Mafic Complex feldspathic websterite sample Md-3.

b. As above, two-pyroxene gabbro sample Md-44.

c. As above, norite sample Md-32.

d. Rb-Sr diagram showing mineral data for Baltimore Mafic Complex norite sample Md-32. Note the lack of an isochron relationship in contrast to the Sm-Nd data.

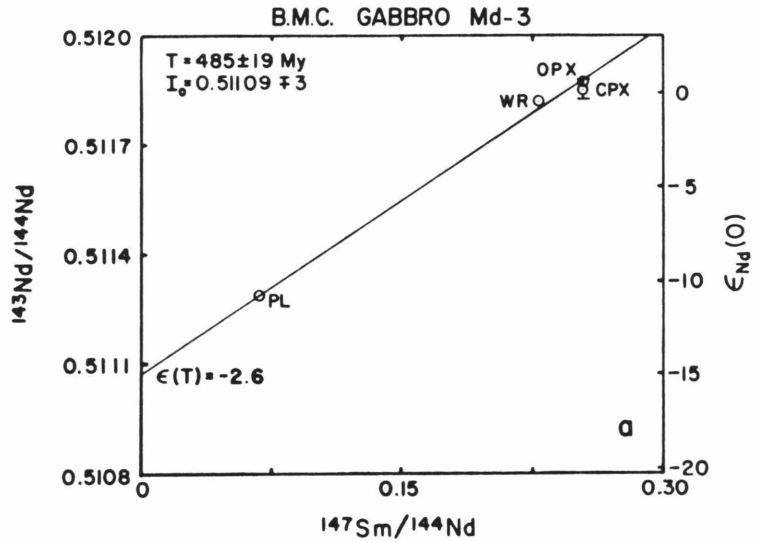
B.M.C. GABBRO Md-3
T = 485 ± 19 My
I_o = 0.51109 ∓ 3
OPX
CPX
WR
PL
ε(T) = -2.6
a
0.5120
0.5117
0.5114
0.5111
0.5108
0
0.15
0.30
0
-5
-10
-15
-20
$^{143}Nd/^{144}Nd$
$^{147}Sm/^{144}Nd$
$\epsilon_{Nd}(0)$

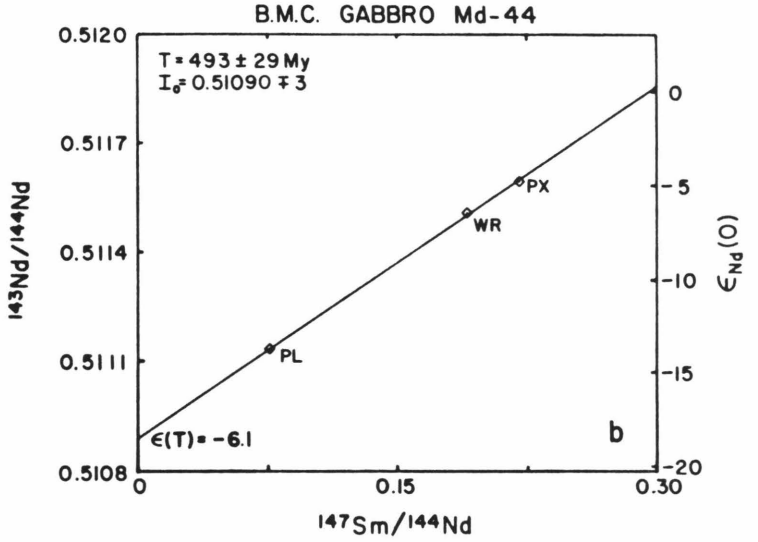
B.M.C. GABBRO Md-44
T = 493 ± 29 My
I_o = 0.51090 ∓ 3
PX
WR
PL
ε(T) = -6.1
b
0.5120
0.5117
0.5114
0.5111
0.5108
0
0.15
0.30
0
-5
-10
-15
-20
$^{143}Nd/^{144}Nd$
$^{147}Sm/^{144}Nd$
$\epsilon_{Nd}(0)$

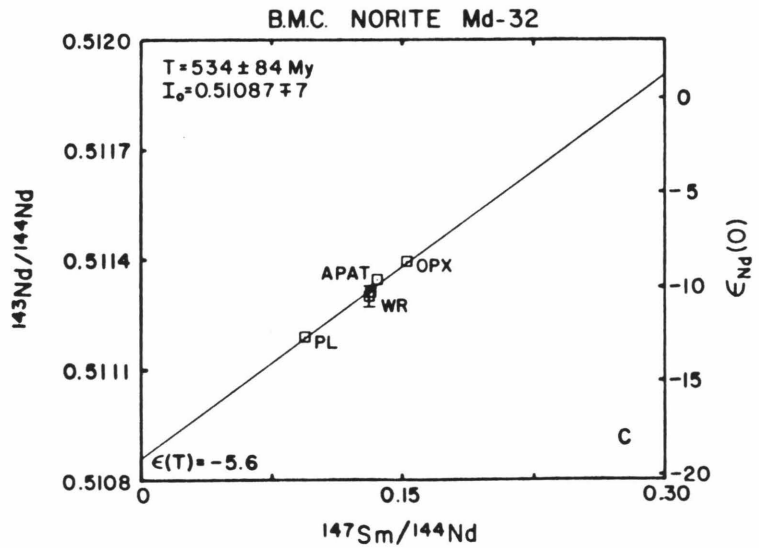
B.M.C. NORITE Md-32
T = 534 ± 84 My
I_o = 0.51087 ∓ 7
APAT
OPX
WR
PL
ε(T) = -5.6
c
0.5120
0.5117
0.5114
0.5111
0.5108
0
0.15
0.30
0
-5
-10
-15
-20
$^{143}Nd/^{144}Nd$
$^{147}Sm/^{144}Nd$
$\epsilon_{Nd}(0)$

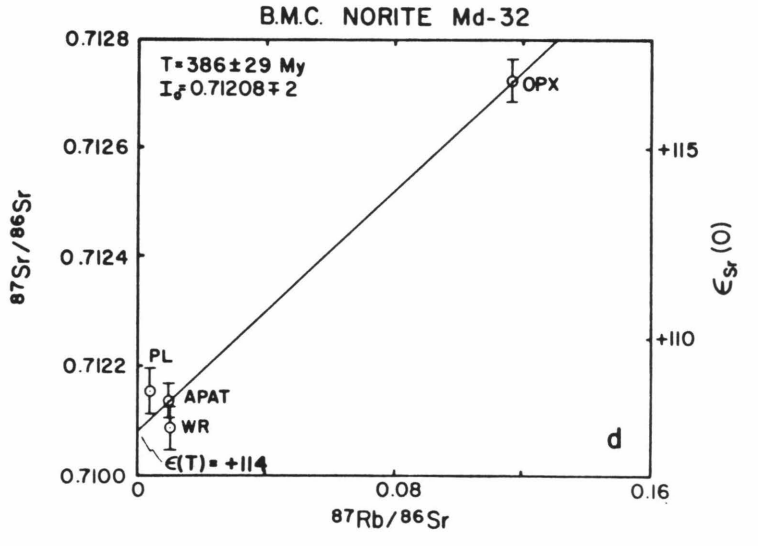
B.M.C. NORITE Md-32
T = 386 ± 29 My
I_o = 0.71208 ∓ 2
OPX
PL
APAT
WR
ε(T) = +114
d
0.7128
0.7126
0.7124
0.7122
0.7100
0
0.08
0.16
+115
+110
$^{87}Sr/^{86}Sr$
$^{87}Rb/^{86}Sr$
$\epsilon_{Sr}(0)$

The large error on the age for the isochron for Md-32 is due to the relatively small spread in Sm/Nd ratios which in turn is probably caused by small amounts of apatite in the plagioclase and orthopyroxene mineral separates. It is important to note that the initial $\varepsilon_{Nd}(T)$ values for these isochrons are different from one another and all are negative. However, the ages obtained for these three samples agree within error at ~ 490 my. This age is in good agreement with zircon U-Pb ages for the BMC [Sinha, pers. com, 1983]. An igneous crystallization age of 490±20 my is therefore assigned to the BMC. This places the time of magmatism prior to or at the earliest stages of the Taconic Orogeny. Samples from both the Susquehanna block (Md-32, Md-44) and the Baltimore block (Md-3) have ages that are identical within error, confirming the close relationship of these two exposures.

The results of Rb-Sr analyses on minerals from sample Md-32 are plotted in Fig. 3.5d. In contrast to the Nd isotopic system, the mineral data fail to define an Rb-Sr isochron with several different mineral phases. The slope is defined only by the orthopyroxene point and the cluster of points with low Rb/Sr ratio. A linear fit to the data yields an age of 386±28 My and a high initial $\varepsilon_{Sr}(T)$ = +114 (0.7121). Although it is tempting to identify this age with the time of metamorphism of the BMC, no age significance should be attached to these results unless further work produces a true isochron.

III.3.3 Whole rock data and discussion

The results of Sm-Nd analyses of whole rocks from the BMC are plotted in Fig. 3.6a and Rb-Sr results for the same samples in Fig. 3.6b. As can be seen from these figures, the whole rock data define neither Sm-Nd nor

Figure 3.6a. Sm-Nd evolution diagram with data for whole rock samples of the Baltimore Mafic Complex. Reference isochrons are drawn for 490 My and $\varepsilon_{Nd}(T) = -3$ and -6. Note the implied range in $\varepsilon_{Nd}(T)$ and general correlation about the 490 My isochron.

b. Rb-Sr evolution diagram with the data for whole rock samples of the Baltimore Mafic Complex. Reference isochron is drawn for 490 My and initial $\varepsilon_{Sr}(T) = +75$. Note the implied range in $\varepsilon_{Sr}(T)$ and limited range of Rb/Sr ratios.

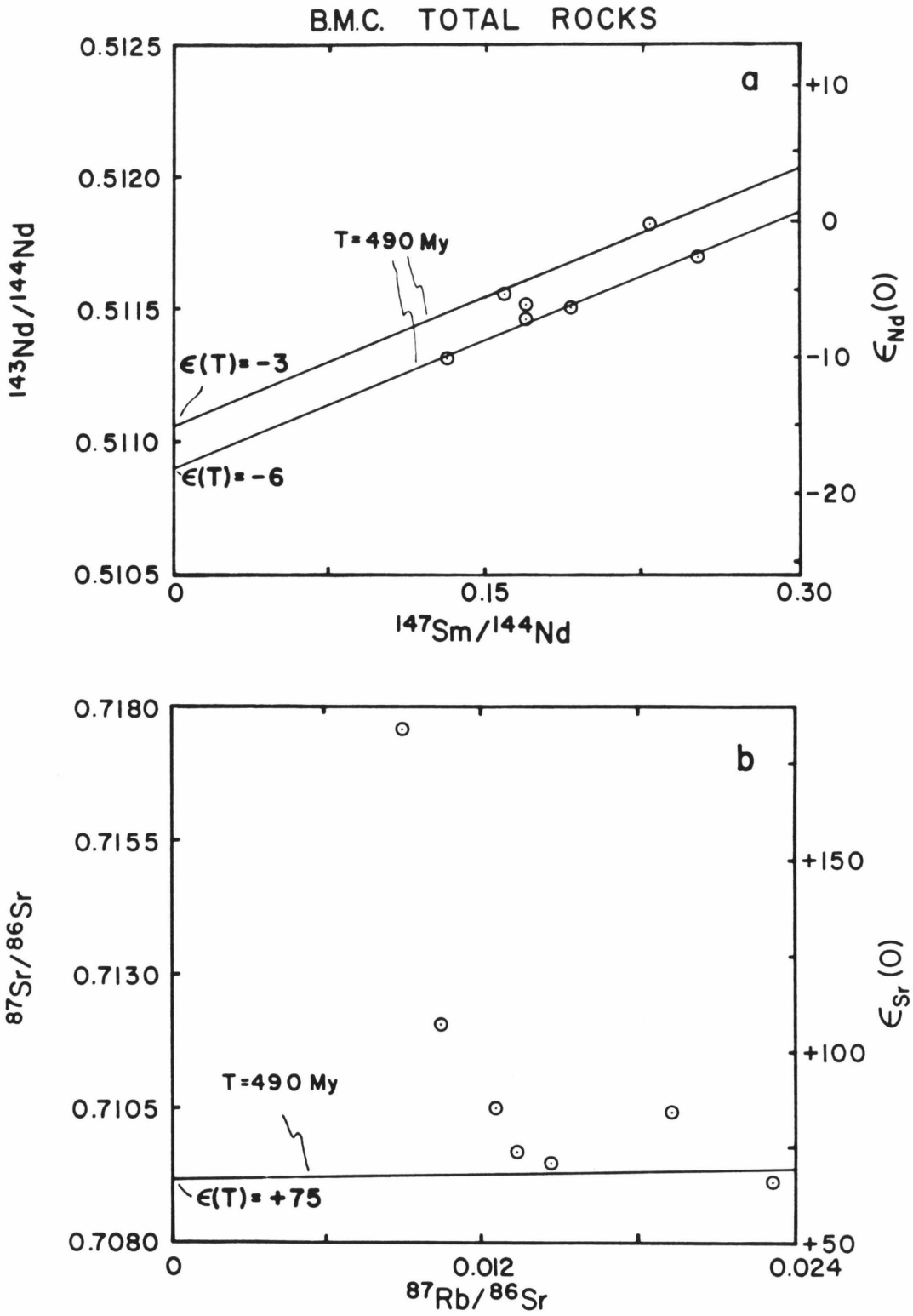
B.M.C. TOTAL ROCKS
a
0.5125
0.5120
0.5115
0.5110
0.5105
$^{143}Nd/^{144}Nd$
T=490 My
ε(T)=-3
ε(T)=-6
0
0.15
0.30
$^{147}Sm/^{144}Nd$
+10
0
-10
-20
$\epsilon_{Nd}(0)$
b
0.7180
0.7155
0.7130
0.7105
0.7080
$^{87}Sr/^{86}Sr$
T=490 My
ε(T)=+75
0
0.012
0.024
$^{87}Rb/^{86}Sr$
+150
+100
+50
$\epsilon_{Sr}(0)$

Figure 3.7. $\varepsilon_{Nd}(T)$ vs. $\varepsilon_{Sr}(T)$ diagram with data for Vermont, North Carolina Thetford, Baltimore and Bay of Islands (BOI) [Jacobsen and Wasserburg, 1979]. Vermont, North Carolina and Bay of Islands samples have the isotopic signature of oceanic crust. The Baltimore (BMC) samples fall on a trend suggesting contamination with continental crust. The Thetford Mines samples (TMC) do not show any obvious trend. Compare with Fig. 3.8.

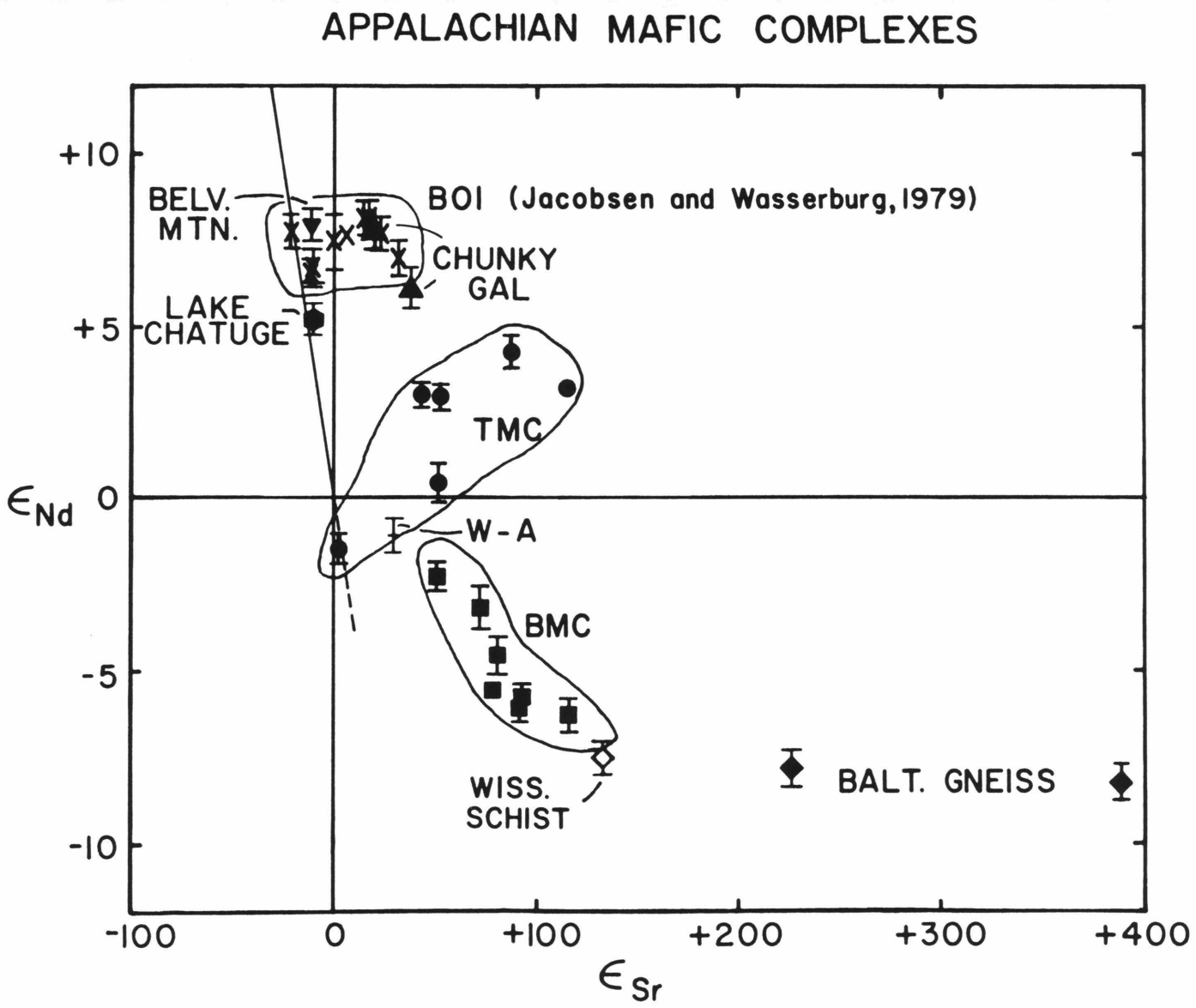
APPALACHIAN MAFIC COMPLEXES
+10
+5
0
-5
-10
ϵ_{Nd}
-100
0
+100
+200
+300
+400
ϵ_{Sr}
BELV. MTN.
BOI (Jacobsen and Wasserburg, 1979)
CHUNKY GAL
LAKE CHATUGE
TMC
W-A
BMC
WISS. SCHIST
BALT. GNEISS

Rb-Sr isochrons, as could have been anticipated from the variation in $\varepsilon_{Nd}(T)$ among the mineral isochrons. Instead, the Nd data vary from $\varepsilon_{Nd}(T)$ = -6.4 to -2.2 and the Sr data from $\varepsilon_{Sr}(T)$ = +115 to +51 (0.7120 to 0.7075) for an age of 490 My. The Nd data show a general correlation between $\varepsilon_{Nd}(0)$ and Sm/Nd about the 490 My reference isochron (Fig. 3.6a.) There is no obvious correlation in the Sr data (Fig. 3.6b).

These isotopic results clearly indicate that the BMC was not derived from depleted oceanic mantle. In particular, the negative values of $\varepsilon_{Nd}(T)$ and positive values of $\varepsilon_{Sr}(T)$ are most like the isotopic signature of old continental crust. The variation in initial isotopic composition of both Nd and Sr does not appear to correlate with stratigraphic position in the complex, rock type, or degree of metamorphism. Hanan [1980, 1981] has shown that $^{87}Sr/^{86}Sr$ ratios are shifted to higher values in metamorphic minerals along late stage fractures in the gabbro. These fractured rocks were avoided in the present study. It is clear from the attempt at an Rb-Sr mineral isochron (Fig. 3.5d) that there has been redistribution of Rb or Sr on a mineral scale during post-crystallization metamorphism. Nevertheless, for reasons which will be shown below, it is believed that the variation in whole rock initial Sr isotopic composition is a magmatic characteristic, and that on the scale of several centimeters, the whole rocks have remained largely closed systems since crystallization. That the variation in initial Nd isotopic composition is a magmatic characteristic is clearly demonstrated by the different initial values obtained for the Sm-Nd mineral isochrons. This interpretation rests on the assumption that the Sm-Nd mineral isochrons record both the time of crystallization from a melt and the melt's isotopic composition. It is possible that the mineral isochrons record a metamorphic event and that the initial isotopic composi-

tions are a result of large scale introduction of Nd and Sr from the surrounding rocks. Such a metamorphic event would have had to have occurred shortly after crystallization in order to account for the agreement between the Sm-Nd mineral isochron and U-Pb zircon ages. In addition, the samples chosen for isochron work have anhydrous, apparently igneous mineralogy (see Appendix II) implying granulite grade metamorphism. Without a hydrous fluid phase to mediate the process, it is unlikely that isotopic exchange can occur over a scale of kilometers. Furthermore, as will be shown below, amphibolite grade metamorphism, presumably in the presence of abundant fluid, did not appreciably disturb the Nd isotopic signature of mafic rocks from North Carolina and Vermont. Therefore, it is not believed that the Nd systematics of the BMC samples record a metamorphic event. The discussion which follows assumes that this is the case. In Fig. 3.7 the results for the BMC are plotted in an $\varepsilon_{Nd}(T)$ vs. $\varepsilon_{Sr}(T)$ diagram. The data define an array lying to higher $\varepsilon_{Sr}(T)$ than the mantle array with $\varepsilon_{Nd}(T)$ inversely correlated with $\varepsilon_{Sr}(T)$. It is this coherence, together with the assumption that the $\varepsilon_{Nd}(T)$ values are magmatic, that leads to the conclusion that the variation in $\varepsilon_{Sr}(T)$ is not due to later metamorphism. The trend in the ε_{Nd}-ε_{Sr} diagram is exactly what one would expect for contamination of a mantle-derived magma with high ε_{Sr} and low ε_{Nd}, old continental crust. Fig. 3.8 schematically illustrates this along with other contamination trends and the isotopic characteristics of endmember rock types. Hanan [1980] suggested that the radiogenic Sr isotopic compositions of the BMC are due to interaction with seawater. This is almost certainly not the case for two reasons: 1) Cambro-Ordovician seawater had $\varepsilon_{Sr} \sim +72$ (0.709) [Peterman et al., 1970; Burke et al., 1982] a value lower than the initial isotopic composition of several of the samples analysed here;
2) interaction with seawater is not expected to shift the Nd isotopic

composition by a significant amount until extremely high water/rock ratios are reached ($\sim 10^5$) due to the extraordinarily low concentration of Nd in seawater ($\sim 2\times10^{-12}$ g/g) [Goldberg et al., 1963; Høgdahl et al., 1968; DePaolo and Wasserburg, 1977]. The mixing line between oceanic crust and seawater is shown in Fig. 3.8. This process is thought to account for the spread of $\varepsilon_{Sr}(T)$ at essentially constant $\varepsilon_{Nd}(T)$ seen in Fig. 3.7 for the Bay of Islands data [Jacobsen and Wasserburg, 1979]. The data for the BMC rocks in Fig. 3.7 do not show this relationship. Instead, it appears that the Baltimore Complex magma was contaminated by or partially derived from older crustal material. Possible candidates for the contaminant are the Grenville age basement rocks exposed in several mantled gneiss domes in the Baltimore area, and the overlying metasediments. The results of analyses of the Baltimore gneiss and Wissahickon schist are plotted on Fig. 3.7 at the isotopic composition they would have had 490 My ago. It is clear from this figure that the Gneisses are suitable candidates for the contaminant in terms of their isotopic composition, as would be sediments or metasediments largely derived from Grenville age basement. The particular sample of Wissahickon schist analyzed appears to have too low a value of $\varepsilon_{Sr}(T)$ to be a reasonable bulk contaminant. Undoubtedly there exists a wide variation in both Rb/Sr and ε_{Sr} within the Wissahickon schist and it is likely that assimilation of portions of this formation could lead to the observed isotopic pattern.

Several other lines of evidence support the idea that the BMC magma was contaminated with older crustal material. Brown primary amphibole is common in the gabbro, suggesting a relatively high f_{H_2O} as might result from the assimilation of hydrous phases, and partially assimilated mafic xenoliths of uncertain origin are present in the upper portions of the

Figure 3.8. ε_{Nd} vs. ε_{Sr} diagram showing contamination trends and possible endmembers for mixing relationships. Isotopic composition of Cambro-Ordovician seawater from Peterman et al. [1970], Burke et al. [1982] and Hooker et al. [1981].

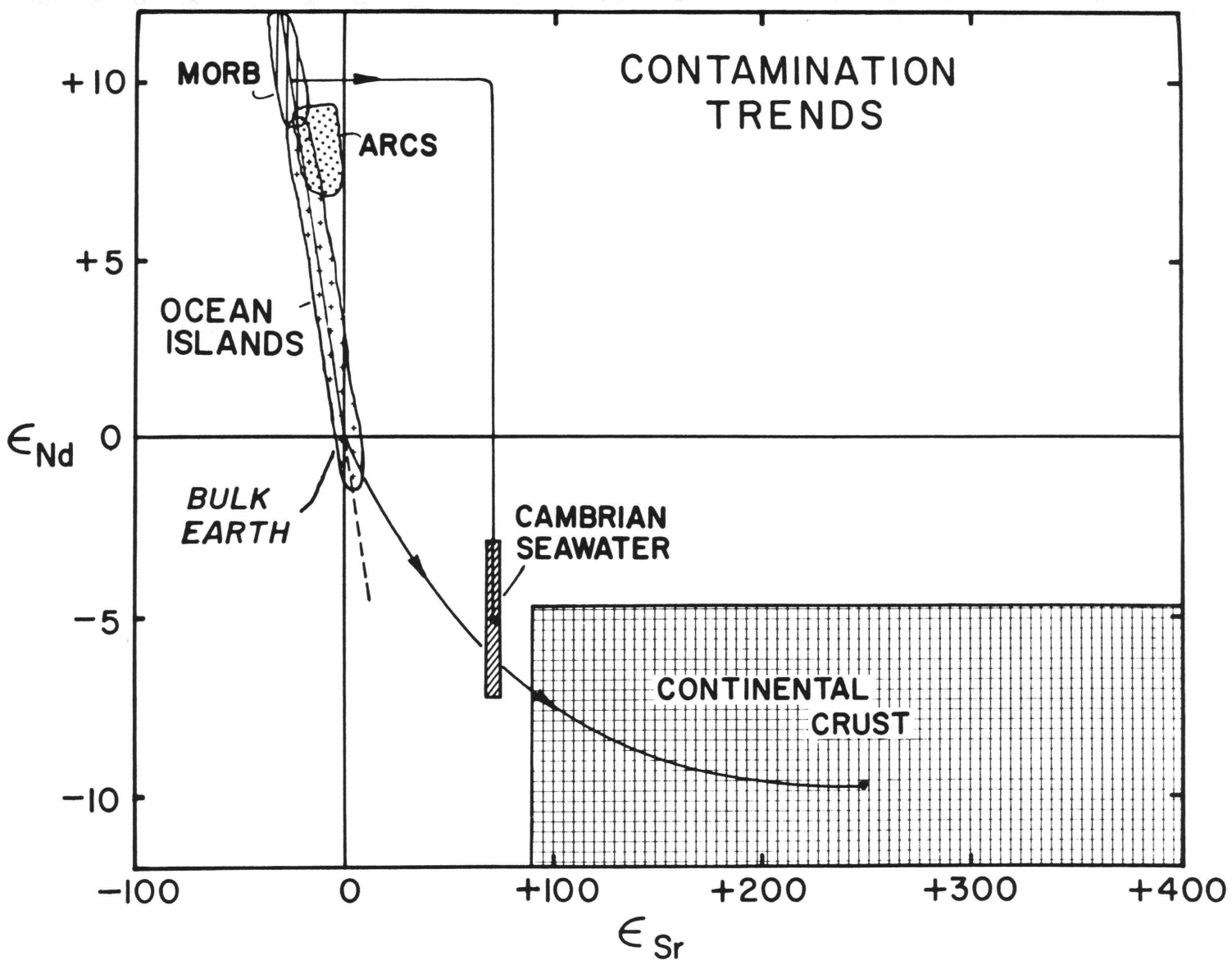
CONTAMINATION
TRENDS
MORB
ARCS
OCEAN
ISLANDS
BULK
EARTH
CAMBRIAN
SEAWATER
CONTINENTAL
CRUST
+10
+5
0
−5
−10
ϵ_{Nd}
−100
0
+100
+200
+300
+400
ϵ_{Sr}

gabbro [Hanan, 1980]. Further evidence is the observation originally due to Bowen [1928] that assimilation of aluminous rocks by basaltic magma should bring orthopyroxene onto the liquidus and increase the anorthite content of the crystallizing plagioclase at the expense of clinopyroxene crystallization according to the generalized reaction:

$$(SiO_2 + Al_2O_3) + CaMgSi_2O_6 = CaAl_2Si_2O_8 + MgSiO_3$$
$$\text{Aluminosilicates} + \text{Diopside} = \text{Anorthite} + \text{Enstatite}$$

More recent experimental work by Irvine [1975] has substantiated Bowen's observation. Both the early appearance of orthopyroxene in the crystallization sequence and high anorthite content of the plagioclase are characteristics of the BMC. Taken to its extreme, this mechanism should produce norites. Note that Md-32, a norite sample, is also the most enriched in incompatible elements of the samples analyzed, as evidenced by the presence of zircon and apatite. This sample also has the highest $\varepsilon_{Sr}(T)$ and lowest $\varepsilon_{Nd}(T)$ and would thus represent the most contaminated sample analyzed. The T^{Nd}_{CHUR} model age for this sample is 1.2 AE, close to that calculated for the samples of Baltimore Gneiss (~ 1.26 AE, see III.4), suggesting that assimilation of the Baltimore Gneiss or a rock with similar isotopic characteristics caused the variation in initial isotopic composition of the BMC. A calculation for simple mixing between a magma with $\varepsilon_{Nd} = \varepsilon_{Sr} = 0$, and 5 ppm Nd, 100 ppm Sr and a contaminant with $\varepsilon_{Nd} = -8$, $\varepsilon_{Sr} = +300$, 50 ppm Nd and 200 ppm Sr shows that > 25% bulk assimilation is necessary to account for the most contaminated samples. This is a rather large amount. This calculation is clearly an oversimplification but serves to give a sense of the magnitude of the effect. A more realistic calculation would include the effects of combined assimilation/fractionation and

selective melting in the contaminant as well as incorporating other isotopic and trace element constraints. In the absence of information on liquid compositions during the evolution of the BMC magma, however, such a detailed calculation is not warranted. Furthermore, the lack of correlation between isotopic composition and rock type or position in the crystallization sequence suggests that the BMC magma chamber was chemically and isotopically heterogeneous and that the magma was therefore not well-mixed, thus this basic assumption of most mixing models cannot be justified in the case of the BMC.

Having documented the probable role of continental crustal material in the genesis of the BMC, one may now ask in what tectonic settings such a process might operate. From the preceding arguments, it appears that the complex did not form at an oceanic spreading center and is therefore not an ophiolite if that term is considered to mean obducted oceanic crust. The remaining possibilities include oceanic island volcanism, subduction-zone related volcanism and continental mafic intrusion of an unspecified nature (not related to a subduction zone). Oceanic island volcanism is an unlikely candidate on the basis of these isotopic data. Although oceanic island basalts are often derived from less depleted mantle sources than normal MORB or a mixture of depleted and enriched mantle, the large negative $\varepsilon_{Nd}(T)$ together with large positive $\varepsilon_{Sr}(T)$ characteristic of the BMC have not been found among oceanic island rocks. The most enriched oceanic island alkali basalts measured to date have $\varepsilon_{Nd} = -5.7$, $\varepsilon_{Sr} = +17$ [Dosso and Murthy, 1980] while the BMC has $\varepsilon_{Sr}(T) \sim +100$ for $\varepsilon_{Nd} \sim -6$. This is simply a statement of the fact that in an ε_{Nd} vs. ε_{Sr} plot, the BMC data lie far to the right of the mantle array (Fig. 3.7).

Subduction related magmas have two mechanisms whereby interaction with continental crustal material may occur: by subduction of continent-derived sediments and by intrusion into continental crust. Although subduction and subsequent melting of sediments has often been called upon to explain some features of andesitic magmas and is probably an important mechanism in their genesis [Brown et al., 1982], it is unlikely that sufficient sediment could be carried down with the subducting plate to produce the strong continental signature seen in the BMC. This possibility cannot be ruled out, however, as the work of Whitford [1975] and Whitford et al. [1977, 1979] has shown that some andesites of the Sunda-Banda Arc, Indonesia, have strongly positive values of $\varepsilon_{Sr}(0)$ and negative values of $\varepsilon_{Nd}(0)$, probably due to large amounts of continental detritus from Australia being subducted beneath the arc. In general, however, only those arcs which are built upon thick continental crust, such as the Andes, have negative ε_{Nd} and positive ε_{Sr} similar to the Baltimore samples. Studies by DePaolo and Wasserburg [1977] and James [1982] of Andean volcanics and Nohda and Wasserburg [1981] of Japanese volcanics have also appealed to contamination by continental material during intrusion in order to explain the observed isotopic and trace element compositions. The last case, continental mafic intrusion of an unspecified nature, is no different in contamination mechanism from the case of a continental arc. Studies of the Stillwater Complex of Montana [DePaolo and Wasserburg, 1979], the Shabogamo Intrusive Suite of Labrador [Zindler et al., 1981], the Kalka Intrusion of Central Australia [Gray et al., 1981] and the Cortlandt Complex of New York [Domenick and Basu, 1982] have similarly suggested on the basis of Nd isotopic evidence that crustal contamination played a role in the genesis of these mafic intrusions.

It is emphasized that the negative values of $\varepsilon_{Nd}(T)$ for the BMC samples rule out a depleted mantle source for the complex, and that the Complex is therefore not a fragment of typical oceanic crust. On the basis of these isotopic data it appears likely that the BMC was intruded into continental crust, possibly as part of a Cambro-Ordovician arc complex, and was contaminated by old LREE enriched crustal material with $\varepsilon_{Nd} << 0$ during emplacement. Its present allochthonous nature [Crowley, 1976] must be due to post-crystallization tectonic movements not related to obduction of oceanic crust. Deep seismic profiles across the Appalachians in Georgia have shown that the entire Piedmont and the Blue Ridge there is allochthonous, having been thrust up to several hundred kms westward over an essentially flat-lying shelf sequence [Cook *et al.*, 1979; Cook and Oliver, 1981]. In addition to the master thrust surface, the profiles also show that the Piedmont is made up of many thrust sheets separated by smaller faults, some of which splay off from the master thrust. Although it is not clear that this structural style can be confidently extrapolated to the Maryland Piedmont, similar thrusting may account for the present position of the BMC.

III.4 Baltimore Gneiss and Wissahickon Formation

It is worthwhile to digress slightly and examine the isotopic results obtained on the Baltimore Gneiss and Wissahickon Fm. in more detail. The samples of basement gneiss Md-7 and Md-11 (Table 3.3) are typical of old upper continental crust and have negative $\varepsilon_{Nd}(0)$ and large positive $\varepsilon_{Sr}(0)$ reflecting the upper crust's LREE- and LIL-enriched nature [McCulloch and Wasserburg, 1978]. The T^{Nd}_{CHUR} model ages for these samples are 1.25 and 1.27 AE which are quite reasonable for Grenville age crust [Tilton *et al.*,

1958, 1970; Grauert, 1974], and appear to accurately reflect the time of crustal formation. Previous isotopic work on the Gneiss has pointed up the complex history of the basement complex: K-Ar and Rb-Sr mineral systems were reset by metamorphic events in the interval 300-500 My ago [Wasserburg et al., 1957; Wetherill et al., 1968], and the U-Th-Pb systematics of zircons show complex patterns of discordance due to episodic and continuous lead loss as well as possible inheritance of older Pb [Tilton et al., 1958, 1970; Grauert, 1974]. The T^{Nd}_{CHUR} model ages appear to be able to see past these later disturbances to the original time of crustal formation of the Grenville Province at ~ 1.25-1.30 AE. Note that there is no evidence for recycling of much older continental crust to form the Baltimore Gneiss. T^{Sr}_{UR} ages (at 1.37 AE and 1.11 AE) are generally less reliable but in this case are close to the T^{Nd}_{CHUR} ages. The sample of Wissahickon schist has T^{Nd}_{CHUR} = 1.04 AE, T^{Sr}_{UR} = 1.72 AE. The Nd model age implies that the Wissahickon sediments were dominantly derived from Grenville age basement such as the Baltimore Gneiss. The Wissahickon schist is known to have been metamorphosed at ~ 330 My from K-Ar studies [Lapham and Bassett, 1964].

III.5 Thetford Mines Complex

III.5.1 Geologic setting

The ophiolites of southern Quebec lie at the southern end of the Baie Verte-Brompton line [St. Julien et al., 1976], a narrow zone of mafic and ultramafic rocks extending from northwest Newfoundland to northern Vermont. Throughout much of its intermediate portion, in the Gaspe Peninsula, the zone is covered by younger Siluro-Devonian metasedimentary rocks (see Fig. 3.1). In Quebec, where the Baie Verte-Brompton line reappears

from under its cover, the backbone of the mafic/ultramafic exposures is formed by the large ophiolitic complexes near Thetford Mines, Asbestos, and Orford. These rocks lie sandwiched between a Cambro-Ordovician shelf sequence to the west and a chaotic ophiolitic melange (St. Daniels Fm.) to the east [Laurent, 1975, 1977]. The Quebec ophiolites are strongly deformed, however, at least at Thetford Mines, the entire ophiolite stratigraphy is present in one more or less continuous package of rocks. The lowermost unit consists of tectonized harzburgite cut by dunnitic dikes and is underlain by a thin, discontinuous sole of amphibolite with a metamorphic gradient increasing toward the ophiolite [Clague et al., 1981]. Above the harzburgite are layered dunites, chromitites, pyroxenites and gabbros. In the intrusive portion of the Complex, the crystallization sequence appears to be: olivine (+ chromite), olivine + clinopyroxene, olivine + clinopyroxene + orthopyroxene, olivine + clinopyroxene + plagioclase, clinopyroxene + plagioclase (+ hornblende). Lying on top of the cumulates is a zone of static gabbro intruded by mafic dikes and sills. Although similar to dike complexes described from other ophiolites, these shallow intrusives do not form a sheeted dike complex. Finally, the sequence is capped by two groups of pillowed basalts separated by a zone of red chert and argillite. The lower lava group is characterized by high Mg, Cr, Ni and is very poor in K, Ti, and P [Laurent, 1977]. The upper pillows are generally smaller and are set in a matrix of epidotized pyroclastic debris. Chemically, the lavas range from basaltic to andesitic [Laurent, 1977]. The entire Complex has been metamorphosed to greenschist facies. Preservation of the original igneous mineralogy varies considerably. Samples of each of the major lithologies with varying degrees of metamorphism have been analysed. Petrographic descriptions of the samples are given in Appendix II along with a description of procedures.

III.5.2 Whole rock data and discussion.

The results for the Thetford Mines Complex (TMC) samples are presented in Table 3.3 and Figures 3.7 and 3.9. It was impossible to obtain a mineral isochron for the TMC due to the pervasive low-grade metamorphic overprint throughout the Thetford area. Conventional K-Ar and $^{40}Ar/^{39}Ar$ incremental heating techniques have yielded an age of ~ 490 my for the metamorphic aureole underlying the TMC [Clague et. al, 1981]. This age presumably dates the time of emplacement of the ophiolite and places a younger limit on the crystallization age of the Complex itself. For the purposes of calculating initial isotopic ratios, an age of 500 my has been assumed. With the exception of Qe 24 (a cumulate clinopyroxenite), all the samples analysed have approximately chondritic Sm/Nd ratios. The calculation of $\varepsilon_{Nd}(T)$ values is therefore nearly independent of the assumed age. As can be seen in Fig. 3.9a, the whole rock samples from Thetford do not define an isochron in either the Sm-Nd or Rb-Sr evolution diagrams. Using the assumed age, one calculates very variable initial isotopic compositions with $\varepsilon_{Nd}(T)$ = +4.2 to -1.5, $\varepsilon_{Sr}(T)$ = -2.6 to +114 (0.7041 to 0.7119). Furthermore, as can be seen in this Figure 3.7, there is no clear correlation between $\varepsilon_{Nd}(T)$ and $\varepsilon_{Sr}(T)$. Like the BMC, the isotopic composition of the Thetford samples does not appear to correlate with rock type, position within the complex, or degree of metamorphism. The range in isotopic composition characteristic of the TMC is not the signature of oceanic crust. Neither can the variations in isotopic composition be generated by simple mixing of oceanic crust with old continental crustal or seawater Sr and Nd. More complicated processes appear to be involved. The TMC is unquestionably an ophiolite sensu stricto in that the complex

Figure 3.9a. Sm-Nd evolution diagram with data for whole rock samples of the Thetford Mines Complex. Reference isochrons are drawn for 500 My and $\varepsilon_{Nd}(T) = +4$ and 0. Note the implied range in $\varepsilon_{Nd}(T)$.

b. Rb-Sr evolution diagram with data for whole rock samples of the Thetford Mines Complex. Reference isochron is drawn for 500 My and $\varepsilon_{Sr}(T) = 0$. Note the implied range of $\varepsilon_{Sr}(T)$ and wide variation in Rb/Sr ratios.

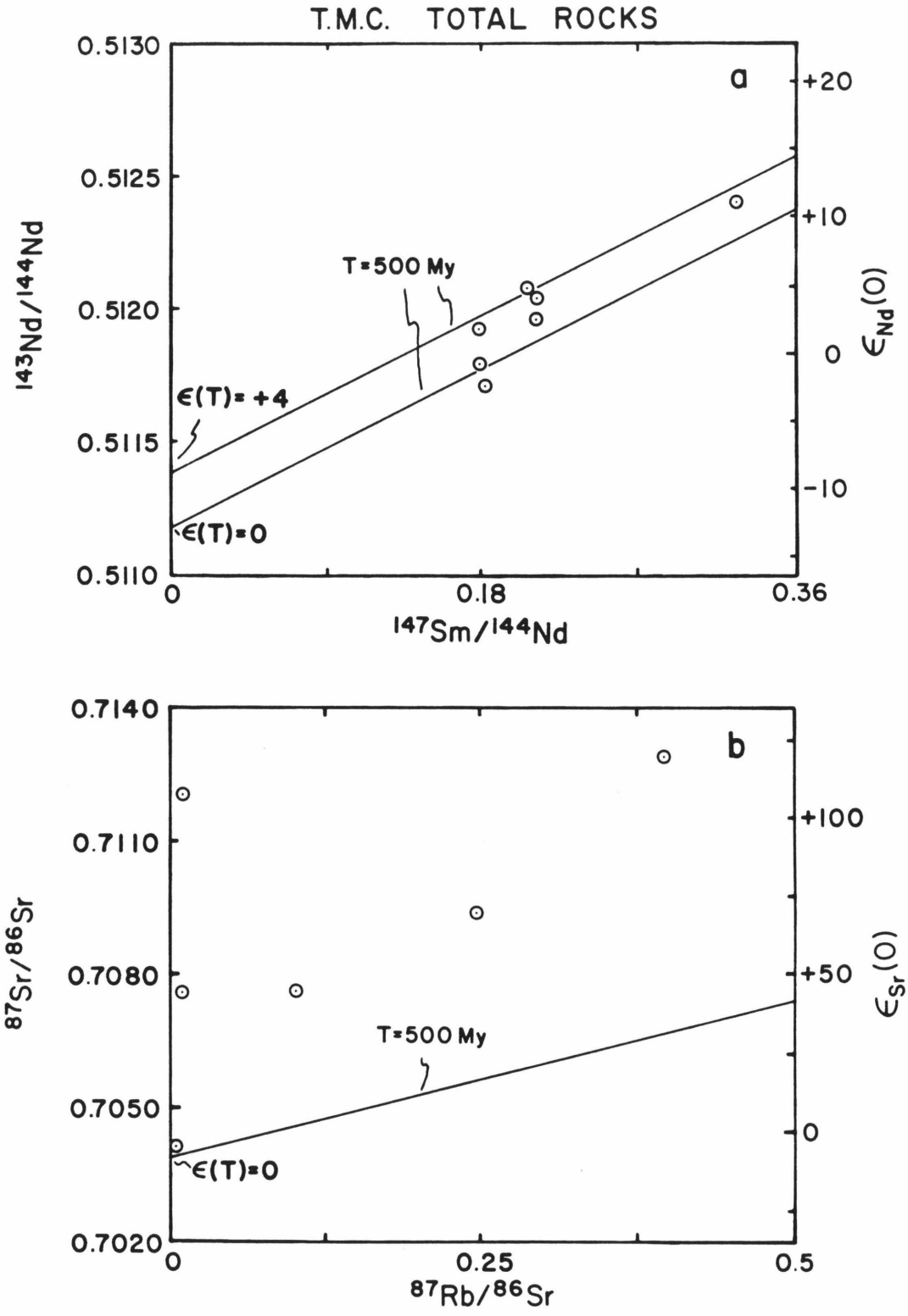
T.M.C. TOTAL ROCKS
a
0.5130
0.5125
0.5120
0.5115
0.5110
$^{143}Nd/^{144}Nd$
T=500 My
ε(T)= +4
ε(T)=0
0
0.18
0.36
$^{147}Sm/^{144}Nd$
+20
+10
0
-10
$\epsilon_{Nd}(0)$
b
0.7140
0.7110
0.7080
0.7050
0.7020
$^{87}Sr/^{86}Sr$
T=500 My
ε(T)=0
0
0.25
0.5
$^{87}Rb/^{86}Sr$
+100
+50
0
$\epsilon_{Sr}(0)$

includes all the elements of the ophiolite stratigraphy. It thus appears that the isotopic and field geologic relationships are in opposition. It is not thought that metamorphism is the primary cause of the variations in isotopic composition in the Nd system. Ophiolites with similar metamorphic histories such as the Josephine Ophiolite and the Kings-Kaweah Ophiolite of California, which have metamorphic assemblages similar to the TMC, preserve the Nd signature and, to a lesser extent, the Sr isotopic signature of oceanic crust (Table 3.1) [Chen and Shaw, 1982]. Furthermore, as will be shown below, relatively high-grade amphibolites from North Carolina and Vermont also preserve the Nd isotopic characteristics of their depleted mantle source. The present data, however, do not exclude the possibility that metamorphism has altered the primary Nd isotopic composition of the TMC On the other hand, the case for the observed Sr isotopic compositions being primary is rather poor. Sr isotopic exchange during metamorphism is a well-documented process [Lanphere et al., 1964, and many later studies] and interaction with metamorphic fluids derived from dehydration reactions in metasedimentary rocks will generally increase the $^{87}Sr/^{86}Sr$ ratio in mantle-derived rocks. Unlike the Baltimore samples, there is no apparent correlation between $\varepsilon_{Nd}(T)$ and $\varepsilon_{Sr}(T)$, suggesting that the behavior of these systems is decoupled. Several of the samples analyzed contained secondary calcite which might be expected to have a large effect on the Sr isotopic composition of the bulk rock, although the presence of calcite does not appear to correlate with $\varepsilon_{Sr}(T)$ or $\varepsilon_{Sr}(0)$. In addition, the samples have quite a wide range of Rb/Sr ratios, possibly indicating rather large Rb-Sr fractionation during metamorphism. In short, the Sr isotopic system cannot be counted upon to preserve primary isotopic composition in complex metamorphic terrains and the following discussion will concentrate on the significance of the Nd data.

Although the isotopic composition of the TMC is unusual for an ophiolite, it is not unique. Recent studies of the Vourinous Complex, Greece [Noiret et al., 1981; Richard and Allegre, 1980], the Troodos Ophiolite, Cyprus [Hannah and Futa, 1982], and the Bett's Cove Ophiolite, Newfoundland [Coish et al., 1982] have shown that, in part, they are also characterized by rocks with $\varepsilon_{Nd}(T)$ between 0 and +4 and with relatively radiogenic Sr, although the latter is usually attributed to interaction with seawater. Both the Troodos and Bett's Cove ophiolites were also found in these studies to include rocks with a more normal oceanic signature of $\varepsilon_{Nd} \sim +8$, a characteristic not seen in the Thetford samples analyzed. The significance of these results for ophiolite genesis is not clear. The implication is that there are ophiolites of varying ages which were derived from a mantle source with modestly positive ε_{Nd} or from a blend of magmas derived from normal depleted oceanic mantle and an enriched reservoir such as enriched mantle, undepleted mantle or continental crust. These characteristics have been attributed to the source for many oceanic island basalts [O'Nions et al., 1977; Dosso and Murthy, 1980]. A mixture of sources might also be expected for arcs and the magmas intruded during the initial stages of continental rifting to form an ocean basin or marginal basin. The latter cases would also allow for interaction of the mantle-derived magma with continental crust.

Church [1977] has pointed out that the TMC is chemically similar to the Bett's Cove ophiolite of Newfoundland [Coish and Church, 1979] in that they are characterized by the presence of orthopyroxene-bearing cumulates and relatively low Ti-basalts, among other features. He contrasts these complexes with ophiolites characterized by dunite-troctolite cumulate sequences and relatively Ti-rich basalts with olivine and plagioclase

phenocrysts such as the Bay of Islands Ophiolite. He further identifies these two endmembers with the ophiolites of the internal and external zones, respectively, of the Tethys region [Rocci et al., 1975]. The isotopic data presented here and the previously mentioned studies seem to indicate that there is a fundamental difference in origin between the two endmembers as defined by Church, but it is unclear what this difference signifies. Clearly, more work is needed to establish the links between the variations in major and minor element geochemistry and isotopic systematics of these ophiolites and to attempt to relate these to modern analogues. Among modern rocks, these complexes have isotopic and chemical affinities to boninites, which are olivine, orthopyroxene, and clinopyroxene-phyric island arc basalts with high MgO and SiO_2 contents but low TiO_2 contents [Kuroda and Shiraki, 1975; Shiraki and Kuroda, 1977]. Recent Nd isotopic data obtained by Hickey and Frey [1982] has shown that boninites, like the Thetford Mines samples, are characterized by a large range in $\varepsilon_{Nd}(0)$ (-0.3 to +6.2) which they attribute to mixing between a strongly depleted mantle peridotite and an enriched component; either subducted sediments or metasomatized, LREE enriched mantle. The TMC may, in part, represent the ancient intrusive and extrusive counterpart to modern boninites and would thus represent an arc complex. Ongoing field and geochemical studies by Laurent and co-workers now suggest that this may indeed be the case [Laurent, pers. com., 1983].

In summary, the Nd and Sr isotopic data from the TMC are not easily reconciled with the geologic relationships. At face value, they preclude the formation of the complex at a normal mid-ocean spreading center. Nevertheless, it is possible that the metamorphism and alteration was so severe that all primary isotopic memory has been erased.

III.6 Mafic rocks from Vermont and North Carolina.

III.6.1 Geologic setting.

In contrast to the large mafic/ultramafic complexes discussed above, this section presents the results of analyses on what are perhaps more typical occurrences of mafic rocks in the Appalachians. By far the majority of the mafic/ultramafic rocks in the orogen occur as small bodies. Samples from four such bodies have been analysed: the Hazens Notch Amphibolite from the Belvidere Mountain Complex, Vt. [Laird, 1977; Chidester et al., 1978; Laird and Albee, 1981]; websterite from the type locality at Webster-Addie, North Carolina [Miller, 1953; Stueber, 1969]; the Chunky Gal Amphibolite from the Buck Creek dunite body, N. C. [Hadley, 1949; Sailor and Kuntz, 1973; McElhaney and McSween, 1983]; and amphibolite from the nearby Lake Chatuge complex, N. C.-Georgia [Hartley, 1973; Jones et al., 1973]. Sample descriptions are given in Appendix III.

The Hazens Notch Amphibolite at Belvidere Mtn. is associated with an extensively serpentinized and rodingitized ultramafic body approximately 3.4 x 1.8 km in size located ~ 200km south of the Thetford Mines Complex on the extension of the Baie Verte-Brompton line. Due to metamorphism and deformation, the genetic relationship between the amphibolite and ultramafic, if any, is unclear. The amphibole in the sample analysed is strongly zoned with barroisitic cores and actinolitic rims [Laird and Albee, 1981], recording a high pressure (> 8 kb) Ordovician metamorphic event followed by a lower temperature and pressure retrograde event, probably during Devonian time.

The amphibolites from North Carolina occur within a belt of mafic and ultramafic rocks in the eastern Blue Ridge province. At the Buck Creek and

Lake Chatuge bodies (each about 7 km in diameter), cores of serpentinized dunite and corona troctolite are enveloped by amphibolite, apparently derived from a troctolitic or gabbroic protolith [McElhaney and McSween, 1983]. As in Vermont, two metamorphic events, probably of Ordovician (granulite to upper amphibolite facies) and Devonian (greenschist facies) age are recorded by the amphibolites. Portions of the contacts between these complexes and the surrounding gneisses are interpreted as major thrust faults.

The Webster-Addie ultramafic body consists of a ring-shaped outcrop pattern of websterite, dunite, and orthopyroxenite ~ 3 x 2 km in size. The maximum width of ultramafic outcrop is ~ 0.7 km. The present outcrop pattern is apparently due to doming of an originally sheet-like mass of ultramafic rocks. Contacts with the enclosing gneiss are faulted and the rocks surrounding the contact strongly granulated [Miller, 1953].

III.6.2 Isotopic results.

Isotopic results for the North Carolina and Vermont samples are presented in Table 3.3 and Figure 3.7. An age of 500 My is again assumed for the purpose of calculating $\varepsilon(T)$ values for these samples. Although this may be in error by as much as ±100 My, in the worst case (XTC-127, leached residue) this corresponds to a shift of only ∓ 1 ε-unit in $\varepsilon_{Nd}(T)$ and does not affect the conclusions.

The samples of amphibolite from the Lake Chatuge district and Chunky Gal amphibolite have initial $\varepsilon_{Nd}(T)$ in the range +5.1 to +7.7. The $\varepsilon_{Sr}(T)$ values for the Chunky Gal amphibolites are moderately radiogenic at +20 and +38 (0.7053 and 0.7066) while the Lake Chatuge Sample has $\varepsilon_{Sr}(T) = -13$ (0.7030). These samples do not define Sm-Nd or Rb-Sr whole rock

isochrons. The Hazens Notch amphibolite sample is similar with $\varepsilon_{Nd}(T) = +8$ and $\varepsilon_{Sr}(T) = -12$.

In contrast to the results for the Baltimore Mafic Complex and Thetford Mines Complex, these amphibolites clearly have the isotopic signature of ancient oceanic crust. In Fig. 3.7, these data generally fall within the field defined by the Bay of Islands complex [Jacobsen and Wasserburg, 1979] although the Lake Chatuge sample has a somewhat lower value of $\varepsilon_{Nd}(T)$ than the other samples. The sample of Hazens Notch amphibolite from Vermont also plots within this field. These samples all have characteristically oceanic values of $\varepsilon_{Nd}(T) > +5$ for T = 500 My but extend from the mantle array to more radiogenic values of $\varepsilon_{Sr}(T)$. The dispersion in $\varepsilon_{Sr}(T)$ may be due to either hydrothermal interaction with seawater or continental metamorphic fluids or both. Previous Sr isotopic work by Stueber [1969] and Jones et al. [1973] has shown that the Sr isotopic composition of ultramafic and mafic rocks from North Carolina is in some cases considerably more radiogenic than plausible seawater values. In addition, these studies suggested that the increase in $^{87}Sr/^{86}Sr$ ratios was correlated with the degree of metamorphism; samples of unmetamorphosed troctolite and dunite had lower isotopic ratios than their metamorphic equivalents, amphibolite and serpentinite. If true, this would clearly indicate exchange of Sr during metamorphism. It is important to note, however, as has been observed in other studies of ophiolite complexes [Jacobsen and Wasserburg, 1979; McCulloch et al., 1981; Chen and Shaw, 1982], that even though the Sr system shows evidence for substantial post-crystallization isotopic exchange, the Nd system appears to preserve the primary isotopic composition, even at the relatively high grade of metamorphism represented by the Vermont and North Carolina amphibolites. This

fact encourages the belief that the Nd isotopic variations observed in the BMC and TMC are primary and not due to later exchange processes.

The results on the Vermont and North Carolina amphibolite samples are significant in that they demonstrate that there are mafic rocks in the Appalachians which are derived from a depleted mantle source and which, at least on isotopic grounds, are good candidates for being fragments of oceanic crust. The isotopic evidence, however is only permissive; mafic rocks derived from a depleted mantle reservior also occur in continental flood basalt provinces [Carlson et al., 1981]. However, when considered together with their association with ultramafic rocks and the general tectonic setting of these amphibolites, an oceanic origin appears likely, perhaps as blocks within an ophiolitic melange.

In order to assess the possibility of contamination along grain boundaries during serpentinization and metamorphism, a split of the powdered Webster-Addie sample was leached briefly in cold 0.1M HCl, rinsed in water, then leached for one hour in sub-boiling 1.5M HCl. The insoluble residue was then analysed. The unleached websterite has $\varepsilon_{Nd}(T) = -1.1$, $\varepsilon_{Sr}(T) = +29.2$ (0.7060) and is slightly LREE depleted. Approximately half of the REE were removed by leaching the sample and the leached residue was strongly LREE depleted (Table 3.3). The measured $^{143}Nd/^{144}Nd$ value, however, increased from the unleached to the leached sample so that the calculated $\varepsilon_{Nd}(T)$ is identical within error for both samples. Leaching the sample has apparently selectively dissolved a relatively LREE enriched phase. No evidence was found for a component with a high value of $\varepsilon_{Nd}(T)$. This sample is clearly different from the nearby amphibolites and does not have the signature of the depleted mantle source typical of oceanic rocks. The leaching experiment shows that the low $\varepsilon_{Nd}(T)$ is not

due to the presence of Nd derived from surrounding metamorphic rocks on grain boundaries. It is difficult to draw any firm conclusions about the origin of the Webster-Addie body on the basis of this single sample; however, the isotopic data do not support an origin at a mid-ocean spreading center.

III.7 Conclusions.

From Sr and Nd isotopic analyses it appears that there is no single origin for the mafic and ultramafic rocks of the Appalachians. The isotopic data support the earlier notions of ensialic mafic intrusions in the case of the Baltimore Mafic Complex, while clearly supporting an oceanic origin for the Bay of Islands Ophiolite, the Belvidere Mountain Complex, and some of the North Carolina bodies. The Thetford Mines Complex appears to belong to a class of ophiolites with peculiar isotopic, and possibly chemical, characteristics, which have affinities to modern-day boninitic rocks found in oceanic arcs. The isotopic data would tend to rule out the formation of these complexes at a mid-ocean spreading center. These conclusions are critically dependent on the observation that the Nd isotopic system appears relatively immune to disturbance during metamorphism and thus preserves the original igneous isotopic signature. Nevertheless, even if the observed isotopic systematics represent a metamorphic effect, these data provide no supportive evidence for an oceanic crustal origin for the Baltimore Mafic Complex, Thetford Mines Complex, or the Webster-Addie body. In contrast, the Sr isotopic system alone is relatively undiagnostic as to the origin of rocks in metamorphic terranes due to the relative ease with which Rb and Sr are mobilized during

metamorphism. The Nd isotopic system can readily be exploited in favorable cases to obtain ages on mafic rocks. When applied to samples of the BMC, this technique yields an age of 490±20 My for this body which is interpreted as the time of crystallization. Old continental crust has a distinctive isotopic signature and combined Nd-Sr isotopic studies provide a sensitive test for the presence of assimiliated crust in igneous bodies. The results on the BMC indicate that a significant fraction of the Nd and Sr in the Complex was derived from old continental material such as the Baltimore Gneiss.

In summary, studies of Appalachian geology have reached a point where the diversity in origins for the mafic and ultramafic rocks of this mountain belt must be recognized and explained. It would appear that simple models involving only obduction of ridge-generated oceanic crust are inadequate to explain the observations. Finally, it is cautioned that not every mafic and ultramafic rock in an orogenic belt is part of an ophiolite nor are all ophiolites formed at mid-ocean spreading centers.

CHAPTER IV

Sm-Nd and Rb-Sr Isotopic Systematics of Marine Phosphates and Carbonates

IV.1 Introduction

The oceans, by receiving the dissolved and suspended load of rivers and by being cycled through hydrothermal circulation systems at oceanic ridges, are constantly imprinted with a record of the upper continental and oceanic crusts. This record can be read in both the detrital sediments filling the ocean basins and in the chemistry of the phases which form from seawater by direct precipitation or by biologic production. This chapter is an attempt to find and read a portion of that record which contains the history of the Nd isotopic composition of seawater as a function of time. If such a record exists, it would reflect the Nd isotopic composition, and hence something about the age of the exposed crust, particularly continental crust as will be shown below. Knowing this would place important constraints on the growth history of the continents. It may also be possible to use the differences in Nd isotopic composition between different ancient oceans to constrain plate reconstructions and as a paleo-oceanographic tool. Although not the main thrust of this work, the analyses presented here also have application to the problem of the transport of REE in the marine environment.

In order to construct the record of Nd isotopic composition in seawater over time, a phase must be identified which contains Nd with the same isotopic composition as seawater at the time of its formation, preserves that composition through sedimentation and diagenesis, and which

is relatively common on the sedimentary record. $CaCO_3$ (calcite and aragonite) and apatite are examined as possible such phases in this chapter.

There have been two previous attempts at establishing the isotopic composition of Nd in past ocean water [Hooker et al., 1981; Chyi et al., 1982]. Both of these studies based their estimates on analyses of metalliferous sediments associated with ophiolites. Their results will be discussed in sections IV.4.4. and IV.5.

IV.2 REE in modern seawater: Implications for ancient seawater.

IV.2.1 Nd isotopic composition.

In order to understand the significance of the Nd isotopic composition of ancient seawater, it is, of course, necessary to have an understanding of the Nd isotopic systematics of modern seawater. This section is a summary of recent work in this area.

Analyses of the isotopic composition of Nd have shown that modern seawater encompasses a wide range of $\varepsilon_{Nd}(0)$ values. Water within each major ocean basin, however, has a relatively limited and characteristic range of Nd isotopic composition. Figure 4.1 is a histogram of $\varepsilon_{Nd}(0)$ values measured both in ferromanganese nodules and seawater. It is clear from this figure that the ferromanganese nodules record the same Nd isotopic composition as the seawater in which they form [Piepgras et al., 1979; Piepgras and Wasserburg, 1980]. As can be seen in Figure 4.1, the modern oceans have the following ranges of $\varepsilon_{Nd}(0)$ values: Atlantic, -15 to -8; Indian, -10 to -7; Pacific, -4 to -1. Much of the variability within a given ocean can be attributed to the existence of distinct water masses with individually characteristic $\varepsilon_{Nd}(0)$ values within that ocean. The Nd

isotopic composition of seawater can therefore be used as a tracer for modern oceanic circulation [Piepgras et al., 1979; Piepgras and Wasserburg, 1980, 1982].

This inter-ocean variability in $\varepsilon_{Nd}(0)$ is markedly different from the analogous case of the Sr isotopic composition of seawater which today has a uniform value of $\varepsilon_{Sr}(0) = +64.5 \pm 2.0$ (0.70905) in all the oceans [Faure et al., 1965; Murthy and Beiser, 1968; Piepgras and Wasserburg, 1980]. The key to the difference between Sr and Nd lies in the residence times of these elements in seawater. The residence time of an element in seawater is defined at steady state as:

$$\tau_{Res} \equiv \frac{\text{Mass of element in seawater}}{\text{Mass flux into seawater}} = \frac{\text{Mass of element in seawater}}{\text{Mass flux out of seawater}} \qquad (4.1)$$

The concentration of Sr in seawater is ~ 8 ppm [Holland, 1978] and its residence time in seawater on the order of 10^6 years [Turner and Whitfield, 1979]. Nd on the other hand has a very low concentration in seawater, ~ 3×10^{-6} ppm [Goldberg et al., 1963; Høgdahl et al., 1968] and an oceanic residence time of tens to hundreds of years [Goldberg et al., 1963; Piepgras et al., 1979; Elderfield and Greaves, 1982]. There is considerable uncertainty in these estimates for the residence time of Nd (and the other REE) because of our lack of knowledge of the fluxes of the REE into and out of seawater. These residence times should be compared with the time required to mix the oceans. Again, this is not a well constrained parameter but ^{14}C studies of deep ocean circulation suggest that mixing of deep water with surface water takes ~ 10^3 years [Broecker et al., 1960]. A minimum mixing rate between oceans is set by the ~ 150 years

Figure 4.1. Histogram of $\varepsilon_{Nd}(0)$ values for ferromanganese nodules and seawater samples from various oceans. Note that each ocean is characterized by a relatively distinct and limited range of $\varepsilon_{Nd}(0)$. Ferromanganese nodules and metalliferous sediments accurately record the $\varepsilon_{Nd}(0)$ value of the seawater in which they form. Typical ranges of $\varepsilon_{Nd}(0)$ for possible crustal sources of the Nd in seawater are indicated in the lower panel. Modern Seawater is dominated by contributions from old continental crust with negative values of $\varepsilon_{Nd}(0)$. Figure modified from Piepgras and Wasserburg, 1982. Data sources: Piepgras et al., 1979, Piepgras and Wasserburg, 1980,1982; O'Nions et al., 1978; Goldstein and O'Nions, 1981; Elderfield et al., 1981b; Piepgras, unpbl. data.

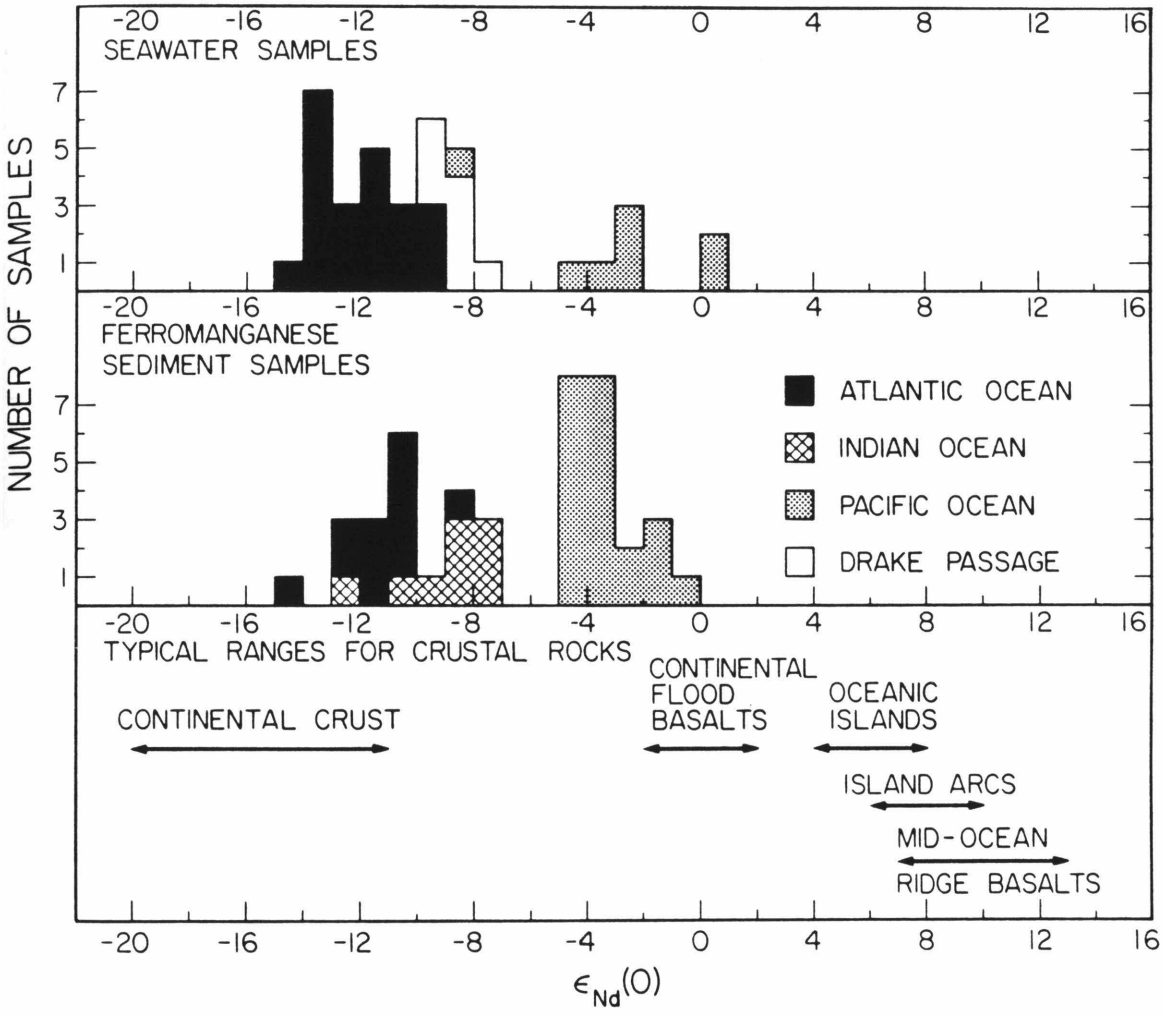
-20 -16 -12 -8 -4 0 4 8 12 16
SEAWATER SAMPLES
FERROMANGANESE SEDIMENT SAMPLES
NUMBER OF SAMPLES
7
5
3
1
ATLANTIC OCEAN
INDIAN OCEAN
PACIFIC OCEAN
DRAKE PASSAGE
TYPICAL RANGES FOR CRUSTAL ROCKS
CONTINENTAL CRUST
CONTINENTAL FLOOD BASALTS
OCEANIC ISLANDS
ISLAND ARCS
MID-OCEAN RIDGE BASALTS
$\epsilon_{Nd}(0)$

it would take to empty the Pacific Ocean by flow of the circum-Antarctic current through the Drake Passage into the Atlantic Ocean [Piepgras and Wasserburg, 1982]. Because the residence time of Sr is so much longer than the oceanic mixing times any isotopic differences in the sources of Sr in seawater can be erased by mixing, resulting in the observed uniform Sr isotopic composition of modern (and ancient) seawater. On the other hand, because of the relatively short residence time of Nd, isotopic differences in the sources for Nd should be manifested by variations in seawater $\varepsilon_{Nd}(0)$, as is observed. In particular, the more negative values of $\varepsilon_{Nd}(0)$ in Atlantic seawater as compared with the Pacific must reflect the dominance of old LREE enriched continental crust as the source for Atlantic seawater Nd. This is in consonance with the fact that ~ 70% of the world's continental runoff flows into the Atlantic Ocean. The modestly negative values of $\varepsilon_{Nd}(0)$ in Pacific waters must reflect the relatively young age of the continental crust surrounding that ocean. Indeed, ~ 80% of the world's sediment load delivered to the oceans is generated by erosion of the young island arc and oceanic island volcanics with $\varepsilon_{Nd}(0)$ averaging ~ +7 in the southwest Pacific [Milliman and Meade, 1983]. Alternatively, the $\varepsilon_{Nd}(0)$ values of Pacific water may reflect a greater injection of Nd with ε_{Nd} ~ +10 from hydrothermal activity at spreading centers. In either case, it is the fact that young crust is a major source for the Nd that results in the modestly negative or even positive values of $\varepsilon_{Nd}(0)$ in Pacific seawater.

One may calculate a model age for the Nd in seawater if it is assumed that all the Nd in seawater is derived from continental crust with a typical value of $f^{Sm/Nd} = -0.4$ [McCulloch and Wasserburg, 1978]. The concentration weighted mean age of the crust contributing Nd to an ocean is then given by $(\varepsilon_{Nd}(T)/(Q^{Nd} \quad -0.4))$. In this way, one calculates that the age of the Atlantic drainages is ~ 1.2AE while that of the Pacific drainages is

~ 0.2AE. One should be able to make similar statements about the age of the sources for Nd in ancient oceans and thus constrain the age of the exposed crust as a function of time. Note that this calculation yields a minimum estimate for the age of the crust by assuming that all the crust which supplies Nd to the oceans was derived from a mantle reservoir with $\varepsilon_{Nd} = 0$. If in fact much of the Nd in seawater is ultimately derived from depleted mantle with $\varepsilon_{Nd} > 0$ then the calculation will underestimate the age of the crust.

Today the different oceans are characterized by different values of $\varepsilon_{Nd}(0)$. Consequently one must expect the same to be true in the past and one cannot expect to be able to generate a single isotopic composition vs. age curve for Nd in the world's oceans as has been done for Sr [Peterman et al., 1970; Veizer and Compston, 1974; Burke et al., 1982]. If it is possible to construct a sufficiently detailed record of the Nd isotopic variations in seawater then this apparent complexity may turn out to be a useful paleo-oceanographic tool for tracing the circulation in ancient oceans. At times in the past, however, such as during the existence of Pangea, there was really only one ocean. The Nd isotopic composition of seawater should be relatively uniform during such times.

The existence of isotopic variations within a given ocean basin is another complication which must be addressed. The carbonate and phosphate samples which will be discussed in the following sections were all formed in relatively shallow water (less than a few hundreds of meters depth). The surface waters of an ocean are quite well mixed by seasonal thermal overturn and wave and current action. The carbonates and phosphates should sample this well mixed reservoir. The isotopic composition of these surface waters, need not, however, be equal to the average isotopic

composition of the whole water column. For example, the isotopic composition of surface water in both the Atlantic and Pacific Oceans today is ~ 3 ε-units less negative than the estimated averages for these oceans [Piepgras and Wasserburg, 1982].

IV.2.2 REE patterns.

Seawater has a distinctive REE pattern which is a useful guide for determining which phases in the sedimentary record derived their REE from seawater. Although the REE as a group have quite low concentrations in seawater, Ce is lower in concentration by up to a factor of 10 than would be predicted from the abundances of its neighboring elements [Goldberg et al., 1963; Høgdahl et al., 1968; Elderfield and Greaves, 1982]. This deficiency of Ce in seawater is generally agreed to be due to the preferential uptake of Ce relative to the other REE by ferromanganese nodules. Analyses of nodules show that they are indeed the major complementary reservoir with a large excess of Ce [Piper, 1974a; Glasby et al., 1978; Elderfield et al., 1981a]. The Ce appears to be preferentially concentrated by the Fe-rich phases in nodules [Elderfield et al., 1981a]. The reason for the anomalous behavior of Ce must involve the ability of Ce to be relatively easily oxidized to a tetravalent ion, unlike the other trivalent rare earths. Theoretical calculations predict, however, that Ce^{3+} should be the stable species in seawater [Turner et al., 1981]. The negative Ce-anomaly of seawater can be inherited by phases which derive their REE from seawater. This characteristic can then be used as a fingerprint to identify those phases which preserve their seawater-derived REE.

There is some evidence that the seawater Ce-anomaly may have been smaller or nonexistent at times in the past [Wright-Clark, et al., 1982].

If marine conditions were more reducing at times in the past, ferromanganese sediments would be less likely to form, Ce would not be preferentially extracted from seawater, and the Ce-anomaly would thus disappear. There is also recent work which demonstrates the existence of positive Ce-anomalies in the surface waters (< 150 m.) of the northwestern Atlantic [DeBaar, et al., 1983]. The same study also found evidence in bottom waters for the re-injection of Ce from the sediments, probably due to the reduction of Ce-rich Fe-hydroxide phases in the sediment. Extensive operation of this process in shallow, nearshore sediments could produce the observed positive Ce-anomalies in surface waters. These complications notwithstanding, the presence of a negative Ce anomaly in a marine sedimentary phase can be taken as good evidence for the derivation of the REE in that phase from seawater.

IV.3 Carbonates.

IV.3.1 Results.

The results of measurements of Sm and Nd concentrations in a variety of modern biogenic $CaCO_3$ samples are presented in Table 4.1 and Figure 4.2. The Nd concentrations range from 0.2 to 9.6 ppb. A sample of inorganically precipitated aragonite in the form of oöliths has 65 ppb Nd. The $f^{Sm/Nd}$ values of these modern carbonates range from -0.16 to -0.45 and are similar to seawater values. Measurements of the Nd isotopic composition of Atlantic samples yield $\varepsilon_{Nd}(0) = -8.3$ and -9.6 and are distinctly different from those of the Pacific samples which have $\varepsilon_{Nd}(0) = -0.1$ and -1.3 (Table 4.1 and Fig. 4.3).

Three extremely well preserved carbonate fossils were investigated and found to have Nd concentrations of 37 ppb, 680 ppb and 31×10^3 ppb with $f^{Sm/Nd}$ values between -0.54 and -0.45 (Table 4.2).

A description of the analytical procedures is given in Appendix III.

IV.3.2 Discussion.

The concentrations of REE in modern biogenic calcite and aragonite reported here are ~ 10^2 times lower than previously reported values for biogenic carbonates [Turekian et al., 1973; Scherer and Seitz, 1980], and up to 10^5 times lower than that reported in the acid soluble portion of limestones [Haskin et al., 1966; Parekh et al., 1977]. Given that the Ca concentration in seawater is ~ 1×10^{-2} moles/kg and the Nd concentration is ~ 2×10^{-5} moles/kg then the Nd concentration would be ~ 3 ppb in a $CaCO_3$ phase formed from seawater with no fractionation of Nd and Ca. The Nd concentrations in the biogenic carbonates are of this order of magnitude (Fig. 4.2). Measured Nd concentrations in seawater vary by about an order of magnitude, between ~ 0.4 to 4.0 × 10^{-12}g/g [Piepgras and Wasserburg, 1982; Elderfield and Greaves, 1982], and it is likely that much of the observed scatter in the biogenic carbonate concentrations can be accounted for by local variations in the concentration of Nd in seawater. Superimposed on this may be possible biologic fractionation.

Although the oölith sample with 65 ppb Nd has significantly higher REE concentration than the biogenic carbonates, the concentration is still much lower than that reported in the literature for carbonate in equilibrium with seawater [Parekh et al., 1977; Scherer and Seitz, 1980]. Individual oöliths are composite objects consisting of an inner nucleus and outer shell of concentric rings of nearly pure aragonite. The nucleus may be composed of a variety of materials, most commonly shell or coral fragments, fecal pellets, lithic fragments, and phosphatic fish debris. It is likely that the bulk of the REE in the oöliths reside in the relatively "dirty" nuclei. Careful partial dissolution experiments could test this assessment. Even at 65ppb Nd, the oöliths have a low REE concentration. This

Table 4.1. Modern Carbonates and Phosphates.

Sample	Locality	Nd (ppb)	$f^{Sm/Nd}$	$\frac{^{143}Nd}{^{144}Nd}$ †	$\varepsilon_{Nd}(0)$
Cc-01 Cressostrea Sp.	Palau	1.37	-0.373	--------	------
Ar-01 Tridaena Sp.	Palau	0.47	-0.449	--------	------
Ar-02 Strombus Gigas	Bermuda	1.96	-0.419	--------	------
Ar-03 Acropora Sp.	Heron Isl., Great Barrier Reef	0.44	-0.162	0.51184 ±.00003	-0.1 ±0.6
Ar-05 Sidereatrae Radians	Bermuda	9.58	-0.249	0.51142 ±.00002	-8.3 ±0.4
Ar-06 Trochus Nilotus	Palau	0.22	-0.294	0.51178 ±.00002	-1.3 ±0.3
Ar-07 Oöliths	Voulter Cays, Bahamas	64.98	-0.184	0.51136 ±.00002	-9.6 ±0.4
Ph-02 Bull Shark Teeth	Mazatlan, Mexico	5.00	------	--------	------
Ph-15 Lingula Sp.	Bahia de Los Angeles, Baja California	150.00	------	--------	------

Errors on aliquot concentration data are ~ 10%, errors on separated sample concentrations are <1%.

† Normalized to $^{142}Nd/^{144}Nd=1.138305$, errors are 2σ of the mean.

Table 4.2 Fossil carbonates.

Sample	Locality	Age	Nd (ppb)	$f^{Sm/Nd}$	Sr (ppm)	$f^{Rb/Sr}$
Ar-04 Baculites Inornatus	Punta San Jose, Baja Calif.	l. Cret.	3.09×10^{4}	-0.453	4744	-0.999
Ar-08	Coon Crk., Tenn.	Maestrictian	6.80×10^{2}	----	2053	----
Cc-02 Belemnites Sp.	Sweden	Campanian	37.0	-0.543	1422	----

Errors on concentrations are ~ 10%.

Figure 4.2. Nd concentration in modern $CaCO_3$ and biogenic apatite. Note logarithmic scale. Indicated are the Nd concentrations in seawater [Nd/S.W.], the Nd concentration in the total dissolved solids in seawater $[(Nd/T.D.S.)_{S.W.}]$, and the Nd concentration expected in $CaCO_3$ or apatite which forms with the Nd/Ca ratio of seawater $[(Nd/CaCO_3)_{S.W.}]$. Also shown is the range of Nd concentrations typical of shales. The Nd concentration in modern carbonates and biogenic phosphate have approximately the Nd/Ca ratio of seawater indicating that there is little tendency for the REE to be concentrated in these phases over seawater.

Nd CONCENTRATIONS IN MODERN $CaCO_3$, APATITE

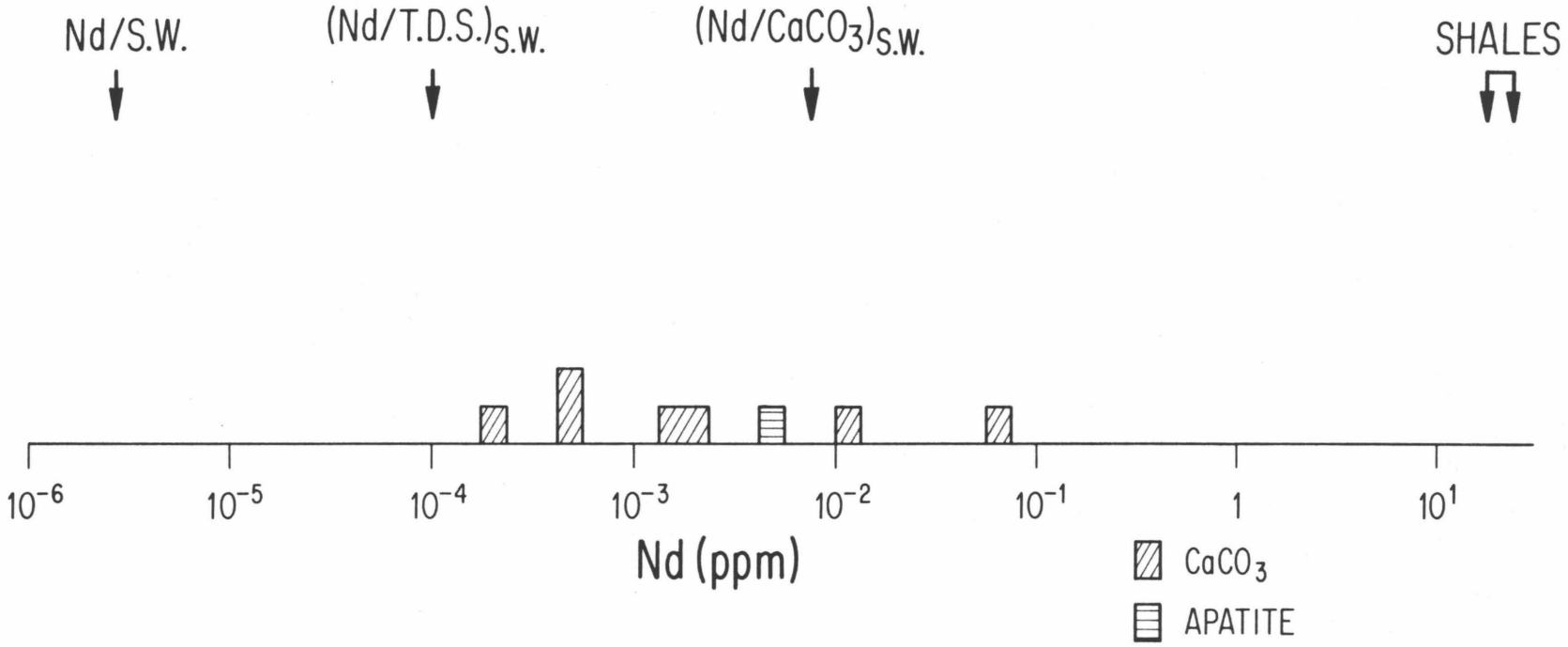

Figure 4.3. Histogram of $\varepsilon_{Nd}(0)$ values for ferromanganese nodules and seawater from Fig. 4.1 with data on $\varepsilon_{Nd}(0)$ in modern carbonates. The isotopic composition of Nd in the carbonates falls in the range of surface seawater isotopic compositions for both Atlantic and Pacific samples. This demonstrates that the REE in the carbonates are derived from seawater.

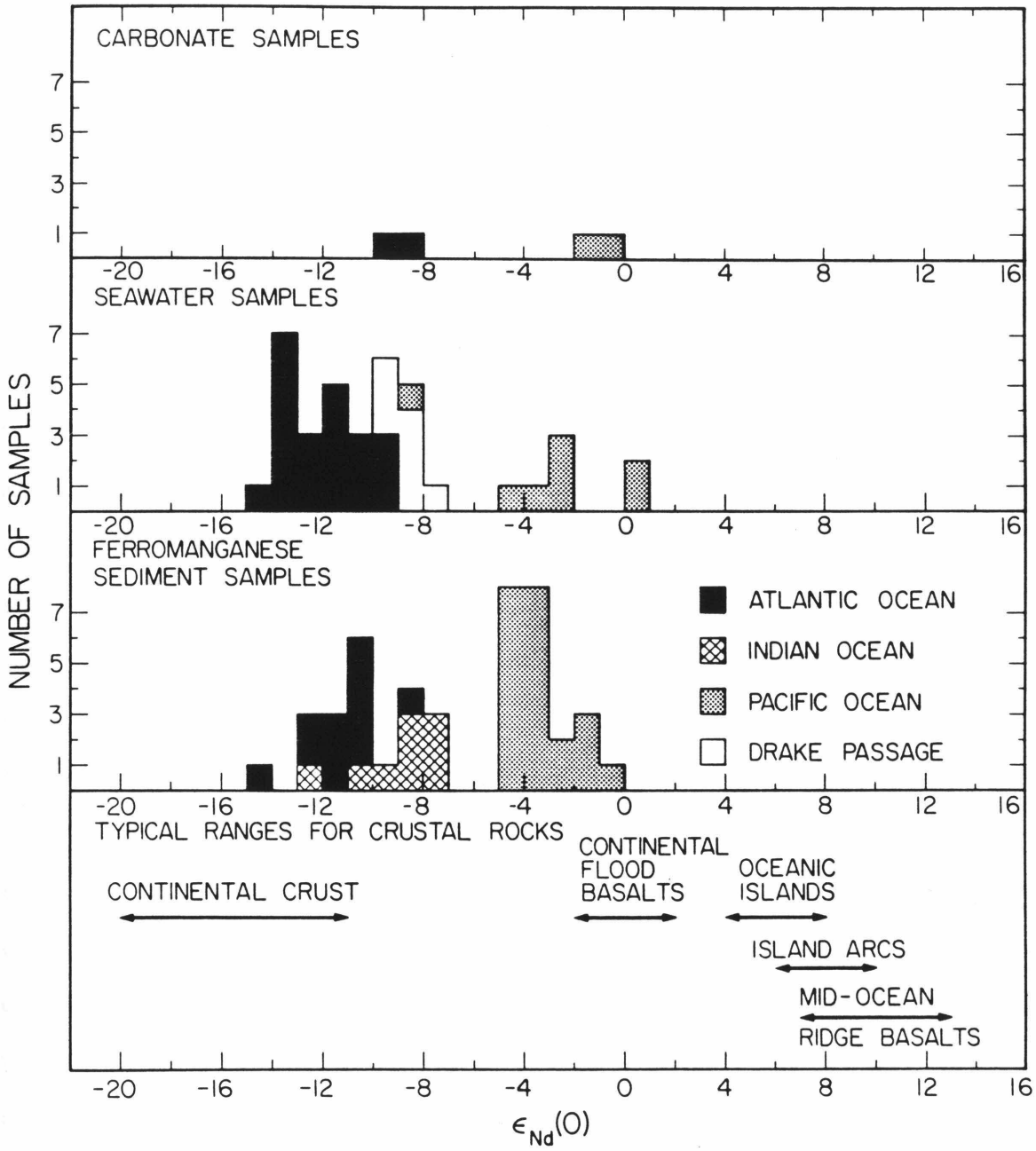
CARBONATE SAMPLES
SEAWATER SAMPLES
FERROMANGANESE
SEDIMENT SAMPLES
NUMBER OF SAMPLES
ATLANTIC OCEAN
INDIAN OCEAN
PACIFIC OCEAN
DRAKE PASSAGE
TYPICAL RANGES FOR CRUSTAL ROCKS
CONTINENTAL CRUST
CONTINENTAL FLOOD BASALTS
OCEANIC ISLANDS
ISLAND ARCS
MID-OCEAN RIDGE BASALTS
$\epsilon_{Nd}(0)$

indicates that biologic effects are not the primary cause of the low concentrations in the biogenic carbonates; biologic fractionation, if active, does not lower the REE concentration in carbonate hard parts by more than a factor of ~ 0.05 over that of inorganically precipitated carbonates. These results are significant in that they demonstrate that the bulk of the REE found in limestones and other carbonate rocks were not present in the primary carbonate materials produced in the marine environment.

Even though the concentration of Nd in the modern carbonates is quite low, the measured $\varepsilon_{Nd}(0)$ values accurately reflect the isotopic composition of Nd in the surface waters in which the shell, coral, or oölith formed. Thus, the Atlantic samples have $\varepsilon_{Nd}(0)$ values of ~ -8 to -10, in the range of Atlantic surface water values, and the Pacific carbonates have $\varepsilon_{Nd}(0)$ values of ~ 0 to -2, similar to Pacific surface waters (Fig. 4.3). This shows that the REE in the carbonates are derived from local seawater.

In contrast to the uniformly low REE concentrations in modern biogenic carbonates, fossil carbonate material spans an enormous range of concentrations (Table 4.2). The samples analysed in the present study were chosen for their excellent state of preservation. Sample Ar-04, a bacculite, is still aragonite and contains primary amino acids [H. Lowenstam, pers. comm., 1983], yet it contains 31 ppm Nd, some 10^4 times the average modern carbonate shell. On the other hand, sample Cc-02, a bellemnite preserving concentric growth rings and primary oxygen isotopic composition, contains only 37 ppb Nd, close to the levels found in the modern samples. As will be discussed in the following section, the high REE concentrations are likely to be a result of diagenesis.

IV.3.3 Occurrence and origin of the REE in carbonates.

Both the origin and mode of occurrence of the REE in the fossil carbonate samples is unclear. These questions also apply to the high REE concentrations reported in some modern biogenic carbonates [Turekian et al., 1973; Scherer and Seitz, 1980], and limestones [Haskin et al., 1966; Parekh et al., 1977]. Based on the low concentrations measured in the modern carbonates in this study, one may confidently state that the REE are not present in the primary marine carbonates. There are several possible reasons for the higher concentrations, among them are adsorption of the REE on grain boundaries, or the presence of a REE-rich minor phase within the carbonate. This section is a review of the literature which bears on the problems of both the location and origin of the REE in carbonates.

Haskin et al. [1966] found that precipitation of a small amount of $CaCO_3$ from a solution of trichloroacetate spiked with radioactive $EuCl_3$ was accompanied by nearly complete removal of the Eu^{3+} from solution. The radioactive Eu was readily brought into solution by placing the precipitate in a dilute $EuCl_3$ solution. Continued precipitation of calcite from the spiked solution did not affect the exchangability of the Eu^{3+}. Calcite prepared in the absence of Eu tracer similarly removed Eu^{3+} from a dilute solution of $EuCl_3$. It appears that in this situation, at least, the REE are scavenged from solution and adsorbed on the surface of the carbonate and that the Ca^{2+} and CO_3^{2-} necessary for continued growth are able to displace the Eu^{3+} from the surface. Thus, one possible explanation for the high REE concentrations in ancient carbonates reported in the literature and in this work is that the REE are adsorbed on the surfaces of the carbonate crystals. The carbonate fossils in particular have a very large surface area on which to adsorb as they are made up of micron-sized crystals of carbonate set in a relatively permeable organic matrix.

The REE may also be located in a minor included phase within the carbonate. In a study of the REE in modern pteropod tests (aragonite), Turekian et al. [1973] found a strong positive correlation between the REE and Fe concentrations. It is well known that Fe-hydroxides efficiently scavenge the REE. Indeed, that property is exploited in the technique used to make the measurements presented here (Appendix III). In the marine environment the most obvious manifestation of this is the high concentrations of seawater-derived REE found in ferromanganese nodules [Piper, 1974a; O'Nions et al., 1978; Piepgras et al., 1979; Elderfield and Greaves, 1981; Elderfield et al., 1981a]. In addition, surfaces of particles in seawater are commonly coated with Fe-hydroxides. Turekian et al. [1973] proposed that the REE resided in sub-microscopic Fe-hydroxide or hydrous Fe-phosphate flocs which were incorporated into the tests as they grew. Fe-hydroxide coatings and particles could also form within and on carbonate fossils and limestones in an oxidizing sedimentary environment. These coatings could then scavenge the REE from pore fluids. This explanation is perhaps more likely than direct scavenging of the REE by carbonate surfaces given the ubiquity of Fe-hydroxides in the marine environment. Although no determinations of the Fe content were made on the samples analysed in this study, it was noted that the solutions containing samples Ar-04 and Ar-08 (30 and 0.7 ppm Nd) were yellow in color, presumably due to the presence of $(FeCl_4)^-_{aq}$ complexes, while the Cc-03 (37 ppb Nd) solution was colorless. Qualitative energy dispersive X-ray fluorescence analysis of sample Ar-04 revealed the presence of only Ca, Sr, K, and Fe. These results are consistent with an Fe-hydroxide phase being the carrier of the REE in the high concentration samples Ar-04 and Ar-08.

Finally, the high REE concentrations reported for acid soluble portions of limestones [Haskin et al., 1966; Jarvis et al., 1975; Parekh et al., 1977; McLennan et al., 1979] must be considered with some caution. In addition to the REE which may be present as adsorbed species on carbonates and Fe-hydroxides, the REE may also be leached from detrital minerals such as clays, or be present in biogenic or authigenic phosphates.

It is clear from the low REE concentrations inferred to be characteristic of modern carbonates that foraminiferal tests and other carbonate debris per se must play a minor role in the transport of the REE in seawater. Carbonate debris, however, may play an important role as a passive carrier for other REE-rich phases. Such particles would accumulate REE in near-surface water and sink. Upon sinking, if the carbonate dissolves, it will release the REE-rich phase to deeper water or to the sediments. This may be an important mechanism in generating the observed REE concentration gradients in seawater [cf. Turekian et al., 1973; Piepgras and Wasserburg, 1982]

The relative abundances of the REE in carbonates can help to determine whether the REE are derived from seawater or from pore fluids during diagenesis. Modern biogenic carbonates, even those with much higher REE contents than the samples reported on in the present study, generally have the negative Ce-anomaly of characteristic of seawater REE pattern [Piper, 1974b; Elderfield et al., 1981a]. The carbonate REE patterns closely mirror the seawater pattern but tend to have somewhat lower LREE enrichments (see $f^{Sm/Nd}$ values in Table 4.1) and are markedly depleted in the HREE relative to seawater [Piper, 1974b; Elderfield et al., 1981a]. Overall, the data strongly suggest that the REE in present day biogenic carbonates are derived directly from seawater. The Nd isotopic data

presented here certainly require this interpretation. The differences between the carbonate and seawater REE patterns requires that there be some fractionation of the REE by whatever mechanism they are incorporated into the carbonates. There are no published REE patterns of modern inorganic carbonates such as the oöliths analysed here. However, the agreement between the Nd isotopic composition of the oöliths and Atlantic seawater implies that they too derive their REE from seawater.

Rare earth patterns of limestones do not have the characteristic negative Ce-anomaly of seawater [Haskin et al., 1966; Jarvis et al., 1975; Parekh et al., 1977; McLennan et al., 1979]. Instead, the limestone patterns are relatively flat when normalized to shales, implying that the REE in the limestones are not derived directly from seawater. These REE must either be located in detrital materials or are introduced during diagenesis by pore fluids carrying REE derived from detrital materials.

IV.3.4 Conclusions

From the foregoing it is apparent that carbonates are unlikely to be a good choice of a phase to analyze to establish the Nd isotopic composition of ancient oceans. The very low REE concentrations in the primary carbonate makes it susceptible to post depositional exchange with Nd from other sources. This Nd may be from a source which also reflects seawater isotopic composition, however, there is no guarantee that this will be the case.

IV.4 Phosphates

IV.4.1 Samples

Two samples of modern biogenic apatite, a shark's tooth and the shells of a species of inarticulate brachiopod, were analysed for Nd concentration. Two types of old phosphate were analysed for Nd and Sr isotopic composition and concentration: biogenic apatite in the form of conodonts, and largely inorganic apatite from phosphorite deposits. These samples are documented in Appendix IV. Procedures are given in Appendix III.

Conodonts are the carbonate-fluorapatite hard parts of an extinct animal that lived from Cambrian to Triassic time. Individual conodont elements range in size from ~ 50 μm to > 1 mm and many elements were grouped together in a single animal to form a functional apparatus. Only recently have fossil impressions of the soft tissue of the organism been found [Briggs et al., 1983]. The animal was a wormlike creature approximately 5 cm long. The conodont apparatus was located in the head and apparently functioned either as teeth or as a structural support for a feeding structure.

Phosphorites are defined as marine sedimentary rocks containing >15 wt. % P_2O_5 and are found in the sedimentary record from the present to ~ 2 AE ago. Carbonate-fluorapatite is the only phosphate mineral found in unaltered phosphorites. The origin of these rocks remains enigmatic. Most of the phosphorite exposed today on the seafloor has been shown to be older than 700,000 yrs. by studies of the $^{234}U/^{238}U$ activity ratio [Kolodny and Kaplan, 1970]. Phosphorites are forming today in only a few, limited geographic areas: off the west coasts of Peru and South Africa [Veeh et al., 1973; Burnett and Veeh, 1977] These are areas of intense coastal

upwelling of deeper waters. Surface waters are essentially devoid of dissolved P (< 3 ppb) because of biologic uptake. Deeper waters (>250 meters) contain 50-100 ppb P and upwelling of this water appears to play a vital role in the formation of phosphates [Bentor, 1980]. Experimental work on the solubility of apatite in seawater has produced conflicting results, but it is clear that seawater with 100 ppb P is not saturated with apatite [Roberson, 1966; Martens and Harriss, 1970; Atlas, 1979]. Furthermore, no one has been successful at precipitating apatite from seawater in the laboratory by addition of P, however, apatite is readily precipitated from Mg^{2+}-free seawater by addition of P. It appears that the Mg^{2+} in seawater poisons the further growth of apatite nuclei by substituting for Ca^{2+} in the growing crystal [Martens and Harriss, 1970]. The situation is quite different in interstitial pore fluids, however, which may contain up to 7500 ppb P [Brooks et al., 1968; Sholkowitz, 1973; Bray et al., 1973; Burnett, 1977]. These high levels are a result of regeneration of soluble P by the breakdown of organic material in the sediment. Interstitial waters are also often depleted in Mg^{2+} by the diagenetic formation of Mg-bearing minerals such as palygorskite, sepiolite, glauconite, and dolomite [Brooks et al., 1968, Bentor, 1980]. Thus, although direct inorganic precipitation of apatite from open seawater seems to be ruled out by the Mg-inhibition effect, formation of apatite in interstitial waters appears to be a reasonable possibility. Upwelling is important insofar as it provides a source of P for organisms which are eventually incorporated into the sediment. Mechanical enrichment of the phosphate by winnowing of lighter minerals by bottom currents may be important for producing the high grade phosphorites one finds in the sedimentary record.

One must be careful when making inferences about the processes which led to the formation of phosphorites in the past from the study of younger deposits. There are considerable differences between relatively young (pre-Miocene) phosphorites and more ancient deposits. The young phosphorites are generally nodular bodies on the order of 10 cm across with concentric layering [Bentor, 1980]. Older deposits have varying textures but are rarely nodular [Trueman, 1971]. Modern phosphorites form only on the continental shelf or upper continental slope; ancient phosphorites formed in a variety of depositional settings, from nearshore to eugeosynclinal [Bentor, 1980]. Finally, there are major differences in the size of the deposits; the older occurrences are by far the larger. The phosphate deposits of the western US (Phosphoria Fm.) contain in excess of 7×10^{17} g of P [British Sulphur Corp., 1973]. The present oceanic reservoir of P contains ~ 9×10^{16} g P [Bentor, 1980]. Under present conditions, ~ 10% of the current annual P-flux to the oceans would have to have been precipitated continuously for 10 My within an area 0.17% of the total ocean floor to form a deposit of this size [Bentor, 1980]. It thus appears that there were times in the past which were more favorable for phosphorite formation [Cook and McElhinny, 1979]. In the case of phosphorites, the present may not be the key to the past.

Although the origin of these rocks is not well understood, using criteria to be discussed below, it will be shown that the REE in phosphatic sediments are largely derived from seawater and may thus contain a record of Nd isotopic variations in ancient seawater.

IV.4.2 Results

The modern biogenic apatite samples have low to very low Nd concentrations (Table 4.1, Fig. 4.2). The shark's tooth has only 5 ppb Nd and is similar in concentration to the modern carbonate samples. The brachiopod shells have higher concentration, 150 ppb, but are still quite low when compared with old apatite samples (see below).

The conodont and phosphorite samples have Nd concentrations between 14 and 876 ppm (Table 4.3, Fig. 4.4). The majority of these samples are LREE enriched with $f^{Sm/Nd}$ values similar to modern seawater, though the phosphates show a greater range in $f^{Sm/Nd}$ than is evident in published seawater analyses. The Sr concentration in all the samples is quite high, between 637 and 7734 ppm. Rb contents are generally low resulting in $f^{Rb/Sr}$ values near -1.0. The $\varepsilon_{Nd}(T)$ values in Table 4.3 range from -15 to -1.7. The $\varepsilon_{Sr}(T)$ values vary from +48 to +79 (0.7078 to 0.7103) and are in excellent agreement with published curves of seawater $^{87}Sr/^{86}Sr$ vs. time (Fig.4.5). These isotopic results are discussed in detail below.

Individual conodont elements, hand-picked from a conodont rich quartzite, were analysed in order to determine the variability in concentrations, isotopic compositions, and parent-daughter ratios in a single deposit. Samples JWC-5-1 numbers I-IV in Table 4.3 are the individual conodont elements. As shown in the Table, the weights of these samples varied between 106 and 528 μg each. Concentrations were also measured in a ~ 5 mg split from 100 mg of hand-picked conodonts (JWC-5-1 bulk). There are significant variations in the concentrations of Sm, Nd, and Sr between the four individuals. The $\varepsilon_{Nd}(T)$ and $\varepsilon_{Sr}(T)$ values, however, are identical within error for all four samples.

Table 4.3 Isotopic Results: Ancient Phosphates.

Sample	Locality	Age (My.)	Nd† (ppm)	$f^{Sm/Nd}$+	$\frac{^{143}Nd}{^{144}Nd}$#	$\varepsilon_{Nd}(T)$§	Sr† (ppm)	$f^{Rb/Sr}$°	$\frac{^{87}Sr}{^{86}Sr}$#	$\varepsilon_{Sr}(T)$§
Phosphorites										
N-33-2	Brewster, Fla.	14 ±9	13.9	-0.365	0.51147 ±.00002	-7.3 ±0.4	1122	-0.938	0.70896 ±.00019	63.5 ±2.7
N-33-1	Gafsa, Tunisia	52 ±2	117.6	-0.395	0.51136 ±.00002	-8.9 ±0.3	1503	-0.973	0.70783 ±.00004	48.1 ±0.6
Mor-15	Oulad-Abdaun Basin, Morocco	68 ±3	99.1	-0.335	0.51150 ±.00002	-6.2 ±0.4	1326	-0.950	0.70782 ±.00006	48.2 ±0.9
Ph-03	Negev, Israel	210 ±5	876.2	-0.398	0.51166 ±.00002	-1.7 ±0.4	744	-0.932	0.70770 ±.00009	48.7 ±1.3
N-33-3	Cokeville, Wy.	250 ±30	40.5	-0.530	0.51142 ±.00002	-5.0 ±0.4	1233	+0.126	0.70751 ±.00006	42.2 ±0.9
NBS-56b	Tennessee	460 ±15	34.0	-0.327	0.51134 ±.00002	-6.2 ±0.4	728	-0.696	0.70838 ±.00003	60.4 ±0.4
Ph-09	Hazara, Pakistan	610 ±30	39.0	-0.382	0.51116 ±.00002	-7.6 ±0.4	997	-0.812	0.71026 ±.00003	90.0 ±0.4
Ph-12	Guizhou, China	610 ±30	16.9	-0.277	0.51129 ±.00002	-6.6 ±0.3	637	-0.866	0.70944 ±.00003	78.9 ±0.4

Table 4.3 (continued).

Sample	Locality	Age (My.)	Nd† (ppm)	$f^{Sm/Nd}$+	$\frac{^{143}Nd}{^{144}Nd}$#	$\varepsilon_{Nd}(T)$§	Sr† (ppm)	$f^{Rb/Sr}$°	$\frac{^{87}Sr}{^{86}Sr}$#	$\varepsilon_{Sr}(T)$§
Ph-05	Parc, Niger	660 ±10	49.4	-0.317	0.51146 ±.00001	-2.2 ±0.3	-----	------	------	----
Ph-08	Kodjari, U. Volta	660 ±10	28.8	-0.313	0.51150 ±.00001	-1.5 ±0.3	1186	-0.838	0.70681 ±.00003	42.0 ±1.0
Ph-04	Rum Jungle, Australia	2000 ±200	14.9	+0.209	0.51162 ±.00002	-15.0 ±1.6	-----	------	------	----
Conodonts										
JWC-35	Bighorn Co., Wy	342 ±3	183.8 ±3.6	-0.321	0.51134 ±.00002	-7.1 ±0.4	3640 ±9	-0.991	0.70802 ±.00005	55.6 ±0.8
JWC-5-1-I[a] (521.8µg)	Missouri	347 ±3	210.8 ±0.2	-0.203	0.51137 ±.00001	-7.5 ±0.3	4070 ±15	-0.998	0.70816 ±.00003	57.8 ±0.4
JWC-5-1-II[a] (266.4µg)	"	"	215.9 ±0.8	-0.142	0.51140 ±.00002	-7.6 ±0.3	4272 ±16	-0.999	0.70818 ±.00003	58.1 ±0.4
JWC-5-1-III[a] (278.8µg)	"	"	220.8 ±0.3	-0.107	0.51139 ±.00002	-8.0 ±0.3	3932 ±7	------	------	----
JWC-5-1-IV[a] (106.6µg)	"	"	184.0 ±1.9	-0.137	0.51140 ±.00002	-7.5 ±0.4	7734 ±99	------	------	----

Table 4.3 (continued).

Sample	Locality	Age (My.)	Nd† (ppm)	$f^{Sm/Nd}$+	$\frac{^{143}Nd}{^{144}Nd}$#	$\varepsilon_{Nd}(T)$§	Sr† (ppm)	$f^{Rb/Sr}$°	$\frac{^{87}Sr}{^{86}Sr}$#	$\varepsilon_{Sr}(T)$§
JWC-5-1-bulk	Missouri	347 ±3	227.4 ±0.1	-----	------	----	-----	------	------	----
JWC-37	Crawford Mtns., Wy.	347 ±3	166.2 ±3.3	-0.352	0.51138 ±.00002	-6.0 ±0.4	2856 ±9	-0.981	0.70807 ±.00003	56.3 ±0.5
JWC-32	Nevada	352 ±3	81.3 ±0.5	-0.390	0.51132 ±.00002	-6.8 ±0.4	4080 ±10	-0.997	0.70812 ±.00004	57.2 ±0.6
JWC-30	Erie Co., N.Y.	357 ±3	171.4 ±2.0	+0.059	0.51152 ±.00002	-6.9 ±0.4	2656 ±13	-0.981	0.70784 ±.00004	53.2 ±0.6

Errors are 2σ mean. $^{143}Nd/^{144}Nd$ normalized to $^{142}Nd/^{144}Nd=1.138305$; $^{87}Sr/^{86}Sr$ normalized to $^{86}Sr/^{88}Sr=0.1194$.

† Uncertainty < 1% except as noted.

+ Uncertainty < 0.2%.

§ Errors are 2σ mean and include the effects of uncertainties in the ages.

° Uncertainty < 0.4%.

a Analyses of individual conodont elements. Weights are given in parentheses.

Figure 4.4. Nd concentration in phosphorite and conodont apatite. Note logarithmic scale. Indicated are the Nd concentration expected in apatite which forms with the Nd/Ca ratio of seawater [$(Nd/APAT)_{S.W.}$], and the range of Nd concentrations typical of shales. Phosphorite and conodont apatite has a high to very high concentration of REE.

Nd CONCENTRATIONS IN PHOSPHORITE AND FOSSIL APATITE

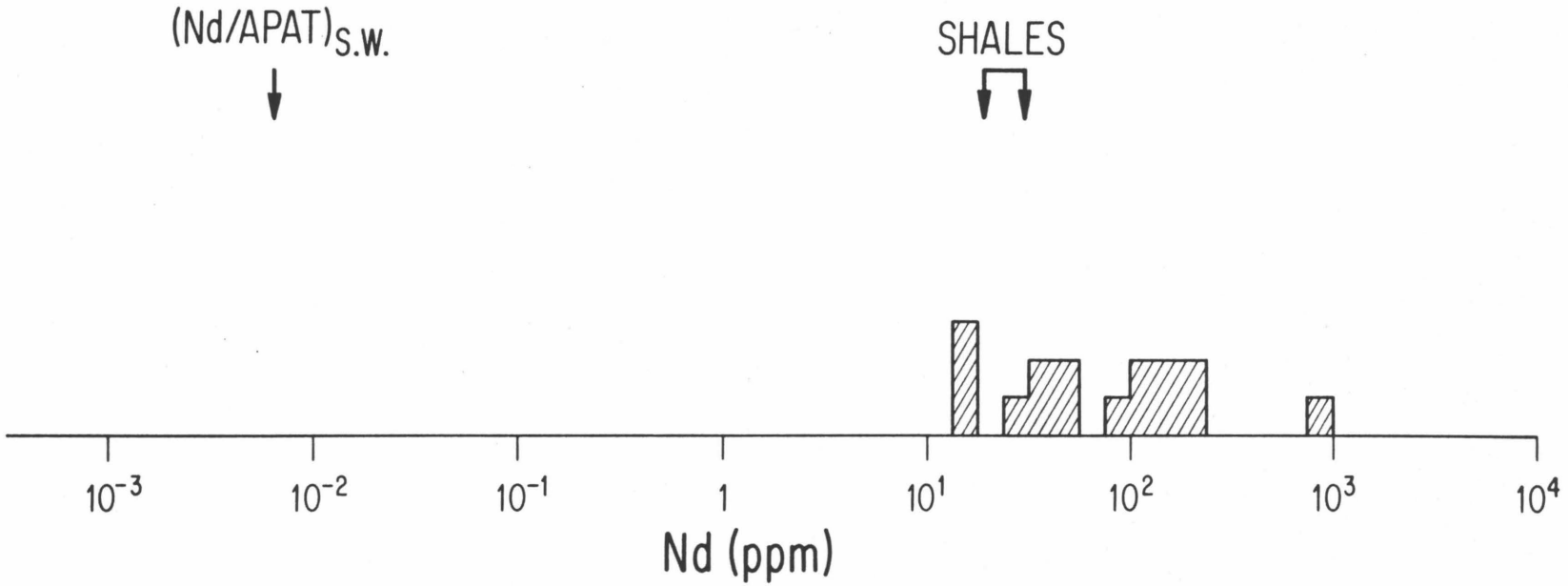

The other conodonts used in this study were isolated from limestones by dissolving the carbonate with dilute (10%) acetic acid. This is a commonly used procedure for the separation of phosphatic fossils from the host rock. As the conodonts were not originally separated with trace element analysis in mind, no special precautions were taken to avoid contamination (i.e. reagent grade acids were used in ordinary plastic buckets). In order to assess the effects of this acetic acid bath, a series of tests was done using ultrapure acetic acid and hand-picked conodonts which had not previously been exposed to acetic acid. The conodonts used in these experiments were representative splits made from ~ 100 mg of crushed, separated conodonts.

In the first experiment, ~ 5 mg of conodonts were covered with 2 ml of 10% acetic acid for 24 hrs. At the end of this time, the conodonts were rinsed with distilled water and the rinses added to the acid. The sample was partially dissolved by this treatment as there was a white residue left after drying down the acid+rinse solution. Approximately 12% of the Nd and Sm originally in the conodonts was found to be in solution. No fractionation of Nd from Sm was effected by this procedure.

The second experiment involved the addition of ~ 495 ng of ^{150}Nd as $NdCl_3$ to 2 ml of 10% acetic acid which was then left to react with 4.51 mg of conodonts (containing ~ 1011 ng Nd) for 29 hrs. At the end of this time, the conodonts were rinsed repeatedly with distilled water and clean 5% acetic acid in an ultrasonic cleaner. Both the conodonts and the solution were analysed. From mass balance considerations it was determined that ~ 6% of the Nd originally in the conodonts went into solution and that 45% of the ^{150}Nd tracer originally in solution was adsorbed by the conodonts. These experiments indicate that the conodonts are attacked to some

extent by acetic acid. The fact that there was no fractionation of Sm from Nd in the first experiment, however, means that this will have no effect on the calculated initial isotopic compositions. More serious is the fact that a large fraction of the ^{150}Nd in solution was picked up by the conodonts. This raises the possibility that similar scavenging may occur during dissolution of limestones to separate conodonts. In practice this does not appear to be a significant problem as will be shown in the following section. It is likely that the ^{150}Nd was adsorbed onto the surface of the conodonts; true isotopic exchange is ruled out by mass balance between the amount of Nd in solution and in the conodonts. Typically, conodonts contribute a small fraction to the total surface area of the insoluble residue in a limestone (abundances are usually on the order of a few tens of conodonts per kg. of limestone). When dissolving a limestone, most of the adsorbable cations in solution are probably taken up by the far more abundant clays, goethite, glauconite and other insoluble phases. Further experiments using radiotracers are being undertaken to clarify the processes involved and whether they will affect the isotopic composition of the conodonts.

IV.4.3 Discussion

Apatite, unlike calcite and aragonite, readily accepts the REE into its lattice. The trivalent rare earths presumably substitute for Ca^{2+} accompanied by a charge-balancing substitution such as Na^{+} for Ca^{2+} or CO_3^{2-} for OH^{-} or F^{-}. The modern biogenic apatites analysed in this study, however, have very low Nd concentrations. Sample Ph-15 with 105 ppb Nd has a concentration some 10^3-10^4 times lower than typical fossil apatite (shark's teeth, fish debris, etc.) [Arrhenius *et al.*, 1957; Bernat, 1975; Dymond and

Eklund, 1978; this work]. The largely inorganically derived apatite in phosphorites also contains REE at 10^2-10^4 times the levels found in the modern biogenic apatites [Altschuler, 1980; this work]. It is clear that an enormous enrichment in REE must occur at some time after the organism's death.

Two related questions are thus raised. How quickly are the REE incorporated into the apatite, and from where are the REE derived? As to the first question, which applies only to the biogenic apatite, there is some evidence that uptake of the REE can occur quite rapidly while the apatite is at the sediment-water interface. A study by Bernat [1975] showed that phosphatic fish debris in the upper 5 mm of sediment from the equatorial Pacific has ~ 1000 ppm of Sm. Assuming a sedimentation rate of 0.01 mm/yr then only 500 years were required to develop this high concentration. Bernat [1975] also found that there was no systematic change in the REE concentration in similar phosphatic material to a depth of 6 meters.

Uranium is also scavenged by biogenic apatite and Kovach and Zartman [1981] have shown that U-Pb ages can be obtained on conodont apatite which are in good agreement with the known stratigraphic age. These studies imply that the trace element enrichment occurs rather rapidly upon sedimentation. This process is likely to be a complicated one. The trace elements are probably first adsorbed onto the surface of the apatite. Incorporation of the adsorbed species into the crystal lattice must take place over a longer period of time during burial and diagenesis. In many cases there is little evidence for recrystallization of the primary microcrystalline biogenic apatite implying that incorporation of the trace elements may be controlled by diffusion.

No analyses are available of the REE in the modern seafloor phosphorite nodules that have a disequilibrium $^{234}U/^{238}U$ activity ratio indicating that they are forming today [Veeh et al., 1973; Burnett et al., 1977; Birch et al., 1983]. It is expected, however, that like ferromanganese nodules, the phosphorite nodules would scavenge and incorporate the REE as the apatite forms.

The question of the origin of the REE in marine apatite applies equally to both biogenic and phosphorite apatite. To the author's knowledge, all published REE analyses of the apatite in phosphorites show a negative Ce-anomaly [Goldberg, et al., 1963; Altschuler et al., 1967; El-Kammar et al., 1979; Altschuler, 1980]. This is strong evidence that in general, the REE in phosphorite apatite are dominantly derived from seawater. It was not possible to obtain REE patterns for the phosphorites analysed here, however, there are REE analyses in the literature for the Florida (N-33-2), Moroccan (Mor-15), and Wyoming (N-33-3) deposits [Altschuler et al., 1967; Altschuler, 1980]. The fact that phosphorite apatite retains a REE abundance pattern with a seawater signature indicates that there has been little exchange with REE derived from detrital components in the phosphorite during diagenesis. This is to be expected as the apatite is the major reservoir for REE in this type of rock. This may be contrasted to the limestone case in which, although the detrital component may be volumetrically insignificant, it is still a major reservoir for REE in the rock.

The evidence that biogenic apatite derives its REE from seawater follows similar reasoning. The REE patterns of the phosphatic fish debris studied by Bernat [1975] all have negative Ce-anomalies. No differences in REE patterns were noted in samples from 0 to 6 meters depth, indicating

that burial and early diagenesis do not disturb the REE in the apatite. A large number of conodont REE patterns have recently been measured by Wright-Clark et al., [ms.]. Conodonts from late Paleozoic (post-Silurian) and Mesozoic sediments all have negative Ce-anomalies. Ordovician through Silurian conodonts from sites around the world have very small to non-existent Ce-anomalies. Lower Ordovician and Cambrian conodonts again show a negative Ce-anomaly. The absence of a Ce-anomaly is correlated with the presence of a negative Eu anomaly. These findings have been interpreted as evidence for reducing conditions and an absence of a Ce-anomaly in the world's oceans during parts of the Paleozoic as discussed in a previous section [Wright-Clark et al., ms.]. The conodonts analysed here are splits of samples analysed by Wright-Clark et al. and do not have Ce-anomalies. Unfortunately, no phosphorite apatite has been analysed from a time during which the Ce-anomaly disappears from the conodonts. Until they can be independently verified by analyses of some other marine phase, the conclusions regarding reducing oceans provided by the conodonts must be considered tentative. Thus, although the conodonts with a modern seawater-like negative Ce-anomaly must certainly have derived their REE from seawater, the conodonts without an anomaly may have been disturbed by post-depositional processes. Several lines of evidence provided by the data presented here, however, suggest that the conodonts without Ce-anomalies do record and preserve seawater-derived REE.

A necessary but not sufficient condition to show that the conodonts reflect seawater ε_{Nd} values is that individual conodonts in the same rock formation must have the same $\varepsilon_{Nd}(T)$ value. Samples JWC-5-1-I through IV in Table 4.3 are individual conodont elements from a single formation. The initial Nd isotopic compositions of these samples are identical within

error as are the initial Sr isotopic compositions, indicating that all the conodonts in this formation equilibrated with an isotopically uniform reservoir.

Further evidence that the the isotopic composition of sedimentary apatite reflects that of the seawater in which it formed is that the initial Sr isotopic compositions of the conodont and phosphorite apatite samples are in excellent agreement with previous estimates of seawater Sr isotopic composition. Figure 4.5 is a plot of the Sr data obtained in this study superimposed on a curve of seawater $^{87}Sr/^{86}Sr$ vs. time showing this agreement. Kovach [1980] has previously shown that the Sr isotopic composition of conodonts defines a closely constrained curve of $^{87}Sr/^{86}Sr$ variations in seawater which agrees with similar curves based on analyses of carbonates. If the phosphates did not preserve seawater Sr isotopic compositions, then there would be good reason to suspect that the Nd isotopic composition was also disturbed in some way. The fact that the Sr in the apatite has not been disturbed by diagenesis, however, does not guarantee that the REE have been similarly unaffected. Samples older than 600 My show larger deviations from the Sr curve than younger samples. In part, this is due to the fact that the curve is poorly defined for times > 600 My.

Perhaps the most important test of whether the Nd isotopic composition of phosphorite apatite and conodonts reflects that of ancient seawater is to compare the isotopic composition of samples from widely separated localities which bordered on a common sea. These samples should record the same initial isotopic composition. This has been done for four different times (Fig. 4.6). Conodonts from localities in Wyoming, Nevada, Missouri and New York of 340-360 My age all have $\varepsilon_{Nd}(T)$ values equal to -7±1. Both conodonts separated using acetic acid and conodonts which were separated

Figure 4.5. Isotopic composition of Sr in seawater vs. time (after Peterman et al., 1970; Veizer and Compston, 1974; Burke et al., 1982, Veizer et al., 1983). Curve is poorly constrained for times > 500My. Symbols show the Sr isotopic composition of the apatite samples analysed in this study. There is good agreement between these samples and previous estimates of seawater $^{87}Sr/^{86}Sr$. There is no obvious long term trend in the Sr curve over the time period shown. Short term variations in $^{87}Sr/^{86}Sr$ must be a consequence of the time-varying relative importance of Sr inputs to seawater from old marine carbonates (~ 0.7080), old silicate continental crust (~ 0.7130), and young continental and oceanic, mantle derived volcanism (~ 0.7030).

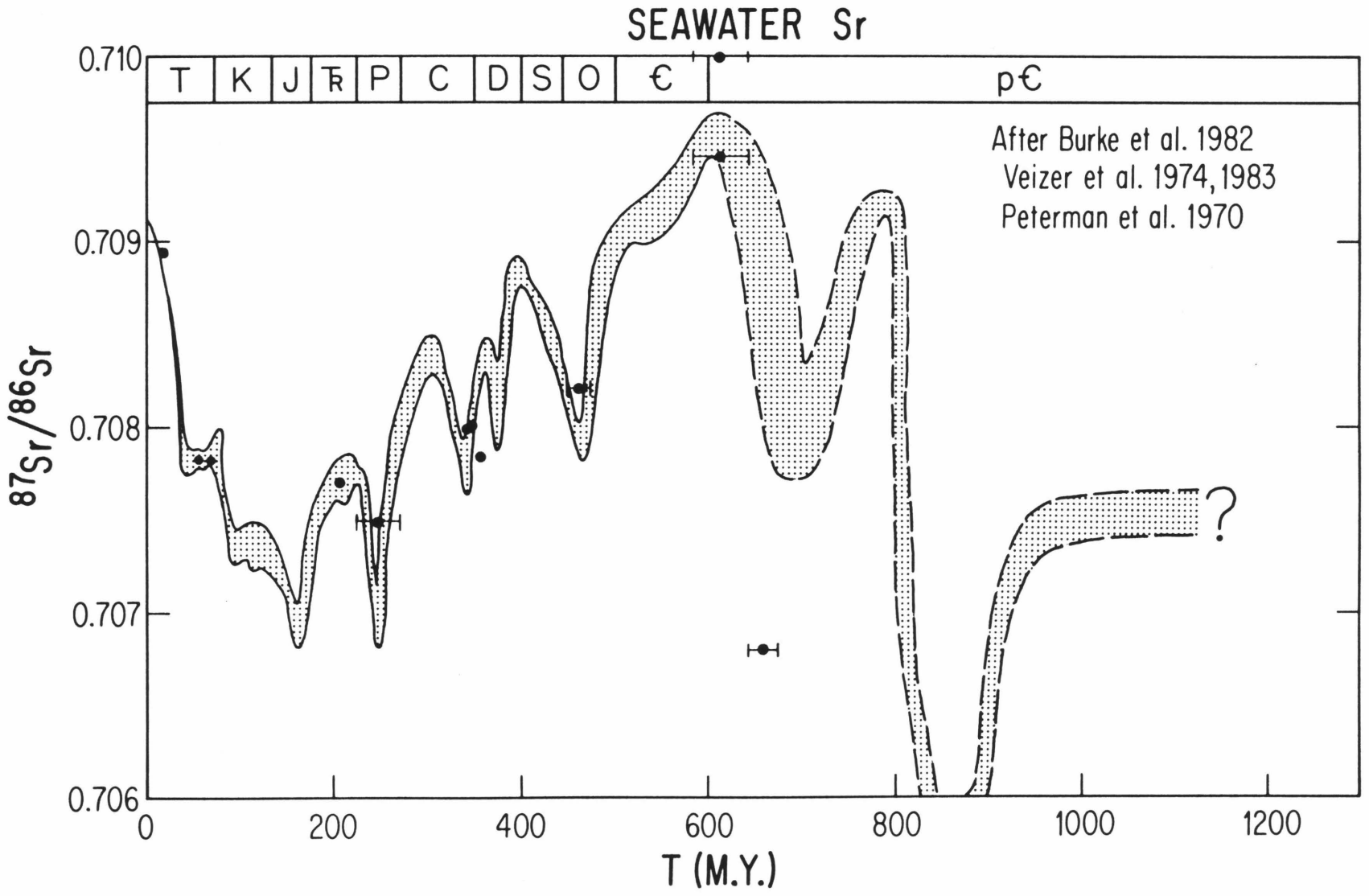
SEAWATER Sr
T
K
J
Tr
P
C
D
S
O
€
p€
After Burke et al. 1982
Veizer et al. 1974, 1983
Peterman et al. 1970
?
0.710
0.709
0.708
0.707
0.706
87Sr/86Sr
0
200
400
600
800
1000
1200
T (M.Y.)

without the use of acetic acid yield the same value of $\varepsilon_{Nd}(T)$ (see IV.4.2). Ordovician phosphorite from Tennessee has an $\varepsilon_{Nd}(T)$ value that overlaps the range of Nd isotopic composition inferred for Cambro-Ordovician seawater from analyses of metalliferous sediments from the southern uplands of Scotland [Hooker et al., 1981]. The lower end of the range given by Hooker et al. [1981] is likely to best reflect seawater values; they found evidence for exchange of the metalliferous sediments with the enclosing ophiolitic basalts ($\varepsilon_{Nd}(T) \sim +8$), a process which would raise the $\varepsilon_{Nd}(T)$ values in the sediments. Two samples of phosphorite of 610±30 My age, one from southern China, the other from Pakistan have $\varepsilon_{Nd}(T) \sim -7\pm1$. Finally, 660±10 My old phosphorite samples from U. Volta and Niger have $\varepsilon_{Nd}(T) \sim -2.0\pm0.5$. This agreement among samples of approximately the same age is encouraging and suggests that sedimentary apatite can be used to establish variations of $\varepsilon_{Nd}(T)$ in seawater through time. Conodonts are especially attractive for this purpose because the detailed biostratigraphies which have been worked out using conodonts offer the possibility of very good time resolution.

Clearly, much more work is needed to elucidate the mechanism of incorporation of the REE into marine apatite and its resistance to exchange during diagenesis. Ideally, any samples which are to be used for isotopic work should also be analysed to obtain a REE pattern. This would aid in selecting samples which are most likely to reflect seawater.

IV.5 Isotopic composition of Nd in ancient oceans

Figure 4.6 summarizes the available data on the isotopic composition of Nd in seawater as a function of time. The majority of the data points plotted in this figure represent the analyses of phosphates presented in

Figure 4.6. Isotopic composition of Nd in seawater as a function of time. Separate curves are drawn for the Pacific and Atlantic oceans back to ~ 200My. Panthalassa (see text) existed between ~ 200 and ~ 275 My so a single curve for the world's oceans is drawn for this period. From ~ 275 to at least 400 My an open seaway to the south of N. America allowed mixing between the "Pacific" and proto-Atlantic oceans and a single curve is also drawn for this period. These curves are speculative and will certainly be modified with the acquisition of new data.

Note that there is no evidence for values of $\varepsilon_{Nd}(T)$ in seawater outside of the range observed in modern oceans for the time period portrayed.

Boxes indicate uncertainties in age and $\varepsilon_{Nd}(T)$. These quantities are correlated. Dashed boxes in the Jurassic and Ordovician are estimates of seawater ε_{Nd} from Chyi et al. [1982] and Hooker et al. [1981] respectively. Also included is the isotopic composition of the Nd leached from Cretaceous-Tertiary sanidine spherules [Shaw and Wasserburg, 1982; this work, Chapter II].

Key to sample localities: A = Atlantic; PA = proto-Atlantic; T = Tethys; P = Pacific (west coast of N. America); PI = "proto-Indian".

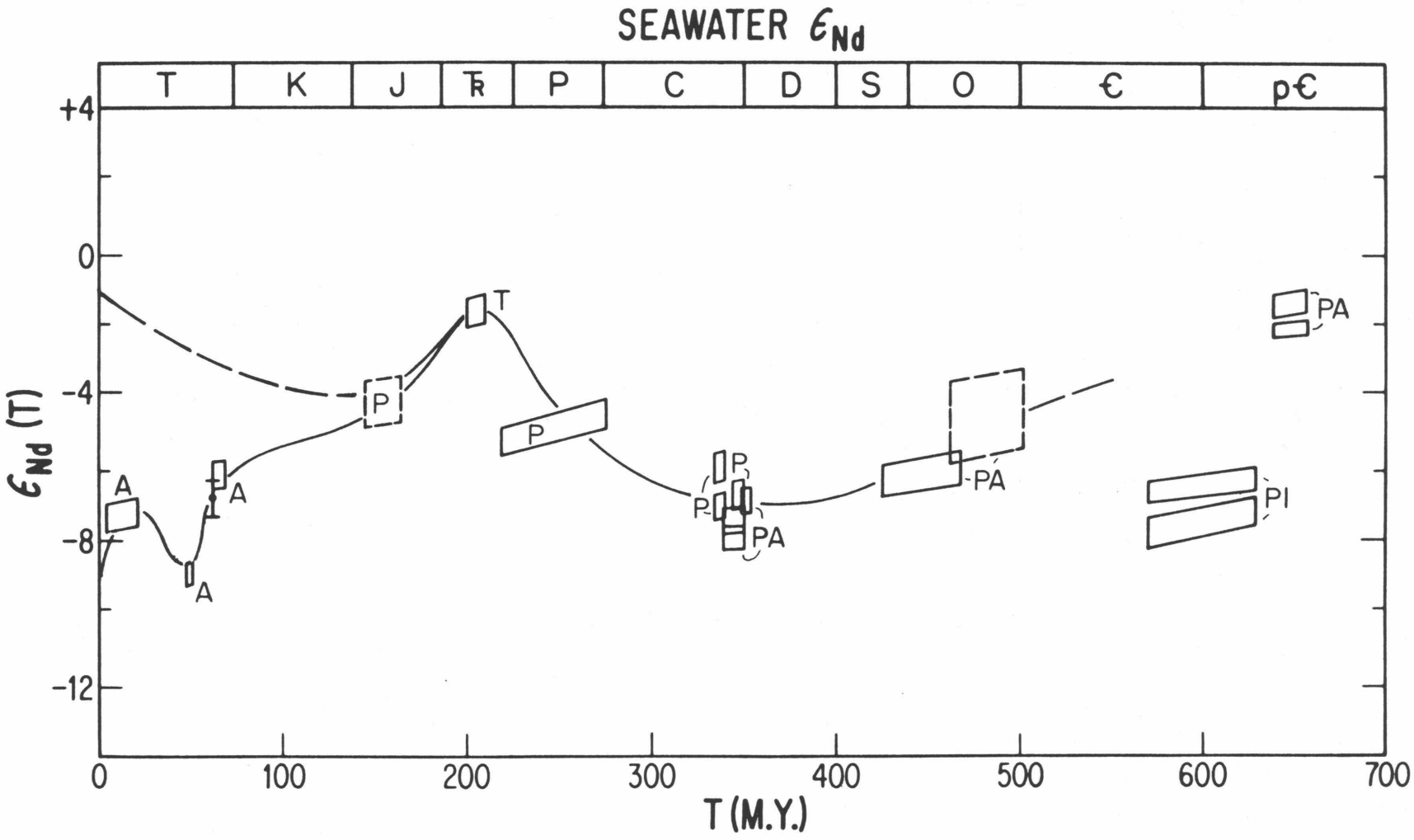
SEAWATER ϵ_{Nd}
T
K
J
Tr
P
C
D
S
O
€
p€
+4
0
-4
-8
-12
ϵ_{Nd} (T)
0
100
200
300
400
500
600
700
T (M.Y.)
A
A
A
P
T
P
P
P
PA
PA
PA
PI

Figure 4.7. Plot of $^{143}Nd/^{144}Nd$ vs. time in 10^9 years. Today is at T=0. Illustrated is the principle of a model age calculation for 2AE seawater using the Rum Jungle phosphorite results. The measured $^{143}Nd/^{144}Nd$ in this sample is 0.51162 ($\varepsilon_{Nd}(0) = -4.4$) with $f^{Sm/Nd} = +0.21$. Going back in time, the Nd isotopic composition of this sample diverges from the chondritic evolution curve (CHUR) and at 2AE had an initial isotopic composition of 0.50872 ($\varepsilon_{Nd}(T) = -15.0$). Assuming that the Nd in seawater at 2AE was derived from continental crust with $f^{Sm/Nd} = -0.4$ then one calculates a model age of ~ 1.5 AE for the age of the crust at the time of phosphorite formation. This crust would be 3.5 AE old today.

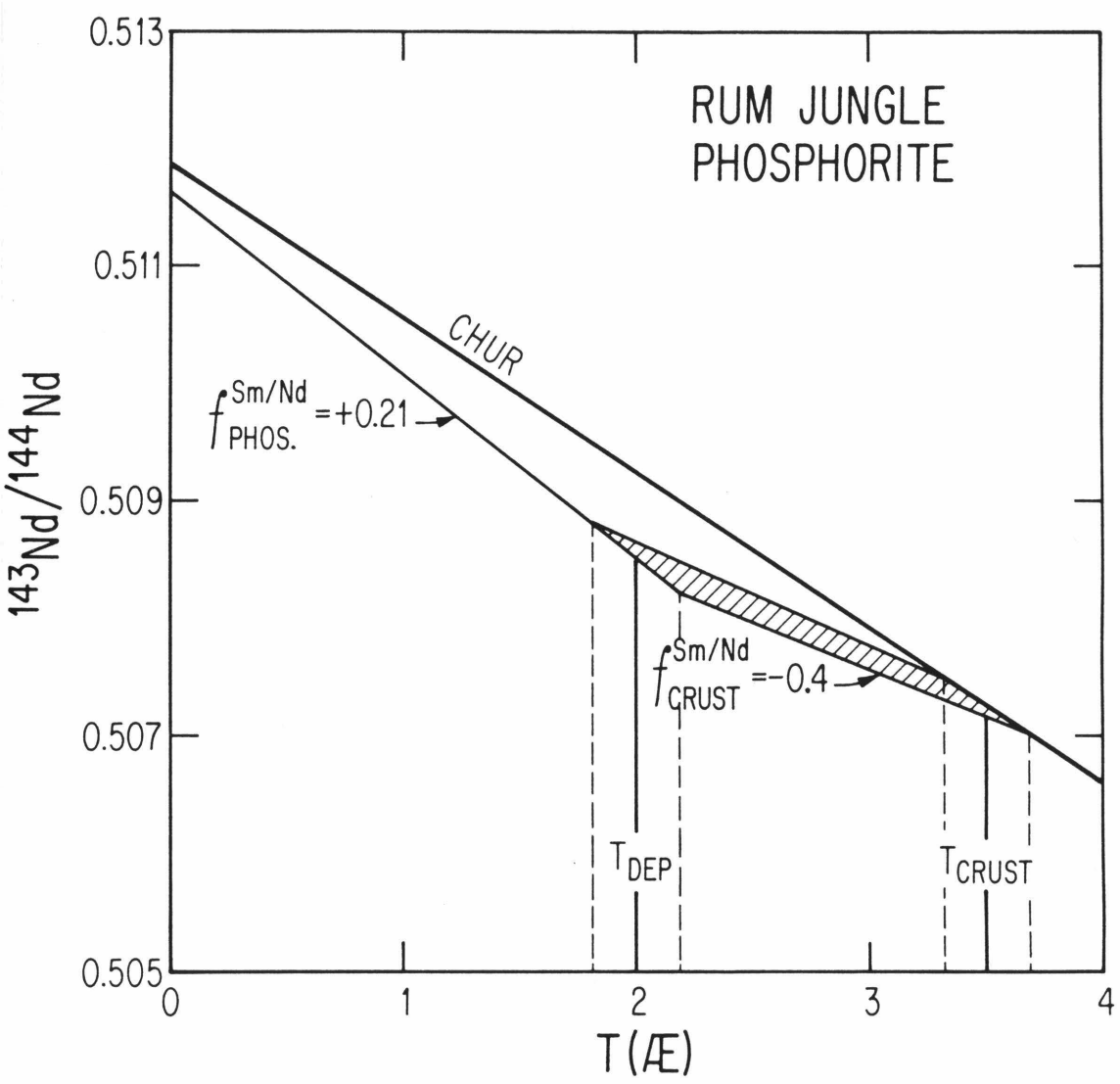
RUM JUNGLE
PHOSPHORITE
CHUR
$f^{Sm/Nd}_{PHOS.}$ =+0.21
$f^{Sm/Nd}_{CRUST}$ =-0.4
T_{DEP}
T_{CRUST}
0.513
0.511
0.509
0.507
0.505
0
1
2
3
4
$^{143}Nd/^{144}Nd$
T(Æ)

this work. Also plotted in Figure 4.6 are the initial isotopic compositions of iron-rich cherts from the Jurassic Franciscan Fm. of California [Chyi et al., 1982] and Cambro-Ordovician metalliferous sediments associated with an ophiolitic melange in the southern Uplands of Scotland [Hooker et al., 1981]. Much of what follows is necessarily speculative given the small data base that currently exists. It is anticipated that many of the details of this discussion will change as more data on ε_{Nd} in seawater are acquired.

There is no evidence among the data in Figure 4.6 for values of $\varepsilon_{Nd}(T)$ in past oceans lying outside the range observed in modern seawater. Values of ε_{Nd} for all the samples less than 700 My old lie between -1.7 and -8.9. It appears that like today, the bulk of the Nd in ancient seawater was derived from old, LREE enriched continental crust. In particular, there are no samples with positive values of $\varepsilon_{Nd}(T)$ which would indicate the dominance of Nd derived from depleted mantle volcanic sources such as midocean ridges, oceanic islands and island arcs. Like the seawater $^{87}Sr/^{86}Sr$ curve (Fig. 4.5), there is no long term trend visible in the ε_{Nd} data over the time period shown in Figure 4.6.

Separate curves of the evolution of the isotopic composition of Nd in the Atlantic and Pacific Oceans are drawn in Figure 4.6 starting at modern seawater $\varepsilon_{Nd}(T)$ values and going back to ~ 200My. The curves are shown as merging at a common point at this time. This assumes that the Nd isotopic composition of the earliest proto-Atlantic Ocean was determined by the influx of seawater from outside the rift zone. This need not be the case. If the Nd in the early proto-Atlantic seawater was derived from continental runoff draining into the rift then the Nd isotopic composition of this water could have been quite different from "Pacific" seawater. At

the present, there is no evidence as to which of these alternatives is correct. From ~ 200My to ~ 275My all the continents were joined together in a single landmass known as Pangea [Berggren and Hollister, 1974; Smith et al., 1981]. As a consequence, there was a single encircling ocean which has been given the name Panthalassa. The Tethys was a western arm of this global sea. It is expected that $\varepsilon_{Nd}(T)$ would have a relatively uniform value in seawater during this time. Correspondingly, a single curve has been drawn on Figure 4.6 for this time period. Analyses of Devonian-Mississippian conodonts from the east, southern, and west coasts of N. America all have approximately the same value of $\varepsilon_{Nd}(T)$, implying that the proto-Atlantic and ancestral Pacific Oceans were well mixed with respect to Nd isotopes at that time. Paleogeographic reconstructions for this time period show a large open seaway between North and South America [Ziegler et al., 1979; Smith et al., 1981] This passage must have allowed relatively free circulation between oceans. The single curve for Panthalassa in Figure 4.6 is extended back to ~ 400My on this basis. For times older than 400My the seawater ε_{Nd} curve is even more poorly constrained. The value of ε_{Nd} in proto-Atlantic seawater appears to have risen between ~ 450 and ~ 630My from ~ -6 to ~ -2. It is not known what relationship the ~ 600My ocean to the south of Pakistan and southern China ("proto-Indian") had to other oceans at that time and no curve has been drawn through these data in Figure 4.6.

It is interesting to note that the times at which seawater $\varepsilon_{Nd}(T)$ is inferred to have been high correspond to times associated with the breakup of large continental landmasses. The Triassic marked the beginning of the breakup of Pangea and the latest Precambrian saw the initial rifting of N. America from Africa to form the proto-Atlantic Ocean. These times also

appear to be local minima in seawater $^{87}Sr/^{86}Sr$ (Fig. 4.5). The Nd and Sr isotopic systems in seawater seem to be reflecting a greater input of young mantle-derived material at these times. Increased volcanism would be a natural corollary to continental breakup. In general, however, there is not a correlation between the $\varepsilon_{Nd}(T)$ and $\varepsilon_{Sr}(T)$ values of the samples analysed in this study.

It should be pointed out that the total range in ε_{Nd} one expects in seawater is on the order of 20 ε-units. Isotopic variations within a single ocean can be on the order of ±3 ε-units. The isotopic composition of Sr in seawater has varied by ~ 40 ε-units over the past 600My (Fig. 4.5) with variations between all oceans being on the order of ±1-2 ε-units. The "signal to noise" ratio of the Nd isotopic system in seawater is thus lower than that of the Sr system and may therefore present a greater problem for interpreting the isotopic record.

The Rum Jungle sample (Ph-04, Table 4.3) is from the oldest known phosphorite deposit (2.0±0.2AE) and represents a large jump back in time from the samples discussed up to now. This sample provides a good example of the sort of information about the age of the exposed crust as a function of time that can be extracted from the record of the Nd isotopic composition of seawater. The measured $\varepsilon_{Nd}(0)$ value of this sample is -4.4. Assuming that the value of $f^{Sm/Nd}$ = +0.21 measured on this sample was acquired at the time of formation of the phosphorite 2AE ago, then one calculates an initial isotopic composition of $\varepsilon_{Nd}(T)$ = -15.0 (Fig. 3.7). This large negative value implies that the Nd in this sample was derived from a LREE source, namely continental crust, which was quite old at the time of phosphorite formation. An estimate of the age of the crust involved can be obtained by assuming a typical value of $f^{Sm/Nd}$ = -0.4 for the crust which

was the source for the Nd in 2AE seawater. One then calculates that the crust bordering on the sea in which the phosphorite formed was already 1.5AE old at 2AE ago, and would thus be 3.5AE old today. This is a powerful statement. These results imply that the exposed continental crust which existed 2AE ago was on average formed 1.5AE earlier and suggest that a substantial amount of continental crust was formed quite early in the earth's history.

Obviously, the conclusions derived from this single sample will require confirmation by analyses of other samples of both Rum Jungle phosphorite and other contemporaneous marine phases. In particular, the value of $f^{Sm/Nd} = +0.21$ is rather different from the values of $f^{Sm/Nd}$ in more recent seawater and suggests that the sample may not have had the simple history assumed here. Nevertheless, the principles involved in obtaining information on the age of the exposed crust as a function of time are well exposed by this example. Analyses of additional phosphorites ranging in age from the Proterozoic to Recent should yield good constraints on the age of the continental crust for the past 2AE. Unfortunately, there are no known Archean phosphorites and a different choice of a phase to analyze will need to be found in order to extend the record of ε_{Nd} in seawater to earlier times. Possible candidates for this include some lithologies of banded iron formations and Archean bedded barite deposits. Finding the record of ε_{Nd} in seawater during the first 2.5AE of the earth's history will not be an easy task, however, it is well worth the attempt for the information it would provide on the early evolution of the crust.

IV.6 Conclusions

Measurements of the Nd and Sm concentrations in modern primary marine calcite and aragonite range from 0.2 to 65 ppb Nd with $f^{Sm/Nd}$ values between -0.16 and -0.45 (Table 4.1, Fig. 4.2). Both biogenic and inorganically precipitated carbonates have low REE concentrations. The concentration of Nd in these samples is within a factor 10 times what would be expected if there were no fractionation of the seawater Nd/Ca ratio upon formation of the carbonate. These concentrations are ~ 10^2 times lower than previously reported for modern biogenic carbonates [Turekian et al., 1973; Scherer and Seitz, 1980], and up to 10^5 times lower than reported for the acid soluble portions of limestones [Haskin et al., 1966; Parekh et al., 1977]. Even though the Nd concentrations are quite low, the $\varepsilon_{Nd}(0)$ values of modern carbonates samples from the Atlantic and Pacific Oceans are distinctly different and reflect the isotopic composition of Nd in the seawater in which they formed (Fig. 4.3). Nd concentrations in three very well preserved carbonate fossils were investigated and found to vary from 37 ppb to 3.1×10^4 ppb Nd (Table 4.2). The high REE concentrations in carbonate fossils and limestones measured in this study and in the literature cannot be primary but must be due to the presence of a second REE-rich phase of the adsorption of REE onto grain boundaries. The fact that the REE patterns of limestones are flat when normalized to shales [Haskin et al., 1966; Jarvis et al., 1975; Parekh et al., 1977; McLennan et al., 1979] implies that the REE in these rocks were not derived from seawater but rather were probably derived from detrital materials or from pore fluids during diagenesis. The low Nd concentration in the primary marine carbonates makes them very susceptible to later isotopic exchange and overprinting of the original isotopic signature by Nd derived from

other sources. Carbonates are thus a poor choice of a phase to analyze in order to determine $\varepsilon_{Nd}(T)$ of ancient seawater.

Modern biogenic apatite was found to have low Nd concentrations (<150 ppb, Table 4.1), but there is some evidence that REE are quickly scavenged from seawater by the apatite upon death of the organism. Quite high REE concentrations can be reached by this process [Arrhenius et al., 1957; Bernat, 1975]. Although the mechanism of its formation is controversial [Bentor, 1980], the inorganically precipitated apatite in phosphorite deposits also has high concentrations of seawater-derived REE [Goldberg et al., 1963; Altschuler et al., 1967; El-Kammar et al., 1979; Altschuler, 1980; this work, Table 4.3 and Fig. 4.4]. Sedimentary apatite of marine origin generally preserves the characteristic negative Ce-anomaly of seawater [see references cited above]. In addition, apatite samples of the same age from geographically separated localities bordering on a common sea record approximately the same $\varepsilon_{Nd}(T)$ value. Apatite thus appears to be a suitable phase to analyze in order to determine variations of $\varepsilon_{Nd}(T)$ in ancient oceans.

Conodont and phosphorite apatite samples have been analysed for Nd and Sr isotopic composition. The $\varepsilon_{Sr}(T)$ values of these samples agree well with previous determinations of the isotopic composition of Sr in seawater (Fig. 4.5). The $\varepsilon_{Nd}(T)$ values lie within the range of modern seawater values indicating that there have been no drastic changes in the sources for Nd in seawater over the past 700My (Fig. 4.6). Pacific and proto-Atlantic seawater during late Devonian to early Mississippian time appears to have been well mixed with respect to Nd isotopes and had a value of $\varepsilon_{Nd}(T) = -7\pm1$. Times of relatively high $\varepsilon_{Nd}(T)$ in seawater during the Triassic and latest Precambrian seem to correlate with the breakup of large

continental landmasses, implying an increased amount of mantle-derived volcanism at these times. The initial $\varepsilon_{Nd}(T)$ value of -15.0 for the 2AE old Rum Jungle phosphorite requires the existence of old continental crust at the time of phosphorite formation. That crust would, on average, be 3.5AE old today. This example demonstrates the possibility of using the variations in ε_{Nd} in seawater over time to constrain the age of the exposed crust in the past.

REFERENCES

Affaton, P., Sougy, J., and Trompette, R., 1980, The tectono-stratigraphic relationships between the upper Precambrian and lower Paleozoic Volta Basin and the Pan-African Dahomeyide orogenic belt (West Africa): Am. J. Sci., v. 280, p. 224-248.

Altschuler, Z. S., 1980, The geochemistry of trace elements in marine phosphorites. Part I. characteristic abundances and enrichment: Soc. Econ. Paleont. and Mineral. Spec. Publ. 29, p. 19-30.

Altschuler, Z. S., Berman, S., and Cuttita, F., 1967, Rare earth elements in phosphorites--geochemistry and potential recovery: U. S. Geol. Surv. Prof. Pap. 575-B, p. B1-B9.

Alvarez, L. W., Alvarez, W., Asaro, F., and Michel, M. V., 1980, Extra-terrestrial cause for the Cretaceous-Tertiary extinction: Science, v. 208, p. 1095-1108.

Alvarez, W., Alvarez, L. W., Asaro, F., and Michel, H. V., 1982a, Current status of the impact theory for the terminal Cretaceous extinction: Geol. Soc. Am. Spec. Pap. 190, p. 305-315.

Alvarez, W., Asaro, F., and Michel, H. V., and Alvarez, L. W., 1982b, Iridium anomaly approximately synchronous with terminal Eocene extinctions: Science, v. 216, p. 886-888.

Arrhenius, G., Bramlette, M. N., and Piccioto, E., 1957, Localization of radioactive and stable heavy nuclides in ocean sediments: Nature, v. 180, p. 85-86.

Atlas, E. L., 1979, Solubility controls of carbonate-fluorapatite in sea-water: Rep. on the Marine Phosphatic Seds. Workshop, Honolulu, p. 18-20.

Baedecker, P. A., 1971, Iridium: in, B. Mason, ed., Handbook of Elemental Abundances in Meteorites, Gordon and Branch, N. Y., p. 463-472.

Bentor, Y. K., 1980, Phosphorites--The unsolved problems: Soc. Econ. Paleont. and Mineral. Spec. Publ. 29, p. 1-18.

Berggren, W. A., and Hollister, C. D., 1974, Paleogeography, paleobio-geography and the history of circulation in the Atlantic Ocean: Soc. Econ. Paleont. and Mineral. Spec. Publ. 20, p. 126-186.

Bernat, M., 1975, Les isotopes de l'uranium et du thorium et les terresreres dans l'environment marin: Cah. ORSTOM, Ser. Geol., v. 7, p. 65-83.

Birch, G. F., Thomson, J., MacArthur, J. M., and Burnett, W. C., 1983, Pleistocene phosphorites off the west coast of South Africa: Nature, v. 302, p. 601-603

Bolten, v. R., and Müller, D., 1969, Das Tertiär im Nördlinger Ries und in seiner Umgebung: Geologica Bavarica, v. 61, p. 87-123.

Bouska, V. I., 1964, Geology and stratigraphy of Moldavite occurrences: Geochim. Cosmochim. Acta, v. 28, p. 921.

Bouska, V. I., Povondra, P., Florenskij, P. V., and Randa, Z., 1981, Irghizites and Zhamanshinites: Zhamanshin Crater, USSR: Meteoritics, v. 16. p. 171-184.

Bowen, N. L., 1928, The Evolution of the Igneous Rocks: Dover Publ., Inc., New York, 1956 reprint, 335 pp.

Bray, J. P., Bricker, O. P., and Troup, B. N., 1973, Phosphate in interstitial water of anoxic sediments: Oxidation effects during sampling: Science, v. 180, p. 1362-1364.

Briggs, D. E. G., Clarkson, E. N. K., and Aldridge, R. J., 1983, The conodont animal: Lethaia, v. 16, p. 1-14.

British Sulphur Corp., 1971, World Survey of Phosphate Deposits, 3rd ed.: London, 180 pp.

Broecker, W. S., Gerard, R., Ewing, M., and Heezen, B., 1960, Natural radiocarbon in the Atlantic Ocean: J. Geophys. Res., v. 65, p. 2903-2931.

Brooks, R. R., Presby, B. J., and Kaplan, I. R., 1968, Trace elements in the interstitial waters of marine sediments: Geochim. Cosmochim. Acta, v. 32, p. 397-414.

Brown, L., Klein, J., Middleton, R., Sacks, I. S., and Tera, F., 1982, ^{10}Be in island-arc volcanoes and implications for subduction: Nature, v. 299, p. 718-720.

Burke, W. M., Denison, R. E., Hetherington, E. A., Kopnick, R. B., Nelson, M. F., and Omo, J. B., 1982, Variation of seawater $^{87}Sr/^{86}Sr$ throughout Phanerozoic time: Geology, v. 10, p. 516-519.

Burnett, W. C., 1977, Geochemistry and origin of phosphorite deposits from Peru and Chile: Geol. Soc. Am. Bull., v. 88, p. 813-823.

Burnett, W. C., and Veeh, H. H., 1977, Uranium-series disequilibrium studies in phosphorite nodules from the west coast of South America: Geochim. Cosmochim. Acta, v. 41, p. 755-764.

Carlson, R. W., MacDougall, J. D., and Lugmair, G. W., 1978, Differential Sm/Nd evolution in oceanic basalts: Geophys. Res. Lett., v. 5, p. 229-232

Carlson, R. W., MacDougall, J. D., and Lugmair, G. W., 1981, Columbia River volcanism: The question of mantle heterogeneity or crustal contamination: Geochim. Cosmochim. Acta, v. 45, p. 2483-2500.

Carlson, R. W., MacDougall, J. D., and Lugmair, G. W., 1983, "Columbia River volcanism: The question of mantle heterogeneity or crustal contamination" (reply to a comment by D. J. DePaolo): Geochim. Cosmochim. Acta, v. 47, p. 845-846.

Chapman, D. R., and Scheiber, L. C., 1969, Chemical investigation of Australasian tektites: J. Geophys. Res., v. 74, p. 6737-6776.

Chen, J. C., and Pallister, J., 1981, Lead isotopic studies of the Samail ophiolite, Oman: J. Geophys. Res., v. 86, p. 2699-2708.

Chen, J. H., and Shaw, H. F., 1982, Pb-Nd-Sr isotopic studies of ophiolites in California, western U. S. [abs]: Geol. Soc. Am. Abstr., v. 14, p. 462.

Chen, J. C., Jacobsen, S. B., and Wasserburg, G. J., 1981, Pb isotopic study of the Bay of Islands Ophiolite complex [abs]: EOS, v. 62, p. 410.

Chidester, A. H., and Cady, W. M., 1972, Origin and emplacement of alpine-type ultramafic rocks: Nat. Phys. Sci., v. 240, p. 27-31.

Chidester, A. H., Albee, A. L., and Cady, W. M., 1978, Petrology, structure and genesis of the asbestos-bearing ultramafic rocks of the Belvidere Mountain area in Vermont: U. S. Geol. Surv. Prof. Paper 1016, 95 pp.

Church, W. R., 1972, Ophiolite: its definition, origin as oceanic crust and mode of emplacement in orogenic belts, with special reference to the Appalachians: Dept. Energy, Mines Res. Canada Publ. 42, p. 71-85.

Church, W. A., 1977, The ophiolites of southern Quebec: Oceanic crust of the Bett's Cove type: Can. J. Earth Sci., v. 14, p. 1668-1673.

Church, W. A., and Stevens, R. K., 1971, Early Paleozoic ophiolite complexes of Newfoundland and Appalachians as mantle-ocean crust sequences: J. Geophys. Res., v. 76, p. 1212-1222.

Chyi, M. S., Carlson, R. W., and Crerar, D. A., 1982, Rb-Sr and Nd isotopic study of the submarine hydrothermal Mn-deposits from the Franciscan assemblage [abs]: Geol. Soc. Am. Abstr., v. 14, p. 463.

Clague, D., Rubin, J., and Brackett, R., 1981, The age and origin of the garnet amphibloite underlying the Thetford Mines ophiolite, Quebec: Can. J. Earth Sci., v. 18, p. 469-486.

Clemens, W. A., 1982, Patterns of extinction and survival of the terrestrial biota during the Cretaceous/Tertiary transition: Geol. Soc. Am. Spec. Pap. 190, p. 407-413.

Cohen, R. S., Evensen, N. M., Hamilton, P. J., and O'Nions, R. K., 1980, U-Pb, Sm-Nd, and Rb-Sr systematics of mid-ocean ridge basalt glasses: Nature, v. 283, p. 149-153.

Coish, R. H., and Church, W. A., 1979, Igneous geochemistry of mafic rocks in the Bett's Cove ophiolite, Newfoundland: Cont. Min. Pet., v. 70, p. 29-39.

Coish, R. H., Hickey, R., and Frey, F. A., 1982, Rare earth element geochemistry of the Bett's Cove ophiolite, Newfoundland: Complexities in ophiolite formation: Geochim. Cosmochim. Acta, v. 46, p. 2177-2134.

Coleman, R. G., 1971, Plate tectonic emplacement of upper mantle peridotites along continental edges: J. Geophys. Res., v. 76, p. 1212-1222.

Compston, W., and Chapman, D. R., 1969, Sr isotope patterns within the southeast Australasian strewn-field: Geochim. Cosmochim. Acta, v. 33, p. 1023-1036.

Cook, F. A., and Oliver, J. E., 1981, The late Precambrian-early Paleozoic continental edge in the Appalachian orogen: Am. J. Sci., V. 281, p. 993-1008.

Cook, F. A., Albaugh, D. S., Brown, L. D., Kaufman, S., Oliver, J. E., and Hatcher, R. D., 1979, Thin-skinned tectonics in the crystalline southern Appalachians; COCORP seismic-reflection profiling of the Blue Ridge and Piedmont: Geology, v. 7, p. 563-567.

Cook, P. J., and McElhinny, M. W., 1979, A reevaluation of the spatial and temporal distribution of sedimentary phosphate deposits in light of plate tectonics: Econ. Geol., v. 74, p. 315-330.

Cook, P. J., and Shergold, J. H., 1979, Proterozoic-Cambrian Phosphorites: Canberra Publishing and Printing, Canberra, 106 pp.

Crocket, J. H., 1981, Geochemistry of the platinum group elements: in, L. J. Cabri, ed., Platinum-Group Elements: Mineralogy, Geology, and Recovery, Canadian Inst. of Mining and Metallurgy Spec. Vol. 23, p. 47-64.

Crowley, W. P., 1976, The geology of the crystalline rocks near Baltimore and its bearing on the evolution of the eastern Maryland Piedmont: Maryland Geol. Surv. Rept. Invest., v. 27, 40 pp.

Dana, J. P., 1873, On some results of the earth's contraction from cooling, including a discussion of the origin of mountains and the nature of the earth's interior: Am. J. Sci., 3rd ser., v. 5, p. 423-443.

Darwin, C., 1844, Geological Observations on Coral Reefs, Volcanic Islands and in South America: D. Appleton and Co., N. Y., 1896 ed., 649 pp.

Dasch, E. J., 1969, Strontium isotopes in weathering profiles, deep-sea sediments, and sedimentary rocks: Geochim. Cosmochim. Acta, v. 33, p. 1521-1552.

David, v. E., 1969, Das Ries-Ereignis als physikalischer Vorgang: Geologica Bavarica, v. 61, p. 350-378.

DeBaar, H. J. W., Bacon, M. P., and Brewer, P. G., 1983, Rare-earth distributions with a positive Ce anomaly in the western North Atlantic Ocean: Nature, v. 301, p. 324-327.

DePaolo, D. J., 1978, Study of magma sources, mantle structure, and the differentiation of the earth using variations of $^{143}Nd/^{144}Nd$ in igneous rocks: Ph. D. dissert., Calif. Inst. of Tech., 360 pp.

DePaolo, D. J., 1983, Comment on "Columbia River volcanism: The question of mantle heterogeneity or crustal contamination": Geochim. Cosmochim. Acta, v. 47, p. 841-844.

DePaolo, D. J., and Wasserburg, G. J., 1976a, Nd isotopic variations and petrogenetic models: Geophys. Res. Lett., v. 3, p. 249-252.

DePaolo, D. J., and Wasserburg, G. J., 1976b, Inferences about magma sources and mantle structure from variations of $^{143}Nd/^{144}Nd$: Geophys. Res Lett., v. 3, p. 743-746.

DePaolo, D. J., and Wasserburg, G. J., 1977, The sources of island arcs as indicated by Nd and Sr isotope studies: Geophys. Res. Lett., v. 4, p. 465-468.

DePaolo, D. J., and Wasserburg, G. J., 1979a, Sm-Nd age of the Stillwater Complex and the mantle curve for neodymium: Geochim. Cosmochim. Acta, v. 43, p. 999-1008.

DePaolo, D. J., and Wasserburg, G. J., 1979b, Nd isotopes in flood basalts from the Siberian platform and inferences about their mantle sources: Proc. Nat'l. Acad. Sci. U. S., v. 76, p. 3056-3060.

DePaolo, D. J., Kyte, F. T., and Marshall, B. D., 1982, Rb-Sr, Sm-Nd, and K-Ca studies of Cretaceous-Tertiary Boundary Sediments: Possible evidence for an oceanic impact [abs.]: 13th Lunar and Planet. Sci. Conf., p. 168.

Dewey, J. F., and Bird, J. M., 1971, Origin and emplacement of the ophiolite suite: Appalachian ophiolites in Newfoundland: J. Geophys. Res., v. 76, p. 3197-3207.

Dietz, R. S., 1977, Elgygytgyn Crater, Siberia: Probable source of Australasian tektite field: Meteoritics, v. 12, p. 145-157.

Domenick, M. A., and Basu, A. R., 1982, Age and origin of the Cortlandt Complex, New York: Implications from Sm-Nd data: Cont. Min. Pet., v. 79, p. 290-294.

Dosso, L., and Murthy, V. R., 1980, A Nd isotopic study of the Kerguelen Islands: Inferences on enriched oceanic mantle sources: Earth Planet. Sci. Lett., v. 48, p. 268-276.

Drake, A. A., and Morgan, B. A., 1981, The Piney Branch Complex--a metamorphised fragment of the central Appalachian ophiolite in northern Virginia: Am. J. Sci., v. 281, p. 484-508.

Dupre, B., and Allegre, C. J., 1980, Pb-Sr-Nd isotopic correlation and the chemistry of the North Atlantic mantle: Nature, v. 286, p. 17-22.

Dymond, J. and Eklund, W., 1978, A microprobe study of metalliferous sediment components: Earth Planet. Sci. Lett., v. 40, p. 243-251.

Edwards, R. L., and Wasserburg, G. J., 1983, Sm-Nd and Rb-Sr systematics of the Kempersai ultramafic complex, South Ural Mountains USSR [abs]: EOS, v. 64, p. 337.

Elderfield, H., and Greaves, M. J., 1981, Negative Ce anomalies in the rare earth element patterns of ferromanganese nodules: Earth Planet. Sci. Lett., v. 55, p. 163-170.

Elderfield, H., and Greaves, M. J., 1982, The rare earth elements in seawater: Nature, v. 296, p. 214-219.

Elderfield, H., Hawkesworth, C. J., Greaves, M. J., and Calvert, S. E., 1981a, Rare earth element geochemistry of oceanic ferromanganese nodules and associated sediments: Geochim. Cosmochim. Acta, v. 45, p. 513-528.

Elderfield, H., Hawkesworth, C. J., Greaves, M. J., and Calvert, S. E., 1981b, Rare earth element zonation in Pacific ferromanganese nodules: Geochim. Cosmochim. Acta, v. 45, p. 1231-1234.

El-Kammar, A. M., Zayed, M. A., and Amer, S. A., 1979, Rare earths of the Nile Valley phosphorites, Upper Egypt: Chem. Geol., v. 24, p. 69-81.

Epstein, S., 1982, The $\delta^{18}O$ of the sanidine spherules at the Cretaceous-Tertiary boundary [abs]: 13th Lunar and Planet. Sci. Conf., p. 205-206.

Epstein, S., and Mayeda, T., 1953, Variations in δO^{18} in natural waters: Geochim. Cosmochim. Acta, v. 4, p. 213-233.

Eugster, O., Tera, F., Burnett, D. S., and Wasserburg, G. J., 1970, The isotopic composition of gadolinium and neutron-capture effects in some meteorites: J. Geophys. Res., v. 75, p. 2753-2768.

Faure, G., Hurley, P. M., and Powell, J. L., 1965, The isotopic composition of strontium in surface water from the North Atlantic Ocean: Geochim. Cosmochim. Acta, v. 29, p. 209-220.

Fleischer, R. L., and Price, P. B., 1964, Fission track evidence for the simultaneous origin of tektites and other natural glasses: Geochim. Cosmochim. Acta, v. 28, p. 755-760.

Fleischer, R. L., Price, P. B., and Walker, R. M., 1965, On the simultaneous origin of tektites and other natural glasses: Geochim. Cosmochim. Acta, v. 29, p. 161-166.

Florenskij, P. V., 1975, The Zamanshin meteorite crater (northern near-Aral) and its tektites and impactites: Prob. Akad. Nauk Izv., v. 10, p. 73-86.

Florenskij, P. V., 1977, The meteorite crater Zamanshin (northern Aral region, U. S. S. R.) and its tektites and impactites: Chem. Erde, v. 36, p. 83-95.

Florenskij, P. V., Perelygin, V. P., Bazhenov, M. L., Lkhaguasuren, D. D., and Stecenko, S. G., 1979, Kompleksnoje opredelenije vozrasta meteoritnogo kratera Zhamansjin: Astronom. vestnik, v. 13, p. 178.

Florenskij, P. V., Dabizha, A. I., Aaloe, A. O., Gorshkov, E. S., and Mikljajev, V. I., 1979, Geologo-geofizicheskajc kharakteristika meteoritnogo kratera Zhamanshin: Meteoritika, v. 38, Ann. CCCR Izd. Nauka, p. 86.

Frey, F. A., 1977, Microtektites: a chemical comparison of bottle green microtektites, normal microtektites, and tektites: Earth Planet. Sci. Lett., v. 35, p. 43-48.

Ganapathy, R., 1982, Evidence for a major meteorite impact on earth 34 million years ago: Implications for Eocene extinctions: Science, v. 216, p. 885-886.

Ganapathy, R., Gartner, S., and Jian, M. J., 1981, Iridium anomaly at the Cretaceous-Tertiary boundary in Texas: Earth Planet. Sci. Lett., v. 45, p.393-396.

Gentner, W., Lippolt, H. J., and Schaeffer, O. A., 1963, Argon-Bestimmungen an Kaliummineralien, XI Die Kalium-Argon Alter der Gläser des Nördlinger, Rieses and der boehmisch-maehrischen tektite: Geochim. Cosmochim. Acta, v. 27, p. 191-200.

Gentner, W., Storzer, D., and Wagner, D. A.,1969, New fission-track ages of tektites and related glasses: Geochim. Cosmochim. Acta, v. 33, p. 1075-1081.

Glasby, G. P., Keays, R. R., and Rankin, P. C., 1978, The distribution of rare earth, precious metal, and other trace elements in Recent and fossil deep-sea manganese nodules: Geochem. Jour., V. 12, p. 229-243.

Glass, B. P., 1968, Microtektites in deep sea sediments: Nature, v. 214, p. 372-374.

Glass, B. P., 1968, Glassy objects (microtektites) from deep-sea sediments near the Ivory Coast: Science, v. 161, p. 891-893.

Glass, B. P., 1970, Comparison of the chemical composition in a flanged australite with the chemical variation among "normal" australasian microtektites: Earth Planet. Sci. Lett., v. 9, p. 240-246.

Glass, B. P., 1978, Zhamanshin crater: Possible source of the Australasian tektites [abs.]: Geol. Soc. Amer. Abstr., Cordilleran Sect., p.107.

Glass, B. P., Baker, R. N., Störzer D., and Wagner, G. A., 1973, North American microtektites from the Caribbean Sea and their fission track ages: Earth Planet. Sci. Lett., v. 19, p. 184-192.

Glass, B. P., and Zwart, P. A., 1979, The Ivory Coast microtektite strewn-field: New data: Earth Planet. Sci. Lett., v. 43, p. 336-342.

Glass, B. P., Swincki, M. B., and Zwart, P. A., 1979, Australasian, Ivory Coast, and North American tektite strewnfields: size, mass, and correlation with geomagnetic reversals and other rare events: Proc. Lunar and Planet. Sci. Conf. 10th, p. 2535-2545.

Glass, B. P., DuBois, D. L., and Ganapathy, R., 1982, Relationship between an iridium anomaly and the North American microtektite layer in core RC9-58 from the Caribbean Sea: Proc. 13th Lunar Planet. Sci. Conf. Pt. I, J. Geophys. Res., v. 87, p. A425-A428.

Goldberg, E. D., Koide, M., Schmitt, R. A., and Smith, J., 1963, Rare earth distributions in the marine environment: J. Geophys. Res., v. 68, p. 4204-4217.

Goldstein, S. L., and O'Nions, R. K., 1981, Nd and Sr isotopic relationships in pelagic clays and ferromanganese deposits: Nature, v. 291, p. 324-327.

Göpel, C. H., Dupré, B., Allegre, C. J., and Xu, R. H., 1982, Lead isotope study on Tibetan ophiolites [abs]: 5th Intl. Conf. on Geochemistry, Cosmochemistry, Isotope Geochemistry, Nikko, Japan, p.117-118.

Grauert, B., 1974, U-Pb systematics in heterogeneous zircon populations from the precambrian basement of the Maryland Piedmont: Earth Planet. Sci. Lett.: v. 23, p. 238-248.

Graup, G., Horn, P., Köhler, M., and Müller-Sohnius, D., 1981, Source material for Moldavites and Bentonites: Naturwissenschaften, v. 67, p. 616.

Gray, C. A., Cliff, R. A., and Goode, A. D. T., 1981, Neodymium-strontium isotopic evidence for extreme contamination in a layered basic intrusion: Earth Planet. Sci. Lett. v. 56, p. 189-198.

Grieve, R. A. F., 1982, The record of impact on earth: Implications for a major Cretaceous/Tertiary impact event: Geol. Soc. Am. Spec. Pap. 190, p. 25-37.

Hadley, J. B., 1949, Preliminary report on corundum deposits in the Buck Creek peridotite, Clay Co., North Carolina: U. S. Geol. Surv. Bull., v. 948E, 25 pp.

Hanan, B. B., 1980, The petrology and geochemistry of the Baltimore Mafic Complex, Maryland: Ph. D. dissert., VA Polytechnic Inst. & State Univ., 218 pp.

Hanan, B. B., 1981, Chemical and isotopic variations related to microfractures in gabbros [abs]: EOS, v. 62, p. 435.

Hannah, J. L., and Futa, K., 1982, Nd, Sr, and O isotope systematics in the Troodos Ophiolite, Cyprus [abs]: Geol. Soc. Am. Abstr., v. 14, p. 506.

Harper, G. D., 1980, The Josephine ophiolite--remains of a late Jurassic marginal basin in northwestern California: Geology, v. 8, p. 333-337.

Harper, G. D., and Saleeby, J. B., 1980, Zircon ages of the Josephine ophiolite and the lower Coon Mountain pluton, western Jurassic belt, northwestern California [abs]: Geol. Soc. Am. Abstr., v. 12, p. 109-110.

Hartley, M. E., 1973, Ultramafic and related rocks in the vicinity of Lake Chatuge: Georgia Geol. Surv. Bull., v. 85, 61 pp.

Hartung, J. B., and Rivolo, A. R., 1979, A possible source in Cambodia for Australasian tektites: Meteoritics, v. 14, p. 153-160.

Haskin, L. A., Wildeman, T. R., Frey, F. A., Collins, K. A., Reedy, C. R., and Haskin, M. A., Rare earths in sediments: J. Geophys. Res., v. 71, p. 6091-6105.

Hawkesworth, C. J., and Vollmer, R., 1979, Crustal contamination versus enriched mantle: $^{143}Nd/^{144}Nd$ and $^{87}Sr/^{86}Sr$ evidence from the Italian volcanics: Cont. Min. Pet., v. 69, p. 151-168.

Hawkesworth, C. J., O'Nions, R. K., Pankhurst, R. J., Hamilton, P. J., and Evensen N. M., 1977, A geochemical study of the island-arc rocks and back-arc tholeites from the Scotia Sea: Earth Planet. Sci. Lett., v. 36, p. 253-262.

Hawkesworth, C. J., Norry, M. J., Roddick, J. C., and Vollmer, R., 1979a, $^{143}Nd/^{144}Nd$ and $^{87}Sr/^{86}Sr$ ratios from the Azores and their significance in LIL-element enriched mantle: Nature, v. 280, p.28-31.

Hawkesworth, C. J., O'Nions, R. K., and Arculus, R. J., 1979b, Nd and Sr isotope geochemistry of island arc volcanics, Grenada, Lesser Antilles: Earth Planet. Sci. Lett., v. 45, p. 237-248.

Hertogen, J., Janssens, M.-J., and Palme, H., 1980, Trace elements in ocean ridge basalt glasses: Implications for fractionations during mantle evolution and petrogenesis: Geochim. Cosmochim. Acta, v. 44, p. 2125-2143.

Hertz, N., 1951, Petrology of the Baltimore Gabbro, Maryland: Geol. Soc. Am. Bull., v. 62, p. 979-1016.

Hess, H. H., 1939, Island arcs, gravity anomalies and serpentine intrusions: Int. Geol. Congr. Moscow 1937, Report 17, v. 2, p. 263-283.

Hess, H. H., 1955, Serpentine, orogeny, and epiorogeny: Geol. Soc. Am. Spec. Pap. 62, p. 391-408.

Hickey, A. L., and Frey, F. A., 1982, Geochemical characteristics of boninite series volcanics: Implications for their source: Geochim. Cosmochim. Acta, v. 46, p. 2099-2115.

Høgdahl, O. T., Melson, S., and Bowen, V. T., 1968, Neutron activation analysis of lanthanide elements in seawater: Adv. Chem. Ser., v. 73, p. 308-325.

Holland, H. D., 1978, The Chemistry of the Atmosphere and Oceans: Wiley, N. Y., 351 pp.

Hooker, P. J., Hamilton, P. J., and O'Nions, 1981, An estimate of the Nd isotopic composition of Iapetus seawater from ca. 490Ma metalliferous sediments: Earth Planet. Sci. Lett., v. 56, p. 180-188.

Hopson, C. A., 1964, The crystalline rocks of Howard and Montgomery Counties, in The Geology of Howard and Montgomery Counties: Maryland Geol. Surv., p. 27-215.

Hopson, C. A., and Frano, C. J., 1977, Igneous history of the Point Sal ophiolite, southern California: in North American Ophiolites, Oregon Dept. of Geol. and Min. Indust. Bull. 95, p. 161-183.

Irvine, T. N., 1975, Olivine-pyroxene-plagioclase relations in the system Mg_2SiO_4-$CaAl_2Si_2O_8$-$KAlSi_3O_8$-SiO_2 and their bearing on the differentiation of stratiform intrusions: Carnegie Inst. Wash. Yearb., p. 492-500.

Jacobsen, S. B., and Wasserburg, G. J., 1979, Nd and Sr isotopic study of the Bay of Islands Ophiolite Complex and the evolution of the source of midocean ridge basalts: J. Geophys. Res., v. 84, p. 7429-7445.

Jacobsen, S. B., and Wasserburg, G. J., 1981, Sm-Nd isotopic evolution of chondrites: Earth Planet. Sci. Lett., v. 50, p. 139-155.

Jahn, B.-M., Bernard-Griffiths, J., Charlot, R., Cornichet, J., and Vidal, F., 1980, Nd and Sr isotopic compositions and REE abundances of Cretaceous MORB (Holes 417D and 418A, Legs 51, 52, and 53): Earth Planet. Sci. Lett., v. 48, p. 171-184.

James, D. E., 1982, A combined O, Sr, Nd, and Pb isotopic and trace element study of crustal contamination in central Andean lavas: I. local geochemical variations: Earth Planet. Sci. Lett., v. 57, p. 47-62.

Jarvis, J. C., Wildman, T. R., and Banks, N. R., 1975, Rare earths in the Leadville limestone and its marble derivates: Chem. Geol., v. 16, p. 27-37.

Johnsen, 1906, Beiträge zur Kenntnis natürlicher und kunstlicher Gläser: Phys.-Oekon. Ges. Koenigsb., Schr., v. 47, p. 105-110.

Jones, L. M., Hartley, M. E., and Walker, R. L., 1973, Strontium isotope composition of Alpine-type ultramafic rocks in the Lake Chatuge district, Georgia-North Carolina: Cont. Min. Pet., v. 38, p. 321-327.

Kieffer, S. W., 1977, Impact conditions required for formation of melt by jetting in silicates: in, Impact and Explosion Cratering, D. J. Roddy, R. O. Pepin, and R. B. Merrill, eds., Pergamon Press, 751 p.

Kolbe, P., Pinson, W. H., Saul, J. M., and Miller, E. W., 1967, Rb-Sr study on country rocks of the Bosumtwi Crater: Geochim. Cosmochim. Acta, v. 31, p. 869-875.

Kolodny, Y., and Kaplan, I. R., 1970, Uranium isotopes in seafloor phosphorites: Geochim. Cosmochim. Acta, v. 34, p. 3-24.

Kovach, J., 1980, Variations in the strontium isotopic composition of seawater during Paleozoic time determined by analysis of conodonts [abs]: Geol. Soc. Am. Abstr., v. 12, p. 465.

Kovach, J., and Zartman, R. W., 1981, U-Th-Pb dating of conodonts[abs]: Geol. Soc. Am. Abstr., v. 13, p. 285.

Kuroda, N., and Shiraki, K., 1975, Boninite and related rocks of Chichi-jima, Bonin Islands, Japan: Rep. Fac. Sci. Shizuoka Univ., v. 10, p. 145-155.

Kyte, F. T., Zhou, Z., and Wasson, J. T., 1980, Siderophile-enriched sediments from the Cretaceous-Tertiary boundary: Nature, v. 288, p. 651-656.

Kyte, F. T., Zhou, Z., and Wasson, J. T., 1981, High noble metal concentrations in a late Pliocene sediment: Nature, v. 292, p. 417-420.

Laird, J. L., 1977, Phase equilibria in mafic schist and the polymetamorphic history of Vermont: Ph. D. dissert., Calif. Inst. of Tech., 445 pp.

Laird, J. L., and Albee, A. L., 1981, Pressure, temperature and time indicators in mafic schist: Their application to reconstructing the polymetamorphic history of Vermont: Am. J. Sci., v. 281, p. 127-175.

Lanphere, M. A., Wasserburg, G. J. F., Albee, A. L., and Tilton, G. R., 1963, Redistribution of strontium and rubidium isotopes during metamorphism, World Beater Complex, Panamint Range, Calif.: in Craig, H. et al., eds., Isotopic and Cosmic Chemistry, North-Holland, Amsterdam, p. 269-320.

Lapham, D. M., and Bassett, W. A., 1964, K-Ar dating of rocks and tectonic events in the piedmont of southeastern Pennsylvania: Geol. Soc. Am. Bull., v. 75, p. 661-668.

Laurent, R., 1975, Occurrences and the origin of the ophiolites of southern Quebec, northern Appalachians: Can. J. Earth. Sci., v. 12, p. 443-455.

Laurent, R., 1977, Ophiolites from the Appalachians of Quebec: in North American Ophiolites, Oregon Dept. of Geol. & Min. Industr. Bull., v. 95, p. 25-40.

Levi, B. G., 1983, The nuclear arsenals of the US and USSR: Physics Today, v. 36, # 3, p. 43-49.

Lippolt, H. J., and Wasserburg, G. J., 1966, Rubidium-Strontium Messungen an Gläsern vom Bosumtwi-Krater und an Elfenbein-Kusten Tektiten: Z. Naturforsch., v. 21a, p. 226-231.

Malpas, J., 1977, Petrology and tectonic significance of Newfoundland ophiolites with examples from the Bay of Islands: in North American Ophiolites, Oregon Dept. of Geol. & Min. Industr. Bull., v. 95, p. 13-23.

Martens, C. S., and Harriss, R. C., 1970, Inhibition of apatite precipitation in the marine environment by magnesium ions: Geochim. Cosmochim. Acta, v. 34, p. 621-625.

McCulloch, M. T., and Wasserburg, G. J., 1978, Sm-Nd and Rb-Sr chronology of continental crust formation: Science, v. 260, p. 1003-1011.

McCulloch, M. T., Gregory, R. I., Wasserburg, G. J., and Taylor, H. P., 1981, Sm-Nd, Rb-Sr and $^{18}O/^{16}O$ isotopic systematics on an oceanic crustal section: Evidence from the Samail Ophiolite: J. Geophys. Res., v. 86, p. 2721-2735.

McCulloch, M. T., and Perfit, M. R., 1981, $^{143}Nd/^{144}Nd$, $^{87}Sr/^{86}Sr$ and trace element constraints on the petrogenesis of Aleutian island arc magmas: Earth Planet. Sci. Lett., v. 56, p. 167-179.

McCulloch, M. T., Jacques, A. L., Nelson, D. R., and Lewis, J. D., 1983, Nd and Sr isotopes in kimberlites and lamproites from western Australia: an enriched origin: Nature, v. 302, p. 400-403.

McDougall, I., and Lovering, J. F., 1969, Apparent K-Ar dates on cores, and excess Ar in flanges of Australites: Geochim. Cosmochim. Acta, v. 33, p. 1057-1070.

McElhaney, M. S., and McSween, H. Y., 1983, Petrology of the Chunky Gal Mountain mafic-ultramafic complex, North Carolina: Geol. Soc. Am. Bull., V. 95, p. 855-874.

McLennan, S. M., Fryer, B. J., and Young, G. M., 1979, The geochemistry of the carbonate-rich Espanola Formation (Huronian) with emphasis on the rare earth elements: Can. J. Earth Sci., v. 16, p. 230-239.

Menzies, M., and Murthy, V. R., 1980, Nd and Sr isotope geochemistry of hydrous nodules and their host alkali basalts: Implications for local heterogeneities in metasomatically zoned mantle: Earth. Planet. Sci. Lett., v. 46, p. 323-334.

Miller, R., 1953, The Webster-Addie ultramafic ring, Jackson County, North Carolina and secondary alteration of its chromint: Am. Mineralogist, v. 38, p. 1134-1147.

Milliman, J. D., and Meade, R. H., 1083, World-wide delivery of river sediment to the oceans: J. Geol., v. 91, p. 1-21.

Misra, K. C., and Keller, F. B., 1978, Ultramafic bodies in the southern Appalachians: A review: Am. J. Sci., v. 278, p. 389-418.

Moores, E. M., and Vine, F. J., 1971, Troodos Massif, Cyprus and other ophiolites as oceanic crust: evaluation and implications: Roy. Soc. London Phil. Trans. A, v. 268, p. 443-466.

Morgan, B. A., 1977, The Baltimore Complex, Maryland, Pennsylvania, and Virginia: in North American Ophiolites, Oregon Dept. of Geol. & Min. Industr. Bull., v. 95, p. 41-49.

Murthy, V. R., and Beiser, E., 1968, Strontium isotopes in ocean water and marine sediments: Geochim. Cosmochim. Acta, v. 32, p. 1121-1126.

Nazarov, M. A., Barsukova, L. D., Kolesov, G. M., Naidin, D. P., Alekseev, A. S., and Vernadsky, V. I., 1982, Extraterrestrial event at the C-T boundary: New geochemical and mineralogical data [abs]: 13th Lunar Planet. Sci. Conf., p. 580.

Nohda, S., and Wasserburg, G. J., 1981, Nd and Sr isotopic study of volcanic rocks from Japan: Earth Planet. Sci. Lett., v. 52, p.264-276.

Noiret, G., Montigny, R., and Allegre, C. J., 1981, Is the Vourinos Complex an island arc ophiolite?: Earth Planet. Sci. Lett., v. 56, p.375-386.

O'Keefe, J. A., 1976, Tektites and their Origin, Elsevier, 254 p.

O'Keefe, J. A., 1981, Comments on "Chemical relationships among irghizites, zhamanshinites, Australasian tektites, and Henbury impact glass": Geochim. Cosmochim. Acta, v. 44, p. 2151-2152.

O'Keefe, J. D., and Ahrens, T. J., 1982, The interaction of the Cretaceous-Tertiary extinction bolide with the atmosphere, ocean and solid earth: Geol. Soc. Am. Spec. Pap. 190, p. 103-120.

O'Nions, R. K., Hamilton, P. J., and Evensen, N. M., 1977, Variations in $^{143}Nd/^{144}Nd$ and $^{87}Sr/^{86}Sr$ ratios in oceanic basalts: Earth Planet Sci. Lett., v. 34, p. 13-22.

O'Nions, R. K., Carter, S. R., Cohen, R. S., Evensen, N. M., and Hamilton, P. J., 1978, Pb, Nd, and Sr isotopes in oceanic ferromanganese deposits and ocean floor basalts: Nature, v. 273, p. 435-438.

Orth, C. J., Gilmore, J. S., Knight, J. D., Pillmore, C. L., Tschudy, R. H., and Fasset, J. E., 1982, Iridium abundance measurements across the Cretaceous/Tertiary boundary in the San Juan and Raton Basins of northern New Mexico: Geol. Soc. Am. Spec. Pap. 190, p. 423-433.

Pal, D. K., Tuniz, C., Moniot, R. K., Kruse, T. H., and Herzog, G. F., 1982, ^{10}Be in Australasian tektites: Evidence for sedimentary precursor: Science, v. 218, p. 787-789.

Papanastassiou, D. A., and Wasserburg, G. J., 1969, Initial strontium isotopic abundances and the resolution of small time differences in the formation of planetary objects: Earth. Planet. Sci. Lett., v. 5, p. 361-372.

Papanastassiou, D. A., and Wasserburg, G. J., 1973, Rb-Sr ages and initial strontium in basalts from Apollo 15: Earth Planet. Sci. Lett., v. 17, p.324-337.

Papanastassiou, D. A., and Wasserburg, G. J., 1981, Microchrons: The ^{87}Rb-^{87}Sr dating of microscopic samples: Proc. 12th Lunar and Planetary Sci. Conf., p. 1027-1038.

Papanastassiou, D. A., DePaolo, D. J., and Wasserburg, G. J., 1977, Rb-Sr and Sm-Nd chronology and genealogy of basalts from the Sea of Tranquillity: Proc. Lunar Sci. Conf. 8th, p. 1639-1672.

Parekh, P. P., Möller, P., Dulski, P., and Bausch, W. M., 1977, Distribution of trace elements between carbonate and non-carbonate phases of limestone: Earth Planet. Sci. Lett., v. 34, p. 39-50.

Peterman, Z. E., Hedge, C. E., and Tourtelot, H. A., 1970, Isotopic composition of strontium in sea water throughout Phanerozoic time: Geochim. Cosmochim. Acta, v. 34, p. 105-120.

Piepgras, D. J., and Wasserburg, 1980, Neodymium isotopic variations in seawater: Earth Planet. Sci. Lett., v. 50, p. 128-138.

Piepgras, D. J., and Wasserburg, G. J., 1982, Isotopic composition of neodymium in waters from the Drake Passage: Science, v. 217, p. 207-214.

Piepgras, D. J., Wasserburg, G. J., and Dasch, E. J., 1979, The isotopic composition of Nd in different ocean masses: Earth Planet. Sci. Lett., v. 45, p. 223-236.

Piper, D. Z., 1974a, Rare earth elements in ferromanganese nodules and other marine phases: Geochim. Cosmochim. Acta, v. 38, p. 1007-1022.

Piper, D. Z., 1974b, Rare earths in the sedimentary cycle: A summary: Chem. Geol., v. 14, p. 285-304.

Pratt, J. H., and Lewis, J. V., 1905, Corundum and the peridotites of western North Carolina: North Carolina Geol. Surv. Bull., v. 1, 464 pp.

Rabken, M. I., 1968, On the depth and condition of regional metamorphism in the Anabar Shield: Proc. 23rd Int. Geol. Congr., p. 61.

Raisbeck, G. M., Yiou, F., Klein, J., and Middleton, R., 1983, $^{26}Al/^{10}Be$ in an Australite tektite; Further evidence for a terrestrial origin [abs]: EOS, v. 64, p. 284.

Rampino, M. R., 1982, A non-catastrophist explanation for the iridium anomaly at the Cretaceous-Tertiary boundary: Geol. Soc. Am. Spec. Pap. 190, p. 455-460.

Richard, P., and Allegre, C. J., 1980, Neodymium and strontium isotopic study of ophiolite and orogenic lherzolite petrogenesis: Earth Planet. Sci. Lett., v. 47, p. 65-74.

Richard, P., Shimizu, N., and Allegre, C. J., 1976, $^{143}Nd/^{144}Nd$, a natural tracer: An application to oceanic basalts: Earth Planet. Sci. Lett., v. 31, p. 267-278.

Roberson, C. E., 1966, Solubility implications of apatite in seawater: U. S. Geol. Surv. Prof. Pap. 550D, p. D178-D185.

Rodgers, J., 1970, The Tectonics of the Appalachians: Wiley-Interscience, N. Y., 271 pp.

Rogers, W. B., and Rogers, H. D., 1843, On the physical structure of the Appalachian chain, as exemplifying the laws which have regulated the elevation of great mountain chains, generally: Assoc. Am. Geologists and Naturalists Repts., p. 474-531.

Rocci, G., Ohnenstetter, D., and Ohnenstetter, M., 1975, La dualité des ophiolites tethysiennes: Petrologie, v. 1, p. 172-174.

Sailor, R. V., and Kuntz, M. A., 1973, Petrofabric and textural evidence for the systectonic recrystallization of the Buck Creek dunite, N. Carolina [abs]: Geol. Soc. Am. Abstr., v. 5, p. 791-792.

St. Julien, P., 1972, Appalachian structure and stratigraphy: Quebec Int. Cong. 24th, Montreal, 1972, Field Excursion A56-C56 Guidebook, 35 pp.

St. Julien, P., Hubert, C., and Williams, H., 1976, The Baie Verte-Brompton Line and its possible tectonic significance in the northern Appalachians [abs]: Geol. Soc. Am. Abstr., v. 8, p. 300.

Saleeby, J. B., 1982, Polygenetic ophiolite belt of the California Sierra Nevada: geochronological and tectonostratigraphic development: J. Geophys. Res., v. 87, p. 1803-1824.

Scherer, M., and Seitz, H., 1980, Rare earth element distribution in Holocene and Pleistocene corals and their redistribution during diagenesis: Chem. Geol., v. 28, p. 279-289.

Schmidt, R. M., and Holsapple, K. A., 1982, Estimates of crater size for large-body impact: Gravity-scaling results: Geol. Soc. Am. Spec. Pap. 190, p. 93-102.

Schnetzler, C. C., and Pinson, W. M., 1964, Variation of strontium isotopes in tektites: Geochim. Cosmochim. Acta., v. 28, p. 953-969.

Schnetzler, C. C., Philpotts, J. A., and Pinson, W. H., 1969, Rubidium-strontium correlation study of moldavites and Ries Crater material: Geochim. Cosmochim. Acta, v. 33, p. 1015-1021.

Schnetzler, C. C., Pinson, W. M., and Hurley, B. M., 1966 , Rubidium-strontium age of the Bosumtwi crater area, Ghana, compared with the age of the Ivory Coast tektites: Science, v. 151, p. 817-819.

Schopf, T. J. M., 1982, Extinction of the dinosaurs; A 1982 understanding: Geol. Soc. Am. Spec. Pap. 190, p. 415-422.

Shaw, H. F., and Wasserburg, G. J., 1982, Sm-Nd and Rb-Sr systematics and the origin of sanidine spherules from a Cretaceous-Tertiary boundary clay: (abs.), Lunar and Planet. Sci. Conf. 13th, p. 716-717.

Shiraki, K., and Kuroda, N., 1977, The boninite revisited: J. Geol. Soc. Japan, v. 86, p. 34-50.

Sholkowitz, E., 1973, Interstitial water chemistry of the Santa Barbara basin sediments: Geochim. Cosmochim. Acta, v. 37, p. 2043-2073.

Smit, J., and Hertogen, J., 1980, An extraterrestrial event at the Cretaceous-Tertiary boundary: Nature, v. 285, p. 198-200.

Smit, J., and Klaver, G., 1981, Sanidine spherules at the Cretaceous-Tertiary boundary, Cometary material?: Nature, v. 292, p. 47-49.

Smith, A. G., Hurley, A. M., and Briden, J. C., 1981, Phanerozoic paleocontinental world maps: Cambridge Univ. Press, Cambridge, 102pp.

Southwick, P. H., 1070, Structure and petrology of the Harford County part of the Baltimore State line gabbro-peridotite complex: in G. W. Fischer et al., eds., Studies of Appalachian Geology: Central and Southern, Wiley-Interscience, New York, 460 pp.

Steinmann, G., 1927, Die ophiolithischen Zonen in dem mediterranen Kettengebirge: 14th Int. Geol. Congr., Madrid, v. 2, p. 638-667.

Störzer, D., and Wagner, W. A., 1971, Fission track ages of the North American tektites: Earth Planet. Sci. Lett., v. 10, p. 435-440.

Störzer, D., and Wagner, G. A., 1977, Fission track dating of meteorite impacts (abs.): Meteoritics, v. 12, p. 368.

Störzer, D., and Wagner, G. A., 1980, Australites older than Indochinites: Naturwissenschaften, v. 67, p. 90.

Stueber, A. M., 1969, Abundances of K, Rb, Sr, and Sr isotopes in ultramafic rocks from western North Carolina: Geochim. Cosmochim. Acta, v. 33, p. 543-553.

Suess, F. E., 1900, Die Herkunft der Moldavite: Jahrb. K. K. Reichanst., Vienna, v. 50, p. 193-382.

Sun, S. S., 1980, Lead isotopic study of young volcanic rocks from mid-ocean ridges, ocean islands, and island arcs: Phil. Trans. R. Soc. Lond., Ser. A, v. 297, p. 409-445.

Tatsumoto, M., 1978, Isotopic composition of lead in oceanic basalts and its implication to mantle evolution: Earth Planet. Sci. Lett., v. 38, p. 63-87.

Taylor, H. P., and Epstein, S., 1962, Oxygen isotope studies on the origin of tektites: J. Geophys. Res., v. 67, p. 4485-4490.

Taylor, H. P., and Epstein, S., 1966, Oxygen isotope studies of Ivory Coast tektites and impactite glasses from the Bosumtwi Crater, Ghana: Science v. 153, p. 173-175.

Taylor, H. P., and Epstein, S., 1969, Correlations between $^{18}O/^{16}O$ ratios and chemical composition of tektites: J. Geophys. Res., v. 74, p. 6834-6844.

Taylor, S. R., 1966, Australites, Henbury impact glass and subgreywacke: a comparison of the abundances of 51 elements: Geochim. Cosmochim. Acta, v. 30, p. 1121-1136.

Taylor, S. R., 1973,Tektites; A Post-Apollo view: Earth Sci. Rev., v. 9, p. 101- 123.

Taylor, S. R., 1975, Lunar Science: A post-Apollo view, Pergamon, 372 p.

Taylor, S. R., and McLennan, S. M., 1979, Chemical relationships among irghizites, zhamanshinites, Australasian tektites, and Henbury impact glasses: Geochim. Cosmochim. Acta, v. 43, p. 1551-1565.

Tera, F., Middleton, R., Klein, J., and Brown, L., 1983, Beryllium-10 in tektites [abs]: EOS, v. 64, p. 284.

Thierstein, H. R., 1982, Terminal Cretaceous plankton extinctions: A critical assessment: Geol. Soc. Am. Spec. Pap. 190, p. 385-399.

Tilton, G. R., Wetherill, G. W., Davis, G. L., and Hopson, C. A., 1958, Ages of minerals from the Baltimore Gneiss, Maryland: Geol. Soc. Am. Bull., v. 79, p. 757-762.

Tilton, G. R., Doe, B. R., and Hopson, C. A., 1970, Zircon age measurements in the Maryland Piedmont, with special reference to Baltimore Gneiss problems: in G. W. Fisher et. al., eds., Studies of Appalachian geology: Central and Southern, Wiley-Interscience, New York, 460 pp.

Trompette, R., Affaton, P., Joulia, F., and Marchand, J., 1980, Stratigraphic and structural controls of the late Precambrian phosphate deposits of the northern Volta basin in Upper Volta, Niger, and Benin, West Africa: Econ. Geol., v. 75, p. 62-70.

Trueman, N. A., 1971, A petrologic study of some sedimentary phosphorite deposits: Bull. Austr. Min. Dev. Lab., v. 11, 71 pp.

Turekian, K. K., Katz, A., and Chan, L., 1973, Trace element trapping in pteropod tests: Limnol and Oceanography, v. 18, p. 240-249.

Turner, D. R., and Whitfield, M., 1979, Control of seawater composition: Nature, v. 281, p. 468-469.

Turner, D. R., Whitfield, M., and Dickson, A. G., 1981, The equilibrium speciation of dissolved components in freshwater and seawater at 25° C and 1 atm. pressure: Geochim. Cosmochim. Acta, v. 45, p. 855-881.

Upadhyay, J. D., Dewey, J. F., and Neale, E. R. W., 1971, The Bett's Cove ophiolite complex, Newfoundland: Appalachian oceanic crust and mantle: Geol. Soc. Canada Proc., v. 24, p. 27-34.

Vachette, M., 1964, Nouvelles mesures d'ages absolus de granites d'age éburén dela cote d'Ivoire: C. R. Acad. Sci. Paris, v. 258, p. 569-577.

Veeh, H. H., Burnett, W. C., and Soutar, A., 1973, Contemporary phosphorites on the continental margin of Peru: Science, v. 181, p. 844-845.

Veizer, J., and Compston, W., 1974, $^{87}Sr/^{86}Sr$ composition of seawater during the Phanerozoic: Geochim. Cosmochim. Acta, v. 38, p. 1461-1484.

Veizer, J., Compston, W., Clauer, N., and Schidlowski, M., 1983, $^{87}Sr/^{86}Sr$ in late Proterozoic carbonates:Evidence for a "mantle event at ~ 900Ma ago: Geochim. Cosmochim. Acta, v. 47, p. 295-302.

Wasserburg, G. J., Pettijohn, F. J., and Lipson, J., 1957, Ar^{40}/K^{40} ages of micas and feldspars from the Glenarm Series near Baltimore, Maryland: Science, v. 126, n. 3269, p. 355-357.

Wasserburg, G. J., Jacobsen, S. B., DePaolo, D. J., McCulloch, M. T., and Wen, T., 1981, Precise determination of Sm/Nd ratios: Sm and Nd isotopic abundances in standard solutions: Geochim. Cosmochim. Acta, v. 45, p. 2311-2323.

Wetherill, G. W., 1975, Radiometric chronology of the early solar system: in, Annual Review of Nuclear Science, v. 25., p. 283-319.

Wetherill, G. W., Davis, G. L., and Lee-Hu, C., 1968, Rb-Sr measurements on whole rocks and separated minerals from the Baltimore Gneiss, Maryland: Geol. Soc. Am. Bull., v. 79, p. 757-762.

White, W. M., and Hofmann, A. W., 1982, Sr and Nd isotope geochemistry of oceanic basalts and mantle evolution: Nature, v. 296, p. 821-825.

Whitford, D. J., 1975, Sr isotopic studies of the volcanic rocks of the Sunda arc, Indonesia and their petrogenetic implications: Geochim. Cosmochim. Acta, v. 39, p. 1287-1302.

Whitford, D. J., Compston, W., Nichols, I. A., and Abbott, M. J., 1977, Geochemistry and late Cenozoic lavas from eastern Indonesia: Role of subducted sediments in petrogenesis: Geology, v. 5, p. 571-575.

Whitford, D. J., White, W. M., Jezek, P. A., and Nichols, I. A., 1979, Nd isotopic composition of recent andesites from Indonesia: Carnegie Inst. Wash. Yearb., 304-307.

Williams, G. H., 1884, On the paramorphosis of pyroxene to hornblende in rocks: Am. J. Sci., 3rd ser., v. 28, p. 259-268.

Williams, G. H., 1886, The gabbros and associated hornblende rocks occurring in the neighborhood of Baltimore, Maryland: U. S. Geol. Surv. Bull. 28, 78 pp.

Williams, G. H., 1890, The non-feldspathic intrusive rocks of Maryland and the course of their alteration: Am. Geologist, v. 6, p. 35-49.

Williams, H., 1971, Mafic/ultramafic complexes in western Newfoundland, the Appalachians and evidence for the transportation: A review and interim report: Geol. Assoc. Canada Proc., v. 24, p. 9-25.

Williams, H., and Talkington, R. W., 1977, Distribution and tectonic setting of ophiolites and ophiolitic melanges in the Appalachian orogen: in North American Ophiolites, Oregon Dept. of Geol. & Min. Industr. Bull., v. 95, p. 1-11.

Williamson, J. M., 1968, Least squares fitting of a straight line: Can. J. Phys., v. 46, p. 1845-1847.

Wilson, J. T., 1966, Did the Atlantic close and then reopen?: Nature, v. 211 p. 696-681.

Wright-Clark, J., Seymour, R. S., and Holzer, W. T., 1982, Geochemistry of conodont apatite -- progress report [abs]: Geol. Soc. Am. Abstr., v. 14, p. 650.

Wright-Clark, J., Seymour, R. S., and Shaw, H. F., ms., REE and Nd isotopes in conodont apatite: Variations with geological age and depositional environment: in review.

Zähringer, J., 1962, K-Ar measurements of tektites in, Radioactive Dating: Proc. NEA Symp., Athens, Nov. 19-23, Int. Atomic Energy Agency, Vienna, p. 289-305.

Ziegler, A. M., Scotese, C. R., McKerrow, W. S., Johnson, M. E., and Baumbach, R. K., 1979, Paleozoic paleogeography: Ann. Rev. Earth and Planet. Sci., v. 7, p. 473-502.

Zindler, A., Hart, S. R., Frey, F. A., and Jakobsson, S. P., 1979, Nd and Sr isotope ratios and rare earth element abundances in Reykjanes Peninsula basalts: Evidence for mantle heterogeneity beneath Iceland: Earth Planet. Sci. Lett., v. 45, p. 249-262.

Zindler, A., Hart, S. R., and Brooks, C., 1981, The Shabogama intrusive suite, Labrador: Sr and Nd isotopic evidence for contaminated mafic magmas in the Proterozoic: Earth Planet. Sci. Lett., v. 54, p. 217-235.

APPENDIX I.

Earth and Planetary Science Letters, 60 (1982) 155–177
Elsevier Scientific Publishing Company, Amsterdam – Printed in The Netherlands

[6]

Age and provenance of the target materials for tektites and possible impactites as inferred from Sm-Nd and Rb-Sr systematics

H.F. Shaw and G.J. Wasserburg

Lunatic Asylum, Division of Geological and Planetary Sciences, California Institute of Technology, Pasadena, CA 91125 (U.S.A.)

Received December 22, 1981
Revised version received June 10, 1982

Sm-Nd and Rb-Sr analyses of tektites and other impactites can be used to place constraints on the age and provenance of target materials which were impact melted to form these objects. Tektites have large negative $\epsilon^{Nd}(0)$ values and are uniform within each tektite group while the $\epsilon^{Sr}(0)$ are large positive values and show considerable variation within each group. Chemical, trace element, and isotopic compositions of tektites are consistent with production by melting of sediments derived from old terrestrial continental crust. Each tektite group is characterized by a uniform Nd model age, T^{Nd}_{CHUR}, interpreted as the time of formation of the crustal segment which weathered to form the parent sediment for the tektites: (1) ~1.15 AE for Australasian tektites; (2) ~1.91 AE for Ivory Coast tektites; (3) ~0.9 AE for moldavites; (4) ~0.65 AE for North American tektites, and (5) ~0.9 AE for high-Si irghizites. Sr model ages, T^{Sr}_{UR}, are variable within each group reflecting Rb-Sr fractionation and in the favorable limit of very high Rb/Sr ratios, approach the time of sedimentation of the parent material which melted to form the tektites. Australasian tektites are derived from ~0.25 AE sediments, moldavites from ~0.0 AE sediments, Ivory Coast tektites from ~0.95 AE sediments. Possible parent sediments of other tektite groups have poorly constrained ages. Our data on moldavites and Ivory Coast tektites are consistent with derivation from the Ries and Bosumtwi craters, respectively. Irghizites are isotopically distinct from Australasian tektites and are probably not related. Sanidine spherules from a Cretaceous-Tertiary boundary clay have initial $\epsilon^{Nd} \sim +2$; $\epsilon^{Sr} \sim +5$ and are not derived from old continental crust or meteoritic feldspar. They may represent a mixture of basaltic oceanic crust and sediments, implying an oceanic impact. These isotopic results are also consistent with a volcanic origin for the spherules.

1. Introduction

The origin of tektites has long been the source of controversy. Since the early part of this century, when it was recognized that tektites are naturally formed objects and not the product of early man's glass-making, many creative theories have been proposed to explain their origin (see O'Keefe [1] for a discussion of the history of these theories). Most of these suggestions have been examined and discarded and today, although some workers favor a lunar volcanic origin for tektites [1,2], most workers agree that the results of analyses on returned lunar samples make a lunar origin highly unlikely. Instead, most feel that the bulk of the physical and chemical data on tektites is consistent with their formation by impact melting of terrestrial rocks or sediments by the fall of a large meteorite or comet nucleus [3,4]. In this paper we present the results of a series of Nd and Sr isotopic measurements made on tektites in order to gain new insight into their origin. We then present a model to explain the observed isotopic systematics.

In order to extend this technique, we have also analyzed sanidine spherules from the Cretaceous-Tertiary boundary clay of the Gredero section, Caravaca, southeast Spain. Alvarez et al. [5] found

Division Contribution No. 3718 (403).

that the sediments marking the end of the Cretaceous in Italy, Denmark, and New Zealand are many-fold enriched in Ir and other noble metals relative to crustal rocks. This has subsequently been confirmed to be a global phenomenon [6–8]. The enrichment of these elements at the Cretaceous-Tertiary boundary has been interpreted as evidence for the impact of a 5–10 km extraterrestrial body. The sanidine spherules are thought to have been produced by this impact event. The lack of geologic evidence on land for the crater which would result from such a large impact has prompted the suggestion that the impact occurred in an ocean basin, a possibility which is in principle addressable by the techniques used in this paper.

Over a decade has passed since the first Sr isotopic measurements were made on tektites [9–13]. Since then, our understanding of the behavior of isotopic systems during various geochemical processes has greatly increased. In addition, the development of techniques to measure precise Nd isotopic ratios has provided a new, powerful tool for dating and determining the provenance of rocks. Advances in Rb/Sr techniques now permit the measurement of $^{87}Sr/^{86}Sr$ ratios to better than 0.1% on samples containing $< 10^{-12}$ moles of Sr [14,15], which has allowed us to include microtektites in this study. Preliminary results of this project were presented at the 12th and 13th Lunar and Planetary Science Conferences [14–17].

2. Samples

Tektites are known to occur in four areas on earth (Fig. 1). Within each area tektites have the same K-Ar or fission track age, presumably dating the time at which the tektites were last molten. These four groups consist of (1) the North American tektites (georgiaites, bediasites, and the Martha's Vineyard tektite), with ages of ~ 35 m.y. [18,19]; (2) the central European moldavites which formed ~ 14 m.y. ago [20,21]; (3) the Ivory Coast tektites of 1.3 m.y. age [18,21]; and (4) the Australasian tektites (australites, indochinites, philippinites, etc.) of ~ 0.7 m.y. age [18,22–24]. In addition, the North American, Ivory Coast, and Australasian occurrences are associated with microtektites found in deep-sea sediments of the same age as the land tektites [25–27]. Recently, glasses associated with the Zhamanshin impact structure have been described from the region north of the Aral Sea, U.S.S.R. [28–31]. The tektite-like objects have been called irghizites and associated impact glasses, zhamanshinite. Determinations of the age of these objects range from 0.81 to 1.1 m.y. [32–33]. Florenskij et al. [34] have determined that the Zhamanshin structure itself is between 0.69 and 0.85 m.y. old.

We have analyzed seven Australasian macrotektites and two Australasian microtektites from the Indian Ocean, six North American tektites (three bediasites, two georgiaites, and the Martha's Vineyard tektite), four moldavites, three Ivory Coast tektites, two high-Si irghizites and one low Si irghizite (zhamanshinite in the nomenclature of Bouska et al. [31]). Samples were chosen to cover the range of representative chemical composition and to cover the geographic distribution of these occurrences. As this work was being completed, it was brought to our attention that a possible parent material for the moldavites had been identified among the Ries Crater materials on the basis of chemical and Sr isotopic analyses [35]. This material is the Tertiary Upper Freshwater Mollase (OSM sands) which formed a thin surficial deposit at the time of formation of the Ries Crater. Through the generosity of Dr. P. Horn at Munich and Drs. Luft and von Engelhardt at Tübingen, we obtained two samples for analysis. Sample OSM 050 is from a surficial deposit near Unterfinnigen and sample OSM D2 is from the 41.9 m level of the NASA drill hole at Demmingen. The OSM sands are of Tortonian age and are made up of freshwater limestones, marls, clay, and sand [36].

In a study of the fossil assemblages across the Cretaceous-Tertiary boundary, Smit [37] found large numbers (50–300 cm^{-3} of sediment) of small (50–1000 μm) spherules in the Ir-rich layer at Caravaca. X-ray diffraction, electron probe and neutron activation analyses showed that the spherules are dominantly sanidine with $K/Na \sim 100$, are rich in As, Se, Sb, Zn, and contain dark inclusions rich in Fe, Ni, and Co [37]. Unlike the

glassy tektites, the spherules are very finely crystalline and contain up to 20% void space which may have been occupied by another phase at one time. We were provided with a concentrate of these spherules by J. Smit. Smit and Klaver [37] have argued that the sanidine spherules have the texture of quickly cooled liquid droplets. At a recent meeting (13th Lunar and Planetary Science Conference, Houston, Texas, 1982), this interpretation was questioned. To some present, the textures were more diagnostic of devitrified glass or authigenic growth. The very heavy oxygen isotopic composition of the spherules ($\delta^{18}O_{SMOW} = +27.5$) reported by Epstein [38] was offered as evidence of high-temperature isotopic exchange with atmospheric oxygen ($\delta^{18}O^{atm}_{SMOW} \sim +24$ [39]). It is possible that low-temperature exchange with seawater ($\delta^{18}O^{sw}_{SMOW} \equiv 0$) during devitrification or authigenic growth could also explain the heavy oxygen of the sanidine.

3. Procedures and data representation

Each macrotektite was crushed and clear interior fragments weighing 50–300 mg were selected, rinsed in clean acetone and distilled water, powdered and set aside for dissolution. A fragment of each tektite was reserved for a thin section. Sample USNM 2082 (Martha's Vineyard) was a powder when received. A 47 mg split was made and used for dissolution. The OSM sand samples were also powders when received. Splits of ~200 mg were used for dissolution. Detailed descriptions of the chemical separation and mass spectrometric procedures are given in references 40–42. A different procedure was followed for the analysis of the microtektites [15]. Rb, Sr, Sm, and Nd concentrations were determined by isotope dilution. Typically, for the macrotektites, 50–100 mg of sample were dissolved and an aliquot (~2%) taken and spiked to determine approximate concentrations. The remainder of the solution was then spiked to determine both isotopic composition and concentration.

Major and minor element concentrations of the tektite samples were determined by electron microprobe analysis. X-ray intensities were reduced using the procedure of Bence and Albee [43] and the correction factors of Albee and Ray [44] and Shaw and Albee [45]. A broad beam (>30 μm) and a low sample current (15 nA on brass) were used to minimize volatile loss. Precision of the analyses is 1–2% of the amount present for major constituents.

Approximately 100 mg of sanidine spherules were hand-picked from other materials in the concentrate. Other materials (~10%) consisted of carbonate nanofossils, lithic fragments, and organic matter. The spherules were crushed, leached in cold 0.5 M HCl, and rinsed with H_2O in an attempt to remove carbonate. The residue (residue 1) was spiked and analyzed. A sequential leaching experiment was carried out on a 262 mg separate of spherules. This separate was subjected to 4 acid leaches of increasing strength: cold 0.1 M, 0.5 M, 1.5 M, and hot 1.5 M HCl. Aliquots of all 4 leaches and the residue (residue 2) were spiked and analyzed. A 7.5 mg aliquot of residue 2 was subjected to a final leach in hot 3 M HCl and the resulting residue (residue 3) analyzed. We have also measured Sr isotopic composition and concentration in a hand-picked separate of carbonate fossils from the boundary clay.

The errors quoted for the $^{143}Nd/^{144}Nd$ and $^{87}Sr/^{86}Sr$ ratios are 2σ of the mean for 150–250 and 100–200 ratios, respectively. Blanks for the procedure are ~50 pg Nd and 150 pg Sr and are negligible. Isotopic ratios are expressed in ϵ notation [46] where $\epsilon^{Nd}(0)$ is the measured deviation in parts in 10^4 of the $^{143}Nd/^{144}Nd$ ratio from the present-day chondritic value of 0.511847 (CHUR):

$$\epsilon^{Nd}(0) = \left[\frac{(^{143}Nd/^{144}Nd)_M}{0.511847} - 1\right] \times 10^4$$

Similarly $\epsilon^{Sr}(0)$ is the deviation in parts in 10^4 of the $^{87}Sr/^{86}Sr$ ratio from the inferred reference value of 0.7045 corresponding to a model undifferentiated mantle reservoir (UR):

$$\epsilon^{Sr}(0) = \left[\frac{(^{87}Sr/^{86}Sr)_M}{0.7045} - 1\right] \times 10^4.$$

The parent-daughter ratios can be referenced to these reservoirs by expressing them as the enrichment factors:

$$f^{Sm/Nd} \equiv [(Sm/Nd)_M/(Sm/Nd)_{CHUR} - 1]$$

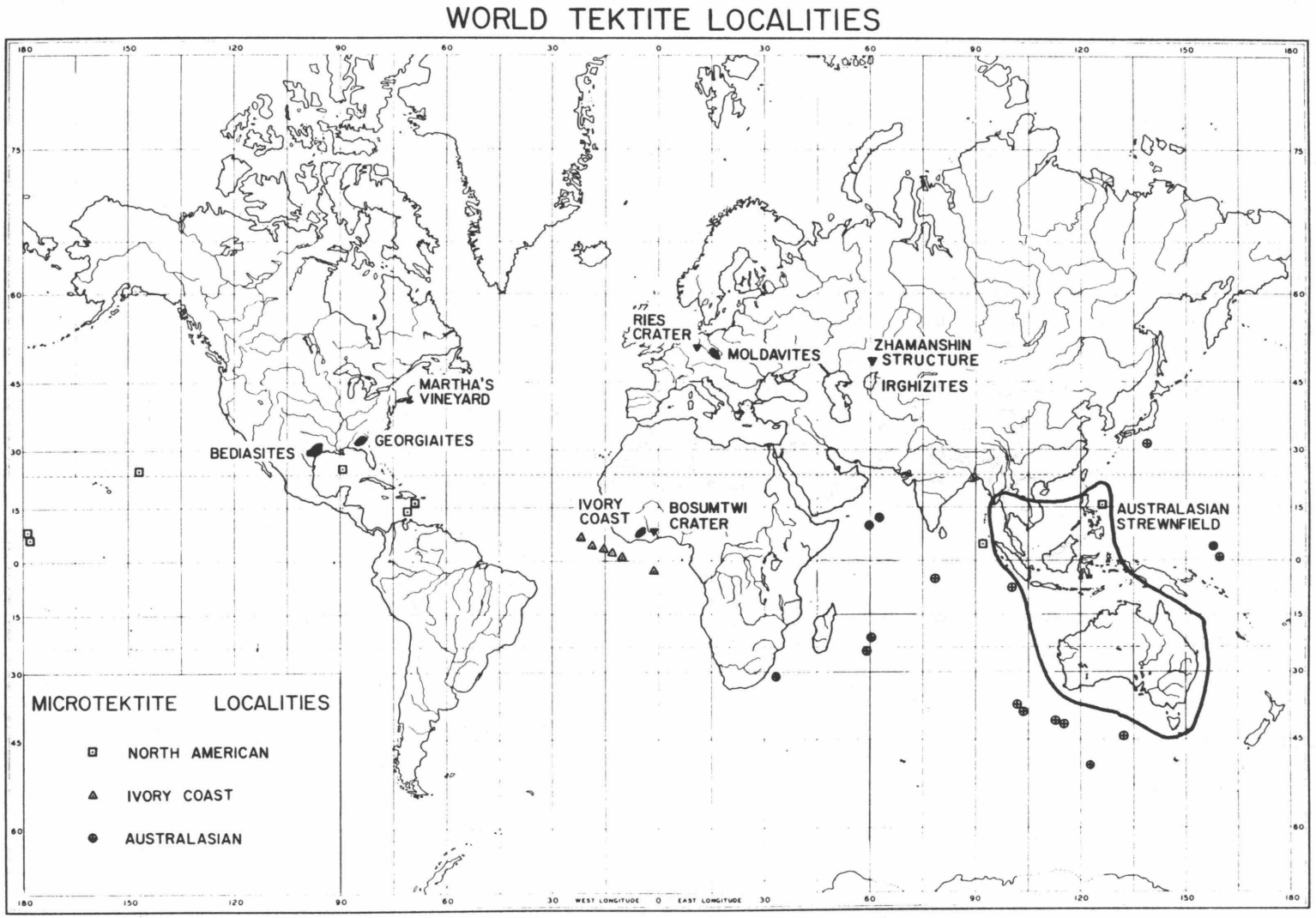

Fig. 1. Map showing the locations of known tektite fields and suggested source craters. Locations of deep-sea cores containing microtektites associated with the North American, Ivory Coast, and Australasian tektites are indicated by the symbols. (After Glass et al. [78].)

TABLE 1

Microprobe analyses of tektites

	Australasian tektites							Moldavites				Ivory Coast tektites		
	Thai A	Thai B	Camb A	Camb B	Camb C	HiCaAus	HiMgAus USNM 2536	USNM 2052	USNM 2051	USNM 2226	USNM 2233	USNM 6011A	USNM 6011B	USNM 6011C
SiO_2	74.16	74.72	75.75	78.15	77.06	75.53	72.84	78.42	76.37	80.91	80.50	68.96	68.73	69.29
TiO_2	0.77	0.74	0.76	0.65	0.83	0.65	0.72	0.36	0.34	0.36	0.27	0.56	0.56	0.57
Al_2O_3	13.95	12.69	11.75	11.13	11.71	11.11	11.84	10.73	10.76	10.73	9.21	17.10	16.21	16.67
Cr_2O_3	0.03	0.04	0.03	0.02	0.03	0.02	0.01	0.03	0.02	0.00	0.13	0.08	0.05	0.04
FeO	4.92	4.57	3.82	4.06	3.55	4.20	4.82	2.00	1.96	1.94	1.43	6.60	6.16	6.28
MgO	1.95	1.85	1.53	1.35	1.31	1.67	2.55	1.82	2.43	1.26	1.69	2.97	3.20	3.07
MnO	0.07	0.08	0.06	0.15	0.07	0.09	0.10	0.04	0.29	0.05	0.09	0.29	0.06	0.06
CaO	1.89	1.83	1.37	1.06	0.96	3.85	2.90	2.02	3.46	1.17	2.69	1.22	1.31	0.93
K_2O	2.67	2.52	2.30	2.45	2.36	2.35	2.30	2.76	3.30	2.86	2.46	1.91	1.79	1.81
Na_2O	0.68	1.05	1.18	1.01	0.92	0.95	1.12	0.43	0.39	0.40	0.38	1.71	1.58	1.54
Total	101.00	100.09	98.55	100.03	98.80	100.41	99.20	98.61	99.32	99.68	98.85	101.40	99.65	100.26

	Bediasites			Georgiaites		Irghizites		
	USNM 1880 B-229	USNM 1880 B-306	USNM 1880 B-312	USNM 2339	USNM 6178	USNM 5939 GpIV 12	USNM 5938 GpIII 3-1	USNM 5938 GpIII 3-6
SiO_2	79.20	78.52	75.69	81.61	80.50	54.27	75.11	74.46
TiO_2	0.72	0.63	0.83	0.51	0.50	0.81	0.76	0.76
Al_2O_3	12.68	11.95	14.85	11.65	11.73	19.47	9.32	9.54
Cr_2O_3	0.01	0.02	0.02	0.04	0.02	0.01	0.03	0.04
FeO	3.52	3.02	4.03	2.92	3.01	7.67	5.34	5.50
MgO	0.40	0.56	0.49	0.54	0.53	2.64	2.65	2.77
MnO	0.03	0.05	0.01	0.00	0.00	0.16	0.08	0.08
CaO	0.41	0.66	0.44	0.48	0.53	8.85	2.30	2.43
K_2O	1.90	2.36	1.69	2.21	2.18	1.39	1.96	1.96
Na_2O	0.90	0.94	0.83	0.52	0.87	3.51	0.81	0.86
Total	99.77	98.75	98.88	100.01	99.87	98.78	98.36	98.42

$f^{Rb/Sr} \equiv [(Rb/Sr)_M/(Rb/Sr)_{UR} - 1]$

where M denotes the measured values and $(^{87}Rb/^{86}Sr)_{UR} = 0.0827$, $(^{147}Sm/^{144}Nd)_{CHUR} = 0.1967$.

4. Results

4.1. Tektites

Chemical compositions are presented in Table 1. With the exception of the low-Si irghizite USNM 5939 #12, all samples are characterized by very high SiO_2 contents and high K_2O and Na_2O contents. These elemental abundances are unlike common terrestrial igneous rocks, having relatively low alkali and high alumina contents as compared to igneous rocks with a similar silica content. This is reflected in the presence of corundum in the norm. The Australasian tektites show a strong positive correlation between the concentrations of CaO and Sr [13]. This correlation does not appear to hold for the other tektite groups. Several authors [30,47,48] have previously determined that the LREE in tektites and irghizites are strongly enriched relative to chondritic abundances. This enrichment is confirmed by our data by the negative values of $f^{Sm/Nd}$ for all samples (Table 3). The values of $f^{Sm/Nd}$ which range from -0.39 to -0.45 are typical of crustal rocks. As many other investigations have shown, tektites and the high Si irghizites are most similar in chemistry to terrestrial sedimentary rocks such as greywackes and arkosic sandstones or soils [49]. There are no known lunar rocks having major and trace element compositions which match those of tektites nor are there any known meteorites with compositions similar to tektites. The low-Si irghizite (USNM 5939 #12) is unlike any of the other tektites analyzed. Its composition is most like a basaltic andesite.

Our isotopic results are presented in Tables 2 and 3. Fig. 2a, b are histograms of isotopic composition comparing our data on tektites and

TABLE 2

Sm-Nd and Rb-Sr isotopic results

	Nd (ppm)	$^{147}Sm/^{144}Nd$ [a]	$^{143}Nd/^{144}Nd$ [b]	Sr (ppm)	$^{87}Rb/^{86}Sr$ [c]	$^{87}Sr/^{86}Sr$ [d]
Australasian tektites						
Thailand A	29.8	0.1165	0.511260 ±24	129.6	2.824	0.71894 ±5
Thailand B	33.8	0.1165	0.511246 ±26	127.9	2.555	0.71880 ±4
Cambodia A	27.0	0.1161	0.511241 ±20	115.9	2.797	0.71857 ±3
Cambodia B	32.2	0.1192 [e]	0.511271 ±35	110.7	2.946	0.71947 ±3
Cambodia C	33.8	0.1155	0.511224 ±23	107.2	3.037	0.71912 ±3
HiCa australite	33.1	0.1170 [e]	0.511258 ±26	291.0	1.327	0.71398 ±4
HiMg australite	31.4	0.1161	0.511290 ±25	162.8	1.750	0.71625 ±5
Microtektites [f]						
BG-1	–	–	–	–	1.528	0.71680 ±70
BG-2	–	–	–	–	0.628	0.71870 ±70
Moldavites						
USNM 2051	28.4	0.1089	0.511345 ±24	159.2	2.206	0.72158 ±4

TABLE 2 (continued)

	Nd (ppm)	$^{147}Sm/^{144}Nd$ [a]	$^{143}Nd/^{144}Nd$ [b]	Sr (ppm)	$^{87}Rb/^{86}Sr$ [c]	$^{87}Sr/^{86}Sr$ [d]
USNM 2233	–	–	–	130.4	2.892	0.72196 ±3
USNM 2226	–	–	–	136.0	3.023	0.72292 ±4
USNM 2052	26.2	0.1165	0.511344 ±27	124.0	3.481	0.72342 ±5
OSM sands						
OSM 050	20.8	0.1094 [e]	0.511317 ±26	56.8	4.508	0.72397 ±4
OSM D2	10.1	0.1013 [e]	0.511345 ±25	64.0	2.194	0.72196 ±6
Ivory Coast tektites						
USNM 6011A	20.5	0.1139	0.510813 ±29	289.6	0.627	0.72334 ±3
USNM 6011B	–	–	–	286.0	0.650	0.72357 ±4
USNM 6011C	21.3	0.1137	0.510849 ±20	259.6	0.787	0.72571 ±3
North American tektites						
Bediasites						
USNM 1880 B-229	31.6	0.1206	0.511514 ±28	123.7	1.212	0.71361 ±5
USNM 1880 B-306	37.7	0.1183	0.511504 ±25	121.6	1.249	0.71310 ±4
USNM 1880 B-312	32.8	0.1194	0.511534 ±25	132.1	–	0.71280 ±7
Georgiaites						
USNM 2339	22.6	0.1180	0.511508 ±21	171.1	–	0.71325 ±7
USNM 6178	–	–	–	114.3	1.184	0.71255 ±3
Martha's Vineyard						
USNM 2082	21.7	0.1178	0.511503 ±25	168.4	1.223	0.71319 ±3
Irghizites						
USNM 5939 GpIV #12, low Si	14.0	0.1399	0.511940 ±33	777.5	0.109	0.70508 ±11
USNM 5938 GpIII 3-1, high Si	17.5	0.1167	0.511410 ±29	142.2	1.215	0.71432 ±6
USNM 5938 GpIII 3-6, high Si	18.2	0.1167	0.511369 ±26	143.7	1.215	0.71427 ±5

[a] Uncertainty = 0.2% except as noted below.
[b] Normalized to $^{146}Nd/^{142}Nd = 0.636151$.
[c] Uncertainty = 1.0%.
[d] Normalized to $^{86}Sr/^{88}Sr = 0.1194$.
[e] Concentration by aliquot only, uncertainty = 2%.
[f] Data from Papanastassiou and Wasserburg [15].

TABLE 3

Parameters for Nd, Sr isotopic evolution

	$\epsilon^{Nd}(0)$ [a]	$f^{Sm/Nd}$ [b]	T_{CHUR} (AE)	$\epsilon^{Sr}(0)$ [c]	$f^{Rb/Sr}$ [d]	T_{UR} (AE)
Australasian tektites						
Thailand A	−11.5 ± 0.5	−0.4078	1.12 ± 0.05	204.4 ± 0.7	33.15	0.371 ± 0.004
Thailand B	−11.8 ± 0.5	−0.4075	1.15 ± 0.05	203.0 ± 0.6	29.90	0.407 ± 0.004
Cambodia A	−11.8 ± 0.4	−0.4047	1.15 ± 0.05	199.8 ± 0.4	32.82	0.365 ± 0.004
Cambodia B	−11.2 ± 0.7	−0.3942	1.14 ± 0.2	212.5 ± 0.4	34.62	0.368 ± 0.004
Cambodia C	−12.2 ± 0.4	−0.4129	1.17 ± 0.07	207.6 ± 0.4	35.72	0.348 ± 0.003
HiCa australite	−11.5 ± 0.5 −11.4 ± 0.4	−0.4050	1.13 ± 0.2	134.6 ± 0.6	15.05	0.536 ± 0.005
HiMg australite						
USNM 2536	−10.9 ± 0.5	−0.4095	1.06 ± 0.05	166.8 ± 0.7	20.17	0.496 ± 0.005
Microtektites [e]						
BG-1	–	–	–	174.6 ± 9.9	17.48	0.59 ± 0.05
BG-2	–	–	–	201.6 ± 9.9	6.59	1.83 ± 0.09
Moldavites						
USNM 2051	−9.8 ± 0.5	−0.4461	0.88 ± 0.04	242.4 ± 0.6	25.68	0.566 ± 0.006
USNM 2233	–	–	–	247.8 ± 0.4	33.96	0.438 ± 0.004
USNM 2226	–	–	–	261.4 ± 0.5	35.56	0.441 ± 0.005
USNM 2052	−9.8 ± 0.5	−0.4077	0.96 ± 0.04	268.6 ± 0.7	41.09	0.392 ± 0.006
OSM sands						
OSM 050	−10.4 ± 0.5	−0.4437	0.93 ± 0.2	276.3 ± 0.5	53.51	0.310 ± 0.004
OSM D2	−9.9 ± 0.5	−0.4851	0.81 ± 0.2	247.9 ± 0.8	25.53	0.583 ± 0.007
Ivory Coast tektites						
USNM 6011A	−20.2 ± 0.6	−0.4207	1.91 ± 0.05	267.4 ± 0.4	6.58	2.44 ± 0.62
USNM 6011B	–	–	–	270.7 ± 0.6	6.85	2.37 ± 0.67
USNM 6011C	−19.5 ± 0.4	−0.4221	1.84 ± 0.05	301.1 ± 0.4	8.52	2.12 ± 0.57
North American tektites						
Bediasites						
USNM 1880 B-229	−6.5 ± 0.6	−0.3870	0.67 ± 0.06	129.3 ± 0.7	13.66	0.568 ± 0.006
USNM 1880 B-306	−6.7 ± 0.5	−0.3983	0.67 ± 0.04	122.1 ± 0.6	14.10	0.519 ± 0.006
USNM 1880 B-312	−6.1 ± 0.5	−0.3929	0.62 ± 0.05	117.8 ± 1.0	–	–
Georgiaites						
USNM 2339	−6.6 ± 0.4	−0.3999	0.66 ± 0.04	124.1 ± 1.0	–	–
USNM 6178	–	–	–	114.3 ± 0.4	13.32	0.515 ± 0.005
Martha's Vineyard						
USNM 2082	−6.7 ± 0.5	−0.4013	0.67 ± 0.04	123.3 ± 0.4	13.79	0.536 ± 0.006
Irghizites						
USNM 5939	+1.8 ± 0.6	−0.2887	−0.25 ± 0.09	7.25 ± 1.6	0.32	1.34 ± 0.30
GpIV #12, low Si						
USNM 5938	−8.5 ± 0.6	−0.4063	0.84 ± 0.05	139.4 ± 0.8	13.70	0.61 ± 0.006
GpIII 3-1, high Si						
USNM 5938	−9.3 ± 0.5	−0.4069	0.91 ± 0.05	138.7 ± 0.7	13.70	0.61 ± 0.006
GpIII 3-6, high Si						

[a] Referenced to $(^{143}Nd/^{144}Nd)_{CHUR} = 0.511847$.
[b] Referenced to $(^{147}Sm/^{144}Nd)_{CHUR} = 0.1967$.
[c] Referenced to $(^{87}Sr/^{86}Sr)_{UR} = 0.7045$.
[d] Referenced to $(^{87}Rb/^{86}Sr)_{UR} = 0.0827$.
[e] Data from Papanastassiou and Wasserburg [15].

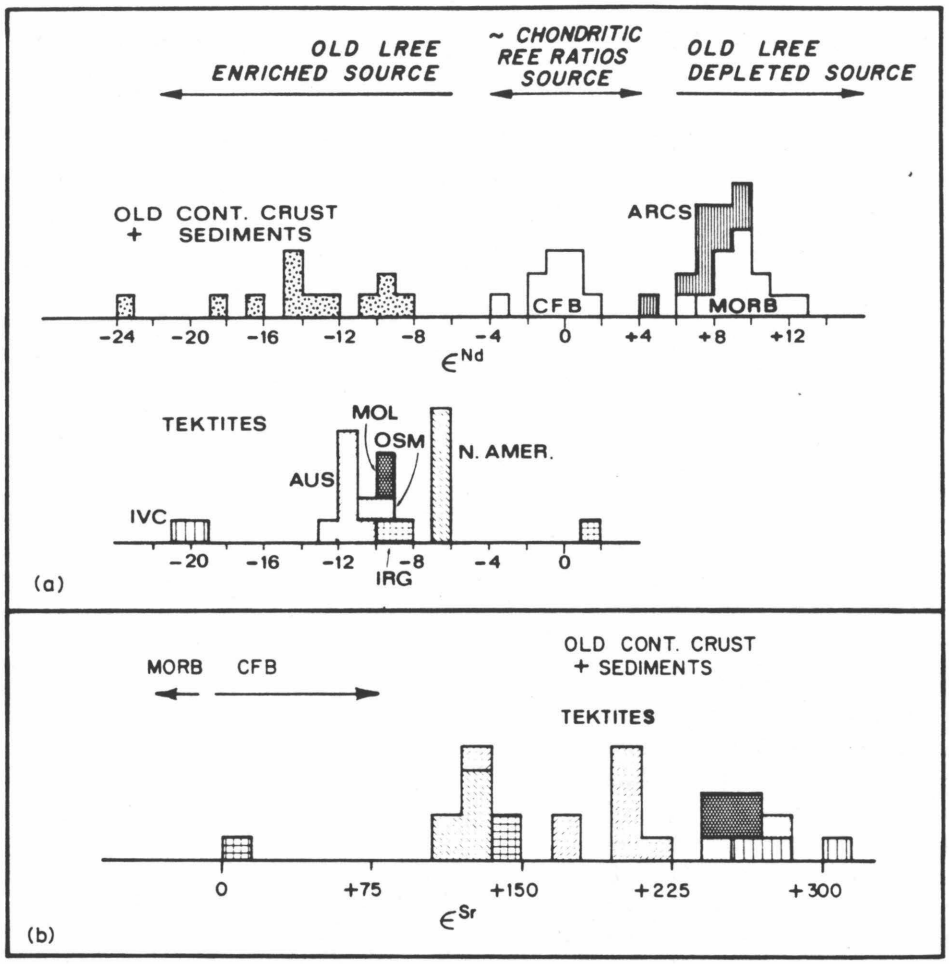

Fig. 2. (a) Histogram of $\epsilon^{Nd}(0)$ comparing the Nd isotopic composition of tektites to other terrestrial materials. Tektites have the Nd isotopic composition of old continental crust. Each tektite group is characterized by a uniform value of $\epsilon^{Nd}(0)$. (b) Histogram of $\epsilon^{Sr}(0)$ for tektites showing range of Sr isotopic composition observed within a given tektite group. Tektites have the Sr isotopic composition of old continental crust. Sr data for old continental crust are not plotted but generally lie in the region $\epsilon^{Sr}(0) > +50$. Patterns within histogram correspond to those used in Fig. 2a. (Data on old continental crust, oceanic island arcs (ARCS), mid-ocean ridge basalts (MORB), and continental flood basalts (CFB) from references 46, 52–55, 79.)

irghizites with various terrestrial rocks. With the exception of the low-Si irghizite, our samples are characterized by negative $\epsilon^{Nd}(0)$ and large positive $\epsilon^{Sr}(0)$ indicating that the parent material for these objects had a time integrated LREE enrichment and high Rb/Sr ratio. The isotopic composition of Nd is extremely uniform within each group of tektites. The Sm/Nd ratios are also quite uniform, though the abundances of Sm and Nd vary. In contrast, Sr isotopic composition within a group is quite variable as is the Rb/Sr ratio. This is particularly true of the Australasian tektites.

The low-Si irghizite is distinctive and has a low $^{87}Sr/^{86}Sr$ and positive $\epsilon^{Nd}(0)$, indicating that although it is now LREE enriched, this enrichment occurred at a recent time and the source material which melted to form this object had a time-integrated LREE depletion.

4.2. Sanidine spherules

In Fig. 3a we have plotted the isotopic composition of Sr for the sequential leaches and residue 2 vs. the cumulative percent Sr released. The bulk

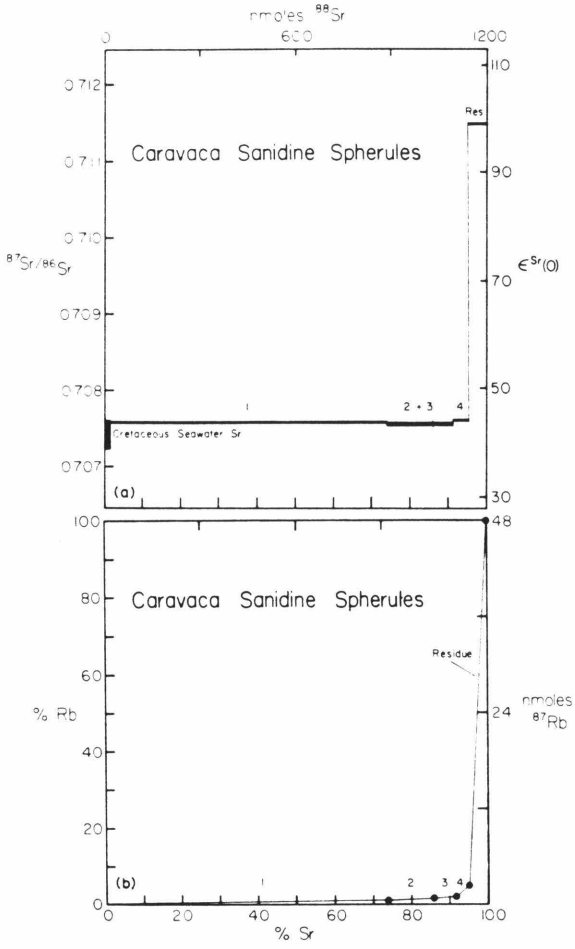

Fig. 3. (a) Plot showing measured $^{87}Sr/^{86}Sr$ vs. cumulative % Sr released in sequential leaching of sanidine spherules. Seawater data from Peterman et al. [50]. (b) Plot of cumulative % Rb vs. cumulative % Sr released during sequential leaching of sanidine spherules.

(~75%) of the Sr was removed in the first leach and ~96% removed in the combined leaches. The isotopic composition of the Sr in the leaches is $\epsilon^{Sr}(0) \sim +45$ which is indistinguishable from that in the carbonate fossils (Table 4) and within the range of Cretaceous seawater Sr [50]. The residue has a significantly different isotopic composition of $\epsilon^{Sr}(0) = +98.4$. The data for the carbonate fossils, residue 1 and residue 2, lie on a straight line mixing line in a plot of $\epsilon^{Sr}(0)$ vs. $1/Sr$ (Fig. 4), showing that the bulk spherules have a Sr isotopic composition which is a mixture of Cretaceous

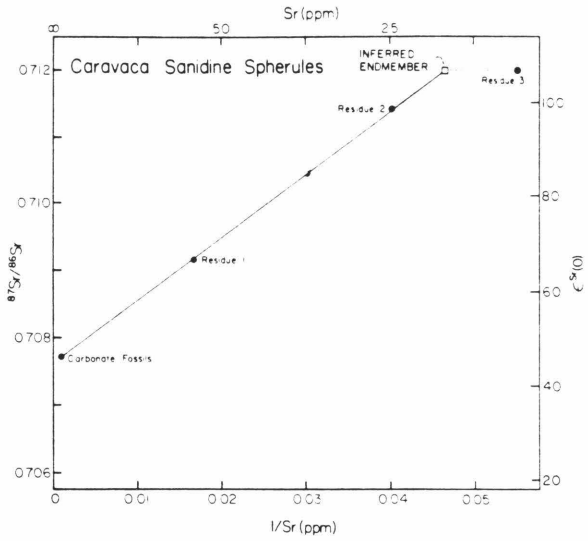

Fig. 4. Plot of $^{87}Sr/^{86}Sr$ vs. $1/Sr$ for Cretaceous-Tertiary boundary clay materials. Sanidine spherules lie on a mixing line between marine Sr and a sanidine Sr endmember.

seawater Sr represented by the fossils and a sanidine Sr endmember at higher $\epsilon^{Sr}(0)$. Residue 3, the most strongly leached residue with $\epsilon^{Sr}(0) = +106.4$ and ~18 ppm Sr does not lie on this mixing line, having lower $\epsilon^{Sr}(0)$ than predicted from the mixing line. We interpret this as representing the onset of Sr leaching from the sanidine itself. We thus infer that $\epsilon^{Sr}(0)$ of the sanidine endmember is +106 as measured in residue 3. Residue 2 closely approached this value in the sequential leaching experiment. This value is higher than that reported by DePaolo et al. [51] for an acid-leached residue with 111 ppm Sr. It is clear that both their sample and that which we originally reported on [17] were insufficiently leached and do not represent the endmember. To determine the initial $\epsilon^{Sr}(T)$ one must look at the behavior of Rb relative to Sr in the leaching experiment. Table 4 and Fig. 3b show that although ~96% of the Sr was removed in the 4 leaches, only 5% of the Rb was extracted. The bulk of the Rb remained in the residue and is associated with the high $\epsilon^{Sr}(0)$ material. Rb in the bulk spherules is strongly fixed in the sanidine unlike Sr which resides in easily acid leachable phases. If we use the Sr mixing relationship to determine the Sr concentration in the sanidine endmember (~22 ppm Sr) and assume that all of

TABLE 4

Isotopic results on sanidine spherules and leaches

	Sr (ppm)	^{87}Rb (nmoles)	^{88}Sr (nmoles)	$^{87}Rb/^{86}Sr$	$\epsilon^{Sr}(0)$ [a]	Nd (ppm)	^{147}Sm (pmoles)	^{144}Nd (pmoles)	$^{147}Sm/^{144}Nd$	$\epsilon^{Nd}(0)$ [b]
Residue 1	60.1	–	–	3.10	$+66.0 \pm 1.4$	0.55	–	–	–	–
0.1 M leach	–	0.515 (1.08%)	886.3 (73.64%)	0.005	$+44.8 \pm 0.7$	–	–	43.9 (7.76%)	–	-6.93 ± 0.50
0.5 M leach	–	0.254 (0.53%)	148.5 (12.34%)	0.014	$+43.7 \pm 0.7$	–	–	253.0 (44.74%)	–	–
1.5 M leach	–	0.262 (0.55%)	68.4 (5.68%)	0.033		–	–	149.0 (26.35%)	–	-5.56 ± 0.49
Hot 1.5 M leach	–	1.400 (2.93%)	43.8 (3.64%)	0.267	$+45.3 \pm 0.6$	–	–	55.6 (9.83%)	–	-4.14 ± 0.46
Residue 2	24.9	45.3 (94.97%)	56.6 (4.70%)	6.70	$+98.4 \pm 0.7$	0.16	12.3	64.0 (11.32%)	0.192	$+1.93 \pm 0.50$
Residue 3	18.0	–	–	8.86	$+106.4 \pm 2.5$	0.11	–	–	–	–
Carbonate fossils	997.6	–	–	0.012	$+45.3 \pm 0.6$	–	–	–	–	–

[a] Referenced to $(^{87}Sr/^{86}Sr)_{UR} = 0.7045$.

[b] Referenced to $(^{143}Nd/^{144}Nd)_{CHUR} = 0.511847$.

Numbers in parentheses refer to the percentage of the element released in a sequential leaching experiment.

the Rb in the bulk spherules is in the sanidine, then we can calculate a lower limit of $\epsilon^{Sr}(T) = +1.1$ at 65 m.y. Similarly, using the same Sr concentration but assuming a Rb concentration equal to that in the most strongly leached residue we calculate an upper limit of $\epsilon^{Sr}(T) = +11.0$. The parent material for the spherules must therefore have had $\epsilon^{Sr}(T)$ between +1 and +11 ($^{87}Sr/^{86}Sr = 0.7045-0.7052$).

Fig. 5 shows $\epsilon^{Nd}(0)$ vs. the cumulative percent Nd released by the leaching. Only 12% of the Nd remained in residue 2 which has a very low Nd concentration of 0.16 ppm and approximately chondritic Sm/Nd (Table 4). The isotopic composition of residue 2 at $\epsilon^{Nd}(0) = +1.9$ is significantly different from any of the leaches and is a lower limit on the endmember composition. We argue on the basis of the Sr results that this value is close to the true isotopic composition in the sanidine endmember. DePaolo et al. [51] also reported a value of $\epsilon^{Nd} = -6.0$ for acid-leached spherules with 1.2 ppm Nd. As noted above, their sample and the sample on which we initially reported [17] were insufficiently leached.

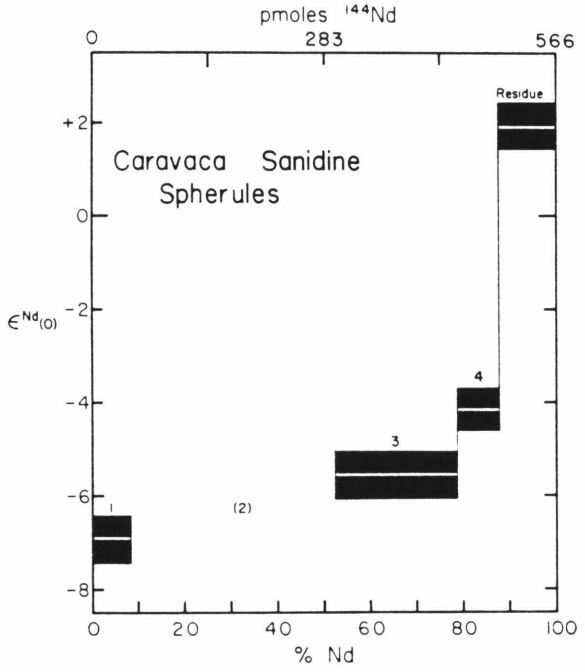

Fig. 5. Plot of $\epsilon^{Nd}(0)$ vs. cumulative Nd released in sequential leaching of sanidine spherules.

5. Discussion

5.1. Tektites

The large negative $\epsilon^{Nd}(0)$ and positive $\epsilon^{Sr}(0)$ characteristic of tektites are clear signatures of old continental crust (Fig. 2) [52]. The isotopic data exclude the possible derivation of tektites from continental material recently derived from the mantle which has $\epsilon^{Nd}(0)$ and $\epsilon^{Sr}(0)$ near zero [46,53]. The data also rule out an oceanic crustal source which would have an $\epsilon^{Nd}(0)$ of +8 to +12 and $\epsilon^{Sr}0)$ of −20 to −30 [46,53–55]. High-Si irghizites also have the characteristic isotopic composition of old continental crust.

A plot of $\epsilon^{Nd}(0)$ vs. $\epsilon^{Sr}(0)$ (Fig. 6) shows that the overlap in Sr isotopic composition between the various tektite groups is spread out in the second dimension provided by the Nd isotopic data. Each tektite group is characterized by a distinctive range of isotopic compositions. The range in isotopic composition is due almost entirely to variations in $\epsilon^{Sr}(0)$ at constant $\epsilon^{Nd}(0)$. This is most clearly displayed by the Australasian tektites. The uniformity of Nd isotopic composition and continuous range of Sr isotopic composition of the Australasian tektites is hard to reconcile with the suggestion that the indochinites and australites are due to different impact events [56]. Instead, our data

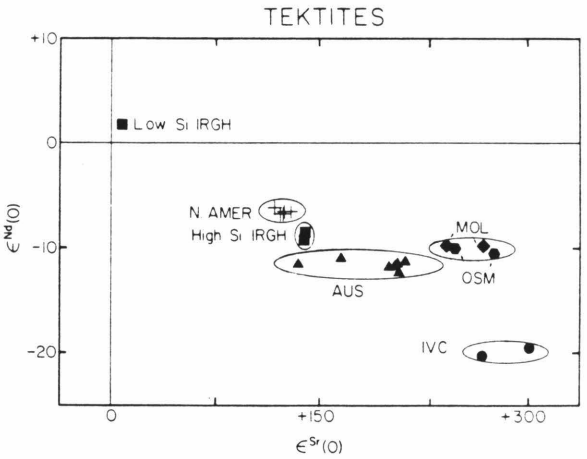

Fig. 6. Plot of $\epsilon^{Nd}(0)$ vs. $\epsilon^{Sr}(0)$ for tektites. Each group has a distinctive range in isotopic composition. Variation in isotopic composition is mainly due to variation in $\epsilon^{Sr}(0)$ at constant $\epsilon^{Nd}(0)$.

support the interpretation that the entire Australasian strewnfield is due to a single impact event.

The OSM sand samples from the Ries Crater site have $\epsilon^{Nd}(0) \sim -10$ and $\epsilon^{Sr}(0) = +250$ to $+280$ and closely match the range in isotopic composition of the moldavites. We fully agree with Graup et al. [35] that this type of material is the likely parent for the moldavites. This result eliminates the problem of identifying a parent material for the moldavites in the Ries which has stood in the way of establishing the strongly suspected relationship between the Ries and the moldavites. It is interesting to note that the OSM sands were a surficial deposit at the time of impact. The thickness of the deposit at the time of impact is unknown but is thought to have been less than a few tens of meters, while cratering effects extend to a depth of 2 km [36,57]. Laboratory experiments on impact processes have demonstrated that directional, high-velocity jets of surficial target material are often produced upon impact [58]. The production of such jets from the surficial OSM sands could explain the highly localized distribution of the moldavites [59].

The isotopic composition of Nd in the irghizites is different from that of the Australasian tektites. Although this does not completely rule out the Zhamanshin impact structure as a possible source for the Australasian strewnfield as suggested by Glass [60], it does demonstrate that high-Si irghizites have a different parent material than the Australasian tektites despite their similarity in chemical composition [30,31], thus reducing the likelihood of there being a connection between these two groups. The higher Ni content of the irghizites as compared with the Australasian tektites [30] raises the possibility that the difference in isotopic composition between these groups may be due to a greater component of meteoritic material in the irghizites. Addition of projectile material with chondritic abundances and isotopic composition ($\epsilon^{Nd}(0) = 0$, $\epsilon^{Sr}(0) > +500$; [61]) to the parent material of the Australasian tektites would displace $\epsilon^{Nd}(0)$ towards 0 but would greatly increase $\epsilon^{Sr}(0)$, contrary to what is observed (Fig. 6). We conclude that this mechanism cannot produce the irghizites and Australasian tektites from a common parent. The difference in isotopic composition between the high-Si and low-Si irghizites establishes that these two types have distinct parent materials and did not acquire their differences in chemistry through selective volatilization, partial melting, or other geologically recent processes acting on a common homogeneous parent material. As described above, meteoritic contamination cannot explain the difference between the high- and low-Si irghizites.

The Martha's Vineyard tektite, USNM 2082, is the only tektite ever found at that locality and questions have been raised as to the authenticity of the find. The Nd and Sr isotopic composition of the Martha's Vineyard sample (Fig. 6, Tables 2 and 3), is indistinguishable from the other North American tektites and it clearly had the same parent material as the bediasites and georgiaites, confirming its relationship to these groups.

5.2. Sanidine spherules

The value of $\epsilon^{Nd} \sim +2$ and relatively unevolved initial $\epsilon^{Sr}(T)$ of $\sim +5$ inferred to be characteristic of the sanidine clearly indicate that unlike tektites, the sanidine spherules could not have been derived from typical LREE-enriched, high-Rb/Sr old continental crust. Strong chemical fractionation during spherule formation is required to explain their present high Rb/Sr ratio and other chemical characteristics (high K/Na, volatile rich, etc.). This means that simple impact melting resulting in a total melt of the target material could not have produced the spherules. Processes which would provide the necessary chemical fractionation include recondensation of volatilized target material and volcanism. Authigenic growth of these objects from a volcanic material at low temperatures could explain both the extremely low Na and Sr contents as well as the oxygen results of Epstein [38]. Our Sr and Nd results are consistent with an oceanic impact in which oceanic crust was a major component of the parent material for the spherules. Oceanic crust alone does not satisfy the isotopic constraints which require a mixture of oceanic crust with $\epsilon^{Nd} \sim +8.0$, $\epsilon^{Sr} \sim -25.0$ and a component with higher $\epsilon^{Sr}(T)$ and lower $\epsilon^{Nd}(T)$ such as marine sediments or seawater. Our results are also consistent with derivation of the sanidine spher-

ules from crustal material which was relatively young at 65 m.y. Thus a volcanic origin for the spherules is not ruled out by our data and impact-induced volcanism would not be an unexpected feature of an impact the size inferred for the Cretaceous-Tertiary event. The sanidine could not have been formed by melting of meteoritic potassium feldspar [37] as $\epsilon^{Sr}(T)$ is too low.

6. Model ages and multistage isotopic evolution

In addition to being useful tracers, isotopic systems can be used to provide information on the timing of events in the history of an object. For $\lambda T \ll 1$, the $^{143}Nd/^{144}Nd$ ratio measured today in a sample derived T years ago from a reservoir with an initial $^{143}Nd/^{144}Nd$ ratio $I(T)$ is given by:

$$(^{143}Nd/^{144}Nd)_M \cong I(T) + (^{147}Sm/^{144}Nd) \cdot \lambda_{Sm} \cdot T$$

Here M denotes the measured value and $\lambda_{Sm} = 6.54 \times 10^{-12}$ yr^{-1} is the decay constant of ^{147}Sm.

The model age is the time at which a sample last had the isotopic composition of a model reservoir. In the case of Nd, this reservoir is taken as the undifferentiated mantle (CHUR) with a nominally chondritic $^{147}Sm/^{144}Nd$ ratio of 0.1967 and a present-day $^{143}Nd/^{144}Nd$ ratio of $I_{CHUR}(0) = 0.511847$ [46,62,63]. The isotopic composition of this model reservoir at time T years ago is then given by:

$$I_{CHUR}(T) \cong I_{CHUR}(0) - (^{147}Sm/^{144}Nd)_{CHUR} \cdot \lambda_{Sm} \cdot T$$

The model age T^{Nd}_{CHUR} is found by solving for $I(T) = I_{CHUR}(T)$ which results in [52]:

$$T^{Nd}_{CHUR} \cong \epsilon^{Nd}(0)/(Q^{Nd} \cdot f^{Sm/Nd})$$

where $\epsilon^{Nd}(0)$ and $f^{Sm/Nd}$ are defined above and $Q^{Nd} = 10^4 \cdot \lambda_{Sm} \cdot (^{147}Sm/^{144}Nd)_{CHUR}/I_{CHUR}(0) = 25.13$ AE^{-1}.

Model ages can also be calculated in a similar manner for Sr using the reference mantle reservoir (UR) with nominal values $(^{87}Rb/^{86}Sr)_{UR} = 0.0827$, $\lambda_{Rb} = 1.42 \times 10^{-11}$ yr^{-1}, $Q^{Sr} = 16.67$ AE^{-1} and $T^{Sr}_{UR} \cong \epsilon^{Sr}(0)/(Q^{Sr} \cdot f^{Rb/Sr})$ [46,55]. Table 3 lists values of T^{Nd}_{CHUR} and T^{Sr}_{UR} calculated in this manner.

If the assumptions built into the model age calculation are fulfilled (that the sample was derived from a reservoir with the isotopic characteristics of the model reservoirs and that the isotopic systems have remained undisturbed since that time), then the model ages T^{Sr}_{UR} and T^{Nd}_{CHUR} should be concordant and will give the age of formation of the sample (i.e., the time at which the sample separated from the model reservoirs with major chemical fractionation of parent and daughter species). Examination of Table 3 shows that although the T^{Nd}_{CHUR} ages within each group are constant, the T^{Sr}_{UR} ages are quite variable and are generally less than T^{Nd}_{CHUR} for the same sample, indicating that the model assumptions are *not* fulfilled.

A plot of T^{Sr}_{UR} vs. $^{87}Rb/^{86}Sr$ using all the available isotopic analyses of Australasian tektites [9,13] defines a hyperbolic array with T^{Sr}_{UR} ranging from ~0.3 to 1.3 AE (1.8 AE if we include the microtektite point) with the model ages decreasing with increasing Rb/Sr ratio. This pattern is a result of the fact that on a Sr evolution diagram, these samples lie about a correlation line (Fig. 7b). A true isochronal relationship would correspond to a hyperbolic curve. These two ways of looking at the isotopic systematics are equivalent; however, we hope to show below the utility of an alternate representation. In the discussion which follows, we use the Sr isotopic system as the example; an analogous development can be carried out for the Nd system.

We wish to obtain an expression which will allow determination of the last time at which major chemical fractionation of the parent-daughter isotopes occurred for the following history. At some time a suite of samples with differing Rb/Sr ratios is derived from a homogeneous reservoir. Each of these samples then evolves isotopically until some later time (or times) when major Rb/Sr fractionation again occurs. It is the last fractionation event of this type which we wish to date and our ability to date this event depends on large Rb/Sr fractionation occurring at that time. The basis for what follows is that for samples with very high Rb/Sr ratios, ages may be obtained

even though the initial isotopic ratio is poorly known. In the limit of infinite Rb/Sr ratio, the initial isotopic ratio plays no part in determining the sample age so long as the initial ratio remains finite. The problem is to determine a method for extrapolating the Rb/Sr ratio of a suite of samples to infinity, making the age determination less ambiguous for a suite of samples which are correlated on an evolution diagram but which do not lie on an isochron.

The isotopic composition of Sr today in a sample which separated from a reservoir (not necessarily the model reservoir) at time T_1 and had an Rb/Sr ratio of R_1, and had been undisturbed since that time, is given by:

$$I^{Sr}(0) \cong I^{Sr}(T_1) + R_1 \cdot \lambda_{Rb} \cdot T_1$$

or in epsilon notation:

$$\epsilon^{Sr}(0) \cong Q^{Sr} \cdot f_1^{Rb/Sr} \cdot T_1 + \epsilon^{Sr}(T_1)$$

Now if that sample had undergone a disturbance at time T_2 possibly changing the isotopic composition by amount ΔI^{Sr} and possibly changing the Rb/Sr ratio to a new value R_2, the isotopic composition would be given by [64]:

$$I^{Sr}(0) \cong I^{Sr}(T_1) + \Delta I^{Sr} + R_1 \cdot \lambda_{Rb} \cdot (T_1 - T_2) + R_2 \cdot \lambda_{Rb} \cdot T_2$$

In general, for $n-1$ disturbances at times $T_2, \ldots, T_n$ we have that:

$$I^{Sr}(0) \cong I^{Sr}(T_1) + \sum_{j=1}^{n-1} \left[(T_j - T_{j+1}) \cdot R_j \cdot \lambda_{Rb} + \Delta I_{j+1} \right] + R_n \lambda_{Rb} T_n$$

Dividing by $R_n \lambda_{Rb}$ we obtain in epsilon notation:

$$\frac{\epsilon^{Sr}(0)}{Q^{Sr} f_n^{Rb/Sr}} \cong \frac{1}{f_n^{Rb/Sr}} \cdot \left[\frac{\epsilon^{Sr}(T_1)}{Q^{Sr}} + \sum_{j=1}^{n-1} \left(f_j^{Rb/Sr}(T_j - T_{j+1}) + \frac{\Delta \epsilon_{j+1}^{Sr}}{Q^{Sr}} \right) \right] + T_n$$

where $\epsilon^{Sr}(T_1)$ is the initial isotopic composition, $\Delta \epsilon_j$ is the change in isotopic composition at time T_j, and $\epsilon^{Sr}(0)/Q^{Sr} f_n^{Rb/Sr} \equiv T_{UR}^{Sr}$. Thus, in a plot of the quantity T_{UR}^{Sr} versus $1/f_n$ a suite of samples which have undergone multistage isotope evolution will lie in the wedge-shaped region defined by the lines having slopes given by the bracketed terms above, and with common y-intercept T_n. This intercept value gives the time at which the suite last underwent parent-daughter fractionation. We note that this formalism provides a connection between the calculated model age T_{UR}^{Sr} and the actual times of disturbance $T_1, \ldots, T_n$. The y-intercept value, however, gives a model-independent estimate of the age of last disturbance and corresponds to the age determined by the slope of an isochron. We shall now apply this analysis to the model age patterns observed in tektites.

Our isotopic results as well as studies of REE patterns ([3,47,48], and others) major, minor, and trace element compositions [30,47,65], and oxygen isotopic work [66–68], all are consistent with the formation of tektites from terrestrial upper crustal rocks by impact melting. The data most closely match the characteristics of sedimentary rocks, sediments and soils, or meta-sediments. We postulate a three-stage model to explain the Sr and Nd systematics of tektites. In the first stage we assume the derivation of a crustal segment with $f_1^{Rb/Sr}$ and $f_1^{Sm/Nd}$ from a uniform mantle reservoir at T_1. At some later time T_2 this segment may undergo weathering and sedimentation producing a sedimentary rock with enrichment factors $f_2^{Sm/Nd}$, $f_2^{Rb/Sr}$, which is then impact melted to form tektites at T_3 ($\cong 0$) at which time selective volatilization may produce enrichment factors $f_3^{Sm/Nd}$, $f_3^{Rb/Sr}$. The Sm-Nd and Rb-Sr isotopic systems will behave quite differently in response to these processes. The major fractionation of Sm and Nd appears to occur during partial melting of mantle sources to produce crustal materials. There are some data which indicate that the Sm-Nd system is relatively undisturbed by weathering and sedimentation [52]. Further, the REE are refractory; Sm and Nd will not be readily fractionated by differential volatilization upon impact melting. For Nd, then, $f_1^{Sm/Nd} \cong f_2^{Sm/Nd} \cong f_3^{Sm/Nd}$ and the equation reduces to that of single-stage growth:

$$T_{CHUR}^{Nd} = T_1 = \epsilon^{Nd}(0) / \left(Q^{Nd} \cdot f_1^{Sm/Nd} \right)$$

The T_{CHUR}^{Nd} model ages correspond to the concentration weighted mean model ages of the sources

of the parent material of tektites (i.e., the original time of formation of the crustal segments from the mantle). In contrast, it is well established that sedimentary processes severely disturb the Rb-Sr system, generally by increasing the Rb/Sr ratio in the sediment through preferential uptake of Rb relative to Sr in clays [52,69], or by decreasing the Rb/Sr ratio by addition of Sr-rich phases. The Rb/Sr system may also be disturbed by selective Rb volatilization upon melting. Depending on which process dominates, the Sr model age T_{UR}^{Sr} may be greater (Rb loss or Sr gain) or less (Rb gain) than T_{CHUR}^{Nd} for a given sample. It should be noted that we are using the term sedimentation in a loosely defined sense. What we are dating is the last major parent-daughter fractionation event. This may occur during weathering, transport, or diagenesis of a sediment.

7. Australites

We now examine the model age systematics for each of the tektite groups. Fig. 7a is a plot of T_{UR}^{Sr} vs. $1/f^{Rb/Sr}$ for Australasian tektites using our data and data from the literature [9,13]. The T_{UR}^{Sr} ages for our samples (Table 3) range from ~ 0.36 to ~ 0.50 AE. The literature data extend this range down to 0.33 AE and up to 1.3 AE. The data define a wedge-shaped, linear array with a clustering in T_{UR}^{Sr} as $1/f^{Rb/Sr}$ tends toward zero. The array has a y intercept of ~ 0.25 AE which we interpret as the age of sedimentation for the parent material for these tektites. This age agrees well with the age of 0.1 to 0.3 AE calculated by Compston and Chapman [13] from the correlation line on the Sr evolution diagram (Fig. 7b). The data point for one of the Indian Ocean microtektites falls within this array indicating that this microtektite shares a common precursor with the macrotektites. The second microtektite is discrepant, having a higher model age than expected for its Rb/Sr ratio. Oddly, its isotopic characteristics are much more similar to those of the Ivory Coast tektites than the Australasian tektites. The general trend displayed in Fig. 7a strongly suggests a two-stage model with major Rb-Sr fractionation at 0.25 AE corresponding to the age of formation of the sediments which were the parent material. We

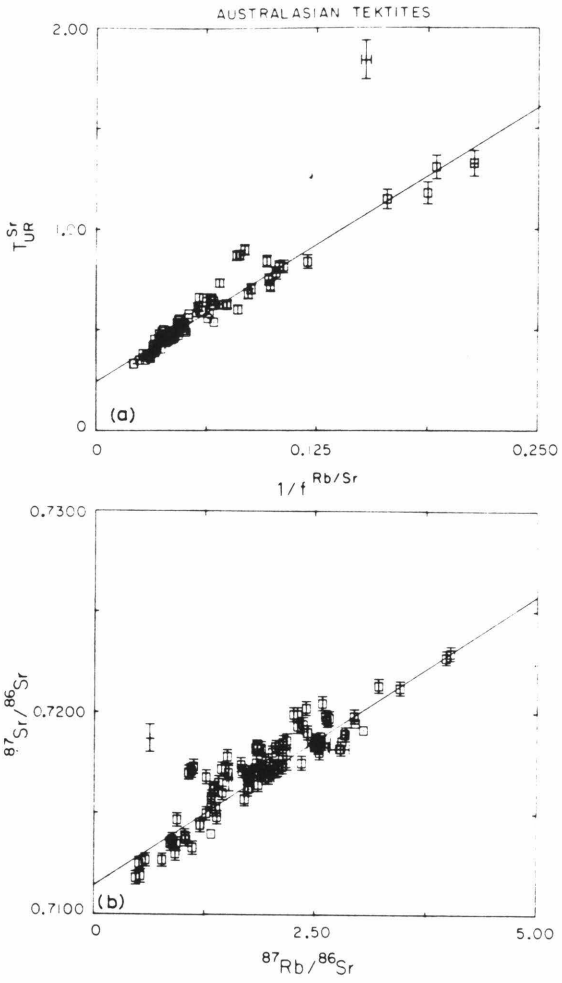

Fig. 7. (a) Plot of T_{UR}^{Sr} vs. $1/f^{Rb/Sr}$ for Australasian tektites. The y intercept gives the time of last Rb-Sr fractionation and corresponds to the time of sedimentation of a sedimentary parent material. Squares = macrotektites, crosses = microtektites. (b) Rb-Sr evolution diagram for Australasian tektites showing correlation line. Symbols as in (a). (Data sources: references 9, 13, 65, and this work.)

see no evidence for significant Rb volatilization during tektite formation as selective volatilization would have produced an intercept of ~ 0 AE in Fig. 7a, corresponding to the time of melting. An exception may be the discrepant microtektite as Rb loss will increase the model age of a sample.

In contrast to the T_{UR}^{Sr} ages, the T_{CHUR}^{Nd} ages are quite uniform with total range in ages of 1.06 to 1.17 AE (Table 3). The uniformity of the Nd model ages suggests that the source terrains for the parent

sediment were of approximately the same age, or that transport and sedimentation were effective at mixing material from sources of different ages. The value of ~ 1.15 AE for the T^{Nd}_{CHUR} ages implies that the parent sediments were dominantly derived from a Precambrian crustal segment.

The majority of these tektites have $T^{Sr}_{UR} < T^{Nd}_{CHUR}$ which is compatible with our model of increased Rb/Sr ratios in sediments by Rb uptake in clays. Four analyses from the literature, all high-Ca philippinites [13,65] have Sr model ages which exceed the Nd model age. These samples also have unusually high CaO and Sr contents. For the samples with $T^{Sr}_{UR} > T^{Nd}_{CHUR}$, we thus infer that the Rb/Sr ratio decreased during sedimentation by addition of Sr, increasing the calculated model age. The strong correlation of Sr with CaO [13] suggests that the carrier of the Sr in the parental sediment was also a Ca-rich phase. Calcite is a common Ca- and Sr-rich and Rb-poor phase in terrestrial sediments and the observed correlations can be explained by variations in the calcite content of the parent material as discussed by Compston and Chapman [13]. The initial Sr ratio for the high T^{Sr}_{UR} samples calculated for an age of 0.25 AE is ~ 0.710, thus the addition of a small amount of Permian marine carbonate with a relatively evolved $^{87}Sr/^{86}Sr$ ratio of ~ 0.708 [50] as compared with $(^{87}Sr/^{86}Sr)_{UR} = 0.7045$ to a detrital sediment with higher $^{87}Sr/^{86}Sr$ is not unreasonable on isotopic grounds and could account for the high model age.

Our data demonstrate that the source crater for the Australasian strewnfield lies in a target of late Paleozoic to early Mesozoic, continental sediment derived from a relatively young Precambrian cratonic source. If the source of the sediments actually contains a substantial amount of Archean crust, then the source area must also include a terrain of much younger rocks so that on average the age of the terrain is 1.15 AE. Our data do not exclude the possibility that the impact structure is located underwater on a continental shelf or deep ocean basin mantled by continentally derived sediments of the above characteristics. Suggested source craters for the Australasian tektites include the Zhamanshin Crater [60] which was discussed and rejected above; the Elgygytgyn Crater of northeast Siberia [70]; and an unnamed northeast Cambodian crater-like structure [71]. The Elgygytgyn Crater is in a terrain of plutonic and volcanic rocks of Mesozoic age (Nekrasov and Riudonis, 1973, cited in Dietz [70]). Unless these rocks have a large component of remelted Precambrian basement with negative $\epsilon^{Nd}(0)$ then it would not be possible to produce tektites with the negative ϵ^{Nd} and Precambrian T^{Nd}_{CHUR} age observed for the Australasian objects. Elgygytgyn crater is therefore an unlikely source for the Australasian tektites. Little is known about the geology in the area of the Cambodian structure. In the absence of more detailed information on the age and lithology of this site we are unable to discuss its merits.

8. North American tektites

The North American tektites are characterized by a uniform T^{Nd}_{CHUR} age with a total range of from 0.62 to 0.67 AE. This means that the material which melted to form the North American tektites came from a crustal segment which formed in very late Precambrian time. This relatively young age eliminates most of the Precambrian shield areas of North America as possible source terrains for the parent material of these tektites as well as sediments derived from these areas. The North American shale (NAS) composite [52,72] has $\epsilon_{Nd}(0) = -14.4$ and $T^{Nd}_{CHUR} = 1.5$ AE, and is thought to be representative of the average mid-continental region. From a comparison with our tektite results it is clear that the Paleozoic sediments making up the NAS composite are derived from older Precambrian crustal material and cannot be typical of the parent material for the North American tektites. Late Precambrian crust of ~ 0.6–0.8 AE age in North America is largely restricted to the eastern and southeastern margin of the Appalachian orogenic belt and may underlie much of the Atlantic and Gulf coastal plains and continental shelves. We suggest that the parent sediment for the North American tektites may have been derived from this terrain. The T^{Nd}_{CHUR} age may reflect a mixture of material from older and younger source terrains so that an average model age of ~ 0.65 AE is obtained. Even in this

case, the older shield areas of North America are still excluded as possible sources for a parent material because of the lack of young crustal material within these areas to mix with material from the ancient crust. Likewise, the Popigai astrobleme of Siberia could not be the source for the North American tektites as suggested by Dietz [70]. This impact occurred on the Archean Anabar shield which gives K-Ar ages in the range of 2.7–1.9 AE [73] and is too old to satisfy the T^{Nd}_{CHUR} ages of the American tektites.

The T^{Sr}_{UR} model ages for the North American tektites in Table 3 range from 0.52 to 0.56 AE (down to 0.42 AE if literature data are included); in all cases slightly younger than the corresponding T^{Nd}_{CHUR} ages. Unfortunately, there is little spread in the Rb/Sr ratios for these samples and, more importantly, the samples do not have the extreme Rb enrichments that were observed in some of the Australasian tektites (Fig. 8). Because of these characteristics, little significant time information can be extracted from the Sr isotopic systematics. The Sr model ages are consistent with derivation of the tektites from a sediment, but do not demand a sedimentary parent. If the parent was a sediment, there was relatively little parent-daughter fractionation at the time of sedimentation as reflected in the small differences between the T^{Nd}_{CHUR} and T^{Sr}_{UR} ages and the $f^{Rb/Sr}$ values which are typical of upper crustal igneous rocks (see Table 3).

In summary, our Nd isotopic data suggest that the source terrain of the parent material for the North American tektites was of ~0.65 AE age and cannot be any of the major ancient shield areas of North America or consequently from the areas covered by Paleozoic sediments derived from these Precambrian terrains. The Sr isotopic data suggest slight parent-daughter fractionation at some time after crustal formation in very late Precambrian time (~0.65 AE).

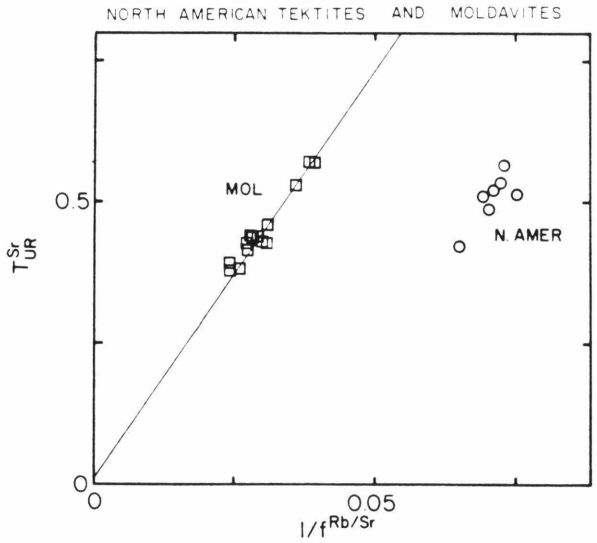

Fig. 8. Plot of T^{Sr}_{UR} vs. $1/f^{Rb/Sr}$ for North American tektites and moldavites. Intercept is well defined at ~0.015 AE and suggests that moldavites were formed from a geologically young parent sediment. North American tektites do not yield any new information. (Data sources North American tektites: reference 9, and this work; moldavites: references 9, 76, and this work.)

9. Ivory Coast tektites

The T^{Nd}_{CHUR} model ages for the Ivory Coast tektites are ~1.9 AE (Table 3), which is in good agreement with whole rock Rb/Sr ages of the rocks around the Bosumtwi Crater and much of western Africa which range from 1.9 to 2.1 AE [11,12,74]. The Sr model ages for these samples

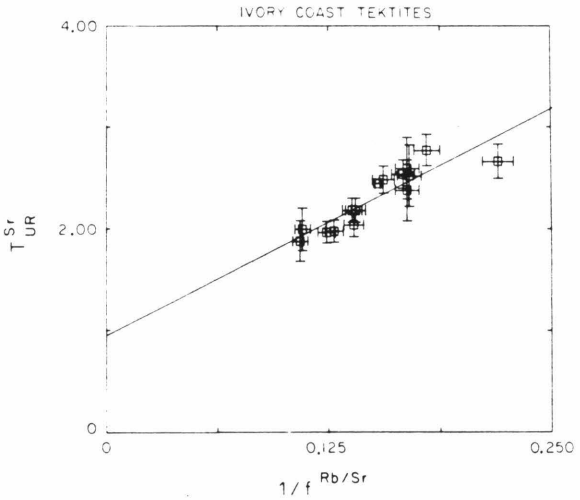

Fig. 9. Plot of T^{Sr}_{UR} vs. $1/f^{Rb/Sr}$ for Ivory Coast tektites. Intercept is reasonably well defined despite the lack of high-Rb/Sr samples. The time of last parent-daughter fractionation is given by the intercept value of ~0.95 AE. (Data sources: references 10, 11, and this work.)

range from 2.1 to 2.4 AE. In a plot of T_{UR}^{Sr} vs. $1/f^{Rb/Sr}$, our data and literature analyses of the Ivory Coast tektites [10–12] appear to define a linear array (Fig. 9). Although these samples are not characterized by high Rb/Sr ratios, they are reasonably well correlated and yield a y intercept of ~ 0.95 AE. These analyses have a range in T_{UR}^{Sr} from 1.9 to 2.8 AE, in all cases greater than T_{CHUR}^{Nd} for our samples. In an evolution diagram the samples plot about a correlation line corresponding to 0.95 AE age. Selective volatilization of Rb during the melting of the tektite parent material, leading to increased values of the Rb/Sr ratio and T_{UR}^{Sr} could be the cause of the younger disturbance. In this case, however, we would expect an intercept value of ~ 0.0 AE in Fig. 9. Thus selective volatilization is not likely to have been an important process for these tektites. Alternatively, the parent material for the Ivory Coast tektites may be a sediment or a metamorphic rock in which the Rb/Sr ratio decreased relative to the crustal source material during sedimentation or metamorphism at ~ 0.95 AE. Taken together, our Nd and Sr data are consistent with formation by melting of material originally derived from the rather ancient basement around the Bosumtwi Crater. The actual target material has not been identified.

10. Moldavites

The T_{CHUR}^{Nd} age for the moldavite samples is ~ 0.9 AE (Table 3), which agrees well with the age of the oldest known basement in the area of the Ries Crater. This basement was remobilized and partially melted at ~ 0.3 AE to form the terrain into which the Ries Crater was emplaced. The Sm-Nd isotopic systematics appear to be seeing through both this orogenic event and the tektite-forming event back to the original time of formation of the crustal segment which was ultimately melted to form the tektites at 14 m.y. The lower Sr model ages of 0.39–0.57 AE (Table 3) indicate that the Rb-Sr system has been disturbed subsequent to the time of crustal formation. A plot of T_{UR}^{Sr} vs. $1/f^{Rb/Sr}$ (Fig. 8) for literature analyses of moldavites [9,75] yields a linear array with y intercept of ~ 0.02 AE and with a variation in T_{UR}^{Sr} of from 0.37 AE to 0.58 AE. Similarly, in an evolution diagram the data plot along a sub-horizontal array of this age. Again the samples have a limited range of Rb/Sr ratios, but the intercept in the model age vs. $1/f^{Rb/Sr}$ plot is reasonably well defined due to the high Rb/Sr ratios. The young Sr age implies parent-daughter fractionation in the Sr isotopic system shortly before the tektite-forming event leading to high Rb/Sr ratios in the parent. These results imply an origin for the moldavites by melting of a young sediment derived locally from the rocks around the Ries Crater. This interpretation of the Rb-Sr systematics is fully compatible with derivation of the moldavites from the Tertiary OSM sands.

11. Irghizites

The two high-Si irghizite samples, USNM 5938 3-1 and USNM 5938 3-6, have T_{CHUR}^{Nd} model ages of ~ 0.88 AE and T_{UR}^{Sr} model ages of ~ 0.61 AE (Table 3), the Nd data giving the original age of formation of the parent material and the Sr data suggesting that this material was disturbed at some later time. Florenskij et al. [34] state that the Zhamanshin structure is in an area of Cretaceous and Tertiary sediments and Quaternary loess deposits underlain by Paleozoic metamorphic rocks. Our data are consistent with derivation of the high-Si irghizites from any of these materials if the crustal source originally formed at ~ 0.9 AE. The low-Si irghizite has a future T_{CHUR}^{Nd} model age of -0.25 AE due to its positive $\epsilon^{Nd}(0)$ but negative $f^{Sm/Nd}$ values. In this case our model fails. Future Nd model ages are not uncommon among modern alkalic basalts of oceanic islands or continental rift settings. These basalts are also characterized by positive $\epsilon^{Nd}(0)$ and are LREE enriched [55,76,77]. It is clear that these basalts are not derived from a mantle reservoir with the isotopic characteristics of CHUR, but instead have had a time-integrated LREE depletion. The observed REE patterns in the erupted basalts were imposed only shortly before eruption yielding the future model ages. We suggest that the low-Si irghizite was derived from similar basaltic material. Identification of the actual parent materials will depend on further field

and laboratory studies of the area around the Zhamanshin structure.

12. Conclusion

Tektites are characterized by negative $\epsilon^{Nd}(0)$ and positive $\epsilon^{Sr}(0)$, which are clear signatures of old terrestrial continental crust. Each tektite group has a rather distinctive ϵ^{Nd} value and a range of ϵ^{Sr}. Chemically and isotopically tektites are similar to terrestrial sediments derived from old continental crustal material. Our results do not exclude the production of tektites by impact into an ocean basin or shelf if the impact site was mantled by sediments of continental derivation. That the moldavites were probably formed by melting of the surficial OSM sands suggests more broadly that the tektite-forming process does not always sample very deeply at the impact site. As a result, we conclude that it is possible to have an impact in an oceanic area which could produce tektites from only surficial sediments and not involve deeper mafic oceanic crust.

Studies of sediments suggest that their Nd model ages reflect the age of their source terrain with major Sm-Nd fractionation occurring during partial melting of the mantle to form new crust. Surficial processes such as weathering do not appear to be effective in fractionating the rare earths. Thus we interpret the uniform Nd model age of each tektite field to be the age of formation of the crustal segment which weathered to form the parent sediment for the tektites. In contrast, it is well known that surficial processes severely disturb the Rb-Sr isotopic system generally by increasing the Rb/Sr ratio during weathering and sedimentation. This results in relatively young T_{UR}^{Sr} ages which reflect more recent events in the history of the tektite parent materials.

Our inferences from the isotopic systematics as to the ages of the source terrains and sedimentary precursors for the various tektite groups are summarized in Table 5. In all cases the T_{CHUR}^{Nd} ages imply a Precambrian age for the crustal source terrains: ~0.6 AE for North American tektites, ~0.9 AE for both the irghizites and moldavites, ~1.15 AE for Australasian tektites, and ~1.9 AE for the Ivory Coast tektites. The T_{UR}^{Sr} ages suggest very young Rb-Sr fractionation in the moldavite

TABLE 5

Summary of age and provenance of tektite parent materials as inferred from isotopic systematics

	Source terrain age (AE)	Sedimentation age (AE)	Target
Australasian tektites	1.15	0.25	middle-late Paleozoic sediments derived from Precambrian craton
North American tektites	0.65	<0.65	material derived from latest Precambrian crust
Moldavites	0.90	0.01	very young sediments derived from late Precambrian crust (Ries Crater)
Ivory Coast tektites	1.90	0.95	Precambrian materials derived from old Precambrian craton (Bosumtwi Crater)
High-Si irghizites	0.88	?	sediments (?) derived from late Precambrian crust (Zhamanshin Crater)
Low-Si irghizites	?	-	basaltic material (Zhamanshin Crater)

parent material, and imply that the moldavites were derived from a very young sediment. The Tertiary OSM sands from around the Ries Crater have the appropriate age and isotopic composition to be the likely parent material for the moldavites. The Australasian tektites are characterized by major parent-daughter fractionation in their Sr isotopic system at ~0.25 AE, which we interpret as the time of formation of a sediment which was melted to form these objects. Parent-daughter fractionation in the Sr system of the Ivory Coast tektites last occurred at ~0.95 AE probably during an ancient sedimentation or metamorphic event producing the parent material which melted to form these objects. Our data are consistent with derivation of the Ivory Coast tektites from Precambrian sediments in the Bosumtwi Crater. This is in consonance with conclusions about the origins of these objects by previous workers [9–12,74]. The Nd isotopic composition of high-Si irghizites rules out any possibility of a common parent with the Australasian tektites.

In summary, our data are consistent with tektite formation by melting of sediments during a meteorite or comet impact onto a continent or continental shelf or ocean basin mantled by sediments of the appropriate age and provenance as described above. The thickness of the sedimentary cover may in some cases be rather modest (less than a few hundred meters).

Unlike the tektites, which are dense homogeneous objects, the sanidine spherules are porous fine-grained inhomogeneous objects. This fact complicates the application of our technique because of the problems of contamination. In spite of this, the results provide insight into the provenance of these materials. The leaching experiment has shown that the sanidine spherules could have been formed by an oceanic impact in which both basaltic oceanic crust and overlying sediments or seawater were involved in the formation of the spherules. The isotopic results are also consistent with a volcanic origin for the spherules or with authigenic growth from volcanic detritus. An old continental source is clearly ruled out by our results. A major problem remains, however, and that is how it is possible to make objects which are dominantly potassium feldspar in composition with extremely low Sr content from any reasonable target material by impact-related processes.

Acknowledgements

We wish to thank B́. Mason and the U.S. National Museum for providing many of the tektite samples used in this study. B.P. Glass kindly provided us with the microtektites used in the study. The Thailand, Cambodian, and high-Ca australite samples were donated by P. Pellas and the French Natural History Museum. We are grateful to S.R. Taylor for his interest in this work and for introducing us to the problem of irghizite genesis. D.A. Papanastassiou shared with us both the microtektite data presented here and his knowledge of things mass spectrometric. This work has been supported by NASA grant NGL 05-002-188.

References

1 J.A. O'Keefe, Tektites and their Origin (Elsevier, Amsterdam, 1976) 254 pp.
2 J.A. O'Keefe, Comments on "Chemical relationships among irghizites, zhamanshinites, Australasian tektites, and Henbury impact glass", Geochim. Cosmochim. Acta 44 (1981) 2151.
3 S.R. Taylor, Tektites, a post-Apollo view, Earth Sci. Rev. 9 (1973) 101.
4 S.R. Taylor, Lunar Science: A Post-Apollo View (Pergamon, New York, N.Y., 1975) 372 pp.
5 L.W. Alvarez, W. Alvarez, F. Asaro and M.V. Michel, Extraterrestrial cause for the Cretaceous-Tertiary extinction, Science 208 (1980) 1095.
6 J. Smit and J. Hertogen, An extraterrestrial event at the Cretaceous-Tertiary boundary, Nature 285 (1980) 198.
7 F.T. Kyte, Z. Zhou and J.T. Wasson, Siderophile-enriched sediments from the Cretaceous-Tertiary boundary, Nature 288 (1980) 651.
8 R. Ganapathy, S. Gartner and M.J. Jian, Iridium anomaly at the Cretaceous-Tertiary boundary in Texas, Earth Planet. Sci. Lett. 54 (1981) 393.
9 C.C. Schnetzler and W.M. Pinson, Variation of strontium isotopes in tektites, Geochim. Cosmochim. Acta 28 (1964) 953.
10 H.J. Lippolt and G.J. Wasserburg, Rubidium-Strontium Messungen an Gläsern vom Bosumtwi-Krater und an Elfenbein-Kusten Tektiten, Z. Naturforsch. 21a (1966) 226.
11 C.C. Schnetzler, W.M. Pinson and B.M. Hurley, Rubidium-strontium age of the Bosumtwi Crater area, Ghana, compared with the age of the Ivory Coast tektites, Science 151 (1966) 817.

12 P. Kolbe, W.M. Pinson, J.M. Saul and E.W. Miller, Rb-Sr study on country rocks of the Bosumtwi Crater, Geochim. Cosmochim. Acta 31 (1967) 869.
13 W. Compston and D.R. Chapman, Sr isotope patterns within the southeast Australasian strewn-field, Geochim. Cosmochim. Acta 33 (1969) 1023.
14 D.A. Papanastassiou and G.J. Wasserburg, Microchrons: the ^{87}Rb-^{87}Sr dating of microscopic samples, 12th Lunar Planet. Sci. Conf. (1981) 802 (abstract).
15 D.A. Papanastassiou and G.J. Wasserburg, Microchrons: the ^{87}Rb-^{87}Sr dating of microscopic samples, Proc. 12th Lunar Planet. Sci. Conf. (1981) 1027.
16 H.F. Shaw and G.J. Wasserburg, Sm-Nd and Rb-Sr isotopic systematics of Australasian tektites, 12th Lunar Planet. Sci. Conf. (1981) 967 (abstract).
17 H.F. Shaw and G.J. Wasserburg, Sm-Nd and Rb-Sr systematics and the origin of sanidine spherules from a Cretaceous-Tertiary boundary clay, 13th Lunar Planet. Sci. Conf. (1982) 716 (abstract).
18 J. Zähringer, K-Ar measurements of tektites, in: Radioactive Dating, Proceedings NEA Symposium, Athens, November 19-23 (International Atomic Energy Agency, Vienna, 1962) 289.
19 D. Störzer and W.A. Wagner, Fission track ages of the North American tektites, Earth Planet. Sci. Lett. 10 (1971) 435.
20 W. Gentner, H.J. Lippolt and O.A. Schaeffer, Argon-Bestimmungen an Kalinmineralien, XI. Die Kalium-Argon Alter der Gläser des Nördlinger, Riesses und der boehmisch-maehrischen Tektite, Geochim. Cosmochim. Acta 27 (1963) 191.
21 R.L. Fleischer, P.B. Price and R.M. Walker, On the simultaneous origin of tektites and other natural glasses, Geochim. Cosmochim. Acta 29 (1965) 161.
22 R.L. Fleischer and P.B. Price, Fission track evidence for the simultaneous origin of tektites and other natural glasses, Geochim. Cosmochim. Acta 28 (1964) 755.
23 W. Gentner, D. Störzer and G.A. Wagner, New fission-track ages of tektites and related glasses, Geochim. Cosmochim. Acta 33 (1969) 1075.
24 I. McDougall and J.F. Lovering, Apparent K-Ar dates on cores, and excess Ar in flanges of australites, Geochim. Cosmochim. Acta 33 (1969) 1057.
25 B.P. Glass, Microtektites in deep-sea sediments, Nature 214 (1967) 372.
26 B.P. Glass, Glassy objects (microtektites) from deep-sea sediments near the Ivory Coast, Science 161 (1968) 891.
27 B.P. Glass, R.N. Baker, D. Störzer and G.A. Wagner, North American microtektites from the Caribbean Sea and their fission track ages, Earth Planet. Sci. Lett. 19 (1973) 184.
28 P.V. Florenskij, The Zamanshin meteorite crater (northern near-Aral) and its tektites and impactites, Prob. Akad. Nauk Izv. 10 (1975) 73.
29 P.V. Florenskij, The meteorite crater Zamanshin (northern Aral region, U.S.S.R.) and its tektites and impactites, Chem. Erde 36 (1977) 83.
30 S.R. Taylor and S.M. McLennan, Chemical relationships among irghizites, zhamanshinites, Australasian tektites, and Henbury impact glasses, Geochim. Cosmochim. Acta 43 (1979) 1551.
31 V.I. Bouska, P. Povondra, P.V. Florenskij and Z. Randa, Irghizites and zhamanshinites: Zhamanshin Crater, USSR, Meteoritics 16 (1981) 171.
32 D. Störzer and G.A. Wagner, Fission track dating of meteorite impacts, Meteoritics 12 (1977) 368 (abstract).
33 P.V. Florenskij, V.P. Perelygin, M.L. Bazhenov, D.D. Lkhaguasuren and S.G. Stecenko, Kompleksnoje opredelenije vozrasta meteoritnogo kratera Zhamansjin, Astronom. Vestn. 13 (1979) 178.
34 P.V. Florenskij, A.I. Dabizha, A.O. Aaloe, E.S. Gorshkov and V.I. Mikljajev, Geologo-geofizicheskajc kharakteristika meteoritnogo kratera Zhamanshin, Meteoritika 38, Ann. CCCR Izd. Nauka (1979) 86.
35 G. Graup, P. Horn, M. Köhler and D. Müller-Sohnius, Source material for moldavites and baritonites, Naturwissenschaften 67 (1981) 616.
36 V.R. Bolten and D. Müller, Das Tertiär im Nördlinger Ries und in seiner Umgebung, Geol. Bavarica 61 (1969) 87.
37 J. Smit and G. Klaver, Sanidine spherules at the Cretaceous-Tertiary boundary; cometary material?, Nature 292 (1981) 47.
38 S. Epstein, The $\delta^{18}O$ of the sanidine spherules at the Cretaceous-Tertiary boundary, 13th Lunar Planet. Sci. Conf. (1982) 205.
39 S. Epstein and T. Mayeda, Variations in $\delta^{18}O$ in natural waters, Geochim. Cosmochim. Acta 4 (1953) 213.
40 D.A. Papanastassiou and G.J. Wasserburg, Rb-Sr ages and initial strontium in basalts from Apollo 15, Earth Planet. Sci. Lett. 17 (1973) 324.
41 D.A. Papanastassiou, D.J. DePaolo and G.J. Wasserburg, Rb-Sr and Sm-Nd chronology and genealogy of basalts from the Sea of Tranquility, Proc. 8th Lunar Sci. Conf. (1977) 1639.
42 D.J. DePaolo, Study of magma sources, mantle structure and the differentiation of the earth using variations of $^{143}Nd/^{144}Nd$ in igneous rocks, Ph.D. Thesis, California Institute of Technology, Pasadena, Calif. (1978).
43 T.A. Bence and A.L. Albee, Empirical correction factors for the electron microanalysis of silicates and oxides, J. Geol. 76 (1968) 382.
44 A.L. Albee and L. Ray, Correction factors for electron probe microanalysis of silicates, oxides, carbonates, phosphates, and sulfates, Anal. Chem. 42 (1970) 1408.
45 H.F. Shaw and A.L. Albee, An empirical investigation into possible nonlinearities of the microprobe correction factors in the system MgO-CaO-Al_2O_3-SiO_2, Proc. 14th Ann. Conf. Microbeam Analysis Soc. (1979) 227.
46 D.J. DePaolo and G.J. Wasserburg, Inferences about magma sources and mantle structure from variations of $^{143}Nd/^{144}Nd$, Geophys. Res. Lett. 3 (1976) 743.
47 S.R. Taylor, Australites, Henbury impact glass and subgreywacke: a comparison of the abundances of 51 elements, Geochim. Cosmochim. Acta 30 (1966) 1121.
48 F.A. Frey, Microtektites: a chemical comparison of bottle

green microtektites, normal microtektites, and tektites, Earth Planet. Sci. Lett. 35 (1977) 43.
49 S.R. Taylor and M. Kaye, Genetic significance of the chemical composition of tektites: a review, Geochim. Cosmochim. Acta 33 (1969) 1683.
50 Z.E. Peterman, C.-E. Hedge and H.A. Tourtelot, Isotopic composition of strontium in sea water throughout Phanerozoic time, Geochim. Cosmochim. Acta 34 (1970) 105.
51 D.J. DePaolo, F.T. Kyte and B.D. Marshall, Rb-Sr, Sm-Nd, and K-Ca studies of Cretaceous-Tertiary boundary sediments: possible evidence for an oceanic impact, 13th Lunar Planet. Sci. Conf. (1982) 168 (abstract).
52 M.T. McCulloch and G.J. Wasserburg, Sm-Nd and Rb-Sr chronology of continental crust formation, Science 260 (1978) 1003.
53 D.J. DePaolo and G.J. Wasserburg, Nd isotopic variations and petrogenetic models, Geophys. Res. Lett. 3 (1976) 249.
54 P. Richard, N. Shimizu and C.J. Allègre, $^{143}Nd/^{144}Nd$, a natural tracer: an application to oceanic basalts, Earth Planet. Sci. Lett. 31 (1976) 267.
55 R.K. O'Nions, P.J. Hamilton and N.M. Evensen, Variations in $^{143}Nd/^{144}Nd$ and $^{87}Sr/^{86}Sr$ ratios in oceanic basalts, Earth Planet. Sci. Lett. 34 (1977) 13.
56 D. Störzer and G.A. Wagner, Australites older than indochinites, Naturwissenschaften 67 (1980) 90.
57 V.E. David, Das Ries-Ereignis als physikalischer Vorgang, Geol. Bavarica 61 (1969) 350.
58 S.W. Kieffer, Impact conditions required for formation of melt by jetting in silicates, in: Impact and Explosion Cratering, D.J. Roddy, R.O. Pepin and R.B. Merrill, eds. (Pergamon Press, New York, N.Y., 1977) 751.
59 V.I. Bouska, Geology and stratigraphy of moldavite occurrences, Geochim. Cosmochim. Acta 28 (1964) 921.
60 B.P. Glass, Zhamanshin crater: possible source of the Australasian tektites, Progr. Geol. Soc. Am., Cordilleran Sect. (1978) 107 (abstract).
61 G.W. Wetherill, Radiometric chronology of the early solar system, Annu. Rev. Nucl. Sci. 25 (1975) 283.
62 S.J. Jacobsen and G.J. Wasserburg, Sm-Nd isotopic evolution of chondrites, Earth Planet. Sci. Lett. 50 (1980) 139.
63 G.J. Wasserburg, S.B. Jacobsen, D.J. DePaolo, M.T. McCulloch and T. Wen, Precise determination of Sm/Nd ratios, Sm and Nd isotopic abundances in standard solutions, Geochim. Cosmochim. Acta 45 (1981) 2311.
64 D.A. Papanastassiou and G.J. Wasserburg, Initial strontium isotopic abundances and the resolution of small time differences in the formation of planetary objects, Earth Planet. Sci. Lett. 5 (1969) 361.
65 D.R. Chapman and L.C. Scheiber, Chemical investigation of Australasian tektites, J. Geophys. Res. 74 (1969) 6737.
66 H.P. Taylor and S. Epstein, Oxygen isotope studies on the origin of tektites, J. Geophys. Res. 67 (1962) 4485.
67 H.P. Taylor and S. Epstein, Oxygen isotope studies of Ivory Coast tektites and impactite glasses from the Bosumtwi Crater, Ghana, Science 153 (1966) 173.
68 H.P. Taylor and S. Epstein, Correlations between $^{18}O/^{16}O$ ratios and chemical composition of tektites, J. Geophys. Res. 74 (1969) 6834.
69 E.J. Dasch, Strontium isotopes in weathering profiles, deep-sea sediments, and sedimentary rocks, Geochim. Cosmochim. Acta 33 (1969) 1521.
70 R.S. Dietz, Elgygytgyn Crater, Siberia: probable source of Australasian tektite field, Meteoritics 12 (1977) 145.
71 J.B. Hartung and A.R. Rivolo, A possible source in Cambodia for Australasian tektites, Meteoritics 14 (1979) 153.
72 L.A. Haskin, T.R. Wildeman, F.A. Frey, K.A. Collins, C.R. Reedy and M.A. Haskin, Rare earths in sediments, J. Geophys. Res. 71 (1966) 6091.
73 M.I. Rabken, On the depth and condition of regional metamorphism in the Anabar Shield, Proc. 23rd Int. Geol. Congr. (1968) 61.
74 M. Vachette, Nouvelles mesures d'âges absolus de granites d'âge éburén de la côte d'Ivoire, C.R. Acad. Sci. Paris 258 (1964) 569.
75 C.C. Schnetzler, J.A. Philpotts and W.H. Pinson, Rubidium-strontium correlation study of moldavites and Ries Crater material, Geochim. Cosmochim. Acta 33 (1969) 1015.
76 C.J. Hawkesworth and R. Vollmer, Crustal contamination versus enriched mantle: $^{143}Nd/^{144}Nd$ and $^{87}Sr/^{86}Sr$ evidence from the Italian volcanics, Contrib. Mineral. Petrol. 69 (1979) 151.
77 M. Menzies and V.R. Murthy, Nd and Sr isotope geochemistry of hydrous nodules and their host alkali basalts: implications for local heterogeneities in metasomatically veined mantle, Earth Planet. Sci. Lett. 46 (1980) 323.
78 B.P. Glass, M.B. Swincki and P.A. Zwart, Australasian, Ivory Coast, and North American tektite strewnfields: size, mass, and correlation with geomagnetic reversals and other rare events, Proc. 10th Lunar Planet. Sci. Conf. (1979) 2535.
79 D.J. DePaolo and G.J. Wasserburg, The sources of island arcs as indicated by Nd and Sr isotope studies, Geophys. Res. Lett. 4 (1977) 465.

APPENDIX II.

As submitted to
Amer. J. Sci.
24 June 1983

ISOTOPIC CONSTRAINTS ON THE ORIGIN OF APPALACHIAN MAFIC COMPLEXES

H. F. Shaw and G. J. Wasserburg

The Lunatic Asylum of the Charles Arms Laboratory
Division of Geological and Planetary Sciences
California Institute of Technology
Pasadena, California 91125

Division Contribution Number 3851 (430)

Abstract

Isotopic analyses of modern oceanic basalts and ophiolites have shown that both modern and ancient oceanic crust have a characteristic Nd and Sr isotopic signature indicative of derivation from a depleted mantle reservoir. It also appears that the Nd isotopic system is not appreciably disturbed by metamorphism. These isotopic characteristics have been extended to the Pt. Sal, Kings-Kaweah, and Josephine ophiolites of California. We have used these characteristics in an attempt to identify pieces of proto-Atlantic oceanic crust among the mafic and ultramafic rocks of the Appalachians. Sm-Nd mineral isochrons for the Baltimore Mafic Complex, Md (BMC) yield an age of 490±20 My which we interpret as the igneous crystallization age. BMC whole rock samples do not define isochrons and have initial isotopic compositions of $-6.4 < \varepsilon_{Nd}(T) < -2.2$, $+51 < \varepsilon_{Sr}(T) < +115$. $\varepsilon_{Nd}(T)$ and $\varepsilon_{Sr}(T)$ are anti-correlated. This is not the signature of depleted mantle and oceanic crust, but is similar to old continental crust. We propose that the BMC is a mafic continental intrusion, possibly subduction related, which was contaminated with old continental crust during emplacement. Whole rock samples from the Thetford Mines Complex, Qe (TMC) do not define isochrons and have $-1.5 < \varepsilon_{Nd}(T) < +4.2$, $+2.6 < \varepsilon_{Sr}(T) < +114$. These data do not in any way reflect the signature of normal oceanic crust. These results are in contrast with geologic relationships which show the TMC to have the characteristics of an ophiolite complex. The TMC is chemically and isotopically similar to a class of other ophiolites which have affinities to modern boninites. The Chunky Gal Amphibolite, N.C., Lake Chatuge complex, N.C., and Hazen's Notch Amphibolite, Vt., were found to have a depleted mantle signature with $+5 < \varepsilon_{Nd}(T) < +8$ and may be fragments of oceanic crust. The Webster-Addie body, N.C., has $\varepsilon_{Nd}(T) \sim -1$, $\varepsilon_{Sr}(T) \sim +30$ and is not isotopically similar to oceanic crust or the other North Carolina

mafic bodies analyzed. From these isotopic results we infer that Appalachian mafic rocks have diverse origins, some are continental intrusives (BMC), others are probably fragments of oceanic crust (Vermont and N. Carolina amphibolites). Future models for the development of the Appalachians must allow for these various origins. The possibility that some ophiolites are not normal oceanic crust but have an origin in a partially continental setting or as anomalous oceanic crust may require further attention.

1. Introduction

The pre-Mesozoic mafic and ultramafic bodies of the Appalachians are largely restricted to the latest Precambrian to Ordovician age eugeosynclinal rocks lying to the east of the chain of anticlinoria cored by Grenville age (~ 1.0-1.3 AE) Precambrian basement. In some places, particularly in the Southern Appalachians, ultramafic bodies also lie enclosed within basement complex rocks. The mafic and ultramafic bodies thus define a belt or series of parallel belts, in places narrow and well-defined, elsewhere broad and diffuse, which extends the length of the Appalachians. The majority of the bodies making up the belt are relatively small (<1 km), apparently rootless pods of peridotite which have been serpentinized to varying degrees. Also found within this belt are larger complexes of mafic and ultramafic rocks which range from relatively complete allochthonous sheets such as the Bay of Islands ophiolite in Newfoundland, through bodies in which metamorphism and deformation have partially obscured an ophiolite stratigraphy, to bodies which have little if any recognizable stratigraphy, but because of their location in the belt and mafic to ultramafic composition, have recently been described as dismembered or fragmented ophiolites.

Historically, the mafic and ultramafic rocks of the Appalachians have been interpreted as intrusive bodies, emplaced into an ensialic eugeosynclinal pile [Pratt and Lewis, 1905; Hess, 1939, 1955; Chidester and Cady, 1972], and which reached their present rootless stratigraphic position by diapiric rise of serpentinized peridotite. More recently, in light of the plate tectonic interpretation of ophiolites as fragments of obducted oceanic crust, the mafic and ultramafic rocks of the Appalachians have been interpreted as large and small fragments of proto-Atlantic oceanic crust and mantle which were incorporated into the Appalachian Orogen during the closure phase of a Wilson cycle

[Church and Stevens, 1971; Williams, 1971; Dewey and Bird, 1971; Upadhyay et al., 1971; St. Julien, 1972; Laurent, 1975, 1977; Crowley, 1976; Morgan, 1977; Williams and Talkington, 1977; Malpas, 1977]. The objective of this study is to use the Sm-Nd and Rb-Sr isotopic systems to place constraints on the origin of several Appalachian mafic bodies in which either extensive metamorphism, or tectonism, or both has made their origin uncertain.

The naturally occurring radioactive isotopes ^{87}Rb and ^{147}Sm decay with halflives $\tau^{Rb}_{1/2}$ = 49 AE and $\tau^{Sm}_{1/2}$ = 106 AE to the respective daughter isotopes ^{87}Sr and ^{143}Nd. Closed systems with differing parent-to-daughter ratios will evolve over time and develop measurable differences in the daughter element isotopic abundances. For Nd, these differences are conveniently represented using epsilon notation [DePaolo and Wasserburg, 1976a,b, 1977] in which $\epsilon_{Nd}(T)$ is the deviation in parts in 10^4 of the sample isotopic composition from that of a nominal chondritic reservoir at time T:

$$\epsilon_{Nd}(T) = \left[\left\{\left(\frac{^{143}Nd}{^{144}Nd}\right)_{SAMPLE}(T)/I_{CHUR}(T)\right\} - 1\right] \times 10^4$$

where $I_{CHUR}(T) = I_{CHUR}(0) - (^{147}Sm/^{144}Nd)_{CHUR} \cdot [\exp(\lambda^{Sm} \cdot T) - 1]$, $\lambda^{Sm} = 6.54 \times 10^{-12}$ yr^{-1}, $I_{CHUR}(0) = 0.511847$, $(^{147}Sm/^{144}Nd)_{CHUR} = 0.1967$, and CHUR stands for Chondritic Uniform Reservoir [DePaolo and Wasserburg, 1976b; Jacobsen and Wasserburg, 1981; Wasserburg et al., 1981]. One can also reference the Sm/Nd ratios to this reservoir by defining the enrichment factor

$$f^{Sm/Nd} \equiv \left\{\left(\left(^{147}Sm/\ ^{144}Nd\right)_{SAMPLE} / \left(^{147}Sm/\ ^{144}Nd\right)_{CHUR}\right) - 1\right\}$$

Positive values of $f^{Sm/Nd}$ thus indicate light rare earth element (LREE) depletion; negative values indicate LREE enrichment. One can similarly define ϵ_{Sr} with respect to a reservoir corresponding to the undifferentiated mantle (UR) with nominal values

$I_{UR}(0) = 0.7045$, $(^{87}Rb/^{86}Sr)_{UR} = 0.0827$, $\lambda^{Rb} = 1.42\times10^{-11}\ yr^{-1}$:

$$\varepsilon_{Sr}(T) = [(\frac{^{87}Sr}{^{86}Sr})_{SAMPLE}(T)/I_{UR}(T))-1]\times10^{4} \quad ;$$

$$I_{UR}(T) = I_{UR}(0) - (^{87}Rb/^{86}Sr)_{UR} \cdot [\exp(\lambda^{Rb}T) - 1];$$

$$f^{Rb/Sr} \equiv \{((^{87}Rb/^{86}Sr)_{SAMPLE} / (^{87}Rb/^{86}Sr)_{UR})-1\}$$

[DePaolo and Wasserburg, 1976b; O'Nions et al., 1977; Jacobsen and Wasserburg, 1981]. There is good reason to believe that the earth has approximately chondritic rare earth ratios. Although these ratios are somewhat variable between different chondrites, the Nd model system parameters are reasonably well established. The Sr model system, on the other hand, is based on a correlation between Nd and Sr isotopic compositions in mantle-derived rocks and on the inference that the bulk earth has a chondritic Sm/Nd ratio. The Sr parameters are therefore less well established. Nevertheless, the current estimate of $(^{87}Sr/^{86}Sr)_{UR} = 0.7045$ appears to be a reasonably close estimate of the bulk earth value.

Isotopic analyses of young rocks thought to have been derived directly from the mantle in oceanic regions have shown that the mantle is isotopically heterogeneous. The largest volume of rock is represented by mid-ocean ridge basalts (MORB) which have low values of $\varepsilon_{Sr}(0)$, and high values of $\varepsilon_{Nd}(0)$ (Fig. 1), implying that these rocks are derived from a large ion lithophile (LIL) and LREE depleted part of the mantle which has existed for a significant fraction of the earth's history. Other oceanic volcanics such as found on oceanic islands show a wide range of isotopic composition. In particular, it appears that there are <u>at least</u> two isotopically distinct, ancient mantle reservoirs

capable of yielding basaltic magmas and which give rise to the general inverse correlation between $\varepsilon_{Nd}(0)$ and $\varepsilon_{Sr}(0)$ known as the mantle array: 1) a LREE and LIL element depleted reservoir characterized by negative values of $\varepsilon_{Sr}(0)$ (~ -20 to -30) and positive values of $\varepsilon_{Nd}(0)$ (~ +8 to +13) that is the source for present-day basaltic oceanic crust, and 2) a reservoir variously referred to as primitive or undepleted mantle with $\varepsilon_{Nd} \sim \varepsilon_{Sr} \sim 0$ [DePaolo and Wasserburg, 1976a,b, 1979; DePaolo, 1983] or enriched mantle with $\varepsilon_{Sr} > 0$, $\varepsilon_{Nd} < 0$ [White and Hofmann, 1982; McCulloch et al., 1983]. Mixtures of magma derived from these two sources appear to be responsible for the isotopic variation of rocks erupted on oceanic islands, in continental volcanic provinces and in kimberlites. The concept of endmember reservoirs is somewhat of an idealization; in actuality it is likely that there is a continuum of sources in the mantle which are either undepleted or were depleted or enriched at a variety of times and which today give rise to the spectrum of isotopic compositions observed in modern mantle-derived rocks [cf. Jacobsen and Wasserburg, 1979]. The conclusions of the present study depend on the fact that the largest volume of basaltic oceanic crust, both modern and ancient, is in general characterized by a depleted mantle signature.

Old, LREE and LIL-enriched continental crust forms a complement to the depleted mantle reservoir and has negative values of $\varepsilon_{Nd}(0)$ and large positive values of $\varepsilon_{Sr}(0)$. Mixing of depleted mantle with crustal rocks has also been proposed as a mechanism for producing the parts of the mantle array populated by some continental flood basalts. The latter point of view has recently been emphasized by Carlson et al. [1981, 1983]. Some of these mixing relationships are shown in Fig. 2 in which $\varepsilon_{Nd}(0)$ is plotted against $\varepsilon_{Sr}(0)$ for rocks from various settings. In this figure, oceanic crust, represented by mid-ocean ridge basalts and island arcs, is seen to have a distinctive isotopic signature of

$\varepsilon_{Nd}(0) \sim +8$ to $+13$ and relatively non-radiogenic values of $\varepsilon_{Sr}(0)$.

Well-characterized ophiolite complexes such as the Samail Ophiolite, Oman, and Bay of Islands Ophiolite, Newfoundland, which are thought to represent sections of fossil oceanic crust also have a depleted mantle isotopic signature (Fig. 1). It should be noted, however, that there are some ophiolites which do not have the isotopic signature of modern oceanic crust. These occurrences are discussed later in light of our results.

In order to extend the isotopic observations on geologically well-characterized ophiolites, we have analyzed samples from three California ophiolites of Mesozoic age: the Josephine Ophiolite [157 My, Harper, 1980; Harper and Saleeby, 1980], the Point Sal Ophiolite [160 My, Hopson and Frano, 1977] and the Kings-Kaweah Ophiolite [200 My, Saleeby, 1982]. The Josephine Ophiolite and Kings-Kaweah Ophiolite have metamorphic histories comparable to that inferred for many of the Appalachian mafic complexes; both were metamorphosed to greenschist or amphibolite facies during regional metamorphic events after their emplacement onto the continental margin. Our data for the California ophiolites are given in Table 1 and Fig. 1. These rocks clearly have the Nd isotopic signature of the depleted mantle source characteristic of modern oceanic crust or oceanic island arcs, especially when allowance is made for the evolution of the source. For a depleted mantle with $f^{Sm/Nd} \sim +0.2$ one would expect this reservoir to evolve by $\sim +0.5$ ε_{Nd} units every 100 My. The present-day range of +8 to +13 ε_{Nd} for the MORB derived from the depleted oceanic mantle would thus correspond to a range of +5.5 to +10.5 at ~ 500 My ago. The value of $\varepsilon_{Nd}(T) = +12.4$ for the Kings-Kaweah sample deserves some comment. This value is among the highest reported for samples from a depleted mantle reservoir and implies that the Kings-Kaweah Ophiolite was derived from mantle which was either more highly

depleted than average or was depleted at a much earlier-than-average time. Ophiolite localities showing such high ε_{Nd} values will require more attention in the future.

The Sr isotopic compositions of ophiolites range from typical depleted mantle values to relatively radiogenic values. This dispersion is due to the relative ease with which the Sr isotopic system is disturbed by exchange during both regional metamorphism and metamorphism on the seafloor [Jacobsen and Wasserburg, 1979; McCulloch et al., 1981]. This fact has limited the utility of the Sr isotopic system for constraining the origin of mafic rocks in complex orogenic terrains. In contrast, the Nd isotopic system appears to be relatively immune to such disturbances, suggesting that the distinctive Nd isotopic signature of oceanic crust is preserved during hydrothermal alteration on the sea floor and during obduction and regional metamorphism. Although the susceptibility of Nd and the REE in general to disturbance in response to different types of metamorphism is not well known, the available data suggest that the REE are quite robust. This feature could be of great importance in the Appalachians where metamorphism has obliterated the original mineralogy and modified the major element chemistry of most of the mafic and ultramafic rocks.

2. Samples and Procedures

We have analyzed samples of two of the largest mafic/ultramafic complexes in the Appalachians south of Newfoundland: the Thetford Mines Complex (TMC) of southern Quebec [Laurent, 1975, 1977] and the Baltimore Mafic Complex (BMC) of Maryland [Hertz, 1951; Hopson, 1964; Southwick, 1970; Morgan, 1977; Hanan, 1980]. Both of these complexes have been called ophiolites in the literature. The TMC has a complete ophiolite stratigraphy although it is strongly deformed. The BMC

on the other hand consists of only a cumulate dunite-chromitite base overlain by cumulate pyroxenites which grade into cumulate and non-cumulate two pyroxene gabbros and norites. The BMC does not include tectonized harzburgite, a dike complex, pillow basalts or overlying marine sediments. A variety of lithologies of varying degrees of metamorphism from both Thetford and Baltimore have been analyzed. For the BMC, mineral separates were made for internal isochrons on three samples having well-preserved igneous mineralogy. In addition, we have analyzed a variety of samples of mafic/ultramafic rocks from diverse localities which have on occasion been suggested to be obducted oceanic crust. These are comprised of one sample of the Hazen's Notch amphibolite associated with the serpentinized dunite of the Belvidere Mountain ultramafic body of northern Vermont [Laird, 1977; Chidester et al., 1978; Laird and Albee, 1981], two samples of Chunky Gal Mountain amphibolite from the Buck Creek peridotite body of North Carolina [Hadley, 1949; Sailor and Kuntz, 1973; McElhaney and McSween, 1982], an amphibolite from the nearby Lake Chatuge complex [Hartley, 1973; Jones et al., 1973] and a sample of websterite from the type locality of Webster-Addie, North Carolina [Miller, 1953; Stueber, 1969]. We have also analyzed two samples of the Grenville age basement gneiss from exposures in the Woodstock and Towsend Domes, Maryland [Tilton et al., 1958, 1970] and one sample of Wissahickon schist as possible representatives of the Appalachian basement and metasedimentary cover through which ensialic mafic rocks may have intruded. Sample locations and brief petrographic descriptions are given in the Appendix.

For the total rock analyses, 10-25 g interior pieces were crushed in a stainless steel mortar and pestle and a ~ 0.5 g split taken for HF + $HClO_4$ dissolution. With the exception of Md-11, an augen gneiss, all the samples analyzed were relatively fine-grained and the powdered material adequately represents the whole rock. No special attempt was made to homogenize a large

volume of sample Md-11. Nevertheless, the Nd isotopic results for this sample are in good agreement with those of fine-grained gneiss Md-7. Similarly, no attempt was made at dissolving the zircons present in Md-7, Md-11, Md-32 and RL80-7, although the HF + $HClO_4$ dissolution used does substantially attack those zircons which are metamict. The lack of dissolution of zircons is unlikely to have any effect on our Rb-Sr results due to the low concentrations of these elements in zircon. One may calculate the expected contribution of the zircons to the REE budget of the whole rock. For the rocks we analyzed, the worst case is for Md-7 which had ~ 2 mg insoluble residue from ~ 700 mg rock. If the residue were entirely zircon at 100 ppm Nd, then the undissolved material would comprise ~ 1% of the total rock Nd. Assuming an improbably large Sm/Nd fractionation between zircon and whole rock leading to a 20 ε-unit difference in isotopic composition between the zircon and rock, the shift in the whole rock ε_{Nd} value due to the lack of zircon dissolution would be only ~ 0.2 ε-units. We therefore believe the undissolved zircons to be an insignificant problem for these rocks.

Mineral separates were made using a combination of magnetic separation, heavy liquids (STBE and MI) and hand-picking. The purity of the mineral separates was ~ 99% for plagioclase and apatite and > 95% for pyroxene with fine-grained magnetite largely making up the remaining < 5%. The mineral separates were rinsed in acetone and distilled water and air dried before weighing.

In order to assess the possibility of contamination along grain boundaries during serpentization and metamorphism, a split of the powdered Webster-Addie sample was leached briefly in cold 0.1M HCl, rinsed in water, then leached for one hour in sub-boiling 1.5M HCl. The insoluble residue was dried, weighed, and dissolved in HF + $HClO_4$.

In order to spike the samples properly, solution aliquots containing 1-2 mg of sample were spiked and approximate Rb, Sr, Sm, and Nd concentrations deter-

mined by isotope dilution. Using these concentrations, the remainder of the sample was spiked and chemically separated to determine both isotopic compositions and concentrations precisely. On many samples, only aliquot data was collected for Rb concentrations. The errors on these data are consequently higher but due to the low Rb/Sr ratios involved, the error in the calculated initial ratios is insignificant. Details of the chemical separation and mass spectrometric procedures are given in Eugster et al. [1970], Papanastassiou and Wasserburg [1973], Papanastassiou et al. [1977], and DePaolo [1978]. Blanks for the complete analytical procedure are < 50 pg Nd and < 200 pg Sr and are negligible.

3. Results

Our results for the Baltimore Mafic Complex are presented in Table 1 and Figs. 3-6. Figs. 3a-3c show our Sm-Nd mineral data on three samples of the BMC. We report 2σ errors for the age and initial values calculated using the regression routine of Williamson [1968]. The large error on the age for the isochron for Md-32 is due to the relatively small spread in Sm/Nd ratios which in turn is probably caused by small amounts of apatite in the plagioclase and orthopyroxene mineral separates. On the basis of these three concordant isochrons, we assign an igneous crystallization age of 490±20 My to the BMC. It is important to note that the initial $\varepsilon_{Nd}(T)$ values for these isochrons are different from one another and all are negative.

The results of our Rb-Sr analyses on minerals from sample Md-32 are plotted in Fig. 3d. In contrast to the Nd isotopic system, the mineral data fail to define an Rb-Sr isochron with several different mineral phases. The slope is defined only by the orthopyroxene point and the cluster of points with low Rb/Sr ratio. A linear fit to the data yields an age of 386±28 My and a high initial $\varepsilon_{Sr}(T) = +114$ (0.7121). The results of our Sm-Nd analyses of

whole rocks from the BMC are plotted in Fig. 4a and our Rb-Sr results for the same samples in Fig. 4b. As can be seen from these figures, the whole rock data define neither Sm-Nd nor Rb-Sr isochrons, as could have been anticipated from the variation in $\varepsilon_{Nd}(T)$ among the mineral isochrons. Instead, the Nd data vary from $\varepsilon_{Nd}(T) = -6.4$ to -2.2 and the Sr data from $\varepsilon_{Sr}(T) = +115$ to $+51$ (0.7120 to 0.7075) for an age of 490 My. The Nd data show a general correlation between $\varepsilon_{Nd}(0)$ and Sm/Nd about the 490 My reference isochron (Fig. 4a). There is no obvious correlation in the Sr data (Fig. 4b). In terms of trace element chemistry, all of the Baltimore samples, with the exception of obvious cumulate rocks, are moderately to strongly LREE-enriched relative to chondrites, as can be seen by the negative values of $f^{Sm/Nd}$ in Table 1. These values lie between typical continental crustal values of $f^{Sm/Nd} \sim -0.4$ and a chondritic value of $f^{Sm/Nd} \sim 0$. The whole rock Rb/Sr ratios have a restricted range and are low relative to nominal undepleted mantle (UR).

Our results for the Thetford Mine Complex samples are presented in Table 1 and Fig. 5. We were unable to obtain a mineral isochron for the TMC due to the pervasive low-grade metamorphic overprint throughout the Thetford locality which has destroyed the igneous mineralogy. For the purpose of calculating initial isotopic ratios we have assumed an age of 500 My. With the exception of Qe 24 (a cumulate clinopyroxenite), all these samples have approximately chondritic Sm/Nd ratios. The calculation of $\varepsilon_{Nd}(T)$ values is therefore nearly independent of the assumed age. As can be seen in Fig. 5, the whole rock samples from Thetford do not define an isochron in either the Sm-Nd or Rb-Sr evolution diagrams. Using the assumed age, we calculate very variable initial isotopic compositions with $\varepsilon_{Nd}(T) = +4.2$ to -1.5, $\varepsilon_{Sr}(T) = -2.6$ to $+114$ (0.7041 to 0.7119). The samples have a wide range of Rb/Sr ratios, ranging from values much less than bulk mantle values to moderately LIL-enriched values. These

are quite reasonable for Grenville age crust [Tilton et al., 1958, 1970; Grauert, 1974]. T_{UR} ages (at 1.37 AE and 1.11 AE) are generally less reliable but in this case are close to the T_{CHUR} ages. The sample of Wissahickon schist has ϵ_{Nd} (490) = -6.6, ϵ_{Sr} (490) = +134 and T_{CHUR} = 1.04 AE, T_{UR} = 1.72 AE. The Nd model age implies that the Wissahickon sediments were dominantly derived from Grenville age basement such as the Baltimore Gneiss. The Wissahickon schist is known to have been metamorphosed at ~ 330 My from K-Ar studies [Lapham and Bassett, 1964].

4. Discussion

An Sm-Nd age of ~ 490±20 My was found for three different rocks from the Baltimore Mafic Complex. This is in agreement with zircon U-Pb ages [Sinha, personal communication]. We therefore interpret these results as the igneous crystallization age of the BMC. This places the time of magmatism prior to or at the earliest stages of the Taconic Orogeny. Samples from both the Susquehanna block (Md-32, Md-44) and the Baltimore block (Md-3) have ages that are identical within error, confirming the close relationship of these two exposures. This age is similar to the age of 505±10 My obtained by Jacobsen and Wasserburg [1979] for the Bay of Islands complex. In contrast to their isotopic results which demonstrated an oceanic signature for the Bay of Islands complex [$\epsilon_{Nd}(T)$ = +6.5 to +8.1, $\epsilon_{Sr}(T)$ = -19.6 to +32.5] our isotopic data clearly indicate that the BMC was not derived from depleted oceanic mantle. In particular, the negative values of $\epsilon_{Nd}(T)$ and positive values of $\epsilon_{Sr}(T)$ are most like the isotopic signature of old continental crust. The variation in initial isotopic composition of both Nd and Sr does not appear to correlate with stratigraphic position in the complex, rock type, or degree of metamorphism. Hanan [1980, 1981] has shown that $^{87}Sr/^{86}Sr$ ratios are shifted to higher values

in metamorphic minerals along late stage fractures in the gabbro. These fractured rocks were avoided in the present study. It is clear from our attempt at an Rb-Sr mineral isochron (Fig. 3d) that there has been redistribution of Rb or Sr on a mineral scale during post-crystallization metamorphism. Nevertheless, for reasons which will be shown below, we believe that the variation in whole rock initial Sr isotopic composition is a magmatic characteristic, and that on the scale of several centimeters, the whole rocks have remained largely closed systems since crystallization. That the variation in initial Nd isotopic composition is a magmatic characteristic is clearly demonstrated by the different initial values obtained for our Sm-Nd mineral isochrons. This interpretation hinges on the assumption that the Sm-Nd mineral isochrons record both the time of crystallization from a melt and the melt's isotopic composition. It is possible that the mineral isochrons record a metamorphic event and that the initial isotopic compositions are a result of large scale introduction of Nd and Sr from the surrounding rocks. Such a metamorphic event would have had to have occurred shortly after crystallization in order to account for the agreement between the Sm-Nd mineral isochron and U-Pb zircon ages. In addition, the samples chosen for isochron work have anhydrous, apparently igneous mineralogy (see Appendix) implying granulite grade metamorphism. Without a hydrous fluid phase to mediate the process, we believe it is unlikely that isotopic exchange can occur over a scale of kilometers. Furthermore, as will be shown below, amphibolite grade metamorphism, presumably in the presence of abundant fluid, did not appreciably disturb the Nd isotopic signature of mafic rocks from North Carolina and Vermont. Therefore, we do not believe that the Nd systematics of the BMC samples record a metamorphic event. In the discussion which follows, we shall assume that this is the case. In Fig. 6 we have plotted our results for the BMC in an $\varepsilon_{Nd}(T)$ vs. $\varepsilon_{Sr}(T)$ diagram. The data define an array lying to

higher $\varepsilon_{Sr}(T)$ than the mantle array with $\varepsilon_{Nd}(T)$ inversely correlated with $\varepsilon_{Sr}(T)$. It is this coherence, together with the assumption that the $\varepsilon_{Nd}(T)$ values are magmatic, that leads us to believe that the variation in $\varepsilon_{Sr}(T)$ is not due to later metamorphism. The trend in the ε_{Nd}-ε_{Sr} diagram is exactly what one would expect for contamination of a mantle-derived magma with high ε_{Sr} and low ε_{Nd}, old continental crust. Fig. 2 schematically illustrates this along with other contamination trends and the isotopic characteristics of endmember rock types. Hanan [1980] suggested that the radiogenic Sr isotopic compositions of the BMC are due to interaction with seawater. This is almost certainly not the case for two reasons: 1) Cambro-Ordovician seawater had $\varepsilon_{Sr} \sim +72$ (0.709) [Peterman et al., 1970; Burke et al., 1982] a value lower than the initial isotopic composition of several of our samples; 2) interaction with seawater is not expected to shift the Nd isotopic composition by a significant amount until extremely high water/rock ratios are reached ($\sim 10^5$) due to the extraordinarily low concentration of Nd in seawater ($\sim 2\times10^{-12}$ g/g) [Goldberg et al., 1963; Høgdahl et al., 1968; DePaolo and Wasserburg, 1977]. The mixing line between oceanic crust and seawater is shown in Fig. 2. This process is thought to account for the spread of $\varepsilon_{Sr}(T)$ at essentially constant $\varepsilon_{Nd}(T)$ seen in Fig. 6 for the Bay of Islands data [Jacobsen and Wasserburg, 1979]. Our data for the BMC rocks in Fig. 6 do not show this relationship. We suggest instead that the Baltimore Complex magma was contaminated by or partially derived from older crustal material. Possible candidates for the contaminant are the Grenville age basement rocks which are exposed in several mantled gneiss domes in the Baltimore area and the overlying metasediments. Our data for the Baltimore gneiss and Wissahickon schist samples are plotted on Fig. 6 at the isotopic composition they would have had 490 My ago. It is clear from this figure that the gneisses are suitable candidates for the contaminant in terms of their

isotopic composition, as would be sediments or metasediments largely derived from Grenville age basement. The particular sample of Wissahickon schist analyzed appears to have too low $\varepsilon_{Sr}(T)$ to be a reasonable bulk contaminant. Undoubtedly there exists a wide variation in both Rb/Sr and ε_{Sr} within the Wissahickon schist and it is likely that assimilation of portions of this formation could lead to the observed isotopic pattern. Several other lines of evidence support the idea that the BMC magma was contaminated with older crustal material. Brown primary amphibole is common in the gabbro, suggesting a relatively high f_{H_2O} as might result from the assimilation of hydrous phases, and partially assimilated mafic xenoliths of uncertain origin are present in the upper portions of the gabbro [Hanan, 1980]. Further evidence is the observation originally due to Bowen [1928] that assimilation of aluminous rocks by basaltic magma should bring orthopyroxene onto the liquidus and increase the anorthite content of the crystallizing plagioclase at the expense of clinopyroxene crystallization according to the generalized reaction:

$$\underset{\text{Aluminosilicates}}{(SiO_2 + Al_2O_3)} + \underset{\text{Diopside}}{CaMgSi_2O_6} = \underset{\text{Anorthite}}{CaAl_2Si_2O_8} + \underset{\text{Enstatite}}{MgSiO_3}$$

More recent experimental work by Irvine [1975] has substantiated Bowen's observation. Both the early appearance of orthopyroxene in the crystallization sequence and high anorthite content of the plagioclase are characteristics of the BMC. Taken to its extreme, this mechanism should produce norites. We note that Md-32, a norite sample, is also the most enriched in incompatible elements of the samples analyzed, as evidenced by the presence of zircon and apatite. This sample also has the highest $\varepsilon_{Sr}(T)$ and lowest $\varepsilon_{Nd}(T)$ and would thus represent the most contaminated sample we have analyzed. The T_{CHUR} model age

for this sample is 1.2 AE, close to that calculated for the samples of Baltimore Gneiss (~ 1.26 AE), suggesting that assimilation of the Baltimore Gneiss or a rock with similar isotopic characteristics caused the variation in initial isotopic composition of the BMC. A calculation for simple mixing between a magma with $\varepsilon_{Nd} = \varepsilon_{Sr} = 0$, and 5 ppm Nd, 100 ppm Sr and a contaminant with $\varepsilon_{Nd} = -8$, $\varepsilon_{Sr} = +300$, 50 ppm Nd and 200 ppm Sr shows that > 25% bulk assimilation is necessary to account for the most contaminated samples. This is a rather large amount. This calculation is clearly an oversimplification but serves to give a sense of the magnitude of the effect. A more realistic calculation would include the effects of combined assimilation/fractionation and selective melting in the contaminant as well as incorporating other isotopic and trace element constraints. In the absence of information on liquid compositions during the evolution of the BMC magma, however, such a detailed calculation is not warranted. Furthermore, the lack of correlation between isotopic composition and rock type or position in the crystallization sequence suggests that the BMC magma chamber was chemically and isotopically heterogeneous and that the magma was therefore not well-mixed, thus this basic assumption of most mixing models cannot be justified in the case of the BMC.

Having documented the probable role of continental crustal material in the genesis of the BMC, we now ask in what tectonic settings such a process might operate. From the preceding arguments, it appears that the complex did not form at an oceanic spreading center and is therefore not an ophiolite if that term is considered to mean obducted oceanic crust. The remaining possibilities include oceanic island volcanism, subduction-zone related volcanism and continental mafic intrusion of an unspecified nature (not related to a subduction zone). Oceanic island volcanism is an unlikely candidate on the basis of our isotopic data. Although oceanic island basalts are often derived from less depleted

mantle sources than normal MORB or a mixture of depleted and enriched mantle, the large negative $\varepsilon_{Nd}(T)$ together with large positive $\varepsilon_{Sr}(T)$ characteristic of the BMC have not been found among oceanic island rocks. The most enriched oceanic island alkali basalts measured to date have $\varepsilon_{Nd} = -5.7$, $\varepsilon_{Sr} = +17$ [Dosso and Murthy, 1980] while the BMC has $\varepsilon_{Sr}(T) \sim +100$ for $\varepsilon_{Nd} \sim -6$. Subduction related magmas have two mechanisms whereby interaction with continental crustal material may occur: by subduction of continent-derived sediments and by intrusion into continental crust. Although subduction and subsequent melting of sediments has often been called upon to explain some features of andesitic magmas and is probably an important mechanism in their genesis [Brown et al., 1982], it is unlikely that sufficient sediment could be carried down with the subducting plate to produce the strong continental signature seen in the BMC. This possibility cannot be ruled out, however, as the work of Whitford [1975] and Whitford et al. [1977, 1979] has shown that some andesites of the Sunda-Banda Arc, Indonesia, have strongly positive values of $\varepsilon_{Sr}(0)$ and negative values of $\varepsilon_{Nd}(0)$, probably due to large amounts of continental detritus from Australia being subducted beneath the arc. In general, however, only those arcs which are built upon thick continental crust, such as the Andes, have negative ε_{Nd} and positive ε_{Sr} similar to the Baltimore samples. Studies by DePaolo and Wasserburg [1977] and James [1982] of Andean volcanics and Nohda and Wasserburg [1981] of Japanese volcanics have also appealed to contamination by continental material during intrusion in order to explain the observed isotopic and trace element compositions. The last case, continental mafic intrusion of an unspecified nature, is no different in contamination mechanism from the case of a continental arc. Studies of the Stillwater Complex of Montana [DePaolo and Wasserburg, 1979], the Shabogamo Intrusive Suite of Labrador [Zindler et al., 1981], the Kalka Intrusion of Central Australia [Gray et al., 1981] and the Cortlandt Complex of New York [Domenick and Basu, 1982] have similarly suggested on the basis of Nd isotopic

evidence that crustal contamination played a role in the genesis of these mafic intrusions. We emphasize that the negative values of $\varepsilon_{Nd}(T)$ for the BMC samples rule out a depleted mantle source for the complex, and that the Complex is therefore not a fragment of typical oceanic crust. We suggest instead, on the basis of our isotopic data, that the BMC was intruded into continental crust, possibly as part of a Cambro-Ordovician arc complex, and was contaminated by old LREE enriched crustal material with $\varepsilon_{Nd} << 0$ during emplacement. Its present allochthonous nature [Crowley, 1976] must be due to post-crystallization tectonic movements not related to obduction of oceanic crust.

We would like to draw attention to our Nd results on the Baltimore Gneiss samples. In particular, we note that the T_{CHUR} model ages [DePaolo and Wasserburg, 1976a] appear to accurately reflect the time of crustal formation. Previous isotopic work on the Gneiss has pointed up the complex history of the basement complex: K-Ar and Rb-Sr mineral systems were reset by metamorphic events in the interval 300-500 My ago [Wasserburg et al., 1957; Wetherill et al., 1968], and the U-Th-Pb systematics of zircons show complex patterns of discordance due to episodic and continuous lead loss as well as possible inheritance of older Pb [Tilton et al., 1958, 1970; Grauert, 1974]. The T_{CHUR}, and to a lesser extent the T_{UR} model ages, appear to be able to see past these later disturbances to the original time of crustal formation of the Grenville Province at ~ 1.25-1.30 AE.

Our Sr and Nd isotopic data for the Thetford Mines complex are plotted in Fig. 6. As can be seen in this figure, there is no clear correlation between $\varepsilon_{Nd}(T)$ and $\varepsilon_{Sr}(T)$. The data scatter from $\varepsilon_{Nd}(T) = -1.5$ to $+4.2$ and $\varepsilon_{Sr}(T) = +2.6$ to $+114.0$ (0.7041 to 0.7119). Like the BMC, the isotopic composition of the Thetford samples does not appear to correlate with rock type, position within the complex, or degree of metamorphism. In particular, note that the upper and lower pillow lava sequences are isotopically indistinguishable.

The range in isotopic composition characteristic of the TMC is not the signature of oceanic crust (compare the data in Fig. 6 with Fig. 2). Neither can the variations in isotopic composition be generated by simple mixing of oceanic crust with old continental crustal or seawater Sr and Nd. More complicated processes appear to be involved. The TMC is unquestionably an ophiolite sensu stricto in that the complex includes all the elements of the ophiolite stratigraphy. It thus appears that the isotopic and field geologic relationships are in opposition. We do not believe that metamorphism is the primary cause of the variations in isotopic composition in the Nd system. Ophiolites with similar metamorphic histories such as the Josephine Ophiolite and the Kings-Kaweah Ophiolite of California, which have metamorphic assemblages similar to the TMC, preserve the Nd signature and, to a lesser extent, the Sr isotopic signature of oceanic crust (Table 1) [Chen and Shaw, 1982]. Futhermore, as will be shown below, relatively high-grade amphibolites from North Carolina and Vermont also preserve the Nd isotopic characteristics of their depleted mantle source. On the other hand, the case for the observed Sr isotopic compositions being primary is rather poor. Sr isotopic exchange during metamorphism is a well-documented process [Lanphere et al., 1964, and many later studies] and interaction with metamorphic fluids derived from dehydration reactions in metasedimentary rocks will generally increase the $^{87}Sr/^{86}Sr$ ratio in mantle-derived rocks. Unlike the Baltimore samples, there is no apparent correlation between $\varepsilon_{Nd}(T)$ and $\varepsilon_{Sr}(T)$, suggesting that these systems are decoupled. Several of the samples analyzed contained secondary calcite which might be expected to have a large effect on the Sr isotopic composition of the bulk rock, although the presence of calcite does not appear to correlate with $\varepsilon_{Sr}(T)$ or $\varepsilon_{Sr}(0)$. In addition, the samples have quite a wide range of Rb/Sr ratios, possibly indicating rather large Rb-Sr fractionation during metamorphism.

In short, the Sr isotopic system cannot be counted upon to preserve primary isotopic composition in complex metamorphic terrains and we shall therefore concentrate our discussion on the significance of the Nd data.

Although the isotopic composition of the TMC is unusual for an ophiolite, it is not unique. Recent studies of the Vourinous Complex, Greece [Noiret et al., 1981; Richard and Allegre, 1980], the Troodos Ophiolite, Cyprus [Hannah and Futa, 1982], and the Bett's Cove Ophiolite, Newfoundland [Coish et al., 1982] have shown that, in part, they are also characterized by rocks with $\varepsilon_{Nd}(T)$ between 0 and +4 and with relatively radiogenic Sr, although the latter is usually attributed to interaction with seawater. Both the Troodos and Bett's Cove ophiolites were also found in these studies to include rocks with a more normal oceanic signature of $\varepsilon_{Nd} \sim +8$, a characteristic not seen in the Thetford samples we have analyzed. The significance of these results for ophiolite genesis is not clear. The implication is that there are ophiolites of varying ages which were derived from a mantle source with modestly positive ε_{Nd} or from a blend of magmas derived from normal depleted oceanic mantle and an enriched reservoir such as enriched mantle, undepleted mantle or continental crust. These characteristics have been attributed to the source for many oceanic island basalts [O'Nions et al., 1977; Dosso and Murthy, 1980]. A mixture of sources might also be expected for arcs and the magmas intruded during the initial stages of continental rifting to form an ocean basin or marginal basin. The latter cases would also allow for interaction of the mantle-derived magma with continental crust.

Church [1977] has pointed out that the TMC is chemically similar to the Bett's Cove ophiolite of Newfoundland [Coish and Church, 1979] in that they are characterized by the presence of orthopyroxene-bearing cumulates and relatively low Ti-basalts, among other features. He contrasts these complexes with

ophiolites characterized by dunite-troctolite cumulate sequences and relatively Ti-rich basalts with olivine and plagioclase phenocrysts such as the Bay of Islands Ophiolite. He further identifies these two endmembers with the ophiolites of the internal and external zones, respectively, of the Tethys region [Rocci et al., 1975]. Our isotopic data together with the previously mentioned studies seem to indicate that there is a fundamental difference in origin between the two endmembers as defined by Church, but it is unclear what this difference signifies. Clearly, more work is needed to establish the links between the variations in major and minor element geochemistry and isotopic systematics of these ophiolites and to attempt to relate these to modern analogues. Among modern rocks, these complexes have isotopic and chemical affinities to boninites, which are olivine, orthopyroxene, and clinopyroxene-phyric island arc basalts with high MgO and SiO_2 contents but low TiO_2 contents [Kuroda and Shiraki, 1975; Shiraki and Kuroda, 1977]. Recent Nd isotopic data obtained by Hickey and Frey [1982] has shown that boninites, like the Thetford Mines samples, are characterized by a large range in $\varepsilon_{Nd}(0)$ (-0.3 to +6.2) which they attribute to mixing between a strongly depleted mantle peridotite and an enriched component; either subducted sediments or metasomatized, LREE enriched mantle. We suggest that the TMC may represent the ancient intrusive and extrusive counterpart to modern boninites.

In summary, our data on the TMC are not easily reconciled with the geologic relationships. At face value, they preclude the formation of the complex at a normal mid-ocean spreading center. Nevertheless, it is possible that the metamorphism and alteration was so severe that all primary isotopic memory has been erased.

Our isotopic results for the North Carolina samples are plotted in Fig. 6. In contrast to the results discussed thus far, the Chunky Gal and Lake Chatuge

amphibolites clearly have the isotopic signature of ancient oceanic crust. In Fig. 6, these data generally fall within the field defined by the Bay of Islands complex [Jacobsen and Wasserburg, 1979] although the Lake Chatuge sample has a somewhat lower value of $\varepsilon_{Nd}(T)$ than the other samples. Similarly, the sample of Hazen's Notch amphibolite from Vermont also plots within this field. These samples all have characteristically oceanic values of $\varepsilon_{Nd}(T) > +5$ for T = 500 My but extend from the mantle array to more radiogenic values of $\varepsilon_{Sr}(T)$. The dispersion in $\varepsilon_{Sr}(T)$ may be due to either hydrothermal interaction with seawater or continental metamorphic fluids or both. Previous Sr isotopic work by Stueber [1969] and Jones et al. [1973] showed that the Sr isotopic composition of ultramafic and mafic rocks from North Carolina was in some cases considerably more radiogenic than plausible seawater values. In addition, these studies suggested that the increase in $^{87}Sr/^{86}Sr$ ratios was correlated with the degree of metamorphism; samples of unmetamorphosed troctolite and dunite had lower isotopic ratios than their metamorphic equivalents, amphibolite and serpentinite. If true, this would clearly indicate exchange of Sr during metamorphism. It is important to note, however, as has been observed in other studies of ophiolite complexes [Jacobsen and Wasserburg, 1979; McCulloch et al., 1981; Chen and Shaw, 1982], that even though the Sr system shows evidence for substantial post-crystallization isotopic exchange, the Nd system appears to preserve the primary isotopic composition, even at the relatively high grade of metamorphism represented by the Vermont and North Carolina amphibolites. This fact encourages our belief that the Nd isotopic variations observed in the BMC and TMC are primary and not due to later exchange processes.

Our results on the Vermont and North Carolina amphibolite samples are significant in that they demonstrate that there are mafic rocks in the Appalachians which are derived from a depleted mantle source and which, at least

on isotopic grounds, are good candidates for being fragments of oceanic crust.

The Webster-Addie sample with $\varepsilon_{Nd}(T) \sim -1$, $\varepsilon_{Sr}(T) \sim +29$ is clearly different from the nearby amphibolites and does not have the signature of the depleted mantle source typical of oceanic rocks. The leaching experiment shows that the low $\varepsilon_{Nd}(T)$ is not due to the presence of Nd derived from surrounding metamorphic rocks on grain boundaries. It is difficult to draw any firm conclusions about the origin of the Webster-Addie body on the basis of this single sample; however, the isotopic data do not support an origin at a mid-ocean spreading center.

5. Conclusions

From Sr and Nd isotopic analyses it appears that there is no single origin for the mafic and ultramafic rocks of the Appalachians. The isotopic data support the earlier notions of ensialic mafic intrusions in the case of the Baltimore Mafic Complex, while clearly supporting an oceanic origin for the Bay of Islands Ophiolite, the Belvidere Mountain Complex, and some of the North Carolina bodies. The Thetford Mines Complex appears to belong to a class of ophiolites with peculiar isotopic, and possibly chemical, characteristics, which have affinities to modern-day boninitic rocks found in oceanic arcs. The isotopic data would tend to rule out the formation of these complexes at a mid-ocean spreading center. These conclusions are critically dependent on the observation that the Nd isotopic system is relatively immune to disturbance during metamorphism and thus preserves the original igneous isotopic signature. Nevertheless, even if the observed isotopic systematics represent a metamorphic effect, we find no supportive evidence for an oceanic crustal origin for the BMC, TMC or the Webster-Addie body. In contrast, the Sr isotopic system alone is relatively undiagnostic as to the origin of rocks in metamorphic terranes due to the

relative ease with which Rb and Sr are mobilized during metamorphism. The Nd isotopic system can readily be exploited in favorable cases to obtain ages on mafic rocks. When applied to samples of the BMC, this technique yields an age of 490±20 My for this body which we interpret as the time of crystallization. Old continental crust has a distinctive isotopic signature and combined Nd-Sr isotopic studies provide a sensitive test for the presence of assimiliated crust in igneous bodies. Our results on the BMC indicate that a significant fraction of the Nd and Sr in the Complex was derived from old continental material such as the Baltimore Gneiss.

In summary, we believe that studies of Appalachian geology have reached a point where the diversity in origins for the mafic and ultramafic rocks of this mountain belt must be recognized and explained. It would appear that simple models involving only obduction of ridge-generated oceanic crust are inadequate to explain the observations. Finally, we caution as others have that not every mafic and ultramafic rock in an orogenic belt is part of an ophiolite nor are all ophiolites formed at mid-ocean spreading centers.

Acknowledgements

We are grateful to T. Fenninger and R. Laurent for assistance in the field in Quebec, and T. Cullen, G. Fisher, B. Marsh and J. Meyers for assistance in Maryland. Discussions with them and with B. Morgan, A. K. Sinha and B. Hanan were most rewarding. We also thank G. Harper, S. Jacobsen, J. Laird, B. Morgan, H. McSween, K. Misra, J. Paque and A. K. Sinha for providing samples. As always, D. A. Papanastassiou was an invaluable source of information on chemical and mass spectrometric procedures. The initial formulation of this project grew out of discussions with A. L. Albee on the nature of the mafic rocks of New England. P. D. Fullagar and an anonymous reviewer provided constructive reviews of this paper. This work was funded by the National Science Foundation Grant Nos. PHY79-23638A2 and EAR79-19786, and the National Aeronautics and Space Association Grant No. NGL 05-002-188.

Appendix

Sample Descriptions and Locations

(Percentages are visual estimates
and intended only as a guide to modal abundances).

Baltimore Mafic Complex

Md-32 - Norite: Plagioclase, 80%; Opx. 14%; Magnetite, 5%; Sulphide, 1%; Tr. apatite, zircon, quartz, green trem-actinolite, chlorite.

Conowingo Dam Quad., Md.-Penn, Road from Oakwood to Susquehanna R. in ravine of Conowingo Creek. 39°41.26'N, 76°11.35'W.

Md-3 - Feldspathic websterite/two pyroxene gabbro: 40% Opx. with Cpx. exsolution lamallae, 40%; Cpx. with opx. exsolution lamallae, 35% plagioclase, 25%; tr opaques, green trem.-actinolite.

Baltimore West Quad., Md. Purnell Dr., 39°19.12'N, 76°47.63'W

Md-40 - Metagabbro: Pale green fibrous trem-actinolite after pyroxene 50%; plagioclase, 30%; cpx., 15%; chlorite, 3%; zoizite + epidote, 1%; opaques, 1%; tr. carbonate, chlorite.

Conowingo Dam Quad. Md.-Penn., RR cut along Susquehanna R., 39°40.43'N, 76°11.13'W.

Md-15 - Feldspathic Orthopyroxenite: Orthopyroxene, 90%; plagioclase, 7%; cpx., 2%; green trem-actinolite 1%; tr. opaques.

Conowingo Dam Quad. Md-Penn, Road from Oakwood to Pilot, 39°41.23'N, 76°10.93'W. Sample from B. Morgan, his #77-BM-65.

Md-39 - Hornblende Gabbro: Plagioclase, 40%; cpx., 20%; opx., 15%; intercumulus brown amphibole, 10%; fibrous green amphibole + ? after pyroxene, 10%; pale green trem-actinolite, 3%; epidote, 1%; opaques, 1%.

Conowingo Dam Quad, Md-Penn; RR cut along Susquehanna R, 39°40.34'N, 76°10.97'W

Md-30 - Two-pyroxene Gabbro: Plagioclase, 45%; opx., 20%; cpx., 15%; fibrous pale green amphibole + ? after pyroxene, 15%; zoizite, 2%; chlorite 2%; opaques, 1%.

Conowingo Dam Quad. Md-Penn; Road from Oakwood to Susquehanna R., 39°41.74'N, 76°11.95'W.

Md-44 - Two-pyroxene Gabbro: Plagioclase, 60%; opx., 20%; cpx., 20%; tr. green trem-actinolite, opaques.

Conowingo Dam Quad. Md-Penn; RR cut along Susquehanna R., 39°41.44'N, 76°12.30'W.

Baltimore Gneiss, Wissahickon Schist

Md-7 - Layered Biotite Gneiss: Quartz, 40%; plagioclase, 30%; microcline, 20%; biotite, 10%; tr. apatite, zircon, sphene.

Ellicott City Quad, Md; Bluff above RR tracks along Patapsco R. west of Woodstock. Woodstock Dome. 39°19.87'N, 76°52.45'W. Near locality sampled by Tilton et al. [1970].

Md-11 - Augen Gneiss: Quartz, 30%; Microcline, 28%; plagioclase, 25%; biotite, 15%; muscovite, 1%; sphene, 1%; tr. epidote, allanite, zircon, apatite, tourmaline.

White Marsh Quad. Md., Hartley Mill Road in Long Green Creek near Crowley's [1976] type locality. Towsend Dome. 39°27.02'N, 76°28.54'W.

RL 80-7 - Wissahickon Schist: Quartz, 40%; plagioclase, 35%; biotite, 10%; epidote + zoizite, 10%; muscovite, 5%; chlorite 1%; tr. opaques, apatite, zircon.

Conowingo Dam Quad. Md-Penn; Rte. 299 NW of Harmony Chapel. 39°39.0'N, 76°8.3'W. Sample from K. Sinha.

Thetford Mines Complex

Qe-40 - Upper Pillow lava (greenschist): Fine-grained chlorite + amphibole, 40%; calcite, 30%; epidote, 20%; quartz + plagioclase, 9%; coarse euhedral green amphibole. 1%; tr. opaques.

Disraeli Sheet Qe. Rt. 34 north of Lac Coulombe, 45°50.70'N, 71°27.63'W.

Qe-13A#3 - Lower Pillow lava (greenschist): Chlorite, 60%; amphibole after cpx (?) microphenocrysts, 39%; opaques, 1%; tr. calcite, zoizite.

Thetford Mines Sheet, Qe. 0.27 km southeast of Colline Poudrier, 46°0.72'N, 71°14.14'W.

Qe-18 - Lower Pillow lava (greenschist): Fine-grained chlorite + amphibole, 55%; quartz + plagioclase, 40%; calcite (in vesicles), 5%; tr. zoizite, opaques.

Thetford Mines Sheet, Qe. On road to Mt. Adstock. 46°1.10'N, 71°12.8'W.

Qe-12A - Metagabbro, screen in dike complex: Amphibole, 55%; Chlorite, 20%; zoizite + ? after plagioclase (?), 15%; quartz, 10%; tr. opaques, cpx. (relict).

Thetford Mines Sheet Qe. Dike and sill complex at Colline Poudrier. 46°0.83'N, 71°14.65'W.

Qe-8B - Metadiabase: Amphibole, 50%; plagioclase, 45%; chlorite, 2%; cpx. phenocrysts (relict), 2%; zoizite, 1%.

Same location as Qe 12A.

Qe-30A - Metagabbro: Dark, fine-grained alteration products of plagioclase [= hydrogrossular (?) + zoizite + clays (?)], 75%; amphibole after cpx., 20%; chlorite, 5%; tr. zoizite, opaques, cpx. (relict).

Disraeli Sheet Qe., Road along northeast end of the northwest arm of Breeches Lake. 45°55.28'N, 71°27.92'W.

Qe-24 - Clinopyroxenite: cpx., 75%; amphibole after cpx., 15%; serpentine after olivine (?), 7%; opaques, 3%.

Disraeli Sheet Qe. Between Lac de l'Est and Colline Lemay. 45°56.89'N, 71°24.36'W.

North Carolina Samples

CG-12-1 - Chunky Gal Amphibolite: Amphibole, 50%; plagioclase, 48%; opaques, 2%; tr. zircon, tourmaline.

Rainbow Springs Quad., N.C., 35°4.8'N, 83°35.4'W, see McElhaney and McSween [1983]. Sample from H. McSween.

CG-2-18 - Chunky Gal Amphibolite: Amphibole, 75%; plagioclase, 20%; zoizite, 5%; tr. zircon.

Shooting Creek Quadrangle, N.C. 35°5.0'N, 83°38.0'W. See McElhaney and McSween [1983]. Sample from H. McSween.

C-1 - Amphibolite from Lake Chatuge ultramafic body: Amphibole, 60%; plagioclase, 40%; tr. epidote, zircon, opaques.

Sample from J. Paque.

XTC-127 - Websterite, webster-addie ultramafic body: cpx., 85%; opx., 15%; tr. green amphibole, spinel, opaques.

Sample from K. Misra.

Vermont Sample

VJL-360C - Hazen's Notch Amphibolite: Blue-green barroisitic amphibole 50%; epidote, 25%; quartz, 20%; garnet + chlorite after garnet, 5%; tr. rutile, zircon, apatite, plagioclase.

Jay Peak Quad., Vermont. Near lookout tower on Belvidere Mountain. 44°46.43'N, 72°33.06'W. See Laird [1977], Laird and Albee [1981]. Sample from J. Laird.

California Samples [Chen and Shaw, 1982]

P-59 - Cumulate gabbro: Plagioclase 80%; cpx. 10%; fibrous trem.-actinolite, 5%; serpentine, 3%; brown amphibole, 2%; Tr. chlorite, opaques.

Point Sal ophiolite. Sample from S. Jacobsen.

JP-042 - Cumulate olivine gabbro: Sericitized plagioclase 65%; olivine 10%; cpx., 10%; serpentine + magnetite after olivine, 10%; fibrous trem.-actinolite, 5%; Tr. green spinel.

Oregon Mountain, Josephine ophiolite. Sample from S. Jacobsen.

Y-13b - Cumulate gabbro: Sericitized plagioclase 70%; cpx. 25%; chlorite + serpentine, 5%; tr. amphibole, opaques.

Josephine ophiolite. Sample from G. Harper.

Ca-10 - Metagabbro: Amphibole after cpx., 70%; plagioclase, 25%; cpx., 5%; tr. opaques, serpentine, chlorite, zoizite.

Kings-Kaweah ophiolite. 45°4.6'N, 119°24.5'W.

References

Bowen, N. L., 1928, The evolution of the igneous rocks: Dover Publications, Inc., New York, 1956 reprint, 335 pp.

Brown, L., Klein, J., Middleton, R., Sacks, I. S., and Tera, F., 1982, ^{10}Be in island-arc volcanoes and implications for subduction: Nature, v. 299, p. 718-720.

Burke, W. M., Denison, R. E., Hetherington, E. A., Koepnick, R. B., Nelson, M. F., and Omo, J. B., 1982, Variation of seawater $^{87}Sr/^{86}Sr$ throughout Phanerozoic time: Geology, v. 10, p. 516-519.

Carlson, R. W., MacDougall, J. D., and Lugmair, G. W., 1978, Differential Sm/Nd evolution in oceanic basalts: Geophys. Res. Lett., v. 5, p. 229-232.

Carlson, R. W., Lugmair, G. W., and MacDougall, J. D., 1981, Columbia River volcanism: The question of mantle heterogeneity or crustal contamination: Geochim. Cosmochim. Acta, v. 45, p. 2483-2500.

Carlson, R. W., Lugmair, G. W., and MacDougall, J. D., 1983, "Columbia River volcanism: The question of mantle heterogeneity or crustal contamination" (reply to a comment by D. J. DePaolo): Geochim. Cosmochim. Acta, v. 47, p. 845-846.

Chen, J. H., and Shaw, H. F., 1982, Pb-Nd-Sr isotopic studies of ophiolites in California, Western U.S. [abs]: Abstract with Programs, Geol. Soc. Amer., v. 14, p. 462.

Chidester, A. H., and Cady, W. M., 1972, Origin and emplacement of alpine-type ultramafic rocks: Nat. Phys. Sci., v. 240, p. 27-31.

Chidester, A. H., Albee, A. L., and Cady, W. M., 1978, Petrology, structure and genesis of the asbestos-bearing ultramafic rocks of the Belvidere Mountain area in Vermont: U. S. Geol. Survey Prof. Paper 1016, 95 pp.

Church, W. A., 1977, The ophiolites of southern Quebec: Oceanic crust of Bett's Cove type: Can. J. Earth Sci., v. 14, p. 1668-1673.

Church, W. A., and Stevens, R. K., 1971, Early Paleozoic ophiolite complexes of Newfoundland and Appalachians as mantle-ocean crust sequences: J. Geophys. Res., v. 76, p. 1212-1222.

Cohen, R. S., Evensen, N. M., Hamilton, P. J., and O'Nions, R. K., 1980, U-Pb, Sm-Nd, and Rb-Sr systematics of mid-ocean ridge basalt glasses: Nature, v. 283, p. 149-153.

Coish, R. H., and Church, W. R., 1979, Igneous geochemistry of mafic rocks in the Bett's Cove ophiolite, Newfoundland: Cont. Min. Pet., v. 70, p. 29-39.

Coish, R. H., Hickey, R., and Frey, F. A., 1982, Rare earth element geochemistry of the Bett's Cove ophiolite, Newfoundland: Complexities in ophiolite formation: Geochim. Cosmochim. Acta, v. 46, p. 2117-2134.

Crowley, W. P., 1976, The geology of the crystalline rocks near Baltimore and its bearing on the evolution of the eastern Maryland Piedmont: Maryland, Geol. Surv. Rept. Invest., v. 27, 40 pp.

DePaolo, D. J., 1978, Study of magma sources, mantle structure, and the differentiation of the earth using variations of $^{143}Nd/^{144}Nd$ in igneous rocks: Ph.D. dissert., California Institute of Technology, 360 pp.

DePaolo, D. J., 1983, Comment on "Columbia River volcanicsm: The question of mantle heterogeneity or crustal contamination": Geochim. Cosmochim. Acta, v. 47, p. 841-844.

DePaolo, D. J., and Wasserburg, G. J., 1976a, Nd isotopic variations and petrogenetic models: Geophys. Res. Lett., v. 3, p. 249-252.

DePaolo, D. J., and Wasserburg, G. J., 1976b, Inferences about magma sources and mantle structure from variations of $^{143}Nd/^{144}Nd$: Geophys. Res. Lett., v. 3, p. 743-746.

DePaolo, D. J., and Wasserburg, G. J., 1977, The sources of island arcs as indicated by Nd and Sr isotopic studies: Geol. Res. Lett., v. 4 no. 10, p. 465-468.

DePaolo, D. J., and Wasserburg, G. J., 1979, Sm-Nd age of the Stillwater Complex and the mantle curve for neodymium: Geochim. Cosmochim. Acta, v. 43, p. 999-1008.

Dewey, J. F., and Bird, J. M., 1971, Origin and emplacement of the ophiolite suite: Appalachian ophiolites in Newfoundland: J. Geophys. Res., v. 76, p. 3197-3207.

Domenick, M. A., and Basu, A. R., 1982, Age and origin of the Cortlandt Complex, New York: Implications from Sm-Nd data: Cont. Min. Pet., v. 79, p. 290-294.

Dosso, L., and Murthy, V. R., 1980, A Nd isotopic study of the Kerguelen Islands: Inferences on enriched oceanic mantle sources: Earth Planet. Sci. Lett., v. 48, p. 268-276.

Edwards, R. L., and Wasserburg, G. J., 1983, Sm-Nd and Rb-Sr systematics of the Kempersai ultramafic complex, South Ural Mountains, USSR [abs]: EOS, v. 64, p. 337.

Eugster, O., Tera, F., Burnett, D. S. and Wasserburg, G. J., 1970, The isotopic composition of gadolinium and neutron-capture effects in some meteorites, J. Geophys. Res., v. 75, p. 2753-2768.

Goldberg, E. D., Koide, M., Schmitt, R. A., and Smith, J., 1963, Rare earth distributions in the marine environment: J. Geophys. Res., v. 68, p. 4204-4217.

Grauert, B., 1974, U-Pb systematics in heterogeneous zircon populations from the precambrian basement of the Maryland Piedmont: Earth. Planet. Sci. Lett., v. 23, p. 238-248.

Gray, C. A., Cliff, R. A., and Goode, A. D. T., 1981, Neodymium-strontium isotopic evidence for extreme contamination in a layered basic intrusion, Earth Planet. Sci. Lett., v. 56, p. 189-198.

Hadley, J. B., 1949, Preliminary report on corundum deposits in the Buck Creek peridotite, Clay County, North Carolina: U.S. Geol. Survey Bull., v. 948E, 25 pp.

Hannah, J. L. and Futa, K., 1982, Nd, Sr and O isotope systematics in the Troodos Ophiolite, Cyprus [abs]: Abstract with Programs, Geol. Soc. Amer., p. 506.

Hanan, B. B., 1980, The petrology and geochemistry of the Baltimore Mafic Complex, Maryland: Ph.D. dissert., VA Polytechnic Inst. & State Univ., 218 pp.

Hanan, B. B., 1981, Chemical and isotopic variations related to microfractures in gabbros [abs]: EOS, v. 62, p. 435.

Harper, G. D., 1980, The Josephine ophiolite--remains of a late Jurassic marginal basin in northwestern California: Geology v. 8, p. 333-337.

Harper, G. D., and Saleeby, J. B., 1980, Zircon ages of the Josephine ophiolite and the Lower Coon Mountain pluton, western Jurassic belt, northwestern California [abs]: Geol. Soc. Am., Abstracts with Programs, v. 12, p. 109-110.

Hartley, M. E., 1973, Ultramafic and related rocks in the vicinity of Lake Chatuge: Georgia Geol. Survey. Bull., v. 85, 61 pp.

Hawkesworth, C. J., O'Nions, R. K., Pankhurst, R. J., Hamilton, P. J., and Evensen, N. M., 1977, A geochemical study of island-arc and back-arc tholeiites from the Scotia Sea: Earth Planet. Sci. Lett., v. 36, p. 253-262.

Hawkesworth, C. J., Norry, M. J., Roddick, J. C., and Vollmer, R., 1979a, $^{143}Nd/^{144}Nd$ and $^{87}Sr/^{86}Sr$ ratios from the Azores and their significance in LIL-element enriched mantle: Nature, v. 280, p. 28-31.

Hawkesworth, C. J., O'Nions, R. K., and Arculus, R. J., 1979b, Nd and Sr isotope geochemistry of island arc volanics, Grenada, Lesser Antilles: Earth Planet. Sci. Lett., v. 45, p. 237-248.

Hess, H. H., 1939, Island arcs, gravity anomalies and serpentine intrusions: Int. Geol. Cong. Moscow 1937, Report 17, v. 2, p. 263-283.

Hess, H. H., 1955, Serpentines, orogeny and epeirogeny: Geol. Soc. Am. Spec. Paper, v. 62, p. 391-408.

Hertz, N., 1951, Petrology of the Baltimore Gabbro, Maryland: Geol. Soc. Amer. Bull., v. 62, p. 979-1016.

Hickey, A. L., and Frey, F. A., 1982, Geochemical characteristics of boninite series volcanics: Implications for their source: Geochim. Cosmochim. Acta, v. 46, p. 2099-2115.

Høgdahl, O. T., Melson, S., and Bowen, V. T., 1968, Neutron activation analysis of lanthanide elements in seawater: Adv. Chem. Ser., v. 73, p. 308-325.

Hooker, P. J., Hamilton, P. J. and O'Nions, P. K., 1981, An estimate of the Nd isotopic composition of Iapetus seawater from ca. 490Ma metalliferous sediments: Earth Planet. Sci. Lett., v. 56, p. 180-188.

Hopson, C. A., 1964, The crystalline rocks of Howard and Montgomery Counties, in, The Geology of Howard and Montgomery Counties: Maryland: Geol. Survey, p. 27-215.

Hopson, C. A. and Frano, C. J., 1977, Igneous history of the Point Sal ophiolite, Southern California: in North American Ophiolites, Oregon Dept. of Geology and mineral industries, Bull. 95, p. 161-183.

Irvine, T. N., 1975, Olivine-pyroxene-plagioclase relations in the system Mg_2SiO_4-$CaAl_2Si_2O_8$-$KAlSi_3O_8$-SiO_2 and their bearing on the differentiation of stratiform intrusions: Carnegie Inst. Wash. Yearbook, p. 492-500.

Jacobsen, S. B., and Wasserburg, G. J., 1979, Nd and Sr isotopic study of the Bay of Islands Ophiolite Complex and the evolution of the source of midocean ridge basalts: J. Geophys. Res., v. 84, p. 7429-7445.

Jacobsen, S. B., and Wasserburg, G. J., 1981, Sm-Nd isotopic evolution of chondrites: Earth Planet. Sci. Lett., v. 50, p. 139-155.

Jahn, B -M., Bernard-Griffiths, J., Charlot, R., Cornichet, J., and Vidal, F., 1980, Nd and Sr isotopic compositions and REE abundances of Cretaceous MORB (Holes 417D and 418A, Legs 51, 52 and 53): Earth Planet. Sci. Lett., v. 48, p. 171-184.

James, D. E., 1982, A combined O, Sr, Nd and Pb isotopic and trace element study of crustal contamination in central Andean lavas: I. Local geochemical variations: Earth Plant. Sci. Lett., v. 57, p. 47-62.

Jones, L. M., Hartley, M. E., and Walker, R. L., 1973, Strontium isotope composition of Alpine-type ultramafic rocks in the Lake Chatuge District, Georgia-North Carolina: Cont. Min. Petr., v. 38, p. 321-327.

Kuroda, N., and Shiraki, K., 1975, Boninite and related rocks of Chichi-jima, Bonin Islands, Japan: Rep. Fac. Sci. Shizuoka Univ., v. 10, p. 145-155.

Laird, J. L., 1977, Phase equilibria in mafic schist and the polymetamorphic history of Vermont: Ph.D. dissert., California Institute of Technology, 445 pp.

Laird, J. L. and Albee, A. L., 1981, Pressure, temperature and time indicators in mafic schist: Their application to reconstructing the polymetamorphic history of Vermont: Amer. Jour. Sci., v. 281, p. 127-175.

Lapham, D. M., and Bassett, W. A., 1964, K-Ar dating of rocks and tectonic events in the piedmont of southeastern Pennsylvania: Geol. Soc. Amer. Bull., v. 75, p. 661-668.

Laurent, R., 1975, Occurrences and origin of the ophiolites of Southern Quebec, Northern Appalachians: Can. J. Earth Sci., v. 12, p. 443-455.

Laurent, R., 1977, Ophiolites from the Appalachians of Quebec in North American ophiolites: Oregon Dept. of Geology & Min. Industries Bull., v. 95, p. 25-40.

Malpas, J., 1977, Petrology and tectonic significance of Newfoundland ophiolites with examples from the Bay of Islands, in Appalachian Ophiolites: Oregon

Dept. of Geology and Min. Industries Bull., v. 95, p. 13-23.

McCulloch, M. T., and Wasserburg, G. J., 1978, Sm-Nd and Rb-Sr chronology of continental crust formation: Science, v. 260, p. 1003-1011.

McCulloch, M. T., Gregory, R. I., Wasserburg, G. J., and Taylor, H. P., 1981, Sm-Nd, Rb-Sr and $^{18}O/^{16}O$ isotopic systematics on an oceanic crustal section: Evidence from the Samail Ophiolite: J. Geophys. Res., v. 86, p. 2721-2735.

McCulloch, M. T., and Perfit, M. R., 1981, $^{143}Nd/^{144}Nd$, $^{87}Sr/^{84}Sr$ and trace element constraints on the petrogenesis of Aleution island arc magmas: Earth Planet. Sci. Lett., v. 56, p. 167-179.

McCulloch, M. T., Jacques, A. L., Nelson, D. R., and Lewis, J. D., 1983, Nd and Sr isotopes in kimberlites and lamproites from Western Australia: an enriched origin: Nature, v. 302, p. 400-403.

McElhaney, M. S., and McSween, H. Y., 1983, Petrology of the Chunky Gal Mountain mafic-ultramafic complex, North Carolina: Geol. Soc. Amer. Bull., in press.

Menzies, M., and Murthy, V. R., 1980, Nd and Sr isotope geochemistry of hydrous mantle nodules and their host alkali basalts: Implications for local heterogeneities in metasomatically veined mantle: Earth Planet. Sci. Lett., v. 46, p. 323-334.

Miller, R., 1953, The Webster-Addie ultramafic ring, Jackson County North Carolina and secondary alteration of its chromite: Amer. Mineral., v. 38, p. 1134-1147.

Morgan, B. A., 1977, The Baltimore Complex, Maryland, Pennsylvania and Virginia, in Appalachian Ophiolites, Oregon Dept. of Geol. and Min. Industries Bull., v. 95, p. 41-49.

Nohda, S., and Wasserburg, G. J., 1981, Nd and Sr isotopic study of volcanic rocks from Japan: Earth Planet. Sci. Lett., v. 52, p. 264-276.

Noiret, G., Montigny, R., and Allegre, C. J., 1981, Is the Vourinos Complex an island arc ophiolite?: Earth Planet. Sci. Lett., v. 56, p. 375-386.

O'Nions, R. K., Hamilton, P. J. and Evensen, N. M., 1977, Variations in $^{143}Nd/^{144}Nd$ and $^{87}Sr/^{86}Sr$ ratios in oceanic basalts: Earth Planet. Sci. Lett., v. 34, p. 13-22.

O'Nions, R. K., Carter, S. R., Cohen, R. S., Evensen, N. M., and Hamilton, P. J., 1978, Pb, Nd and Sr isotopes in oceanic ferromanganese deposits and ocean floor basalts: Nature, v. 273, p. 435-438.

Papanastassiou, D. A., and Wasserburg, G. J., 1973, Rb-Sr ages and initial strontium in basalts from Apollo 15: Earth Planet. Sci. Lett., v. 17, p. 324-337.

Papanastassiou, D. A., DePaolo, D. J., and Wasserburg, G. J., 1977, Rb-Sr and Sm-Nd chronology and genealogy of basalts from the Sea of Tranquility: Proc. Lunar Sci. Conf. 8th, p. 1639-1672.

Peterman, Z. E., Hedge, C. E., and Tourtelot, H. A., 1970, Isotopic composition of strontium in seawater throughout Phenerozoic time: Geochim. Cosmochim. Acta, v. 34, p. 105-120.

Pratt, J. H., and Lewis, J. V., 1905, Corundum and the peridotites of western North Carolina: North Carolina Geol. Survey Bull., v. 1, 464 p.

Richard, P., Shimizu, N., and Allegre, C. J., 1976, $^{143}Nd/^{144}Nd$, a natural tracer: An application to oceanic basalts: Earth Planet. Sci. Lett., v. 31, p. 267-278.

Richard, P., and Allegre, C. J., 1980, Neodymium and strontium isotopic study of ophiolite and orogenic lherzolite petrogenesis: Earth Planet. Sci. Lett., v. 47, p. 65-74.

Rocci, G., Ohnenstetter, D. and Ohnenstetter, M., 1975, La dualité des ophiolites tethysiennes: Petrologie, v. 1, p. 172-174.

Sailor, R. V., and Kuntz, M. A., 1973, Petrofabric and textural evidence for the syntectonic recrystallization of the Buck Creek dunite, N. Carolina [abs]:

Geol. Soc. Amer., Abstract with Programs, v. 5, p. 791-792.

Saleeby, J. B., 1982, Polygenetic ophiolite belt of the California Sierra Nevada: geochronological and tectonostratigraphic development: J. Geophys. Res., v. 87, p. 1803-1824.

St. Julien, P., 1972, Appalachian structure and stratigraphy: Quebec Int. Geol. Cong. 24th Montreal, 1972 Field Excursion A56-C56 Guidebook, 35 p.

Shiraki, K., and Kuroda, N., 1977, The boninite revisited: J. Geol. Soc. Japan, v. 86, p. 34-50.

Southwick, P. H., 1970, Structure and petrology of the Harford County part of the Baltimore State line gabbro: Peridotite Complex: in G. W. Fischer et al., eds., Studies of Appalachian Geology: Central and Southern, Wiley-Interscience, New York, 460 pp.

Stueber, A. M., 1969, Abundances of K, Rb, Sr and Sr isotopes in ultramafic rocks and minerals from western North Carolina: Geochim. Cosmochim. Acta, v. 33, p. 543-553.

Tilton, G. R., Doe, B. R., and Hopson, C. A., 1970, Zircon age measurements in the Maryland Piedmont, with special reference to Baltimore Gneiss problems, in Fisher, G. W. et al., eds., Studies of Appalachian geology: Central and Southern: Wiley-Interscience, New York, 460 pp.

Tilton, G. R., Wetherill, G. W., Davis, G. L., and Hopson, C. A., 1958, Ages of minerals from the Baltimore gneiss, Maryland: Geol. Soc. Am. Bull., v. 79, p. 757-762.

Upadhyay, J. D., Dewey, J. F., and Neale, E. R. W., 1971, The Bett's Cove ophiolite complex, Newfoundland: Appalachian oceanic crust and mantle, Geol. Assoc. Canada Proc., v. 24, p. 27-34.

Wasserburg, G. J., Jacobsen, S. B., DePaolo, D. J., McCulloch, M. T., and Wen, T., 1981, Precise determination of Sm/Nd ratios: Sm and Nd isotopic

abundances in standard solutions: Geochim. Cosmochim. Acta, v. 45, p. 2311-2323.

Wasserburg, G. J., Pettijohn, F. J., and Lipson, J., 1957, Ar^{40}/K^{40} ages of micas and feldspars from the Glenarm Series near Baltimore, Maryland: Science, v. 126, n. 3269, p. 355-357.

Wetherill, G. W., Davis, G. L., and Lee-Hu, C., 1968, Rb-Sr measurements on whole rocks and separated minerals from the Baltimore Gneiss, Maryland: Geol. Soc. Amer. Bull., v. 79, p. 757-762.

White, W. M., and Hofmann, A. W., 1982, Sr and Nd isotope geochemistry of oceanic basalts and mantle evolution: Nature, v. 296, p. 821-825.

Whitford, D. J., 1975, Strontium isotopic studies of the volcanic rocks of the Sunda arc, Indonesia and their petrogenetic implications: Geochim. Cosmochim. Acta, v. 39, p. 1287-1302.

Whitford, D. J., Compston, W., Nichols, I. A., and Abbott, M. J., 1977, Geochemistry and late Cenozoic lavas from eastern Indonesia: Role of subducted sediments in petrogenesis: Geology, v. 5, p. 571-575.

Whitford, D. J., White, W. M., Jezek, P. A., and Nichols, I. A., 1979, Nd isotopic composition of recent andesites from Indonesia: Carnegie Inst. Washing. Yearbook, 304-307.

Williams, H., 1971, Mafic/ultramafic complexes in western Newfoundland, the Appalachians and the evidence for the transportation: A review and interim report: Geol. Assoc. Canada Proc., v. 24, no. 1, p. 9-25.

Williams, H., and Talkington R. W., 1977, Distribution and tectonic setting of ophiolites and ophiolitic melanges in the Appalachian orogen: in Appalachian Ophiolites, Oregon Dept. of Geology and Min. Industries Bull, v. 95, p. 1-11.

Williamson, J. M., 1968, Least squares fitting of a straight line: Can. J. Phys., v. 46, p. 1845-1847.

Zindler, A., Hart, S. R., Frey, F. A., and Jakobsson, S. P., 1979, Nd and Sr isotope ratios and rare earth element abundances in Reykjanes Peninsula basalts: Evidence for mantle heterogeneity beneath Iceland: Earth Planet. Sci. Lett., v. 45, p. 249-262.

Zindler, A., Hart, S. R., and Brooks, C., 1981, The Shabogama Intrusive Suite Labrador: Sr and Nd isotopic evidence for contaminated mafic magmas in the Protozoic: Earth Planet. Sci. Letter., v. 54, p. 217-235.

Table 1. Rb-Sr and Sm-Nd isotopic results.

Sample	$\frac{^{143}Nd}{^{144}Nd}$*	ppm Nd	$\frac{^{147}Sm}{^{144}Nd}$‡	$f^{Sm/Nd}$	$\varepsilon_{Nd}(T)^a$	$\frac{^{87}Sr}{^{86}Sr}$*	ppm Sr	$\frac{^{87}Rb}{^{86}Sr}$+	$f^{Rb/Sr}$	$\varepsilon_{Sr}(T)^a$
Baltimore Mafic Complex										
Md-32 Norite	0.51132 ±2	16.1	0.131	-0.334	-6.2 ±0.5	0.71209 ±4	302.9	0.0104#	-0.874	+114.9 ±0.6
	0.51131 ±3	16.3	0.130	-0.337	-6.4 ±0.5	0.71214 ±4	302.9	--	--	--
Md-32 Plagioclase	0.51120 ±2	6.7	0.093	-0.526	--	0.71254 ±4	494.4	.0042#	0.949	
Md-32 Orthopyroxene	0.51140 ±2	4.0	0.152	-0.228	--	0.71272 ±4	8.55	.1161#	0.404	--
Md-32 Apatite	0.51135 ±2	796.9	0.135	-0.314	--	0.71214 ±3	205.6	.0100#	0.879	--
Md-3 Feldspathic websterite	0.51183 ±2	0.68	0.227	0.516	-2.2 ±0.4	0.70756 ±2	93.6	.0089	-0.893	+50.8 ±0.3
Md-3 Plagioclase	0.51130 ±2	0.12	0.068	-0.656	--	--	--	--	--	--
Md-3 Orthopyroxene	0.51188 ±2	0.21	0.253	0.285	--	--	--	--	--	--
Md-3 Clinopyroxene	0.51186 ±3	1.86	0.253	0.285	--	--	--	--	--	--

Table 1. (Continued).

Sample	$\frac{^{143}Nd}{^{144}Nd}$*	ppm Nd	$\frac{^{147}Sm}{^{144}Nd}$‡	$f^{Sm/Nd}$	$\varepsilon_{Nd}(T)^a$	$\frac{^{87}Sr}{^{86}Sr}$*	ppm Sr	$\frac{^{87}Rb}{^{86}Sr}$+	$f^{Rb/Sr}$	$\varepsilon_{Sr}(T)^a$
Md-44 Gabbro	0.51152 ±2	1.16	0.190	-0.035	-6.0 ±0.4	0.71052 ±8	131.0	0.0125	-0.849	+92.5 ±1.1
Md-44 Pyroxene	0.51160 ±2	1.55	0.220	0.119	--	--	--	--	--	--
Md-44 Plagioclase	0.51114 ±2	0.38	0.076	-0.612	--	--	--	--	--	--
Md-40 Metagabbro	0.51152 ±3	5.36	0.168	-0.143	-4.5 ±0.6	0.70970 ±3	85.1	0.0133	-0.839	+80.7 ±0.4
Md-30 Gabbro	0.51147 ±1	2.48	0.168	-0.144 ±0.3	-5.5 ±0.3	0.70950 ±3	180.0	0.0146	-0.823	+77.7 ±0.4
Md-15 Orthopyroxenite	0.51171 ±2	0.51	0.250	0.273	-6.1 ±0.4	0.71047 ±3	25.8	0.0193	-0.767	+91.0 ±0.4
Md-39 Hornblende Gabbro	0.51156 ±3	4.84	0.159	-0.194	-3.1 ±0.7	0.70916 ±4	142.5	0.0230#	-0.721	+72.1 ±0.6
Thetford Mines Samples										
Qe-18 Lower Pillow Basalt	0.51194 ±2	0.86	0.178	-0.097	+3.0 ±0.4	0.70763 ±3	53.5	0.1009	-0.220	+42.5 ±0.4
Qe-13A #3 Lower Pillow Basalt	0.51181 ±3	1.94	0.178	-0.097	+0.4 ±0.6	0.70761 ±4	72.3	0.0101	-0.878	+51.5 ±0.6

Table 1. (Continued).

Sample	$\frac{^{143}Nd}{^{144}Nd}$*	ppm Nd	$\frac{^{147}Sm}{^{144}Nd}$‡	$f^{Sm/Nd}$	$\varepsilon_{Nd}(T)^a$	$\frac{^{87}Sr}{^{86}Sr}$*	ppm Sr	$\frac{^{87}Rb}{^{86}Sr}$+	$f^{Rb/Sr}$	$\varepsilon_{Sr}(T)^a$
Qe-40 Upper Pillow Basalt	0.51197 ±2	1.05	0.201	0.022	+2.2 ±0.4					
Qe-8B Metadiabase	0.51209 ±2	1.43	0.205	0.044	+4.7 ±0.5	0.71287 ±4	98.6	0.3957	3.784	+87.2 ±0.6
Qe-12A Metagabbro	0.51205 ±1	0.96	0.211	0.072	+3.2 ±0.3	0.71202 ±3	94.5	0.0106	-0.872	+114.0 ±0.4
Qe-30A Metagabbro	0.51172 ±2	0.11	.1813	-0.078	-1.5 ±0.4	0.70412 ±4	88.4	0.0039	-0.953	+2.6 ±0.6
Qe-24 Clinopyroxenite	0.51242 ±2	0.11	0.326	0.655	+2.9 ±0.4	0.70936 ±5	6.58	0.2457	1.971	+52.6 ±0.7
Vermont Sample										
VJL-360C Hazens Notch Amphibolite	0.51232 ±3	6.9	0.217	0.101	+8.0 ±0.5	0.70412 ±3	63.1	0.1509#	0.824	-12.3 ±0.4
North Carolina Samples										
CG 12-1 Chunky Gal Amphibolite	0.51241 ±2	3.42	0.248	0.259	+7.7 ±0.4	0.70543 ±6	95.2	0.0143#	-0.827	+20.1 ±0.8

Table 1. (Continued).

Sample	$\frac{^{143}Nd}{^{144}Nd}$*	ppm Nd	$\frac{^{147}Sm}{^{144}Nd}$‡	$f^{Sm/Nd}$	$\varepsilon_{Nd}(T)^a$	$\frac{^{87}Sr}{^{86}Sr}$*	ppm Sr	$\frac{^{87}Rb}{^{86}Sr}$+	$f^{Rb/Sr}$	$\varepsilon_{Sr}(T)^a$
CG 2-18 Chunky Gal Amphibolite	0.51210 ±3	12.7	0.182	-0.073	+6.0 ±0.5	0.70680 ±5	340.4	0.0290	-0.649	+38.1 ±0.7
C-1 Lake Chatuge Amphibolite	0.51220 ±2	2.09	0.226	0.137	+5.1 ±0.5	0.70320 ±4	162.0	0.0258#	-0.688	-12.7 ±0.6
XTC-127 Webster-Addie websterite	0.51190 ±2	0.57	0.231	0.176	-1.1 ±0.4	0.70691 ±4	8.13	0.1323#	0.599	+29.2 ±0.6
XTC-127 leached residue	0.51207 ±1	0.31	0.278	0.414	-0.9 ±0.3	0.70654 ±4	7.30	--	--	--
Baltimore Gneiss, Wissahickon Schist Samples										
Md-7 Biotite Gneiss	0.51119 ±2	24.6	0.117	-0.407	-7.8† ±0.4	0.72947 ±3	199.0	1.363#	15.48	+227.4† ±0.4
Md-11 Augen Gneiss	0.51117 ±2	69.8	0.115	-0.415	-8.2† ±0.4	0.75406 ±6	128.8	3.225#	37.99	+393.2† ±0.9
RL 80-7 Wissahickon schist	0.51120 ±2	22.4	0.102	-0.484	-6.6† ±0.3	0.71773 ±3	123.6	0.6253#	6.561	+134.2† ±0.4

Table 1. (Continued).

Sample	$\frac{^{143}Nd}{^{144}Nd}$*	ppm Nd	$\frac{^{147}Sm}{^{144}Nd}$‡	$f^{Sm/Nd}$	$\varepsilon_{Nd}(T)^a$	$\frac{^{87}Sr}{^{86}Sr}$*	ppm Sr	$\frac{^{87}Rb}{^{86}Sr}$+	$f^{Rb/Sr}$	$\varepsilon_{Sr}(T)^a$
California Ophiolites[b]										
P-59	0.51229	1.25	0.223	0.134	+8.2	0.70333	298.7	0.0061	-0.926	-14.2
Pt. Sal Gabbro	±4				±0.9	±4				±0.6
JP-042	0.51238	0.74	0.275	0.396	+8.8	0.70349	88.4	0.0686	-0.171	-13.9
Josephine Gabbro	±2				±0.4	±3				±0.4
Y-13b	0.51238	1.14	0.257	0.305	+8.4	0.70342	214.7	0.0470#	-0.431	-14.2
Josephine Gabbro	±2				±0.4	±3				±0.4
Ca-10	0.51254	1.57	0.243	0.237	+12.4	0.70232	131.6	0.0061	-0.926	-27.9
Kings R. Gabbro	±3				±0.5	±3				±0.4

*Errors are 2σ of the mean; $^{143}Nd/^{144}Nd$ normalized to $^{146}Nd/^{142}Nd = 0.636151$; $^{87}Sr/^{86}Sr$ normalized to $^{86}Sr/^{88}Sr = 0.1194$.

‡Uncertainty = 0.2%

+Uncertainty = 1.0%. Rb measured on aliquot only--except as noted.

#Uncertainty = 0.4%. Rb measured on separated sample.

†Initial ε values calculated for 490 My.

[a]Errors on initial ε values reflect only the analytical uncertainty and do not include errors due to age estimates.

[b]Initial ε values calculated using the ages: Pt. Sal = 160 My; Josephine Ophiolite = 157 My; Kings R. Ophiolite = 200 My.

Figure Captions

Fig. 1. Histogram of $\varepsilon_{Nd}(T)$ values comparing mid-ocean ridge basalts, (MORB), oceanic island arcs and ocean island basalts [Carlson et al., 1978; Cohen et al., 1980; DePaolo, 1978; DePaolo and Wasserburg, 1976b, 1977; Dosso and Murthy, 1980; Hawkesworth et al., 1977; 1979a,b; Jahn et al., 1980; McCulloch and Perfit, 1981; Menzies and Murthy, 1980; O'Nions et al., 1977; 1978; Richard et al., 1976; Zindler et al., 1979] and ophiolites (key to ophiolites: Tr - Troodos, V - Vourinos, BC - Bett's Cove, BOI - Bay of Islands, S - Samail, PS - Pt. Sal, Jo - Josephine, KR - Kings-Kaweah, U - Kempersai, Urals, To - Toba, Japan) [Chen and Shaw, 1982; Coish et al., 1982; Edwards and Wasserburg, 1983; Hannah and Futa, 1982; Jacobsen and Wasserburg, 1979; McCulloch et al., 1981; Richard and Allegre, 1980].

Fig. 2. ε_{Nd} vs. ε_{Sr} diagram showing contamination trends and possible endmembers for mixing relationships. Isotopic composition of Cambro-Ordovician seawater from Peterman et al. [1970], Burke et al. [1982] and Hooker et al. [1981].

Fig. 3. a. Sm-Nd evolution diagram showing internal isochron relationship for Baltimore Mafic Complex feldspathic websterite sample Md-3.

b. As above, two-pyroxene gabbro sample Md-44.

c. As above, norite sample Md-32.

d. Rb-Sr diagram showing mineral data for Baltimore Mafic Complex norite sample Md-32. Note the lack of an isochron relationship in contrast to the Sm-Nd data.

Fig. 4. a. Sm-Nd evolution diagram with data for whole rock samples of the Baltimore Mafic Complex. Reference isochrons are drawn for 490 My and $\varepsilon_{Nd}(T) = -3$ and -6. Note the implied range in $\varepsilon_{Nd}(T)$ and general correlation about the 490 My isochron.

b. Rb-Sr evolution diagram with the data for whole rock samples of the Baltimore Mafic Complex. Reference isochron is drawn for 490 My and initial $\varepsilon_{Sr}(T) = +75$. Note the implied range in $\varepsilon_{Sr}(T)$ and limited range of Rb/Sr ratios.

Fig. 5. a. Sm-Nd evolution diagram with data for whole rock samples of the Thetford Mines Complex. Reference isochrons are drawn for 500 My and $\varepsilon_{Sr}(T) = +4$ and 0. Note the implied range in $\varepsilon_{Nd}(T)$.

b. Rb-Sr evolution diagram with data for whole rock samples of the Thetford Mines Complex. Reference isochron is drawn for 500 My and $\varepsilon_{Sr}(T) = 0$. Note the implied range of $\varepsilon_{Sr}(T)$ and wide variation in Rb/Sr ratios.

Fig. 6. $\varepsilon_{Nd}(T)$ vs. $\varepsilon_{Sr}(T)$ diagram with data for Vermont, North Carolina Thetford, Baltimore and Bay of Islands (BOI) [Jacobsen and Wasserburg, 1979]. Vermont, North Carolina and Bay of Islands samples have the isotopic signature of oceanic crust. The Baltimore (BMC) samples fall on a trend suggesting contamination with continental crust. The Thetford Mines samples (TMC) do not show any obvious trend. Compare with Fig. 2.

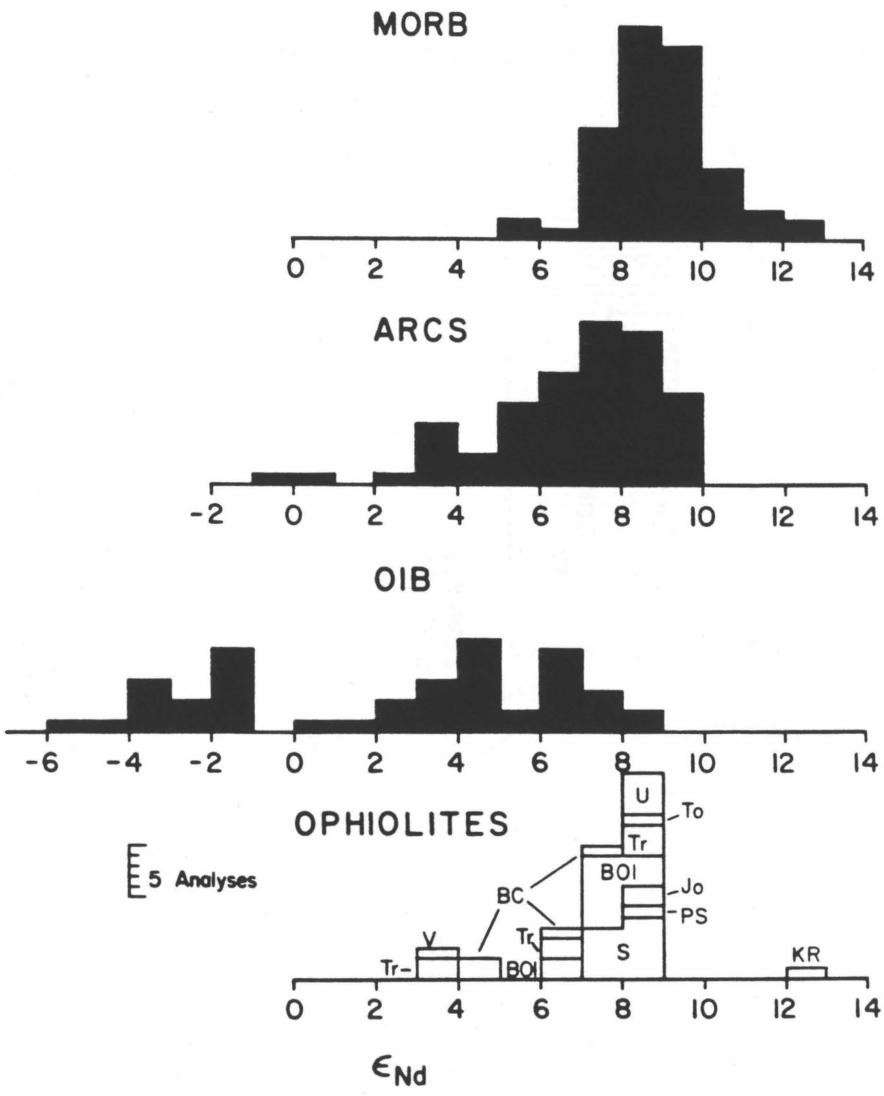
MORB
0 2 4 6 8 10 12 14
ARCS
-2 0 2 4 6 8 10 12 14
OIB
-6 -4 -2 0 2 4 6 8 10 12 14
OPHIOLITES
5 Analyses
U
To
Tr
BOI
Jo
PS
BC
V
Tr
S
Tr-
BOI
KR
0 2 4 6 8 10 12 14
ϵ_{Nd}

Figure 1.

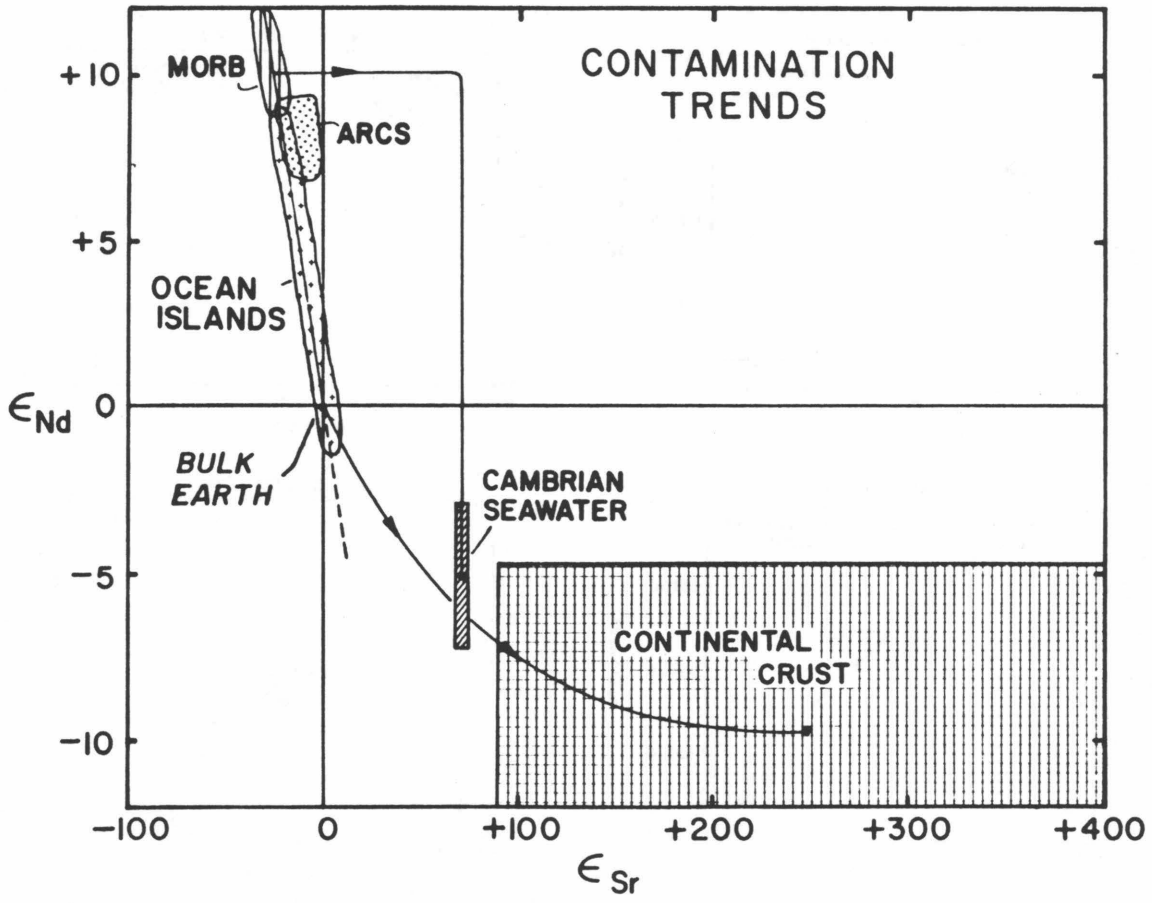
CONTAMINATION
TRENDS
MORB
ARCS
OCEAN
ISLANDS
BULK
EARTH
CAMBRIAN
SEAWATER
CONTINENTAL
CRUST
+10
+5
0
−5
−10
ϵ_{Nd}
−100
0
+100
+200
+300
+400
ϵ_{Sr}

Figure 2.

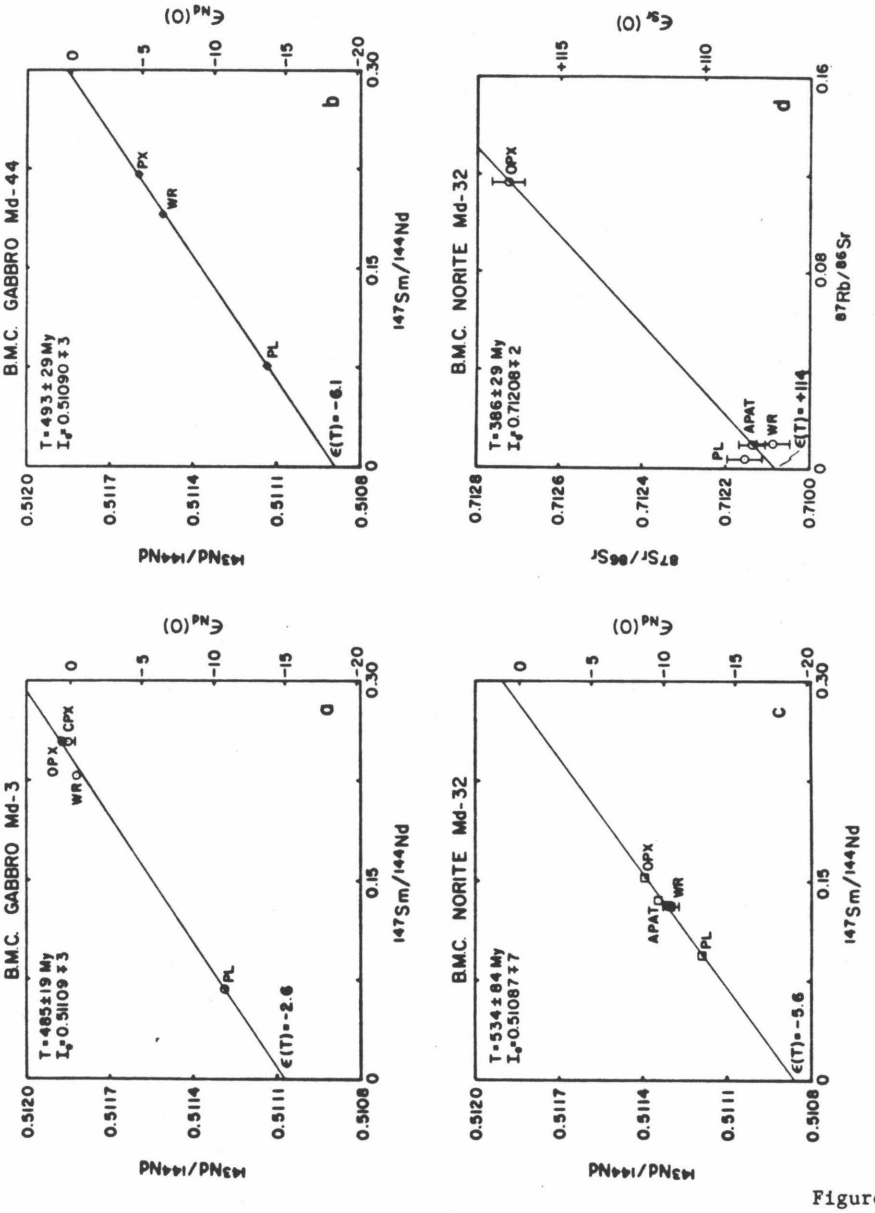
B.M.C. GABBRO Md-44
T = 493 ± 29 My
I_o 0.51090 ± 3
ε(T) = -8.1
PX
WR
PL
b
B.M.C. NORITE Md-32
T = 386 ± 29 My
I_o 0.71208 ± 2
ε(T) = +114
OPX
APAT
WR
PL
d
B.M.C. GABBRO Md-3
T = 485 ± 19 My
I_o 0.51109 ± 3
ε(T) = -2.6
OPX
CPX
WR
PL
a
B.M.C. NORITE Md-32
T = 534 ± 84 My
I_o 0.51087 ± 7
ε(T) = -5.6
OPX
APAT
WR
PL
c
$\varepsilon_{Nd}(0)$
$\varepsilon_{Sr}(0)$
$^{143}Nd/^{144}Nd$
$^{87}Sr/^{86}Sr$
$^{147}Sm/^{144}Nd$
$^{87}Rb/^{86}Sr$

Figure 3.

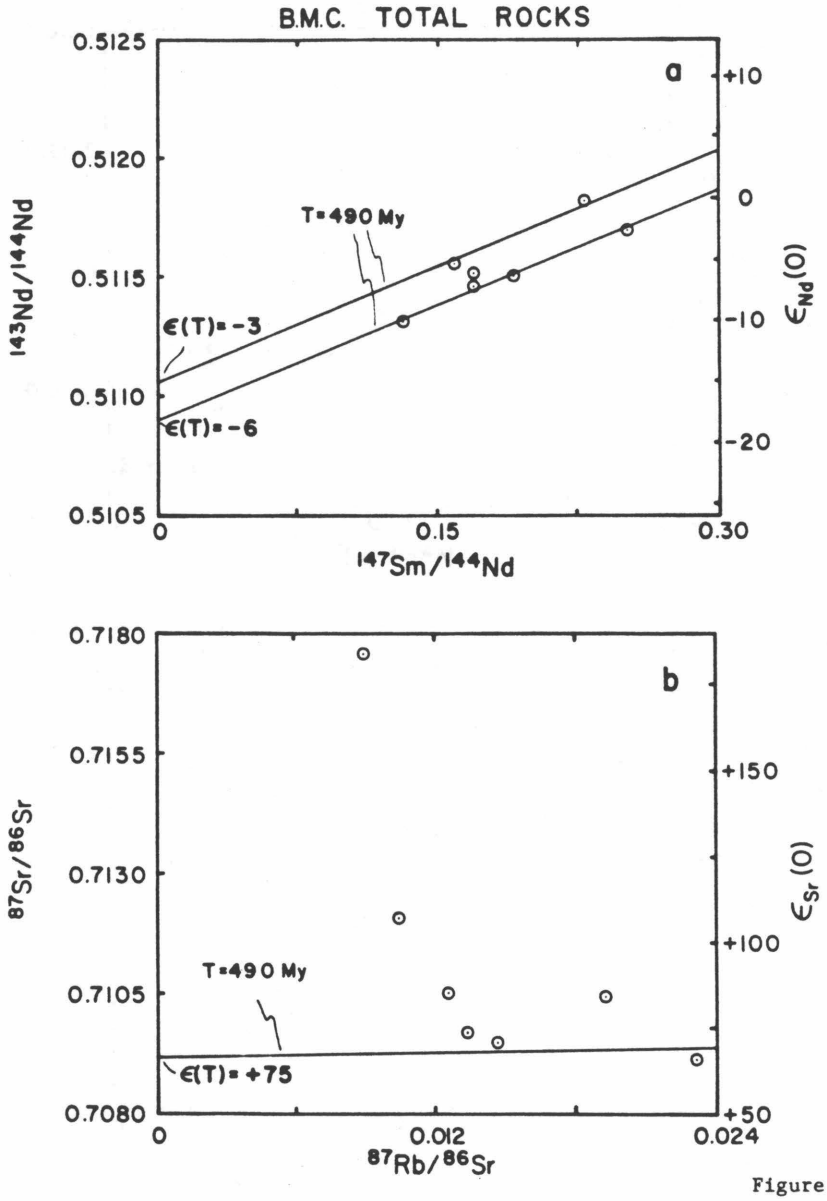
B.M.C. TOTAL ROCKS
a
0.5125
0.5120
0.5115
0.5110
0.5105
143Nd/144Nd
T=490 My
ε(T)=-3
ε(T)=-6
0
0.15
0.30
147Sm/144Nd
+10
0
-10
-20
εNd(0)
b
0.7180
0.7155
0.7130
0.7105
0.7080
87Sr/86Sr
T=490 My
ε(T)=+75
0
0.012
0.024
87Rb/86Sr
+150
+100
+50
εSr(0)

Figure 4.

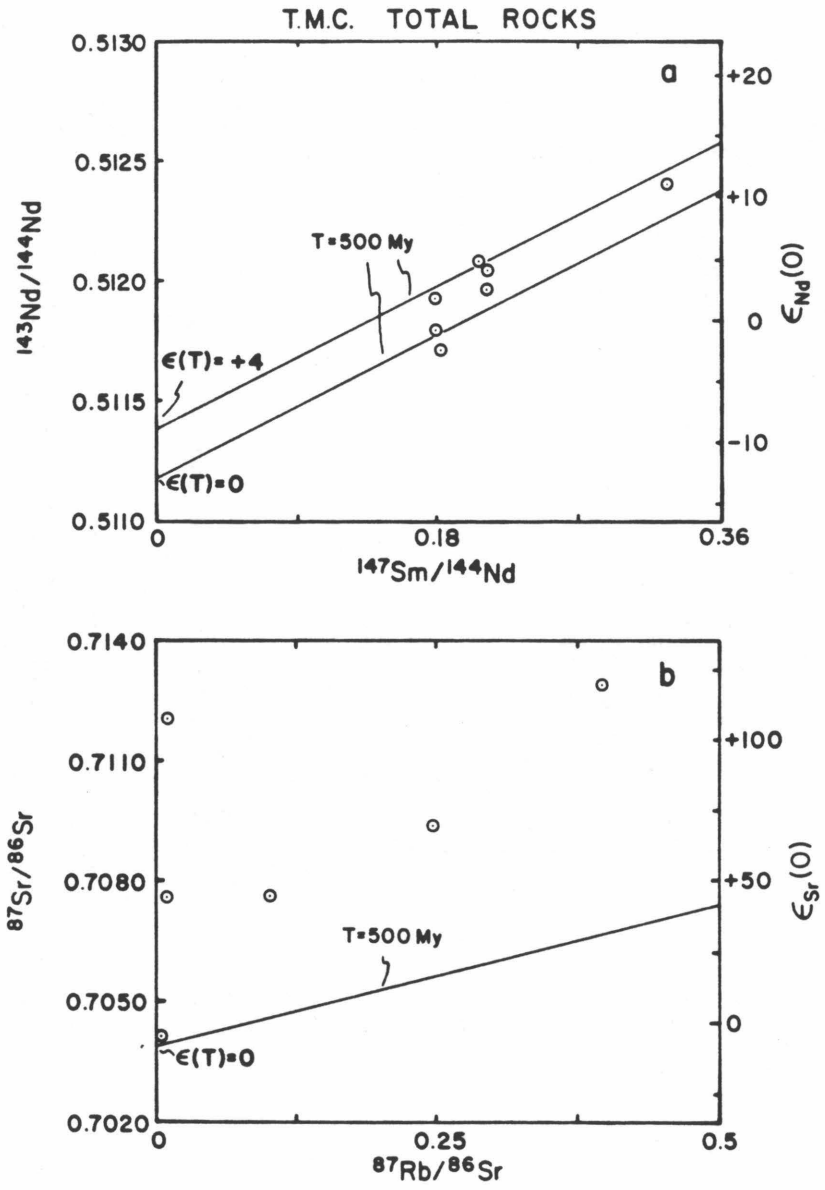
T.M.C. TOTAL ROCKS
a
0.5130
0.5125
0.5120
0.5115
0.5110
$^{143}Nd/^{144}Nd$
T=500 My
ε(T)= +4
ε(T)=0
0
0.18
0.36
$^{147}Sm/^{144}Nd$
+20
+10
0
-10
$\epsilon_{Nd}(0)$
b
0.7140
0.7110
0.7080
0.7050
0.7020
$^{87}Sr/^{86}Sr$
T=500 My
ε(T)=0
0
0.25
0.5
$^{87}Rb/^{86}Sr$
+100
+50
0
$\epsilon_{Sr}(0)$

Figure 5.

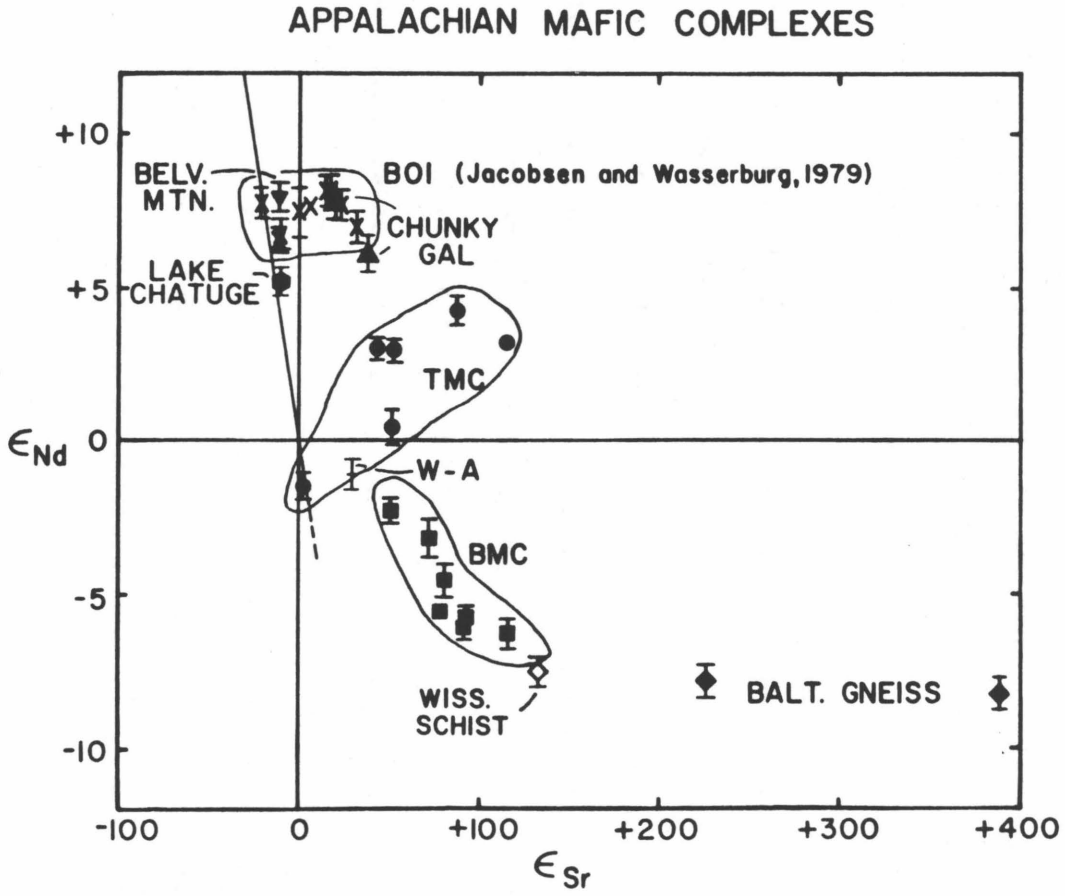
APPALACHIAN MAFIC COMPLEXES
+10
+5
0
-5
-10
ϵ_{Nd}
-100
0
+100
+200
+300
+400
ϵ_{Sr}
BELV. MTN.
BOI (Jacobsen and Wasserburg, 1979)
CHUNKY GAL
LAKE CHATUGE
TMC
W-A
BMC
WISS. SCHIST
BALT. GNEISS

Figure 6.

Appendix III

Procedures Used for Analysis of Phosphates and Carbonates

AIII.1 Carbonates

Because of the low concentration of REE found in the modern carbonates studied, a procedure was devised to extract the REE from a relatively large quantity of material. This procedure is a modification of the Fe-hydroxide co-precipitation technique used extensively for seawater analysis [Goldberg et. al., 1963].

Samples were first cleaned of adhering material in several distilled water rinses in an ultrasonic cleaner. The surface of each sample was then etched by brief reaction with ~ 0.05M HCl to remove possible surface contamination, followed by a final ultrasonic rinse in distilled water. The samples were then dried and weighed. Sample weights varied from ~ 0.5 to 35.0 g. Dissolution was carried out by addition of 2.5M HCl over a period of 1-2 days to a teflon beaker initially containing the sample and distilled water to cover. The slow dissolution was necessary to avoid excessively vigorous reaction of the carbonate with the acid, leading to overflow from the beaker. The solution was then heated to dryness. At this point, the organic material present was usually digested by the addition of several ml. of aqua regia and the solution dried down. The dry residue was then dissolved in ~ 1.5M HCl and an aliquot corresponding to ~ 0.5g. of sample taken. This aliquot was spiked for Sm and Nd concentration measurements. The spiked solution was dried down once more to equilibrate the spike with the sample. The aliquot was then dissolved in 0.5M HCl. To this solution, ~ 2-3 mg. of Fe as $FeCl_3$ solution were added. The Fe was

then precipitated as hydroxides by the addition of a solution of ammonia produced by bubbling NH_3 gas through distilled water. The Fe-hydroxides quantitatively scavenge the REE from solution. The precipitate was allowed to settle overnight or longer and as much of the supernatant as possible poured off. The solution and precipitate were then centrifuged and the remaining supernatant pipetted off. The precipitate was rinsed with distilled water to remove NH_4Cl and again centrifuged. The Fe precipitate was finally dissolved in ~ 0.25 ml. of 1.5M HCl. This solution was centrifuged and the supernatant loaded on a 2 cm. x 0.4 cm. column of AG 50W-8X, 100-200 mesh resin. The sides of the column were rinsed with 2-3 drops of 1.5M HCl and the Fe eluted with 2.5 ml. of 2.5M HCl. The REE were then eluted with 3.5 ml. of 4.0M HCl. This eluant was collected, dried down and loaded onto a flat Re filament for mass spectrometry. The yield for this procedure is > 95% with a blank of < 8 pg. Nd.

For the measurements of isotopic composition, the remaining sample solution was spiked using the aliquot concentration data as a guide so that both isotopic composition and concentration could be measured on the same aliquot. As above, ~ 3 mg. of Fe were added to the solution and precipitated with ammonia solution and the precipitate cleaned as described above. After separating the REE from the Fe using the first ion exchange column, Sm and Nd were separated from the other REE using a second column as described by DePaolo [1978]. Yield for this procedure is > 85% with a blank of < 35 pg. Nd.

AIII.2 Modern phosphates

The samples of modern biogenic phosphate were cleaned, dissolved, and spiked in the same way as the modern carbonates. Unfortunately, the same

technique of Fe-hydroxide precipitation could not be used to concentrate the REE from the phosphate solution. Upon addition of ammonia solution to the acid sample solution, a large amount of white precipitate, probably hydrous Fe and Ca phosphates, forms at a lower pH than that at which Fe-hydroxides precipitate. The procedure followed was to load ~ 0.5 g. of sample dissolved in ~ 3 ml. of 1.5M HCl on a 17 cm. column of AG50W-8X, 100-200 mesh resin. The walls of the column were rinsed with another 2 ml. of 1.5M HCl, followed by 90 ml. of 2.5M HCl then 15 ml. of 4.0M HCl. The REE were eluted with an additional 35 ml. of 4.0M HCl. This solution was dried down and loaded on a flat Re filament for mass spectrometry. Yield for this procedure is > 90% with a blank of < 30 pg. Nd. This procedure is not entirely satisfactory; considerable amounts of organic material are left in the REE cut. The NdO^+ beam in the mass spectrometer is somewhat unstable even for an unseparated sample and it is exceedingly difficult to obtain a good Sm^+ or SmO^+ beam.

AIII.3 Ancient phosphates

These samples, either as chips of phosphorite rock or conodonts were cleaned in distilled water in an ultrasonic cleaner, were weighed and dissolved in ~ 1.0M HCl. The solution was separated from any insoluble residue by centrifuging. The insoluble residue was repeatedly rinsed and centrifuged in 0.1M HCl. These rinses were added to the sample solution. The residue was then washed into a clean pre-weighed teflon beaker, dried, weighed and stored for possible future use. An aliquot of the sample solution was then taken and spiked for Rb, Sr, Sm, and Nd concentration measurements. These concentrations were then used as a guide to spike a second aliquot for both concentration and isotopic composition

measurements. The chemical and mass spectrometric procedures followed those given by Eugster et. al. [1970], Papanastassiou and Wasserburg [1973], Papanastassiou et. al. [1977], and DePaolo [1978]. When aliquots taken for isotopic composition measurements contained more than ~ 4 mg. sample, it was often necessary to pass the Sr cut through the first cation exchange column a second time in order to obtain a clean separation of Ca from Sr. It is obvious when this is necessary as the $CaCl_2$ in the cut is quite hygroscopic and a small droplet of water quickly accumulates in the spot in the beaker where the sample dried down. Poor separation of Ca from Sr results in unsatisfactory Sr runs in the mass spectrometer.

All reported concentrations refer to the weight of the soluble portion of the sample only (i.e. bulk sample weight minus the weight of the insoluble residue). Blanks for the chemical procedure are < 45 pg. Nd and < 250 pg. Sr and are negligible. Yields are > 80%.

APPENDIX IV

Localities and Sources of Phosphate Samples

Sample #	Description	Locality	Source	Reference
N-33-2	Land pebble phosphorite	Brewster, Fla.	CIT collection	Altschuler et al., 1967
N-33-1	Bedded sandy phosphorite	Gafsa, Tunisia	CIT collection	
Mor-15	Pelletal phosphorite	Oulad-Abdaun Basin Morocco, Composite of Bed #3	Z. S. Altschuler	Altschuler, 1980
Ph-03	Coprolitic phosphate nodules in limestone	Magdesh Ramon, Negev, Israel	H. A. Lowenstam	
N-33-2	Oölitic phosphorite	Phosphoria Fm. Cokeville, Wy.	CIT collection	Altschuler et al., 1967 Altschuler, 1980
NBS-56-b	Weathered phosphorite	Tennessee "Brown Rock"	CIT collection	
Ph-09	Siliceous pelletal-oölitic phosphorite. Slightly recrystallized	Hazara, Pakistan	IFDC†	Cook and Shergold, 1979
Ph-12	Dolomitic phosphorite. Slightly recrystallized	Guizhou, China	IFDC	British Sulphur Corp., 1971 Cook and Shergold, 1979
Ph-05	Siliceous phosphorite	Parc, W. Niger	IFDC	Affaton et al., 1980 Trompette et al., 1980
Ph-08	Interbedded phosphate/ sand-shale basin deposits.	Kodjari, U. Volta	IFDC	"

Sample #	Description	Locality	Source	References
Ph-04	Siliceous, hematitic phosphorite. Recrystallized.	Rum Jungle, Australia	IFDC	British Sulphur Corp., 1971 Cook and Shergold, 1979
JWC-35	Conodonts	Madison Ls. (Cottonwood Cyn. Mbr.) Bighorn Co., Wy.	J. Wright-Clark	Wright-Clark et al., ms.
JWC-5-1	"	Holt's Summit Ss. Missouri	"	"
JWC-37	"	Lodgepole Ls. East Crawford Mtns. Lincoln Co., Wy.	"	"
JWC-32	"	Devils Gate Ls. (type Locality) Nevada	"	"
JWC-30	"	Genesee Fm. (Genundewa Mbr.) Erie Co., N.Y.	"	"

† IFDC = International Fertilizer Development Corp., Muscle Shoals, Ala.

APPENDIX V.

Sm-Nd AND Rb-Sr ISOTOPIC SYSTEMATICS OF AUSTRALASIAN TEKTITES

H.F. Shaw and G.J. Wasserburg, The Lunatic Asylum, Division of Geological and Planetary Sciences, Caltech, Pasadena, CA 91125

We report Nd and Sr isotopic measurements made on tektites. The purpose of our study is to use the Sm-Nd and Rb-Sr systems to gain new insights into the origin of tektites. Over a decade has passed since the first Sr isotopic measurements were made on Australasian tektites [1,2]. Since that time our understanding of the behavior and significance of isotopic systems with respect to geochemical processes has greatly increased. In addition, the development of techniques to measure Nd isotopic ratios has provided a new and powerful tool for dating and determining the provenance of rocks. The analysis of returned lunar samples in the last ten years has clearly shown that a lunar origin for tektites is highly unlikely [3]. We must, therefore, return to earth in our search for possible parent materials for these objects.

Results. Our measurements of the $^{143}Nd/^{144}Nd$, $^{87}Sr/^{86}Sr$, $^{147}Sm/^{144}Nd$, and $^{87}Rb/^{86}Sr$ ratios are presented in Table 1. The measured ε^{Nd} are identical within errors at approximately -11.35; however, the $^{147}Sm/^{144}Nd$ ratios range from 0.117 to 0.149. Our measured ε^{Sr} lie in the range of published values of +108 to +240. Likewise, $^{87}Rb/^{86}Sr$ for our samples lie in the published range of 0.471 to 4.01 [1,2].

Discussion. The large negative measured ε^{Nd} and positive ε^{Sr} are clear signatures of old continental crust. The isotopic data, taken alone, is sufficient to exclude the possible derivation of tektites from young, recently mantle derived, continental material. The data also clearly exclude any possible oceanic crustal source. Several authors have determined that the LREE abundances in tektites are strongly enriched relative to chondritic abundances [4,5,6,this study]. These studies have also noted the close similarity between the REE patterns (as well as major and other trace element abundances) of terrestrial sedimentary rocks and tektites. Oxygen isotope analyses of tektites also suggest affinities to sedimentary rocks [7]. Our results support the interpretation that Australasian tektites are produced by impact melting of sediments or metasediments derived from old continental crust. The production of tektites from a sediment implies that their isotopic systems have undergone at least a 2-stage growth history. In the first stage we assume the derivation of a crustal segment with $f_1(Rb/Sr) \equiv ((Rb/Sr)_{crust}/(Rb/Sr)_{UR}-1)$ and $f_1(Sm/Nd) \equiv ((Sm/Nd)_{crust}/(Sm/Nd)_{CHUR}-1)$ from a uniform reservoir (the mantle) at time T_o. At some later time, T_s, this segment of crust may undergo weathering and sedimentation producing a sedimentary rock with enrichment factors $f_2(Rb/Sr)$ and $f_2(Sm/Nd)$. A third possible stage would involve volatilization upon impact melting leading to a third set of enrichment factors, f_3. We will defer consideration of this possibility for a moment. For the 2-stage model we measure today the enrichment factor f_2 and isotopic composition ε. From these we calculate model ages $T^{Sr}_{UR} = \varepsilon^{Sr}/(f_2(Rb/Sr) \cdot Q_{Sr})$ and $T^{Nd}_{CHUR} = \varepsilon^{Nd}/(f_2(Sm/Nd) \cdot Q_{Nd})$. These ages are related to the times T_o and T_s by:

$$T^{Sr}_{UR} = \frac{f_1(Rb/Sr)}{f_2(Rb/Sr)} (T_o - T_s) + T_s$$

with a similar equation for T^{Nd}_{CHUR}. We now consider the specific behavior of the Nd and Sr isotopic systems in this model.

The Sm-Nd system has been shown to be relatively undisturbed by sedimentary and some metamorphic processes [8]. Further, the REE are notably refractory and will not be readily subject to disturbance by volatile loss upon

Sm-Nd, Rb-Sr IN TEKTITES

Shaw, H.F. and Wasserburg, G.J.

TABLE 1. Sm-Nd, Rb-Sr Results.

	ε^{Nd}	$^{147}Sm/^{144}Nd$	f(Sm/Nd)	T^{Nd}_{CHUR}	ε^{Sr}	$^{87}Rb/^{86}Sr$	f(Rb/Sr)	T^{Sr}_{UR}
Australite	-11.3 ±0.4	0.117	-0.405	1.11	134.6 ±0.6	1.327	15.045	0.54
Cambodia A	—	0.142	-0.281		199.8 ±0.4	2.797	32.817	0.36
Cambodia B	-11.2 ±0.7	0.119	-0.394	1.14	212.5 ±0.4	2.945	34.612	0.37
Thailand A	-11.5 ±0.5	0.149	-0.242	1.88	204.9 ±0.7	2.824	33.142	0.37

ε^{Nd} relative to $(^{143}Nd/^{144}Nd)_{CHUR} = .511836$.
ε^{Sr} relative to $(^{87}Sr/^{86}Sr)_{UR} = .7045$.
Errors are 2σ of the mean. Errors on Sm/Nd and Rb/Sr ratios are ~ 1%.
$(^{87}Rb/^{86}Sr)_{UR} = .0827$, $\lambda^{Rb} = .0142\ AE^{-1}$, $(^{147}Sm/^{144}Nd)_{CHUR} = .1967$,
$\lambda^{Sm} = .00654\ AE^{-1}$.

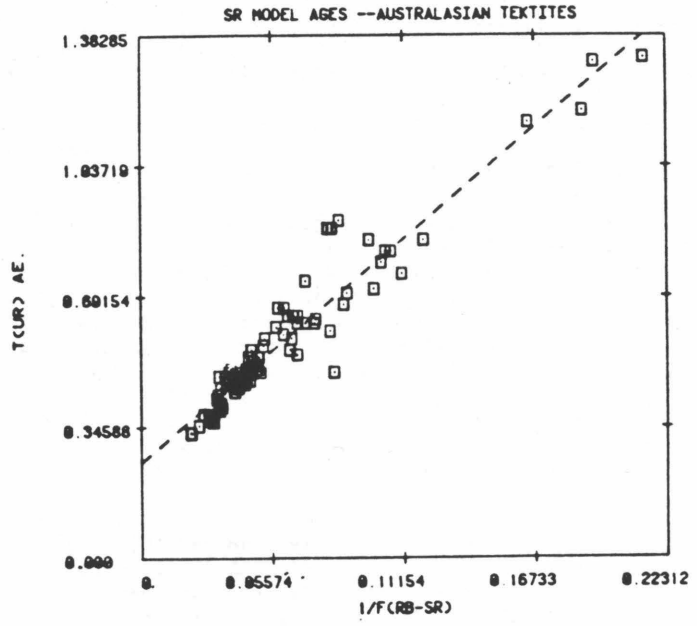

Fig.1. T^{Sr}_{UR} plotted against 1/f(Rb/Sr) showing the lowering of model ages in a 2-stage model as a result of increasing Rb/Sr during sedimentation. The y intercept gives the age of sedimentation. The age of the source region can be obtained from T^{Nd}_{CHUR} data. Plotted are data for all analyzed Australasian tektites, excluding high Na/K types. Data sources: this work, [1], [2].

Sm-Nd, Rb-Sr IN TEKTITES

Shaw, H.F. and Wasserburg, G.J.

melting. For Nd then, $f_1(Sm/Nd) = f_2(Sm/Nd)$ ($= f_3(Sm/Nd)$) and the model age equation reduces to that of single stage growth: $T^{Nd}_{CHUR} = T_o = \epsilon^{Nd}/Q^{Nd} \cdot f_1(Sm/Nd)$. It is thus possible to use our Sm-Nd data to obtain a concentration weighted, mean model age of the sources of the parent material of tektites. In contrast, sedimentary processes severely disturb the Rb-Sr system, generally by increasing the Rb/Sr ratio in the sediment through preferential Rb uptake relative to Sr by clays [8]. In the 2-stage model we have for Sr, $f_2 > f_1$ (and for continental crust $f_1 > 0$) so that the calculated model age, T^{Sr}_{UR}, will be greater than the age of sedimentation by the quantity $(f_1(Rb/Sr)/f_2(Rb/Sr)) \cdot (T_o - T_s)$. In the limit $f_2 >> f_1$, T^{Sr}_{UR} will approach T_s, the age of sedimentation. Selective Rb loss by volatilization during melting of the sediment will increase the calculated model age so that Sr model ages place a lower limit on the age of sedimentation of a tektite precursor. Table 1 lists T^{Nd}_{CHUR} and T^{Sr}_{UR} model ages calculated for our samples. As expected from the preceding discussion, T^{Nd}_{CHUR} are uniformly older than the T^{Sr}_{UR} ages and imply a significant contribution of crustal material greater than 1.9 AE age to any sedimentary precursor of Australasian tektites. We attribute the variability of T^{Nd}_{CHUR} to similar variations in the sedimentary material. The suite of mineral inclusions found in tektites [9] implies a variety of sources for the sediment so that this variation is not surprising. In Fig. 1 we have plotted T^{Sr}_{UR} vs. 1/f(Rb/Sr) for all available data on Australasian tektites (excluding the peculiar high Na/K types). A 2-stage growth history results in a linear plot on this graph, with the y intercept giving the age of sedimentation. The data indeed define a linear array with intercept ~ 0.25 AE which we interpret as the maximum age of sedimentation for the tektite parent material. This estimate compares favorably with Rb-Sr errorchron "ages" of 0.1 to 0.3 AE obtained by Compston and Chapman [3] from some of the data in Fig. 1. With decreasing Rb/Sr (i.e., less Rb enrichment during sedimentation), T^{Sr}_{UR} approaches our values of T^{Nd}_{CHUR}. In this limit, the $^{87}Rb/^{86}Sr$ value appears to approach a value of ~ 0.3, this being the averaged ratios of the sources of the sedimentary parent material. This value is at the low end of estimates of this ratio for average continental crust [10]. We conclude that the Sm-Nd and Rb-Sr isotopic systems can be used to infer the provenance of impact derived materials and, in particular, place significant new constraints on the age of the source regions for a sedimentary precursor of Australasian tektites. We believe that Sm-Nd analysis of microtektites should be possible and would provide insight into their origin and relationship to normal tektites. Finally, Sm-Nd data on late Cretaceous clays may help identify the location of the meteorite impact postulated to be the cause of anomalously high Ir contents in these clays [11], particularly if the impact occurred in an ocean basin.

Refs.: [1] Schnetzler and Pinson (1964) GCA 28, 953. [2] Compston and Chapman (1969) GCA 33, 1023. [3] Taylor (1973) E. Sci. Rev. 9, 101. [4] Taylor(1966) GCA 30,1121. [5] Frey (1977) EPSL 35, 43. [6] Taylor and McLennon (1979) GCA 43, 1551. [7] Taylor and Epstein (1970) Proc. Lunar Sci. Conf. 1st GCA 1, 1613. [8] McCulloch and Wasserburg (1978) Science 200, 1003. [9] Glass and Barlow (1979) Meteoritics 14, 55. [10] Jacobsen and Wasserburg (1979) JGR 84, 7411. [11] Alvarez et al. (1979) Science 208, 1095.
Div. Contrib. No. 3553 (379).

APPENDIX VI.

Sm-Nd, Rb-Sr SYSTEMATICS OF MAFIC COMPLEXES AND OPHIOLITES OF THE APPALACHIANS AND WESTERN U.S.

H. F. Shaw (Div. of Geological Sciences, Calif. Inst. Tech., Pasadena, CA 91125)
G. J. Wasserburg and A. L. Albee

We have examined the Sm-Nd and Rb-Sr isotopic systematics of the Baltimore Mafic Complex (BMC) of MD and the Thetford Mines Complex (TMC) of southern Qe. in an effort to identify remnants of Cambro-Ordovician oceanic crust in the Appalachians south of Newfoundland. For comparison, we also report measurements of Mesozoic ophiolites of the western U.S. Sm-Nd internal isochrons on 3 BMC gabbros give ages of 490±30My in accord with zircon ages (Sinha,pers.com.). We interpret this as the igneous age. BMC samples do not define Sm-Nd or Rb-Sr whole rock isochrons. Initial ε_{Nd}=-2.6 to -6.2, ε_{Sr}=+51.2 to +115.3 and these values are strongly anticorrelated. The isotopic composition of BMC samples does not depend on degree of metamorphism. An overlying pillow basalt has ε_{Nd}=+2.6,ε_{Sr}=+43.8 and appears unrelated to the BMC. TMC samples have ε_{Nd}=-1.5 to +4.2, ε_{Sr} = +2.6 to +114.2 (T~500My) and do not form Sm-Nd or Rb-Sr isochrons. Neither the BMC nor TMC has the Nd isotopic signature of oceanic crust (ε_{Nd} = +8 to +12). Instead, the data imply that much of the BMC Nd and Sr is derived from older continental crust. The ε_{Nd} of the TMC implies derivation from a relatively undepleted mantle source or a blend of sources. In contrast to these results, metagabbros from the King's River Ophiolite (200My,Saleeby,in press) and the Josephine Ophiolite (157My, Harper and Saleeby, 1980) of CA have ε_{Nd}=+12.4, ε_{Sr}=-27.9; ε_{Nd}=+8.6, ε_{Sr}=-13.9 respectively. These results are consistent with an oceanic origin for these complexes and are similar to isotopic data reported for other ophiolites. In particular, ε_{Nd} has been unaffected by obduction and metamorphism of these complexes. Comparing the data for the BMC and TMC with that of modern oceanic crust and ophiolites, we must conclude that the mafic and ultramafic bodies of the Appalachians south of Newfoundland are not pieces of oceanic crust, if the BMC and TMC are representative of these bodies.

APPENDIX VII.

Sm-Nd AND Rb-Sr SYSTEMATICS AND THE ORIGIN OF SANIDINE SPHERULES FROM A CRETACEOUS-TERTIARY BOUNDARY CLAY

H. F. Shaw and G. J. Wasserburg, The Lunatic Asylum, Div. Geological and Planetary Sciences, Calif. Inst. of Tech., Pasadena, CA 91125

Isotopic measurements were made on sanidine spherules from the Cretaceous-Tertiary Boundary Clay of the Gredero section, Caravaca SE Spain. Sediments marking the end of the Cretaceous in Italy, Denmark, and New Zealand were found by Alvarez et al. [1] to be many-fold enriched in Ir and other noble metals. This has subsequently been confirmed to be a world-wide phenomenon [2,3,4]. The enrichment of these elements (relative to crustal rocks) has been interpreted as evidence for the impact of a large (~5 km) extraterrestrial body, a possibility which has stimulated discussion about the role of such an event in the extinction of a wide variety of species at the end of Cretaceous time. In his study of the fossil assemblages across the Cretaceous-Tertiary Boundary, Smit [5] found large numbers (50-300 cm^{-3} sediment) of small (50-1000 μm) sanidine spherules in the Ir-rich layer at Caravaca. The spherules appear to have crystallized from quickly cooled liquid droplets. Smit found that chemically and structurally the spherules are pure sanidine with K/Na ~ 100, rich in As, Se, Sb, Zn, contain dark inclusions rich in Fe, Ni, and Co and up to 20% void space [5]. These objects may have been produced by the postulated impact event. The lack of geologic evidence on land for the crater which would be produced by such a large impact has prompted suggestions that the impact occurred in an ocean basin. We have previously demonstrated that the Nd and Sr isotopic composition of tektites can be used to infer the age and location of impact targets [6]. We apply this approach to the sanidine spherules. Procedures and Results. Spherules (~100 mg) were picked from a concentrate provided us by J. Smit. This sample was crushed, leached in cold ~0.5M HCL and rinsed with water in an attempt to remove carbonate. The residue was analyzed. We also measured the Sr isotopic composition of carbonate nanofossils associated with the spherules. The spherules have low Nd concentration (0.8 ppm, see Table 1), they are LREE enriched ($f^{Sm/Nd} = -0.21$), and the measured $\varepsilon^{Nd}(0)$ is -7.9. The measured $\varepsilon^{Sr}(0)$ is +66.0 ($^{87}Sr/^{86}Sr$ = 0.70915) with $f^{Rb/Sr} = +36.5$ and Sr concentration 60 ppm. Using the measured values of $f^{Sm/Nd}$ and $f^{Rb/Sr}$ to correct for in situ decay of Sm and Rb gives $\varepsilon^{Nd}(T) = -7.6$, $\varepsilon^{Sr}(T) = +26.4$ for T = 65 My. The carbonate fossils have $\varepsilon^{Sr}(0) = +45.3$ ($^{87}Sr/^{86}Sr$ = 0.70769) with $f^{Rb/Sr} = -0.85$ and Sr concentration 998 ppm, in good agreement with values for latest Cretaceous seawater [7]. Discussion. The rather large negative $\varepsilon^{Nd}(T)$ result demonstrates that the spherules were derived from an old LREE enriched source. $T^{Nd}_{CHUR} = 1.5$ AE, suggesting a Precambrian source if the Sm/Nd ratio of the spherules is close to that of the source. The small positive $\varepsilon^{Sr}(T)$ implies a slightly Rb enriched source. In Fig. 1 we have plotted $\varepsilon^{Nd}(T)$ vs $\varepsilon^{Sr}(T)$ for the spherules together with data on tektites. Tektites lie in the field occupied by typical upper crustal rocks in this diagram. The spherule point has lower $\varepsilon^{Sr}(T)$ than typical upper crustal rocks, implying that its source had lower Rb/Sr. Lower crustal granulites with low Rb/Sr have isotopic compositions which plot in the area of the spherule point [8,9]. Thus we infer from the low $\varepsilon^{Sr}(T)$ and high T^{Nd}_{CHUR} age that the high Rb/Sr ratio measured in the spherules was not characteristic of the source but is related to the formation of the spherules. The T^{Sr}_{UR} model age of 0.1 AE is consistent with this. We recognize that incomplete removal of carbonate from the sanidine may be the cause of the low $\varepsilon^{Sr}(T)$ value. This would remove the constraint of low Rb/Sr in the source but would not eliminate the requirement of strong Rb/Sr fractionation upon spherule formation as the Sr concentration of the sanidine must then be <10 ppm which results in a very large $f^{Rb/Sr}$ for the sanidine. In summary, the isotopic

Sm-Nd and Rb-Sr of Sanidine Spherules

Shaw, H. F. and G. J. Wasserburg

data require an old LREE enriched, probably low Rb/Sr and hence low K source for the sanidine spherules and a mechanism for strong Rb enrichment relative to Sr during spherule formation. Isotopically, the spherules resemble crustal rocks; either lower crustal granulites or if carbonate contamination is a problem, upper crustal granitic rocks. Clearly excluded as a source is the impacting projectile [5] which should have $\varepsilon^{Nd}(T) \sim 0$ for chondritic REE abundances. The moon is an unlikely source as $\varepsilon^{Sr}(T)$ is much too high. The spherules could not have been derived from oceanic crust which has distinctly different ε^{Nd} of +8 to +12, thus the ocean basins are ruled out as an impact site. There remains the problem of producing melt droplets of >80% K-feldspar composition. Any mechanism for the formation of the spherules must provide for the strong chemical fractionation of Rb and Sr, K and Na, and enrichment in volatile elements required by the isotopic and chemical data. Because of this, total melting of a target by impact is ruled out. Mechanisms which do provide for fractionation are 1) condensation of target material volatilized upon impact and 2) impact triggered explosive volcanism of partially remelted crustal material. The former possibility implies that chemical fractionation of a Precambrian crustal target occurred during volatilization and condensation such that K-feldspar-rich condensates with high Rb/Sr and K/Na were effectively separated as liquid droplets from any more refractory earlier condensates (Ca,Mg rich?) and any less refractory vapor (Na rich?). The volcanic mechanism implies that a melt of the above characteristics was produced by partial melting and fractional crystallization processes acting on an original Precambrian crustal source. Contribution No. 3739 (409). Ref.: [1] Alvarez et al. (1979) Science 208, 1095; [2] Smit and Hertogen (1980) Nature 285, 198; [3] Kyte et al. (1980) Nature 288, 651; [4] Ganapathy et al. (1981) EPSL 54, 393; [5] Smit and Klaver (1981) Nature 292, 47; [6] Shaw and Wasserburg (1981) Proc. LPSC XII, 967; [7] Peterman et al. (1970) GCA 34, 105; [8] Hamilton et al. (1979) Nature 277, 25; [9] DePaolo (1980) Nature 291, 193.

Table 1.

	$\varepsilon^{Nd}(0)$	ppm Nd	$f^{Sm/Nd}$	$\varepsilon^{Sr}(0)$	ppm Sr	$f^{Rb/Sr}$
Sanidine spherules	-7.9±0.4	0.81	-0.21	+66.0±1.4	60.1	+36.5
Carbonate fossils	-	-	-	+45.3±0.6	997.6	-0.85

ε^{Nd} relative to $(^{143}Nd/^{144}Nd)_{CHUR} = 0.511847$; ε^{Sr} relative to $(^{87}Sr/^{84}Sr)_{UR} = 0.7045$; Errors are 2σ of the mean.

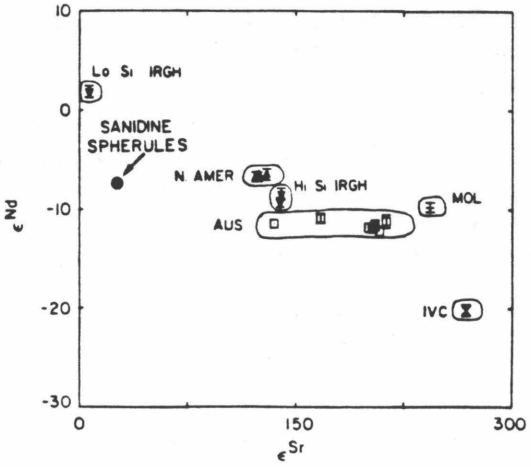

Fig. 1. Plot of initial ε^{Nd} vs initial ε^{Sr} comparing sanidine spherules with tektite data. Spherules lie to lower ε^{Sr} in the field of lower crustal rocks.

APPENDIX VIII.

ISOTOPIC CONSTRAINTS ON THE ORIGIN OF APPALACHIAN MAFIC COMPLEXES

SHAW, Henry F., WASSERBURG, G. J., and ALBEE, A. L., Division of Geological and Planetary Sciences, California Institute of Technology, Pasadena, California 91125

Current models for the origin of the belt of mafic and ultramafic complexes extending the length of the Appalachians stress the role of obducted oceanic crust and mantle. We have tested these models for several complexes using the initial isotopic composition of Nd and Sr. Ophiolites and modern oceanic crust have $\varepsilon^{Nd} > +7$ and $^{87}Sr/^{86}Sr < 0.705$. These values are distinct from those of ensialic mafic rocks with $\varepsilon^{Nd} < +3$, $^{87}Sr/^{86}Sr > 0.704$. Jacobsen and Wasserburg (1979) found that the Bay of Islands Complex, Newfoundland, has the isotopic signature of oceanic crust. Our results on amphibolite (Hazens Notch Fm.) associated with the Belvidere Mtn. Complex, N. Vt., are similar ($\varepsilon^{Nd} = +8$, $^{87}Sr/^{84}Sr = 0.7031$, for $T \sim 500$ My) and imply an oceanic origin. In contrast, the Thetford Mines Complex (TMC) of S. Quebec has variable initial ε^{Nd} of +4.2 to -1.5 and $^{87}Sr/^{86}Sr$ of 0.7041 to 0.7119 for $T \sim 500$ My. Sm-Nd internal isochrons on 3 gabbro samples from the Baltimore Mafic Complex (BMC), Md., give ages of 490±30 My in accord with zircon ages (Sinha, pers. com.). Whole rock initial values are $\varepsilon^{Nd} = -2.6$ to -6.2, $^{87}Sr/^{86}Sr = 0.7075$ to 0.7120 and are inversely correlated. Isotopic composition in the TMC and BMC does not correlate with degree of metamorphism or rock type. Neither the TMC nor BMC has the isotopic signature of oceanic crust. The isotopic data imply that much of the Nd and Sr in the BMC is derived from older continental crust. The isotopic composition of the TMC implies a relatively undepleted source or blend of sources. These results demonstrate that simple models involving obduction of oceanic crust cannot explain the origin of all Appalachian mafic complexes; instead, these rocks must have formed by diverse processes in a variety of geologic settings. Contribution Number 3773 (420).

APPENDIX IX.

Pb-Nd-Sr ISOTOPIC STUDIES OF CALIFORNIA OPHIOLITES

CHEN, J.H. AND H. F. SHAW, Div. Geol. Sci., California Institute of Technology, Pasadena, CA 91125

We report Pb-Nd-Sr isotopic results on gabbroic rocks from the Kings River (KR, 200 m.y.), the Point Sal (PS, 160 m.y.), and the Josephine (JP, 157 m.y.) ophiolites in an effort to identify the geological environments in which these ophiolites formed. The Pb isotopic composition of the KR metagabbro (α = 17.56, β = 15.41, γ = 37.11) plots within the field of present-day MORB and is similar to the least radiogenic Pb found in MORB. The low ε_{Sr}(-27.9) value for the KR ophiolite is typical of oceanic samples. Initial ε_{Nd} (+12.4) for the KR ophiolite is very high but within the range of modern MORB. These data indicate that the magma which formed the KR ophiolite was derived from a depleted mantle similar in Pb, Nd, and Sr isotopic composition to the source of MORB. In contrast, Pb from the PS ophiolite is more radiogenic, (α = 18.41-18.58, β = 15.56-15.58, γ = 38.03-38.13) in particular, the β value is about 5°/$_{oo}$ higher than that in the MORB for the same α value and is similar to those found in volcanic rocks from island-arcs. The Pb isotopic composition (α = 18.21, β = 15.51, γ = 37.86) for the JP ophiolite is intermediate between those of the KR and PS, and the β value is 1-2°/$_{oo}$ higher than that for typical MORB. The ε_{Nd} and ε_{Sr} values for the PS ophiolite (+8.2, -16.6) and the JP ophiolite (+8.8, -14.3) indicate an oceanic affinity, but do not distinguish between MOR or island-arc environments. These isotopic data clearly show signature of oceanic crust for these ophiolites and the presence of the depleted oceanic mantle on the west of the Mesozoic North American plate. These isotopic data also indicate that some of the California ophiolites may have formed in geologic environments other than spreading centers.

Contribution Number 3787 (391)

'PENDIX X.

Sm,Nd in Modern and Ancient Marine $CaCO_3$ and Apatite

H. F. SHAW and G. J. WASSERBURG (both at Calif. Inst. of Technology, Pasadena, California 91106)

We report C_{Sm},C_{Nd} (concentrations) and ε_{Nd} of modern and ancient marine $CaCO_3$ and apatite (ap.). We wish to determine the role of these phases in the marine REE budget and assess their suitability for tracing ε_{Nd} variations in seawater through time. Modern coral and mollusk calcite and aragonite have 0.2-9.0ppb Nd and Sm/Nd = 0.18-0.27. The ε_{Nd} of modern biogenic $CaCO_3$ reflect surface water: Pacific samples have ε_{Nd} = 0 to -2, Atlantic have ε_{Nd} = -8 to -9. Oöliths have ~65ppb Nd and Sm/Nd ~ 0.27. These C_{Nd} are 10^2-10^4 lower than previously reported for $CaCO_3$. Well preserved $CaCO_3$ fossils have C_{Nd} = 37ppb to 25×10^3ppb. High values must be due to diagensis or Fe-OH coatings. High REE concentrations reported for limestones cannot be primary but must but due to diagnesis or to detrital components. Modern biogenic ap. (shark's teeth) has ~ 4ppb Nd, 10^6-10^5 lower than fish debris and 10^5-10^4 lower than fossil and phosphorite ap. The REE are not enriched by primary biologic production of ap. or $CaCO_3$: Nd/Ca (seawater) ~ 7×10^{-9}g/g. REE enrichment must occur after death of the organism. Negative Ce anomalies in marine ap. imply that the REE are extracted from seawater. Although neither this process nor the formation of phosphorites is well understood, $\varepsilon_{Nd}(T)$ of fossil and phosphorite ap. may record ε_{Nd} of ancient seawater. We determined $\varepsilon_{Nd}(T)$ and $\varepsilon_{Sr}(T)$ of conodonts and phosphorites. All samples have $\varepsilon_{Sr}(T)$ in excellent agreement with seawater Sr curves. U. Dev. -L. Miss (360-340 My) conodonts from E. and W. N. America have $\varepsilon_{Nd}(T)$ = -6 to -7 suggesting a common Nd source. Israeli Tethyan phosphorite (205 My) has $\varepsilon_{Nd}(T)$ = -1.7 and ~660 My. W. African phosphorite has $\varepsilon_{Nd}(T)$ = -1.5 implying a contribution of depleted oceanic mantle volcanics to seawater at these times. Rum Jungle, Australia phosphorite (~2AE) has $\varepsilon_{Nd}(T)$ ~ -15, requiring a 3.5AE crustal Nd source and demonstrating the presence of significant amounts of ancient continental crust ~ 2 AE ago. Div. Cont. 3885 (438).